1975

VOLUME II

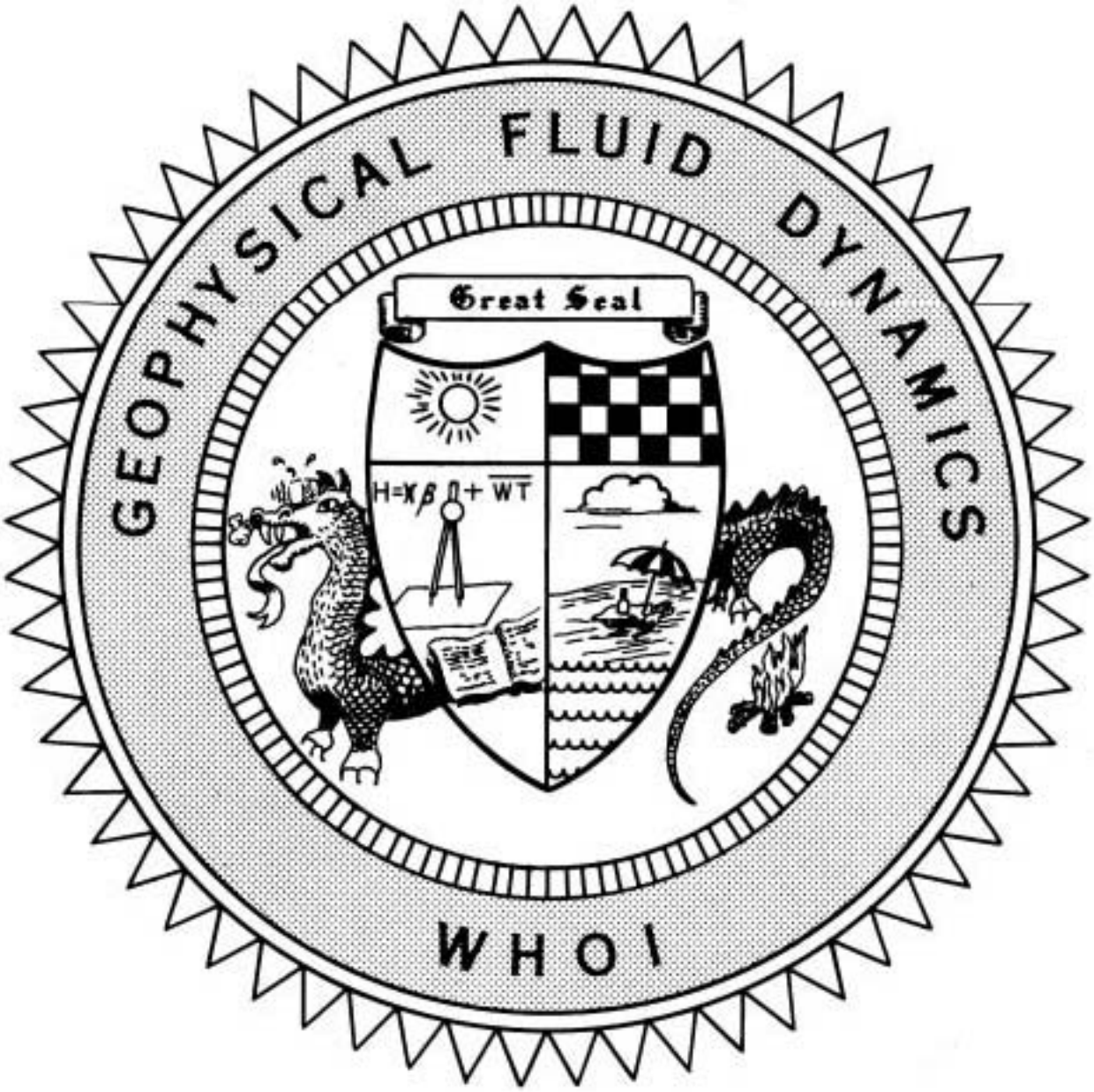

FELLOWSHIP **LECTURES**

Notes on the 1975

Summer Study Program
in
GEOPHYSICAL FLUID DYNAMICS
at
The WOODS HOLE OCEANOGRAPHIC INSTITUTION

Reference No. 75-58

Contents of the Volumes

Staff Members and Participants

Atwater, Tanya M.	Massachusetts Institute of Technology
Benton, Edward R.	University of Colorado
Busse, Friedrich H.	University of California at Los Angeles
Davis, Stephen H.	The Johns Hopkins University
Fitzjarrald, Dan	NOAA, Boulder, Colorado
Huppert, Herbert E.	Cambridge University, England
Keller, Joseph B.	Courant Institute of Mathematical Sciences
Loper, David E.	Florida State University
Malkus, Willem V.R.	Massachusetts Institute of Technology
McKenzie, Dan P.	University of Cambridge, England
Molnar, Peter	Massachusetts Institute of Technology
Newell, Alan C.	Clarkson College of Technology, N.Y.U.
Pedlosky, Joseph	University of Chicago
Peltier, W. R.	University of Toronto, Canada
Robbins, Kay Ann	Massachusetts Institute of Technology
Runcorn, S. Keith	University of Newcastle on Tyne, England
Sclater, John G.	Massachusetts Institute of Technology
Smith, Ronald B.	University of Colorado
Spiegel, Edward A.	Columbia University
Stern, Melvin E.	University of Rhode Island
Suess, Steven T.	NOAA, Boulder, Colorado
Turcotte, Donald	Cornell University
Veronis, George	Yale University
Whitehead, John A.,Jr.	Woods Hole Oceanographic Institution

Postdoctoral Fellows

Melosh, H. Jay	California Institute of Technology,Pasadena
Parsons, Barry E.	University of Cambridge, England
Proctor, Michael	University of Cambridge, England
Saito, Masanori	University of Tokyo, Japan

Predoctoral Fellows

Colella, Phillip	Appl.Mathematics.	University of California at Berkeley
Facinelli, William A.	Fluid Mechanics	Yale University
Hansen, Kirk S.	Meteorology	University of Chicago
Houben, Howard C.	Astronomy	Cornell University
Jones, Stephen	Appl.Mathematics.	University of Cambridge, England
Koenigsberg, Mark	Appl.Mathematics.	Massachusetts Institute of Technology
Skilbeck, John N.	Mathematics	University of Cambridge, England
Waxman, Allen M.	Astronomy	University of Michigan

Editor's Preface

This volume contains the manuscripts of research lectures by the twelve fellows of the summer program. The list of titles of these lectures indicates both the broad range of topics touched upon during the program as well as the central summer theme. The four postdoctoral fellows gave polished lectures which probably will appear in journals soon. The eight predoctoral contributions range from through work which already is of thesis caliber to work which is just the first product of a novel idea.

These lecture reports have not been edited or reviewed in a manner appropriate for published papers. They therefore should be regarded as unpublished manuscripts. Readers who would like to quote or use the material should write directly to the authors.

In addition to these volumes, which record the first pressed fruit of the program, more cautious professional results invariably emerge from the exchange of the summer. For this opportunity, we wish to thank the Woods Hole Oceanographic Institution and the National Science Foundation for encouragement and financial support.

Mary C. Thayer

Willem V.R. Malkus

Standing: Davis, Busse, Melosh, Proctor, Jones, Bullard, McKenzie, Malkus and Koenigsberg
Middle row: Thayer, Keller, Skilbeck, Dixie, Stern, Houben, Pedlosky, Waxman. Front row: Veronis, Colella, Facinelli, Hansen and Saito.

CONTENTS OF VOLUME II

Fellows' Lectures

ON NONLINEAR RAYLEIGH-TAYLOR INSTABILITY

Phillip Colella

In (1), Whitehead and Luther describe a set of experiments demonstrating viscous Rayleigh-Taylor instability. In these experiments, they float on top of a dense viscous fluid a thin layer of less dense viscous fluid, seal the container (which is made of plexiglass) so there are no air bubbles, and invert the container, Initially the interface between the two fluids is flat but this configuration is unstable, After about thirty seconds, one sees spouts of light fluid welling up, surrounded by downwelling heavy fluid.

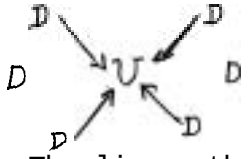

D = regions of downwelling fluid

U = region of upwelling fluid (as seen from above)

The linear theory (which is outlined in an appendix to (1) predicts the magnitude of the wavenumber of the disturbance which grows the fastest, but does not determine the shape. Whitehead and Luther conjectured that one particular planform - hexagon - has the greatest growth rate in the first nonlinear corrections to the theory. A method is outlined here to determine which planform gives rise to the maximum growth rate in the nonlinear theory for a restricted range of the physical parameters.

Scaline and Linear Theory

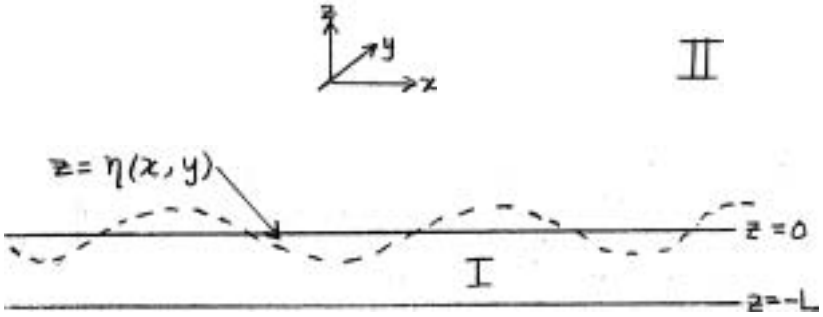

We consider a system of two incompressible, immiscible fluids of equal constant viscosity μ, separated by a boundary $z = ?(x, y)$. Fluid I is of density ρ_0, fluid II of density $\rho_0 + \Delta\rho$, $\Delta\rho > 0$. The equations of motion and the boundary conditions are

$$\rho_0 \frac{\partial}{\partial t} \underset{\sim}{v} = \mu \Delta \underset{\sim}{v} - \nabla(p - \rho_0 g z) + (\underset{\sim}{v} \cdot \nabla)\underset{\sim}{v} \qquad \text{IN REGION I} \qquad (1)$$

$$(\rho_0 + \Delta\rho) \frac{\partial}{\partial t} \underset{\sim}{v} = \mu \Delta \underset{\sim}{v} - \nabla(p - (\rho_0 + \Delta\rho) g z) + \underset{\sim}{v} \Delta \underset{\sim}{v} \qquad \text{IN REGION II}$$

$$\nabla \cdot \underset{\sim}{v} = 0 \qquad \underset{\sim}{v} = (u, v, w)$$

$$[\underset{\sim}{v}]_{z=\eta} = 0 \qquad \text{continuity of velocity across the free boundary} \qquad (2)$$

$$\left.\begin{aligned}[\underset{\sim}{t}\cdot\underset{\approx}{\sigma}\cdot\underset{\sim}{n}]_{z=\eta} &= 0\\ [\underset{\sim}{s}\cdot\underset{\approx}{\sigma}\cdot\underset{\sim}{n}]_{z=\eta} &= 0\end{aligned}\right\}$$ continuity of tangential stress across free boundary (3), (4)

$$[\underset{\sim}{n}\cdot\underset{\approx}{\sigma}\cdot\underset{\sim}{n}]_{z=\eta} = [p]_{z=\eta}|n|^2$$ continuity of normal stress across free boundary (5)

$$\frac{\partial\eta}{\partial t} + u\frac{\partial\eta}{\partial x} + v\frac{\partial\eta}{\partial y} = w,$$ where u, v, w are evaluated at $z = \eta(x,y)$ (6)

$$\underset{\sim}{v} = 0 \text{ AT } z = -L, \quad \underset{\sim}{v} \longrightarrow 0 \text{ AS } z \longrightarrow \infty$$ (7)

$$\sigma_{ij} = \mu\left(\frac{\partial u_i}{\partial x_j} + \frac{\partial u_j}{\partial x_i}\right),$$ THE RATE OF STRAIN TENSOR

$$\underset{\sim}{n} = \left(\frac{\partial\eta}{\partial x}, \frac{\partial\eta}{\partial y}, -1\right)$$ normal vector to $z = \eta(x,y)$

$$\left.\begin{aligned}\underset{\sim}{t} &= \left(1, 0, \frac{\partial\eta}{\partial x}\right)\\ \underset{\sim}{s} &= \left(0, 1, \frac{\partial\eta}{\partial y}\right)\end{aligned}\right\}$$ linearly independent tangent vectors to $z = \eta(x,y)$

$[A]_{z=\eta}$ is the discontinuity of A across the surface $z = \eta$, i.e. the function whose value at the point (x,y) is $A(x,y,\eta(x,y)+) - A(x,y,\eta(x,y)-)$. We non-dimensionalize the equations writing down, for the moment, only the linearized boundary conditions (the dimensional quantities are starred).

$$\vec{x}_* = Lx \qquad \eta_* = L\eta$$

$$t_* = \frac{\Delta\rho}{\rho_0}\frac{\nu}{gL}t \qquad p_* = \frac{\rho_0\nu U}{L}p - \rho_0 g z \quad \text{IN REGION I}$$

$$\underset{\sim}{v}_* = \frac{gL^2}{\nu}\underset{\sim}{v} \qquad p_* = \frac{\rho_0\nu U}{L}p - (\rho_0+\Delta\rho)gz \quad \text{IN REGION II}$$

$$\frac{\Delta\rho}{\rho_0}\frac{gL^3}{\nu^2}\frac{\partial}{\partial t}\underset{\sim}{v} = -\nabla p + \Delta\underset{\sim}{v} - \frac{gL^3}{\nu^2}(\underset{\sim}{v}\cdot\nabla)\underset{\sim}{v} \quad \text{IN REGION I}$$ (8)

$$\left(\frac{\Delta\rho}{\rho_0} + \left(\frac{\Delta\rho}{\rho_0}\right)^2\right)\frac{gL^3}{\nu^2}\frac{\partial}{\partial t}\underset{\sim}{v} = -\nabla p + \Delta\underset{\sim}{v} - \frac{gL^3}{\nu^2}(\underset{\sim}{v}\cdot\nabla)\underset{\sim}{v} \quad \text{IN REGION II}$$

$$\nabla\cdot\underset{\sim}{v} = 0 \quad \text{IN BOTH REGIONS}$$

$$[\underset{\sim}{v}]_{z=0} = 0$$ (9)

$$\left[\frac{\partial w}{\partial x}+\frac{\partial u}{\partial z}\right]_{z=0}=0 \tag{10}$$

$$\left[\frac{\partial w}{\partial y}+\frac{\partial v}{\partial z}\right]_{z=0}=0 \tag{11}$$

$$2\left[\frac{\partial w}{\partial z}\right]_{z=0}=[p]_{z=0}-\frac{\Delta\rho}{\rho_0}\eta \tag{12}$$

$$\frac{\Delta\rho}{\rho_0}\frac{\partial\eta}{\partial t}=w \tag{13}$$

$$\underset{\sim}{v}=0 \text{ AT } z=-1, \quad \underset{\sim}{v}\longrightarrow 0 \text{ AS } z\longrightarrow+\infty \tag{14}$$

We expand the solutions in $\frac{\Delta\rho}{\rho_0}=\varepsilon$, which we take to be small. We also assume $\frac{gL^3}{\nu^2}=O(\varepsilon^2)$ or smaller. With this ordering, the time dependence of $\underset{\sim}{v}$, p is completely determined by the boundary conditions to order ε^3, and $(\underset{\sim}{v}\cdot\nabla)\underset{\sim}{v}$ is negligible to the same order. We expand $\underset{\sim}{v}, p$ and η in powers of ε about $\underset{\sim}{v}$, p and η identically zero for $\varepsilon=0$.

$$\underset{\sim}{v}=\varepsilon\underset{\sim}{v}_0+\varepsilon^2\underset{\sim}{v}_1+\varepsilon^3\underset{\sim}{v}_2+\cdots$$

$$p=\varepsilon p_0+\varepsilon^2 p_1+\varepsilon^3 p_2+\cdots$$

$$\eta=\varepsilon\eta_0+\varepsilon^2\eta_1+\cdots$$

$\underset{\sim}{v}_0, p_0$ turn out to be zero, since η does not enter the ε-equation. The ε^2-equations are

$$\Delta\underset{\sim}{v}_1=\nabla p_1 \quad \text{in both regions} \tag{15}$$
$$\nabla\cdot\underset{\sim}{v}_1=0$$

$\underset{\sim}{v}_1$ satisfies the boundary conditions (9), (10), (11), and (14).

$$2\left[\frac{\partial w_1}{\partial z}\right]_{z=0}=[p_1]_{z=0}-\eta_0 \tag{16}$$

$$\frac{\partial\eta_0}{\partial t}=w_1(x,y,0,t) \tag{17}$$

The reason for scaling the time is in Eqs. (16) and (17); it gives a very simple form to the time dependence of η_0 and $\underset{\sim}{v}$ in the linear theory, and, as we will see, in the first nonlinear corrections as well.

To solve these equations, we assume

$$\underset{\sim}{v}_1=\underset{\sim}{v}'(z)f(x,y)C_1(t)$$
$$p_1=p'(z)f(x,y)C_1(t)$$
$$\eta_0=f(x,y)C_1(t) \qquad \underset{\sim}{v}'=(u',v',w')$$

where f satisfies $\frac{\partial^2 f}{\partial x^2}+\frac{\partial^2 f}{\partial y^2}+k^2 f=0$. By taking the curl of (15) twice, using the fact that $\nabla\cdot\underset{\sim}{v}_1=0$, we see that $\underset{\sim}{v}_1$ satisfies the biharmonic equation

$$(D^2-k^2)^2\underset{\sim}{v}'C_1 f=0 \qquad D=\frac{\partial}{\partial z} \tag{18}$$

Differentiating the x-component of (15) with respect to x, and the y-component of (15) with respect to y, adding them, and using $\nabla \cdot \underset{\sim}{v} = 0$ we get

$$C_1 f \frac{1}{k^2}\left(D^2 - k^2\right) D w' = \rho' C_1 f \tag{19}$$

Once we determine w', we know ρ' using (19), then u_1 and v_1, using (15).

The general solution for w_1 is

$$\left(A e^{-kz} + B z e^{-kz}\right) f C_1 = w_1 \quad \text{IN REGION II.}$$

$$\left(E \sinh(z+1) + F z \sinh(z+1)\right) f C_1 = w_1 \quad \text{IN REGION I.}$$

The boundary conditions can be arranged to be a set of four linear equations for (A, B, E, F). $\left[\underset{\sim}{v}_1\right]_{z=0}$ implies $\left[w'\right]_{z=0} C_1 f = 0$ (20)

and $\left[u'(z)\frac{\partial}{\partial x} + \frac{\partial f}{\partial y}\right]_{z=0} = 0$ which implies

$$\left[D w'\right]_{z=0} C_1 f_z = 0 \tag{21}$$

We differentiate (9) with respect to x, (10) with respect to y, and add them.

$$\left[\frac{\partial^2 w_1}{\partial x^2} + \frac{\partial^2 w_1}{\partial y^2} + \frac{\partial}{\partial z}\left(\frac{\partial u_1}{\partial x} + \frac{\partial v_1}{\partial y}\right)\right]_{z=0} = 0$$

from which follows

$$\left[\left(D^2 + k^2\right) w'\right]_{z=0} C_1 f = 0 \tag{22}$$

(16) and (21) imply

$$\left[\rho'\right]_{z=0} C_1 f = C_1 f. \tag{23}$$

Schematically, Eqs. (19-23) are of the form

$$C_1 f \, T \vec{a} = C_1 f \, \vec{e}_4 \tag{24}$$

where T is a 4 x 4 matrix depending on k, $\vec{a}$ = (A,B,E,F), and $\vec{e}_4 = (0,0,0,1)$. This system of equations can be solved, and the results used in (17) to determine the time evolution of $\eta_0 = C_1(t) f(x,y)$, and therefore of the whole system.

$$f(x,y)\frac{dC_1}{dt} = A C_1 f(x,y) \qquad A = \left\{k(\coth(k)+1) + k\tanh(k)\,\middle|\,\frac{\coth(k)-1}{1-\tanh(k)}\right\}^{-1} \tag{25}$$

$A > 0$ for $k > 0$.

Nonlinear Analysis

To order ε^3, the equations are $\Delta \underset{\sim}{v}_2 = \nabla p_2$ in both regions (26)

$$\nabla \cdot \underset{\sim}{v}_2 = 0$$

$$\left[\underset{\sim}{v}_2\right]_{z=0} = \left[\frac{\partial \underset{\sim}{v}_1}{\partial z}\right]_{z=0} \eta_0 \tag{27}$$

$$\left[\frac{\partial w_2}{\partial y} + \frac{\partial v_2}{\partial z}\right]_{z=0} = \eta_0 \left[\frac{\partial}{\partial z}\left(\frac{\partial w_1}{\partial y} + \frac{\partial v_1}{\partial z}\right)\right]_{z=0} \tag{28}$$

$$\left[\frac{\partial u_2}{\partial z} + \frac{\partial w_2}{\partial x}\right]_{z=0} = \eta_0\left[\frac{\partial}{\partial z}\left(\frac{\partial w_1}{\partial x} + \frac{\partial u_1}{\partial z}\right)\right]_{z=0} \tag{29}$$

$$\left[2\frac{\partial w_2}{\partial z} - P_2\right]_{z=0} - g\eta_1 = \eta_0\left[2\frac{\partial w_1}{\partial z} - P_1\right] \tag{30}$$

$$\frac{\partial \eta_0}{\partial t} = w_2 + \eta_0\frac{\partial w_1}{\partial z} - u_1\frac{\partial \eta_0}{\partial x} - v_1\frac{\partial \eta_0}{\partial y} \tag{31}$$

$$\underline{v}_2 = 0 \quad \text{AT} \quad z = -1, \qquad \underline{v}_2 \longrightarrow 0 \quad \text{AS} \quad z \longrightarrow +\infty \tag{32}$$

We assume $\underline{v}_2 = \underline{v}_2'(z) f(x,y) C_2(t)$, $P_2 = P_2'(z) f(x,y) C_2(t)$ and $\eta_1 = C_1(t) f(x,y)$, where the f is the same as in the order ε^2 problem.

$$w_2' = A_1 e^{-kz} + B_2 z e^{-kz} \qquad \text{IN REGION II}$$

$$= E_2 \sinh(k(z+1)) + F_2 z \sinh(k(z+1)) \qquad \text{IN REGION I}$$

As before, the boundary conditions (-) can be expressed as an equation for A_2, B_2, E_2, F_2 of the form $C_2 f T\vec{a}_2 = C_2 f \vec{e}_4 + \vec{b}(fC_1)$, where T is the same as in (24), $a_2 = (A_2, B_2, E_2, F_2)$, and $\vec{b}$ is four-vector with a quadratic dependence on $C_1 f$. So

$$C_2 f A_2 = (C_2 f T^{-1} e_4)_A + (T^{-1}(\vec{b}(fC_1)))_A$$

$$= C_2 f A + G_1(fC_1)$$

A here is the A in (25). Using the expression in (31), we get

$$f\frac{dC_2}{dt} = fAC_2 + G_1(fC_1) + G_2(fC_1) \tag{33}$$

where $G_2(fC_1)$ is a quadratic expression in fC_1 arising from the last three terms in (31).

Let us consider again (25) $f\frac{dC}{dt} = fA_1C_2$. Solutions to (25) and (33) are iterative approximations to the equation

$$\frac{d}{dt}(fC) = AfC + G_1(fC) + G_2(fC)$$

We project this equation along f :

$$\frac{dC}{dt} = AC + \bar{G}C^2, \text{ where } \bar{G} = \int_0^{2\pi}\int_0^{2\pi} G_1(f)f + G_2(f)f)\,dx\,dy$$

The planform f for which $\bar{G}$ is maximum should correspond to the one observed in the experiments in (1).

Reference

Whitehead and Luther 1975 J.Geophys.Res. 80(5): 705-717.

GEOSTROPHIC ADJUSTMENT - THEORY AND EXPERIMENT

William A. Facinelli

Introduction

To provide some background for our work this summer, we first consider a problem solved by Rossby (1938), which has since been referred to as the Rossby Adjustment Problem. This is best described by the following figure:

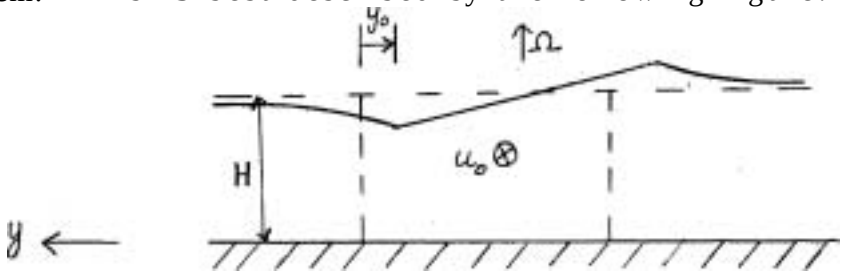

The fluid extends infinitely far to the left and right and into the plane of the paper. Initially there is a velocity jet with uniform speed u_0 confined by the dashed lines, with the free surface horizontal. The system is rotating with angular velocity Ω. Rossby took the final state to be geostrophic, i.e., the velocity is everywhere balanced by a pressure gradient due to a variation in the height of the free surface. In calculating what the final state would be, he neglected frictional and transient effects. The resulting free surface is shown by the solid line in the figure. The main velocity jet shifts a distance y_0 to the right, and there are weak countercurrents (directed out of the paper) on each side of the central stream.

The second case which Rossby analyzed was a two-layer, stratified system, with an initial velocity jet in the upper layer:

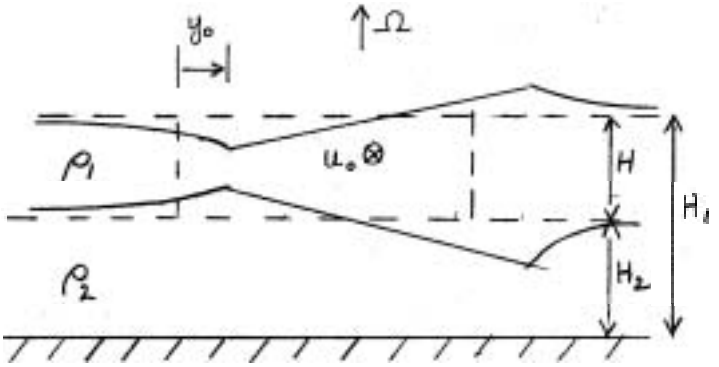

Assuming that the bottom layer remains motionless, he found the adjusted free surface and interface to be as shown in the figure. Once again, the main jet moves to the right a distance y_0, and there are weak countercurrents on each side of it.

The characteristic length scale of these problems (and those which follow) is called the Rossby radius of deformation. When the system is two-layer, there are actually two such parameters:

$$\lambda_1 = \frac{\sqrt{gH_1}}{f} \quad \text{and} \quad \lambda' = \frac{\sqrt{g'H}}{f}, \text{ where } g' = \frac{\rho_2 - \rho_1}{\rho_2} g.$$

λ_1 depends on the overall depth of the fluid, H_1, and is associated with the "baratropic" mode of response. λ' is a function of the density contrast and the depth of the upper layer. It is the length scale of the "baroclinic" mode, (These

ideas will be clarified later, when the mathematical solution to a two-layer problem is presented.

To close this introductory section, mention will be made of work done by Veronis (1956), in which he treated the response of the ocean to an applied wind stress. As a special case, he considered the process of "quasi-static" geostrophic adjustment, and obtained a final state identical to that found by Rossby in the first problem above.

Use of the Fundamental Equations

The Rossby Adjustment Problem is characterized by discontinuous velocities in the initial state of the fluid. Our work this summer had to do with fluid systems starting out with discontinuous depths. The first such problem to be discussed here is the following:

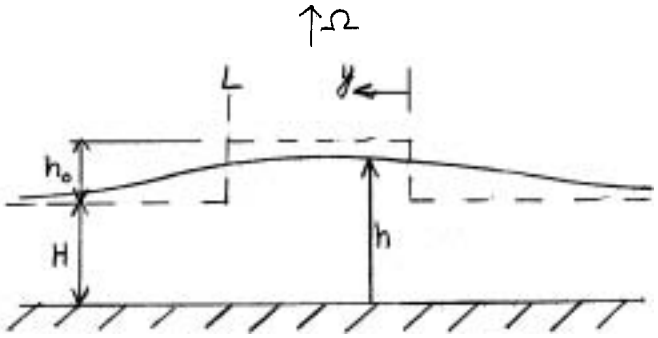

The fluid is incompressible and extends to infinity to the left and right and into the plane of the paper. It starts with height $H+h_o$ between $y=0$ and $y=L$, and height H everywhere else. The height in the final state is $h(y)$. The x-direction is positive into the paper.

In all that follows, the frictional terms will be ignored. There is no pressure gradient (and height variation) in the x-direction, so the first equation of motion is:

$$\frac{\partial u}{\partial t} - fv = 0 \qquad (1)$$

where f is the Coriolis parameter (here assumed constant). In the equation of motion in the y-direction, we neglect $\frac{\partial v}{\partial t}$ compared with the other terms, thus:

$$fu = -g\frac{dh}{dy} \qquad (2)$$

This is the geostrophic relation. Finally, vertical integration of the equation of continuity for an incompressible fluid yields:

$$h\frac{\partial v}{\partial y} + \frac{\partial h}{\partial t} = 0 \qquad (3)$$

When the bump (h_o) is small compared with H, this can be approximated by:

$$H\frac{\partial v}{\partial y} + \frac{\partial h}{\partial t} = 0. \qquad (4)$$

Then combining Eqs.(1), (3), and (4) gives a linear equation in h:

$$\frac{\partial^3 h}{\partial y^2 \partial t} - \frac{f^2}{gh}\frac{\partial h}{\partial t} = 0 \qquad \text{or} \qquad \frac{\partial^3 h}{\partial x^2 \partial t} - \frac{1}{\lambda^2}\frac{\partial h}{\partial t} = 0. \qquad (5)$$

In the region between $y=0$ and $y=L$ (call this region I), the height goes from $H+h_0$ initially to h at some later time, so integrating with respect to time yields

$$\frac{d^2h}{dy^2} - \frac{1}{\lambda^2}(h-H-h_0) = 0, \text{ in I.} \tag{6}$$

For $y \geq L$ (region II) and $y \leq 0$ (region 111), the height goes from H to h, so integrating (5) gives

$$\frac{d^2h}{dy^2} - \frac{1}{\lambda^2}(h-H) = 0, \text{ in II and III.} \tag{7}$$

Taking into consideration the required symmetry about $y = \frac{L}{2}$ and that $h \to H$ as $|y|$ gives as the solutions for (6) and (7)

$$\text{I: } h-(H+h_0) = A \qquad \left(\frac{y-\frac{L}{2}}{\lambda}\right)$$

$$\text{II: } h-H = Be^{-\frac{y-L}{\lambda}}$$

$$\text{III: } h-H = Be^{\frac{y}{\lambda}}.$$

The boundary conditions are that h be continuous at $y=0$ (and $y=L$) and that $u = -\frac{g}{f}\frac{dh}{dy}$ be continuous at the same locations. This enables us to find A and B:

$$A = -h_0 e^{-L/2\lambda}$$

$$B = h_0 e^{-L/2\lambda} \sinh L/2\lambda.$$

Therefore:

$$\text{I: } h-H = h_0\left[1-e^{-L/2\lambda}\cosh\left(\frac{y-\frac{L}{2}}{\lambda}\right)\right.$$

$$\text{II: } h-H = h_0 \sinh\frac{L}{2\lambda}\, e^{-\frac{y-\frac{L}{2}}{\lambda}}$$

$$\text{III: } h-H = h_0 \sinh\frac{L}{2\lambda}\, e^{\frac{y-\frac{L}{2}}{\lambda}}$$

The corresponding velocities are:

$$\text{I: } u = \frac{g h_0}{f\lambda} e^{-\frac{L}{2\lambda}} \sinh\left(\frac{y-\frac{L}{2}}{\lambda}\right)$$

$$\text{II: } u = \frac{g h_0}{f\lambda} e^{-\frac{y-\frac{L}{2}}{\lambda}} \sinh\frac{L}{2\lambda}$$

$$\text{III: } u = -\frac{g h_0}{f\lambda} e^{\frac{y-\frac{L}{2}}{\lambda}} \sinh\frac{L}{2\lambda}$$

These "adjusted" heights and velocities look like the sketch on the following page.

This problem illustrates the concept of the geostrophic adjustment of an initial imbalance in the height of a fluid, and also shows how the equations of motion and continuity are sometimes sufficient to completely solve a problem. This problem was tractable using only these equations because of the requirement that $h_0 \ll H$, so that $h \approx H$ in the equation of continuity. The reaulting differential equation for h was linear. If the "bump" is not very small, the differ ential equation is nonlinear.

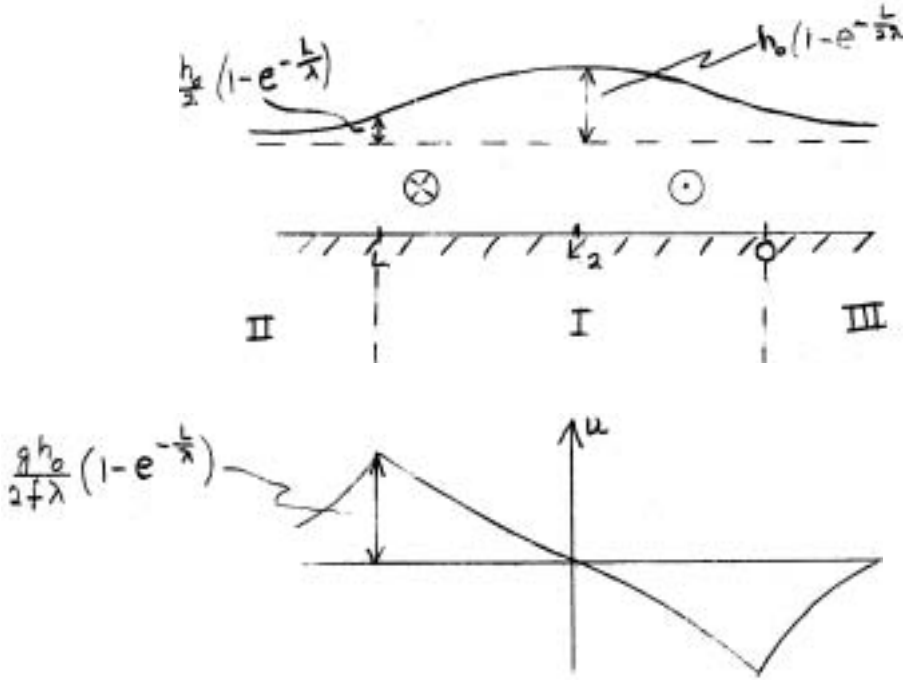

The continuity equation is also nonlinear for a two-layer system in which the initial height of the upper layer vanishes at some point, such as:

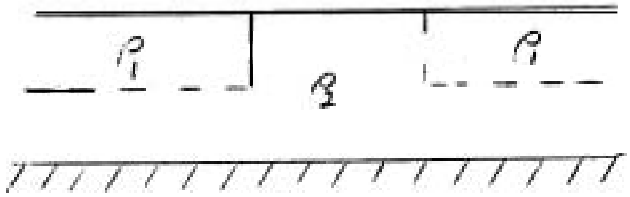

We shall give the solution of such a problem, using the conservation of potential vorticity.

Conservation of Potential Vorticity

The only problem for which we obtained a complete analytical solution using conservation of potential vorticity was the following:

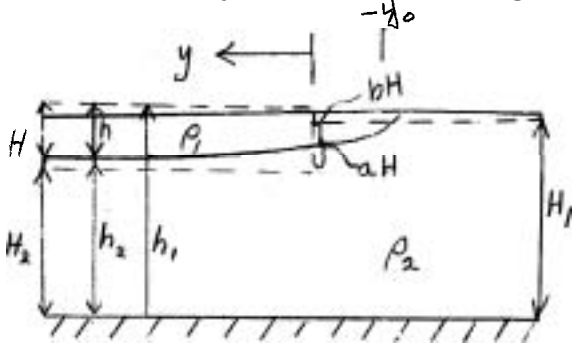

The initial depth of the top layer is H_1, and it extends from $y=0$ to $y=m$. The bottom layer has depth H_2 for $y>0$ and H_1 for $y<0$. The free surface for $y>0$ is bH (where $b=\frac{\rho_2-\rho_1}{\rho_2}$) higher than it is for $y<0$. This is so that the pressure is constant at any given depth in the bottom layer. (The extra head of fluid 1 on the left compensates for fluid 1 being lighter than fluid 2.) The adjusted profile is given by the solid lines in the figure.

The principle of conservation of potential vorticity - which holds for all frictionless flows - is:

$$\frac{d}{dt}\left(\frac{f+\zeta}{d}\right)=0,$$

where ζ is the relative vorticity and d is the depth of the fluid layer. In the problem at hand, this implies that for $y>0$ for the top layer

$$\frac{f-\frac{du_1}{dy}}{h}=\frac{f}{H},$$

and for positive y for the bottom layer

$$\frac{f-\frac{du_2}{dy}}{h_2}=\frac{f}{H}.$$

Eliminating the velocities by means of the geostrophic relation for each layer and substituting $h=h_1-h_2$ yields two coupled differential equations for h_1 and h_2:

$$h_{1yy}-\frac{1}{A}(h_1-h_2-H)=0$$

$$a h_{1yy}+b h_{2yy}-\frac{1}{\lambda_2^2}(h_2-H_2)=0,$$

where

$$\lambda=\frac{\sqrt{gH}}{f},\quad \lambda_2=\frac{\sqrt{gH_2}}{f}.$$

These equations can be made homogeneous by substituting

$$\eta_1=h_1-H_1-bH,\quad \eta_2=h_2-H_2=h_2-H_1+aH.$$

The equations thus become

$$\eta_{1yy}-\frac{1}{\lambda_2}(\eta_1-\eta_2)=0$$

$$a\eta_{1yy}+b\eta_{2yy}-\frac{1}{\lambda_2^2}\eta_2=0$$

It is easiest to solve this system using normal modes, which is essentially another change of variables that decouples the system of equations. We will skip the mathematical details (a description of the method is in Veronis and Stommel (1956), and state the results. The differential equations are:

$$R_{iyy}-k_i R_i=0,\quad i=1,2, \tag{8}$$

where

$$k_1=\frac{f^2}{gH_1}\equiv\frac{1}{\lambda_1^2}$$

$$k_2=\frac{f^2}{g'H}\left(1+\frac{H}{H_2}\right)\equiv\frac{1}{\lambda'^2}$$

(Note that this λ' is identical to the one originally defined when H/H_2 is very small.) In the problem we are considering, (8) is valid for $y>-y_0$ only, so we require that $R_i\to 0$ as $y\to\infty$. Therefore

$$R_1=A_1 e^{-\frac{y+y_0}{\lambda_1}}$$

$$R_2 = A_1 e^{-\frac{y+y_0}{\lambda'}}$$

where A_1 and A_2 are arbitrary constants. The expressions for η_1, η_2, and h in terms of these normal modes are:

$$\eta_1 = \frac{H}{H_1} A_1 e^{-\frac{y+y_0}{\lambda'}} + \frac{H_2}{H_1} A_2 e^{-\frac{y+y_0}{\lambda'}}$$

$$\eta_2 = \frac{HH_2}{H_1^2} A_1 e^{-\frac{y+y_0}{\lambda_1}} - \frac{1}{b} A_2 e^{-\frac{y+y_0}{\lambda'}}$$

$$h = H + \frac{H^2}{H_1^2} A e^{-\frac{y+y_0}{\lambda_1}} + \frac{1}{b} A_2 e^{-\frac{y+y_0}{\lambda'}}$$

Note how each of these expressions involves a λ_1 term (the barotropic mode) and a λ' term (the baroclinic mode).

For $y < 0$ (initially) and $y < -y_0$ (finally), conservation of potential vorticity and the geostrophic relation yields a differential equation in h_1 alone:

$$h_{1yy} - \frac{1}{\lambda_1^2}(h_1 - H_1) = 0$$

In terms of η_1 as previously defined, this is:

$$\eta_{1yy} - \frac{1}{\lambda^2}(\eta_1 + bH) = 0$$

Requiring that $\eta_1 \to 0$ as $y \to -\infty$ means that the solution is

$$\eta_1 = -bH + A_3 e^{\frac{y+y_0}{\lambda'}}$$

We now have four unknown constants: A_1, A_2, A_3, and y_0. Hence, four boundary conditions are necessary. These are:

continuity of η_1 at $y = -y_0$,

$h = 0$ at $y = -y_0$,

conservation of fluid 1,

continuity of u_2 at $y = -y_0$.

Using the resulting four equations to solve for the four constants completes the problem.

The most interesting results of this analysis concern the formulas for u_1 and u_2 for $b \ll 1$:

$$u_1 = \frac{g}{f}\left(\frac{H}{\lambda_1 H_1} A_1 e^{-\frac{y+y_0}{\lambda_1}} + \frac{H_2}{\lambda' H_1} A_2 e^{-\frac{y+y_0}{\lambda'}}\right)$$

$$u_2 = \frac{g}{f}\left[\frac{H}{\lambda' H_1} A_1 e^{-\frac{y+y_0}{\lambda_1}} + \left(\frac{aH_2}{\lambda' H_1} - \frac{1}{\lambda'}\right) A_2 e^{-\frac{y+y_0}{\lambda'}}\right].$$

There are three important conclusions which follow:

1) When $y + y_0 \gg \lambda'$ (far away from y_0 compared with λ'), the baroclinic (λ') terms drop out, and we see that $u_1 = u_2$. Thus the response far away from the position of zero depth of the upper layer is barotropic.

2) Numerical evaluation of u_1 and u_2 at $y = -y_0$ for values of the parameters in our experiments (with $b \ll 1$) gives that $u_2 \sim -\frac{1}{20} u_1$.

3) When $H/H_1 \to 0$ and $H_2/H_1 \to 1$, $u_2 = -b u_1$.

Experimental Problem

We will now turn to an analysis of the problem done in our experiments. The system again consists of two layers of densities ρ_1 and ρ_2, but results 2 and 3 above imply that when the bottom layer is much deeper than the upper layer, the bottom is nearly motionless. Incorporating the assumption of a motionless bottom into our analysis of the experimental problem made it much more tractable.

Viewed from the side and from the top, the initial state and the final (adjusted) state of the system look like this:

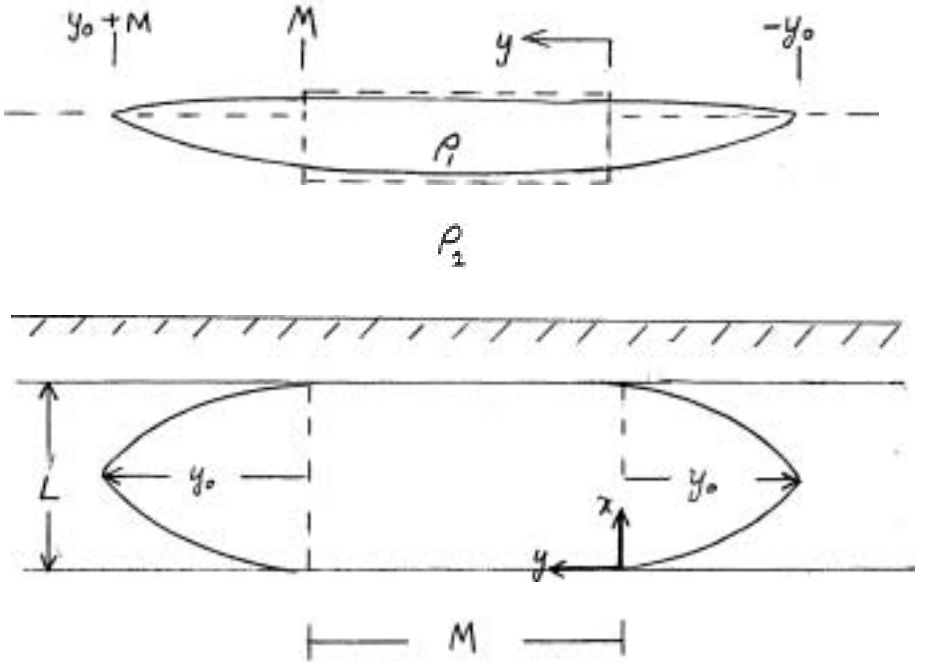

As in the previous problem, the initial and final depths of the top layer are H and h, respectively. The bottom layer starts with depths H_2 for $0 \le y \le M$ and H_1 for other y. Its final depth is given by h_2, with h_1 being the adjusted height of the free surface.

In this problem, conservation of potential vorticity of the upper layer implies that

$$\frac{f + \frac{\partial v_1}{\partial x} - \frac{\partial u_1}{\partial y}}{h} = \frac{f}{H}$$

Use of the geostrophic formulas for u_1 and V, then gives

$$h_{1xx} + h_{1yy} - \frac{1}{\lambda^2}(h - H) = 0. \qquad (9)$$

We now make the assumption of a motionless bottom, and set $u_2 = 0$ in the geostrophic relation for the bottom layer

$$u_2 = -\frac{g}{f}(a h_{1y} + b h_{2y})$$

Therefore

$$a h_{1y} + b h_{2y} = 0$$

$h_2 = h_1 -$ implies $a h_{1y} + b h_{1y} - b h_y = 0$

$h_{1y} = b h_y$.

Similarly, $v_2 = 0$ leads to

$$h_{1x} = b h_x .$$

Now h_1 can be eliminated from (9) to give:

$$b(h_{xx} + h_{yy}) - \frac{1}{\lambda^2}(h - H) = 0 \qquad (10)$$

or

$$h_{xx} + h_{yy} - \frac{1}{\lambda'^2}(h - H) = 0,$$

where $\lambda' = \sqrt{\frac{g' H}{f}}$.

Choosing the solution to (10) which is symmetric about $x = \frac{L}{2}$ and about $y = \frac{M}{2}$, and using the boundary conditions that $h = 0$ at $(0, \frac{M}{2})$ and $(\frac{L}{2}, -y_0)$ gives the following solution for h:

$$= \left(\frac{c_1 - 1}{1 - c_1 c_2}\right)\cosh\left(\frac{x - \frac{L}{2}}{\lambda'}\right) + \left(\frac{c_2 - 1}{1 - c_1 c_2}\right)\cosh\left(\frac{y - \frac{M}{2}}{\lambda'}\right)\Bigg] ,$$

with

$$c_1 = \cosh\left(\frac{y_0 + \frac{M}{2}}{\lambda'}\right), \quad c_2 = \cosh\frac{L}{2\lambda'} .$$

This expression still contains the unknown y_0 . This could be determined from conservation of mass:

$$H\left(\frac{L}{2}\right)\left(\frac{M}{2}\right) = \int_0^{L/2} \int_{y = y(x) \text{ on } h = 0}^{M/2} h \, dy \, dx ,$$

requiring numerical integration. However, predictions for y_0 can rather easily be made for limiting values of λ' :

$\lambda' \gg L$

Solving far h at $(\frac{L}{2}, \frac{M}{2})$ and setting $\cosh\frac{L}{2\lambda'} = 1 + \frac{L^2}{8\lambda'^2}$ gives:

$$h\left(\frac{L}{2}, \frac{M}{2}\right) = \frac{L^2}{8\lambda'^2} H .$$

This is the maximum depth of the fluid. A lower bound for y_0 can be obtained by using conservation of mass:

$$H\left(\frac{L}{2}\right)\left(\frac{M}{2}\right) = \frac{L^2}{8\lambda'^2} H\left(\frac{L}{2}\right)\left(\frac{M}{2} + y_0\right)$$

$$4LM = \frac{L^3}{\lambda'^2}\left(\frac{M}{2} + y_0\right)$$

$$y_0 = M\left(\frac{4\lambda'^2}{L^2} - \frac{1}{2}\right) \approx \frac{4M\lambda'^2}{L^2} \qquad (11)$$

$\therefore y_0 \gg M, \; y_0 \gg \lambda'$ (if $M \sim L$).

Equation (11) actually gives a lower bound because the depth is less than $\frac{L^2}{8\lambda'^2} H$ everywhere but at $(\frac{L}{2}, \frac{M}{2})$, and because the upper layer does not extend out to $-y_0$ uniformly across the channel.

This shows that for very large λ', the adjusted upper layer should extend far out from where it was originally confined.

$\lambda' \ll L, M$

In this case, we make use of the approximations

$$c_1 = \tfrac{1}{2} e^{\frac{y_0 + \frac{M}{2}}{\lambda'}}, \quad c_2 = \tfrac{1}{2} e^{\frac{L}{2\lambda'}},$$

and find the following expression for h near $(\frac{L}{2}, 0)$:

$$h = H(1 - e^{\frac{y+y_0}{\lambda'}}).$$

The x dependence has dropped out, and the solution is the same as that which we have found (but not presented in this report) for the one-dimensional (no sidewalls), motionless bottom problem. We have also found that in this problem

$$y_0 = \bar{A}',$$

Thus for very small λ', the upper layer should almost remain confined to the starting region.

With this analysis behind us, we can now turn to a discussion of the actual experimental results.

Experiments

The experiments were done in a channel 160 cm long by 8.0 cm wide ($L = 8.0$cm). The barriers which at first confined the upper layer fluid to the central region were spaced 16.9 cm apart ($M = 16.9$ cm).

The channel was mounted on the large 2-meter diameter rotating table at the Woods Hole Oceanographic Institution. This apparatus was well-suited for taking photographs, for which we used a 16 mm movie camera.

For each experiment, we first inserted the barriers astride the center of the trough, then poured in salty water of known density to a depth of 11 cm ($H_1 = 11$ cm). The table was spun up to the desired rotation rate Ω. ($f = 2\Omega$). At this point fresh, dyed water was carefully siphoned atop the denser water in the center region, until the top layer reached a depth H. When all was ready, the camera was turned on and then the barriers were raised.

In every case, the dyed fluid at first moved rapidly away from the center region, and then slowed down considerably. The distance of spreading varied with λ' as expected. (Distance down the channel was measured by strips of black tape, each 10 cm long and spaced 10 cm apart.)

Geostrophic adjustment is well illustrated by the frames selected from experiments 2 and 3. In both cases, the flow of the dyed fluid had just slowed nearly to a halt. In the first, the main body of the fluid extends about 5 cm out from where it was originally confined, and $h' = 3$ cm. In the second, most of the dyed water is within roughly 11 cm of the starting region, with $\lambda' = 7$ cm. Both pictures show a non-geostrophic flow down the channel in jets hugging the wall to their right.

Experiment #4 had $\lambda' = 8.2$, which was nearly the same as in #3. However, we have selected from the #4 film a frame which was taken 26 sec further into the experiment than the frame above it. Thus the flow is further down the channel, probably due to non-geostrophic, viscous effects. (The flow pattern is asymmetric because the right barrier was raised just before the left one.) Also, the upper layer water was more darkly dyed in #4 than it was in #3 (and in #2), so the appearance of the jets is greatly enhanced.

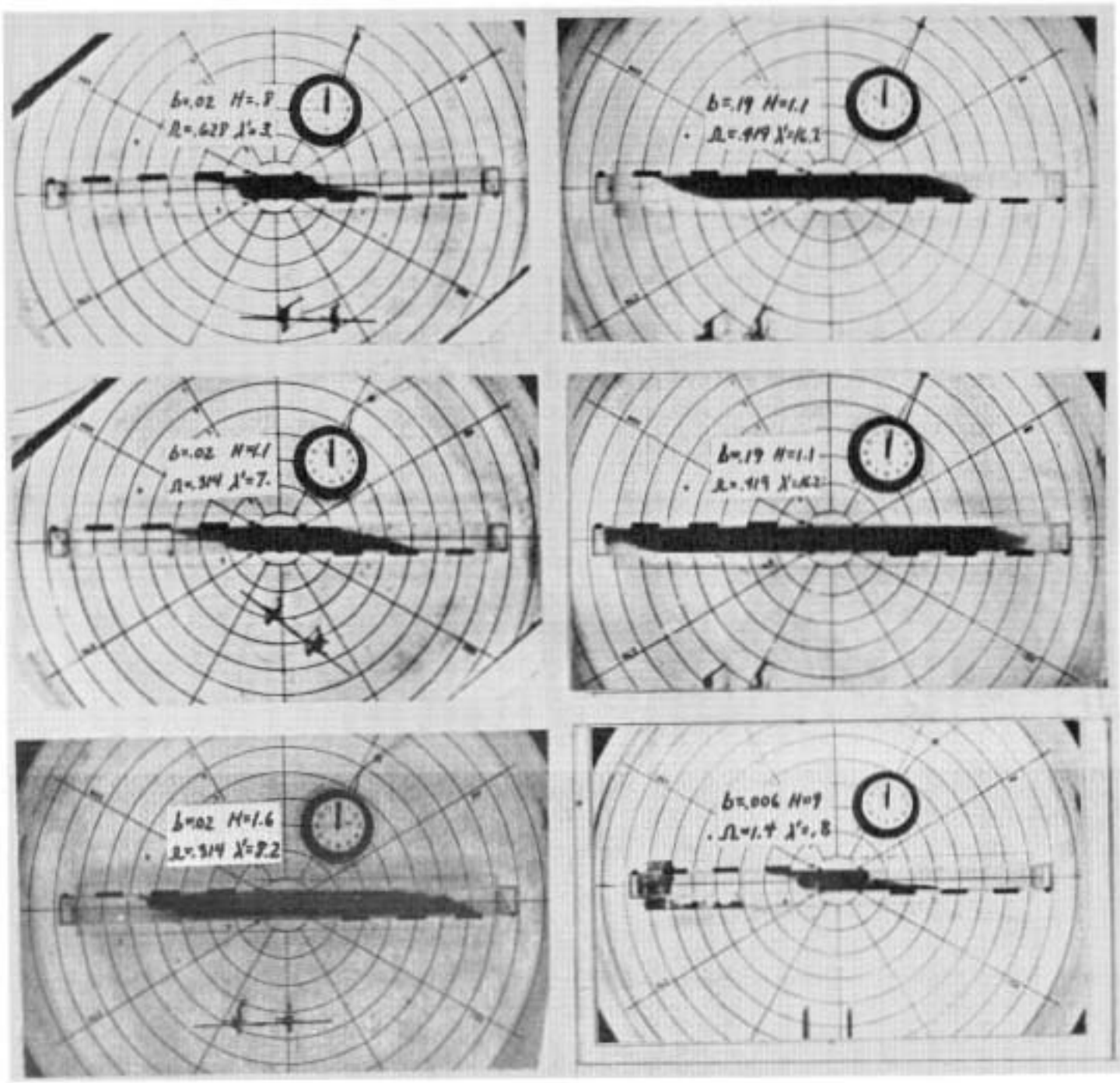

Left **fog:** Experiment #2, 12 sec after barriers raised. Left center: #3, 17 sec. Left bottom: #4, 43 sec. Right top: #5, 17 sec. Right Center: #8, 116 sec. Right bottom: #6, 24 sec.

In the #4 picture we see an instability breaking off from the left of the jet in the right side of the channel. These are the instabilities discussed by Jones (1975) elsewhere in this volume. Unfortunately, our main series of experiments did not demonstrate such motions very well, but a preliminary, unphotographed experiment very clearly showed a succession of eddies breaking away from a jet.

The first frame from experiment #8 shows the flow after it had just slowed down. Again we see that most of the dyed fluid slows when it is approximately λ' away from the starting region. The second photograph was taken nearly 100 sec later, and illustrates how the flow continues to slowly move along as it is influenced by viscosity. This displays a rather prominent instability breaking away from the jet on the right.

Finally, we will discuss the #6 photograph. In our experiments with very small λ', ageostrophic processes became apparent much sooner than when λ' was on the order of L or larger. In this last picture, a large circular eddy in the left part of the trough has nearly completed its flow across the channel, Its counterpart on the right side has already done so. (The unfortunate asymmetry is again, apparent.) Thus the geostrophic adjustment is quickly swamped by viscosity when λ is very small.

Conclusion and Future Work

The time-independent and inviscid theory of geostrophic adjustment presented in this report was at least qualitatively verified by the experiments. There is now a basis for future work in this area, both theoretically and in the laboratory. The following are some suggestions:

1) Apply the same concept of ideal geostrophic adjustment to other problems. This will probably involve use of a computer.

2) Extend the theory to include transient and/or viscous effects.

3) Perform more extensive and more careful experiments similar to those described above, with the goal being the investigation of non-geostrophic processes.

The author would like to thank Dr. George Veronis for his invaluable guidance in this project. I am also grateful to Drs. Melvin Stern and John Whitehead for several helpful suggestions, and to Mr. Robert Frazel for much technical assistance.

References

Jones, S., 1975 On the Stability of a Boundary Jet, G.F.D. Woods Hole Oceanog.Inst.

Rossby, C.G. 1938 On the Mutual Adjustment of Pressure and Velocity Distributions in Certain Simple Current Systems. J.Mar.Res. 1: 239.

Veronis, G. 1956 Partition of Energy between Geostrophic and Non-geostrophic Oceanic Motions. Deep Sea Res., 3: 157-175.

Veronis, G. and H. Stommel 1956 The Action of Variable Wind Stresses on a Stratified Ocean. J.Mar.Res., 15: 43-95.

A PROPOSED LABORATORY STUDY OF PLANETARY VORTICES

Kirk S. Hansen

Introduction

This report is concerned with the feasability of generating vortex motions in a rotating fluid of variable depth. Such motions are called "planetary vortices" because the depth variation introduces a β-effect analogous to that introduced by variable Coriolis parameter on the β-plane.

Interest in the laboratory study of planetary vortices evolved from a geophysical dynamics lecture by Alan Newell (1975) on nonlinear wave packets. Consider a packet of slightly dispersive, slightly nonlinear waves grouped around wave number K. The normal-mode solutions to this problem are of two types. One set of solutions decay exponentially, as in the linear case. In addition, there are permanent waves called 'solitons'. Two such waves may collide with each other and interact in a nonlinear fashion, but once the collision is completed, each soliton retains its initial identity almost exactly. This ability to retain initial identities is the distinguishing feature of solitons from other nonlinear wave types.

At the conclusion of Newell's lecture, the question was raised as to what extent 'modons' behave like solitons. (A modon is a particular type of barotropic vortex on the β-plane. Modons have been studied by Stern (1974, 1975) in connection with their relation to mid-ocean eddies.) Do modons also retain their identities after interacting with one another or with other types of vortices? Is the governing differential equation for modons amenable to the methods of solution described by Newell? The results of this discussion were inconclusive, and it was suggested that a laboratory study of modons might provide some insight to the above questions.

As a first step toward realizing the interaction of a modon with other vortex motions in the laboratory, I will investigate the possibility of generating a single modon of known characteristics.

Theoretical description of modops

The vorticity balance maintained by modons is between the nonlinear and Coriolis terms:

$$\vec{V} \cdot \nabla \zeta + \beta V = 0 \qquad (1)$$

The velocity vector $\vec{V} = (U, V)$ where U is in the x-direction (eastward) and V is in the y-direction (northward). The two-dimensional gradient operator is represented by ∇; $\zeta = \partial V/\partial x - \partial U/\partial y$ is the vertical component of vorticity; and the Coriolis parameter f is taken as a linear function of y on the β-plane ($f = f_0 + \beta y$).

A modon is defined in part as an isolated barotropic disturbance in equilibrium on the β-plane. Equilibrium requires the modon to have a dipole structure, with a cyclonic vortex to the north and an anticyclonic vortex to the south (Fig.1). Isolation requires the pressure perturbation and the velocity to vanish with increasing distance r from the center of the disturbance. At large r, therefore, the first term in (1) is small to order V^2 while the second term is small only to order V. The vorticity constraint cannot then be satisfied unless the far-field vorticity equals zero. This requires a discontinuous change in ζ at some distance R, where $\zeta = 0$ for all $r > R$.

A solution to the modon problem may be obtained following Stern (1975). The conservation of absolute vorticity serves as a starting point:

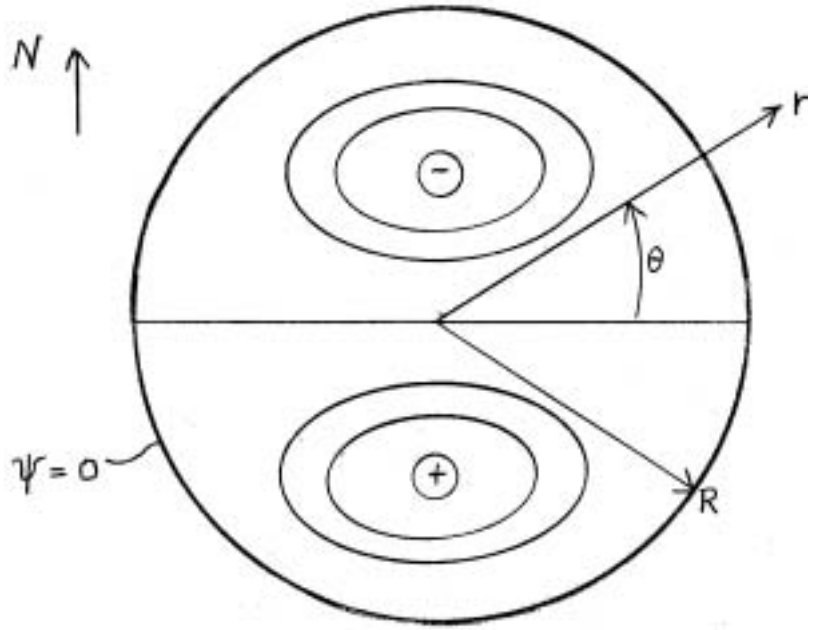

Fig.1 Schematic representation of a modon (Stern, 1975).

$$\frac{d}{dt}(\zeta + f) = 0 \tag{2}$$

For a steady state, and with $f = f_0 + \beta y$ Eq.(2) becomes:

$$\vec{\nabla} \cdot \nabla(\zeta + \beta y) = 0 \tag{3}$$

Since $\nabla \cdot \vec{V} = 0$ on the β-plane, the velocity may be written in terms of a stream function as $U = -\partial\psi/\partial y$ and $V = \partial\psi/\partial x$. The vorticity is then $\zeta = \nabla^2\psi$, and Eq.(3) may be written as

$$\vec{\nabla} \cdot \nabla(\nabla^2\psi + \beta y) = 0 \tag{4}$$

which is equivalent to (1). The quantity in parentheses must be constant along a given streamline, or equivalently, equal to some function of ψ only.

$$\nabla^2\psi + \beta y = F(\psi) \tag{5}$$

Boundary conditions are a free streamline $\psi = 0$ across which the vorticity change is discontinuous. Choose

$$\psi(R, \theta) = 0 \tag{6}$$

where (r, θ) are polar coordinates defined in Fig.1 and R is the radius of the streamline. Also, the isobaric boundary condition requires uniform pressure for $r \geq R$. Application of Bernoulli's equation along the free streamline $\psi = 0$ indicates that $|\vec{V}|^2$ is uniform on the streamline. Hence $(\nabla\psi)^2$ is uniform on $r = R$ and

$$\frac{\partial^2\psi(R, \theta)}{\partial r\, \partial \theta} = 0, \tag{7}$$

The problem is to pick $F(\psi)$ in such a manner that (5) can be solved subject to boundary conditions (6) and (7). Stern chose $F(\psi) = -\lambda\psi$, where $\lambda > 0$. The governing differential equation is then

$$\nabla^2 \psi + \lambda \psi = -\beta y \tag{8}$$

A particular solution is $\psi_p = -\frac{\beta y}{\lambda} = -\frac{\beta r \sin\theta}{\lambda}$. The homogeneous solution for $\nabla^2 \psi_h + \lambda \psi_h = 0$ that satisfies boundary condition (6) can be written in terms of $J_1(r\lambda^{1/2})$, where J_1 is the Bessel function of the first kind and order one. The total solution $\psi = \psi_p + \psi_h$ is given by

$$\psi = -\frac{\beta \sin\theta}{\lambda}\left[r - R\frac{J_1(r\lambda^{1/2})}{J_1(R\lambda^{1/2})}\right] \tag{9}$$

Further, boundary condition (7) requires

$$J_2(R\lambda^{1/2}) = 0 \tag{10}$$

Substitution of (9) into (8), with $\nabla^2\psi = \zeta$, gives

$$\zeta = -\beta R \sin\theta \frac{J_1(r\lambda^{1/2})}{J_1(R\lambda^{1/2})} \tag{11}$$

for any value of $R\lambda^{1/2}$ satisfying (10). The root-mean-square vorticity provided by (11) is

$$\zeta_{rms} = \frac{\beta R}{\sqrt{2}} \tag{12}$$

More complicated functions $F(\psi)$ may be chosen, but the particular $F(\psi)$ illustrated above gives the minimum value of ζ_{rms} for all possible solutions within the circular region of area πR^2. The final defining property of a modon is that its rms vorticity be the minimum possible value for a given class of solutions. Thus the vorticity distribution (11) is a unique modon solution to Eqs. (5) - (7). Different modons may be generated, however, by choosing other shapes for the free streamline $\psi = 0$ (that is, by choosing different boundary conditions (6) and (7)).

Modons are likely unstable to small perturbations so that the $\frac{\partial \zeta}{\partial t}$ term in the vorticity equation becomes significant given enough time. For this reason modons probably do not exist in the actual oceans. But their idealized vortex motion may prove to be useful in modeling (in a statistical sense) some features of the more complicated vortex motions observed in the ocean. For example, if ζ_{rms} can be derived from observed data, then (12) can be used to estimate the mean eddy radius.

Plan of attack

A pilot experiment was conducted in an attempt to generate a positive and negative vortex pair resembling a modon in the laboratory. The experimental setup is shown schematically in Fig.2. A rotating tank with flat bottom, but with depth variation due to the parabolic shape of the free surface, was used. Water was the working fluid. A pump was attached to the rotating table, with the source and sink inserted into the fluid along a radial direction from the center of the tank as indicated. The plan was to turn on the pump for a moment, allowing a positive (anticyclonic) vortex to form around the source and a negative (cyclonic) vortex to form around the sink. The pump could then be turned off, allowing the study of free vortices on a "β-plane". The flow pattern was observed using a potassium permanganate dye.

The results of this test were erratic, Often only one of the expected vortices would form. In other cases, a vortex pair would form initially but dissipate almost immediately. The difficulties with this experiment indicated that a simpler case, for which the flow pattern can be accurately predicted, should be examined first.

The next section of this paper is a discussion of potential flow in a rotating fluid of constant depth. Solutions have been obtained for both the interior flow and

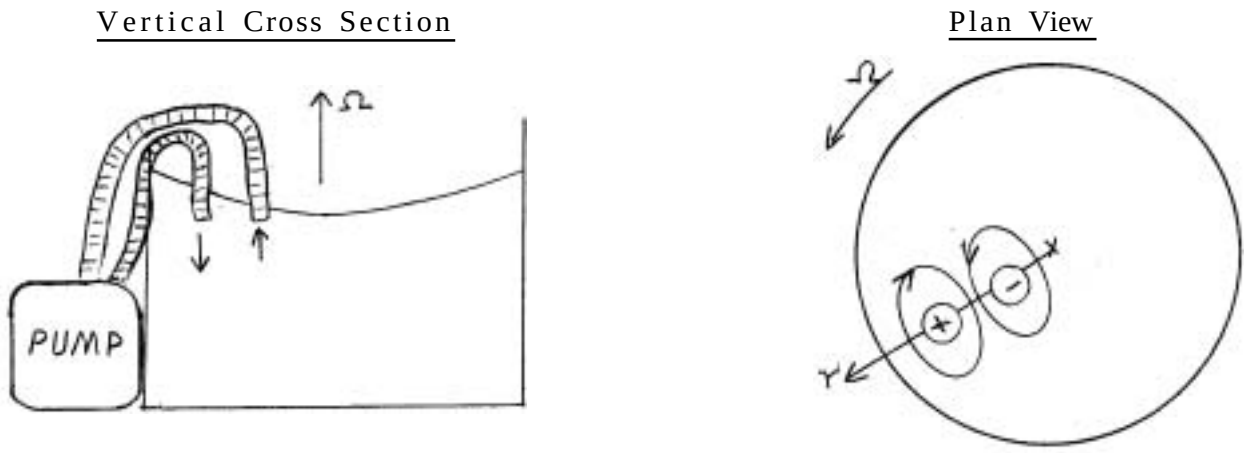

Fig.2 Pilot experiment for generating modons.

the Ekman boundary layer transport. The remaining sections consider the progressively more complicated cases of vortex motion in general in a variable-depth fluid and, finally, the specific case of modons in the laboratory.

Rigid top

Consider a rotating fluid of constant depth bounded by infinite planes on the top and bottom. A circular source and sink each of radius a are separated by a distance R as measured from their centers (Fig.3). The theory of source-sink flows

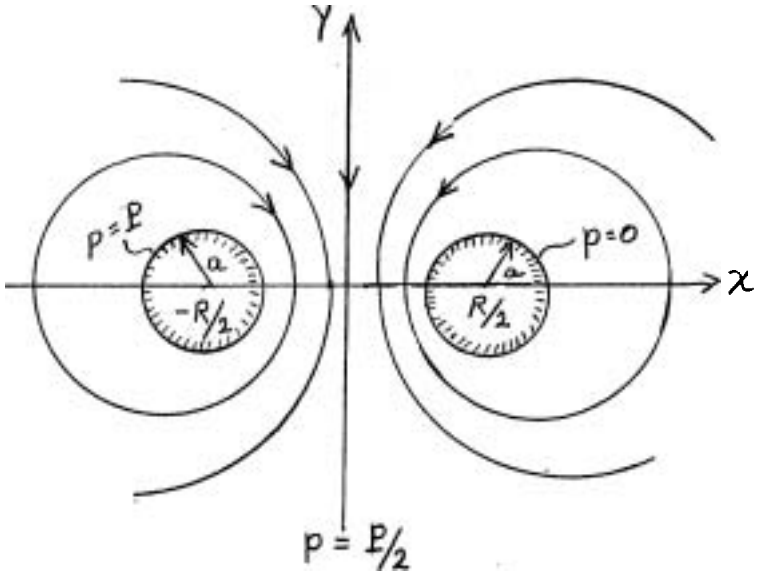

Fig.3 Isobars (or streamlines) for interior flow of source-sink experiment.

such as this has been described by Greenspan (1968). The column of fluid beneath the source is a high-pressure region, and the column beneath the sink is a low-pressure area. For the appropriate parameter range, the interior flow will be geostrophic with a positive vortex around the source and a negative vortex around the sink. Since the streamlines form closed contours around the high- and low-pressure centers, the transport of fluid from source to sink cannot occur through the interior but must be confined to the top and bottom Ekman boundary layers.

The geostrophic relations for the interior flow are

$$V_g = \frac{1}{\rho f}\frac{\partial p}{\partial x} \qquad U_g = -\frac{1}{\rho f}\frac{\partial p}{\partial y} \tag{13 a,b}$$

where ρ is the fluid density and p is the pressure. The coriolis parameter f is a constant equal to 2Ω, where Ω is the rate of rotation, and (U_g, V_g) are in the (x,y) directions as shown in Fig.3.

Taking $\frac{\partial}{\partial n}$ $\frac{\partial(13b)}{\partial y}$ gives

$$\zeta = \frac{1}{\rho f}\nabla^2 p \tag{14}$$

For steady, incompressible, and two-dimensional flow the continuity equation is

$$\nabla \cdot \vec{V} = 0 \tag{15}$$

and for irrotational flow

$$\nabla \times \vec{V} = 0 \tag{16}$$

Equations (15) and (16) define a problem in potential flow, and (16) substituted into (14) yields the relevant differential equation

$$\nabla^2 p = 0 \tag{17}$$

with boundary conditions

$$p = P \text{ at the source and } p = 0 \text{ at the sink.} \tag{18}$$

The solution to (17) and (18) may be deduced in the following manner. For a point source located at the origin,, the pressure is proportional to $\ln r$

$$\text{or } p = -K \ln (x^2+y^2)^{1/2} + C.$$

For a point source and sink of equal and opposite strengths located at $(\mp r_o, 0)$, the pressure is given by

$$p = -K \ln \left[\frac{(x+r_o)^2+y^2}{(x-r_o)^2+y^2}\right] + C \tag{19}$$

The isobars are circles with centers at $\left(-F\left(\frac{p-c}{K}\right)r_o, 0\right)$ and radii of $r_o\sqrt{F^2\left(\frac{p-c}{K}\right)-1}$

where

$$F\left(\frac{p-c}{K}\right) = \frac{\exp\left(\frac{p-c}{K}\right)+1}{\exp\left(\frac{p-c}{K}\right)-1}.$$

Equation (19) may also be used for the case of circular source and sink of finite radii by choosing K and r_o so that the isobaric contours with centers at $(\mp R/2, 0)$ have radii = a and pressure = $\pm P/2 + C$.

$$\frac{R}{2} = -F\left(\frac{P}{2K}\right)r_o \tag{20}$$

$$a = r_o\sqrt{F^2\left(\frac{P}{2K}\right)-1} \tag{21}$$

Solving (20) and (21) for r_o and K results in

$$r_o = \frac{\sqrt{R^2-4a^2}}{2} \tag{22}$$

$$K = \frac{P}{2\ln\left(\frac{R+\sqrt{R^2-4a^2}}{R-\sqrt{R^2-4a^2}}\right)} \tag{23}$$

Finally, boundary conditions (18) are satisfied by picking the constant C equal to $P/2$ so that

$$p = -K \ln \left[\frac{(x+r_o)^2 + y^2}{(x-r_o)^2 + y^2} \right] + P/2 \tag{24}$$

where r_o and K are defined by (22) and (23).

The flow rate Q from source to sink may be related to the pressure difference P as follows. Consider the Ekman boundary layer equations

$$-fv = -\frac{1}{\rho} \frac{\partial p}{\partial x} + \nu \frac{\partial^2 u}{\partial z^2} \tag{25}$$

$$fu = -\frac{1}{\rho} \frac{\partial p}{\partial y} + \nu \frac{\partial^2 v}{\partial z^2} \tag{26}$$

It is convenient for this problem to work along the axis of symmetry $x = 0$ so that $\partial p/\partial y = 0$. The z-axis points vertically upward with $z = 0$ at the bottom boundary. Boundary conditions are:

$$(u, v) = (0, V_g) \quad \text{at} \quad z = \infty \tag{27}$$

$$(u, v) = (0, 0) \quad \text{at} \quad z = 0 \tag{28}$$

The addition of (25) and (26) $\times i$ yields

$$\nu \frac{\partial^2 V}{\partial z^2} + \frac{fV}{i} = \frac{1}{\rho} \frac{\partial p}{\partial x} \tag{29}$$

where $V = u + iv$. The solution of (29) satisfying boundary conditions (27) and (28) is

$$V = iV_g - iV_g e^{-(1+i)z/\delta} \tag{30}$$

where $\delta = \sqrt{\frac{2\nu}{f}}$ is the boundary layer thickness.

Only the x-component of flow contribures to the transport from source to sink, as the y-component is parallel to the geostrophic contour. The local transport T is therefore equal to $\int_0^\infty u\,dz$, or $\int_0^\infty \mathrm{Re}\, V\,dz$ Evaluation using V from (30) gives

$$T = -V_g \frac{\delta}{2} \tag{31}$$

The total flow rate Q equals $2\int_{-\infty}^{\infty} T\,dy$, where the factor 2 is due to the presence of both top and bottom boundary layers. From (31)

$$Q = -\frac{\delta}{\rho f} \int_{-\infty}^{\infty} \left(\frac{\partial p}{\partial x} \right)_{x=0} dy \tag{32}$$

and using the expression for p given by (24), $Q = \frac{4\pi K \delta}{\rho f}$. This may be written as

$$Q = P/R \tag{33}$$

where R is the total resistance to the flow encountered between source and sink:

$$R = \frac{\rho f}{2\pi\delta} \ln \left(\frac{R + \sqrt{R^2 - 4a^2}}{R - \sqrt{R^2 - 4a^2}} \right) \tag{34}$$

A convenient means of measuring P and Q in the laboratory, without sophis-

ticated instrumentation, is the simple spin-down experiment illustrated in Fig.4.

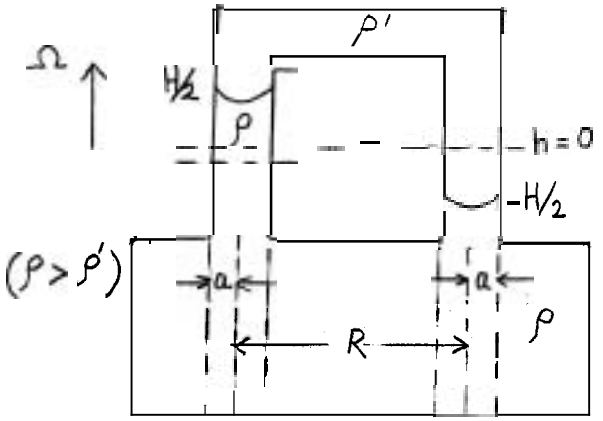

Fig.4 Spin-down experiment with reduced gravity.

Consider first the case where the fluid in the tank is water and the "primed" fluid is air ($\rho >> \rho'$). Suppose there exists a pressure head H at time $t = 0$, say, so that $P = \rho g H$. As fluid is transported from source to sink, the flow pattern discussed previously is established, and the head is related to the flow rate by (33):

$$H = \frac{QR}{\rho g} \tag{35}$$

One may in principle make H large enough to easily measure provided large flow rates can be tolerated without introducing large Rossby numbers. Let the Rossby number be given by

$$\epsilon = \frac{1}{fa}\left(\frac{Q}{2\pi a \delta}\right) \tag{36}$$

where the quantity in parentheses is a typical velocity. With $\nu = 10^{-2}\text{cm}^2\text{sec}^{-1}$, $f = 1\ \text{sec}^{-1}$, $R = 20$ cm, $a = 1$ cm, and $Q = 1\ \text{cm}^3\text{sec}^{-1}$, the Rossby number is order one, which is probably the largest tolerable value without drastically altering the predicted flow pattern. Use of the same numerical values in (35) results in $H \approx 10^{-2}$cm, which is too small to be of practical value in the laboratory.

The value of H may be magnified, however, by using a reduced gravity effect. Let the rotating tank contain salty water, and let the primed fluid be fresh water. For this case $P = \rho g^* H$ and

$$H = \frac{QR}{\rho g^*} \tag{37}$$

where the reduced gravity $g^* = \left(\frac{\rho - \rho'}{\rho}\right) g$. If $\rho = 1.001\,\rho'$, then $g^* = 10^3 g$ and H is of order 10 cm, which is a convenient value.

The only remaining requirement is that the appropriate time constant τ for this experiment be large compared with the spin-up time τ_{sp}. Let the pressure head at time t be represented by $2h$ so that

$$2h = \frac{QR}{\rho g^*} \tag{38}$$

The time-dependent flow rate is given by

$$Q = -\pi a^2 \, dh/dt \tag{39}$$

Substitution of (38) into (39) and integration as $-\int_{H/2}^{h} dh/h = \int_0^t \frac{2\rho g^* h}{R^2 \pi a^2}\, dt$ yields

$$h = H/2 \exp -t/\tau \tag{40}$$

where τ is the e-folding time constant and

$$\tau = \frac{R \pi a^2}{2\rho g^*} \tag{41}$$

For τ sufficiently large, P (or, equivalently h) can be related to Q merely by recording the value of h at two different times. Equation (39), with dh/dt approx-

imated by $\Delta h/\Delta t$, may then be used to evaluate Q. The corresponding value of h may be taken as $\frac{h(t_1)+h(t_2)}{2}$. These experimental values of Q and h can be checked for theoretical agreement through (38). With $g^* = 10^{-3} g$, and other parameters as before, the value of τ is about 10 sec. The spin-up time is $\tau_{sp} = \sqrt{\frac{D^2}{\nu}}$, where D is the depth of the fluid. For a depth of 10 cm, $\tau_{sp} \approx 2\text{min} \gg \tau$. Thus the proposed spin-down experiment, even with reduced gravity, fails to satisfy the requirement of large τ.

Generation of a positive and negative vortex pair using a source-sink flow therefore requires a strictly steady state to be maintained by continuously adding fluid at the source and withdrawing fluid from the sink, Experiments of this nature were performed by Buzyna (1967).

The working fluid used by Buzyna was water. The experimental geometry was shown in Fig.3, with the origin of the coordinate axes located at the center of the rotating tank, R = 14.5 cm, and a = 0.65 cm. The flow rates considered by Buzyna were 0.1 to 0.3 $cm^3 sec^{-1}$, and f was varied from 0.3 to 1.4 sec^{-1}. Evaluation of the Rossby number using (36) indicates that Buzyna was working with ϵ of order 0.1 to one.

The qualitative features of the interior flow agreed with the streamline pattern indicated in Fig.3, and the transport from source to sink was largely confined to the Ekman boundary layers. Buzyna made no attempt, however, to measure the pressure difference P as a function of Q. The fact that Buzyna was able to reproduce the expected flow pattern, even for large Rossby numbers, is probably due to the potential character of the problem. For potential flow, ζ is identically zero and the $\epsilon(\vec{\nabla} \cdot \nabla \zeta)$ term drops out of the vorticity equation independently of the value chosen for ϵ.

Details of the interior and boundary layer flows were more complicated than predicted by theory, however. The column of fluid beneath the source became larger with time and did not always remain located directly beneath the source. Below the sink region, fluid moved from the bottom toward the surface in a spiral pattern rather than in a simple column. In the Ekman layers, there was a certain amount of recirculation and mixing near the source. At the higher flow rates, instabilities were observed in the boundary layer flow.

Free-surface experiments

For rotating fluids with a rigid, flat bottom and a free upper surface, depth increases in the radial direction as shown in Fig.5.

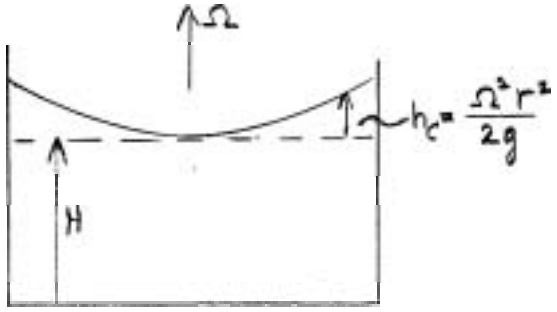

Fig.5 Shape of free surface for fluid in a rotating tank

The total depth is $h = H + h_c$. For a steady state, and ignoring lateral friction, the vorticity equation is $\vec{v} \cdot \nabla \zeta + f(\nabla \cdot \vec{v}) = 0$. ecall that for the rigid-top case $\nabla \cdot \vec{v} = 0$ but with the free surface $\nabla \cdot \vec{v} = -\frac{\partial w}{\partial z}$ from the continuity equation and

$$\vec{v} \cdot \nabla \zeta = f \frac{\partial w}{\partial z} \qquad (42)$$

As a consequence of shallow-water theory, w varies linearly with depth and

$$\partial w/\partial z = \Delta w/\Delta z :$$

$$\frac{\partial w}{\partial z} = \frac{\vec{v}\cdot\nabla h - W_E}{H} \tag{43}$$

Here H has been assumed large with respect to h_c so that $h \simeq H$, and W_E is the Ekman suction velocity. Substituting (43) into (42) and nondimensionalizing all of the variable yields

$$\epsilon(\vec{v}\cdot\nabla\zeta) = \beta\vec{v}\cdot\nabla h - E^{1/2}\zeta \tag{44}$$

where ϵ (as before) is the Rossby number, E is the Ekman number, and β is a scale factor for the β-effect. Higher-order terms in ϵ and E have been neglected.

Buzyna (1967) also conducted source-sink experiments for the free-surface case. All experiments were performed with the same value of Ω, and the depth was varied from a few cm up to about 20 cm. For shallow depths, the spatial variation in h was large and the ensuing flow pattern was very complicated. For large depths, the relative variation in depth from center to edge of tank was small, and the flow pattern was qualitatively similar to the constant-depth experiments described in the previous section. The only significant difference was a shift in the streamline pattern (Fig.6) so that the line of symmetry was no longer orthogonal to the line joining source and sink.

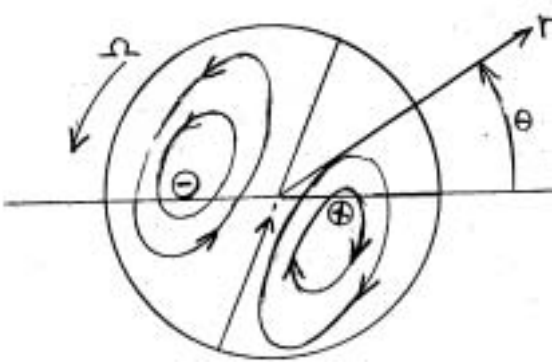

Fig.6 Streamlines for interior flow in free-surface case (Buzyna, 1967).

Since this result was not observed in any of the experiments with the rigid top, it is likely due to the β-effect. If $\epsilon \ll E^{1/2}$, then by (44) β must scale as $E^{1/2}$ to balance the vorticity constraint. Evaluating this vorticity balance in dimensional quantities, $\vec{v}\cdot\nabla h - W_E = 0$ or, ignoring adjustments in the free-surface elevation due to the geostrophic flow

$$U\frac{\partial h}{\partial r} - \frac{\delta}{2}\zeta = 0 \tag{45}$$

where (U,V) are in the (r,θ) directions.

With $\zeta = \frac{1}{\rho f}\nabla^2 P$ and $U = -\frac{1}{\rho f r}\frac{\partial P}{\partial\theta}$ Eq.(45) becomes

$$\nabla^2 p + \alpha\frac{\partial p}{\partial\theta} = 0 \tag{46}$$

where $\alpha = \frac{2\Omega^2}{g\delta}$ is a positive constant. It would be useful to solve (46) subject to the boundary conditions.

$$p = 0 \text{ at the sink and } p = P \text{ at the source} \tag{47}$$

and compare the result with Buzyna's experiment. Equations (46) and (47) have not been solved, but their qualitative effect may be understood from the following thermal analogy.

Consider a rotating fluid moving past cold and hot heat sources fixed in the inertial frame of reference (Fig.7). The thermal diffusion equation is

$$\frac{dT}{dt} = K\nabla^2 T,$$

and for a steady state

$$\vec{v}\cdot\nabla T = K\nabla^2 T.$$

For the experiment presented in Fig.7

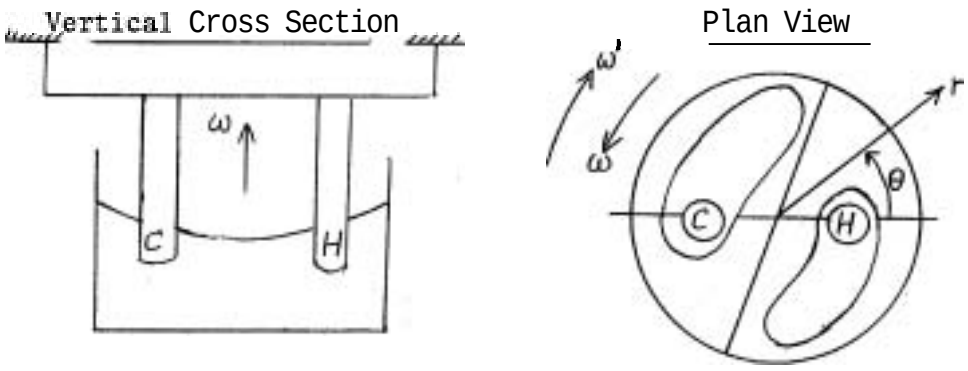

Fig.7 Thermal wake in a rotating fluid,

this reduces to

$$\nabla^2 T - \frac{\omega}{K}\frac{\partial T}{\partial \theta} = 0 \qquad (48)$$

With $\omega = -\omega'$ Eq.(48) may be written as

$$\nabla^2 T + \frac{\omega'}{K}\frac{\partial T}{\partial \theta} = 0 \qquad (49)$$

where ω'/K is a positive constant. Equation (49) has the analogous form as (46). With rotation in the ω'-direction, the thermal wake will cause the isotherms to orient themselves as shown in Fig.7. This is identical to the orientation of the isobars in Buzyna's experiment (Fig.6).

Although the vorticity balance represented by (45) apparently explains the experimental result in a qualitative sense, there is reason to believe that it may not do so in derail. This is because the derivation of (45) assumes $\epsilon << E^{1/2}$ whereas the parameter range explored by Buzyna was $\epsilon > E^{1/2}$.

Modons in the laboratory

Although the modons studied analytically by Stern (1974, 1975) were free vortices, it may be possible to generate a modon in the laboratory by using a continuous source-sink flow. Imagine the source and sink to be located in just the right place and to have the required shapes so that their outer edges correspond to isobars of a modon (Fig. 8).

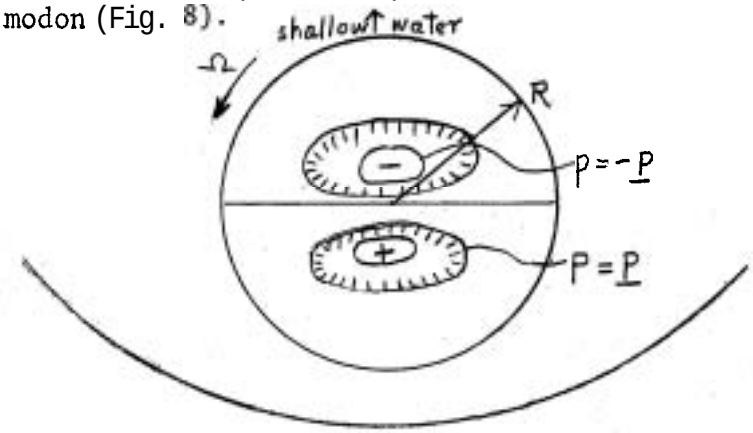

Fig.8 A modon in a rotating tank.

The fluid located outside the immediate vicinity of the sink or source does not know whether it is part of a free vortex or if it is being forced by a source-sink flow. So if the fluid beneath the source and sink is neglected, a vortex pair forced by the above flow should behave like a modon.

Also, in the laboratory there will be no free streamline $\Psi = 0$. This does not matter, as long as the viscous term in (44) is able to balance the far-field velocity. For a modon, scale β as $\epsilon \gg E^{1/2}$. The nondimensional vorticity equation is then

$$\epsilon(\vec{v}\cdot\nabla\zeta - \vec{v}\cdot\nabla h) = -E^{1/2}\zeta \qquad (50)$$

with boundary conditions

$$p = P \text{ at the source and } p = -P \text{ at the sink.} \qquad (51)$$

Near the center of the modon, the principal balance is on the left-hand side (LHS) of Eq. 50. For $r \gg R$, the first term on the LHS becomes small to order V^2 and the second term is small only to order V. The balance for $r > R$ is therefore between the β and viscous terms.

Solutions to (50) for boundary conditions (51) may or may not exist, and the possibility of their existence needs to be more thoroughly examined before attempting to generate a modon in the laboratory. Niiler (1966) has solved (51) in his study of wind-driven ocean circulation, but for different boundary conditions. If solutions do exist for the laboratory problem, then the source and sink should be arranged along the radial direction (as in Fig.2), and with the sink closest to the center. This is because shallow water in the laboratory models is northward in direction on the β-plane.

Summary

Vortices on the f-plane that behave as predicted in a qualitative sense have been generated in the laboratory by Buzyna (1967) using source-sink flows. Theoretical work still needs to be done on the problem, however. The effects of the sidewall boundary layers, especially those surrounding the source and sink, should be studied, and the Ekman layer instabilities need to be analyzed.

Solution of Eq.(46) would aid in understanding the results of Buzyna's experiments on the β-plane. Equation (50) must be solved before modons can be modeled in the laboratory. Even if solutions do exist, there is still a question as to whether it is experimentally possible to realize the appropriate parameter space.

Acknowledgments

I would like to thank Dr. Melvin Stern for suggesting this problem and for guiding my work throughout the summer. Helpful advice was received from Drs.George Veronis and Joseph Pedlosky. Laboratory assistance was provided by Dr. John Whitehead and Mr. Robert Frazel.

References

Buzyna, George 1967 GFD Lectures. Source-sink experiments in a rotating fluid. Vol.II: 17-33.

Greenspan, H.P. 1968 The Theory of Rotating Fluids. Cambridge, Univ.Press. 327 pp.

Newell, Alan 1975 GFD Lectures. Integrable systems of nonlinear evolurion equations. Vol.I.

Niiler, Pearn P. 1966 On the theory of wind-driven ocean circulation. Deep-sea Research, 13: 597-606.

Stern, Melvin E. 1974 GFD Lectures. Modons. Vol.I: p.125.
Stern, Melvin E. 1975 Minimal properties of planetary eddies. J.Mar.Research, 33: 1-13.

GRAVITATIONAL TIDES IN THE EARTH'S CORE

Howard C. Houben

The motions within the Earth's liquid core are an important subject of inquiry mainly because they are most certainly responsible for the generation of the geomagnetic field. However, in some ways our understanding of these motions has grown worse over the last twenty years, At that time it seemed clear that convection in the outer core would give rise to dynamo action. While this conviction still has not been disproved the following difficulties must be met:

1) The simplified convection model of Bullard and Gellman (1954) apparently does not give rise to dynamo action as previously thought (Gibson and Roberts 1969).

2) More complex and detailed convective models, which do apparently give rise to a magnetic field, have not yet been worked out for the precise physical state and geometry of the Earth's core (Busse 1975).

3) The low efficiency of a thermal engine operating in the Earth's core would require a large heat flux to maintain the geodynamo (Stacey 1969). The source of this energy is unclear. Indeed the possibility that Mercury has a magnetic field of similar origin to the Earth's (Ness et *al*. 1975) is a serious embarassment since the cosmochemical arguments which indicate that the Earth could have substantial radioactive heat sources in its core would exclude this possibility for Mercury (Lewis 1971).

4) The possibility that the lunar-solar precession could drive the dynamo (Malkus 1968) does not have the same problem with energetics and has recently been favored by many authors (Stevenson 1974).

The core paradox.

5) The physical properties of the Earth's core may be such as to exclude convection. On the assumption that the inner core is solid, current studies of the physical properties of molten iron (at high pressure) would indicate that the temperature gradient in the outer core should be shallower than the adiabatic gradient (Higgins and Kennedy 1971; Kennedy and Higgins 1973; Stacey 1975), rendering the core stably stratified. Convection would be possible in only the innermost part of the fluid core and the instabilities due to the precessional force would be inhibited. These results would require all dynamo theories to be reexamined.

In light of the above it is of interest to study a different source of core motions - the lunar and solar tides. The total energy dissipated within the Earth by the tides is $\sim 3 \times 10^{19}$ ergs/sec. Although this dissipation takes place largely within the oceans, it is quite possible that on the order of a percent of this is actually dissipated in the core - probably enough to drive the geomagnetic dynamo. The general effect of the tides is to distort the core, i.e. the container of the fluid, into an ellipsoid. Thus a periodic radial velocity is imposed on the fluid at the boundaries, The previously-mentioned core stratification which would tend to inhibit radial motions is not operative here because the radial velocity is externally imposed. Indeed the effect of the stratification is to enhance motions in the other directions. The magnitude of the radial motions is about 10 cm (as will

later be derived) and for the tidal frequency of about $10^{-4}\,\mathrm{sec}^{-1}$ this gives a velocity of 10^{-3} cm/sec. For an assumed core conductivity of 3×10^{-6} emu, the resultant magnetic Reynolds number $= 4\pi\sigma V L$ is ~ 10, indicating that the tidally-forced motions are something to be reckoned with in relation to the magnetic field. It should also be noted that the tidal and precessional forces, having similar origins, are about equal in magnitude and so it is quite natural to consider the two together, independent of the question of core stratification.

The tidal potential at position $\underline{r}$ due to the Moon may be expressed as (Chapman and Lindzen, 1970)

$$\Psi = -G\frac{M_D}{R_D^2}\sum_{n=2}^{\infty}\left(\frac{r}{R_D}\right)^n P_n(\cos\Theta)$$

where Θ is the angle between the observer and the Moon as seen from the center of the Earth. The P_n are the Legendre polynomials. In turn Θ can be written (in terms of ordinary spherical coordinates) as

$$\cos\Theta = \cos\theta\cos\Delta + \sin\theta\sin\Delta\cos(\varphi + ft)$$

where Δ = the colatitude of the Moon and $f = 2\pi/$ lunar day $= \Omega - \omega_D$ where $\Omega = 2\pi/$sidereal day and $\omega_D = 2\pi/$sidereal month. Now Δ itself varies with frequency ω_D (as well as slower time dependences) and so the tides may be separated into forces with a large variety of frequencies (Bartels 1957). (The solar tides may be similarly analyzed.) The most important tidal components for our study will be

1) M_2, the lunar quasi-semidiurnal tide $\propto P_2^2(\cos\theta)\cos 2(\varphi + ft)$. This tide has the largest amplitude and is the one most evident in ocean tides.

2) K_2, the lunisolar semidiurnal tide $\propto P_2^2(\cos\theta)\cos 2(\varphi + \Omega t)$. The exact semidiurnal time dependence comes from the combination of the time-dependent latitude and longitude terms in the expression for $\cos\Theta$. This component may be expected to excite a resonance in the rotating fluid core.

3) K_1, the lunisolar diurnal tide $\propto P_2^1(\cos\theta)\sin(\varphi + \Omega t)$. The exact diurnal dependence comes about in the same way as for the previous component, This term has the same time dependence as the precessional force (in the rotating frame) and also may excite a natural resonance in the core.

The response of the core boundary to the tidal potential is a displacement equal to $-\frac{h}{g}\Psi$ (Munk and MacDonald 1960) where h is a Love number of order unity. The amplitude (neglecting angular factors) of these displacements is thus

$$h\left(\frac{M_D}{M_e}\right)\left(\frac{r_e}{R_D}\right)^3 r_e \equiv h\varepsilon r_e \quad \text{where } \varepsilon \sim 3\times 10^{-8}$$

and the resultant velocity is $-\frac{h}{g}\frac{\partial\Psi}{\partial t} \sim 2\Omega h\varepsilon r_e \sim 10^{-3}$ cm/sec as previously given.

We have now established the boundary condition for our tidal analysis and will turn to the equation of motion. We wish to write this in a frame attached to the Earth which is precessing and rotating. In addition to the coriolis and centrifugal forces there is the transverse force which must be considered. It is equal to $\dot{\underline{\Omega}} \times \underline{r}$ where the time derivative is evaluated in the rotating frame $\dot{\underline{\Omega}} = \underline{\Omega} \times \underline{\omega}$ where $\underline{\omega}$ is the precessional vector about which $\underline{\Omega}$ rotates in the clockwise (retrograde) direction. (Since $\underline{\omega}$ is fixed in space, in our rotating frame it apparently rotates with frequency Ω.)

The equation of motion is

$$\frac{D\underline{v}}{Dt} + 2\underline{\Omega}\times\underline{v} + (\underline{\Omega}\times\underline{\omega})\times\underline{r} + \frac{1}{\rho}\nabla p + \nabla\chi = \nabla\cdot\underline{\underline{\tau}} \qquad (1)$$

where ρ and p are the fluid density and pressure, χ is the sum of self-gravitational, centrifugal and tidal potentials, and $\underline{\underline{\tau}}$ is the deviatonic stress. For completeness it would be necessary to include the Lorentz force in Eq.(1). We will do this later in the analysis when the form of magnetic field which our tidal velocity field may sustain is found.

We will non-dimensionalize Eq.(1) with the help of the velocity scaling derived from our tidal analysis. Replacing dimensional variables with dimensional quantities (in brackets) times non-dimensional variables:

$$\underline{v} \Rightarrow [2\Omega\varepsilon r_c]\underline{v}$$

$$t \Rightarrow [\tfrac{1}{2}\Omega]t$$

$$\underline{\nabla} \Rightarrow [1/r_c]\underline{\nabla}$$

$$\underline{r} \Rightarrow [r_c]\underline{r}$$

$$\psi \Rightarrow [\varepsilon g r_c]\psi$$

$$\chi = \bar{\chi} + \chi' \Rightarrow [g r_c](\bar{\chi} + \varepsilon\chi')$$

$$\rho = \bar{\rho} + \rho' \Rightarrow [\rho_0](\bar{\rho} + \varepsilon\rho')$$

$$p = \bar{p} + p' \Rightarrow [\rho_0 g r_c](\bar{p} + \varepsilon p')$$

$$\underline{\underline{\tau}} \Rightarrow [2\Omega\varepsilon\nu]\underline{\underline{\tau}}$$

$$\underline{\omega} \Rightarrow [2\Omega\varepsilon]\underline{\omega}$$

In the above, the overbars refer to time average quantities. Equation (1) becomes

$$[4\Omega^2\varepsilon r_c]\frac{\partial \underline{v}}{\partial t} + [4\Omega^2\varepsilon^2 r_c]\underline{v}\cdot\underline{\nabla}\underline{v} + [4\Omega^2\varepsilon r_c]\hat{k}\times\underline{v} + [2\Omega^2\varepsilon r_c](\hat{k}\times\underline{\omega})\times\underline{r} + \\ + [g]\frac{1}{\bar{\rho}+\varepsilon\rho'}\underline{\nabla}(\bar{p}+\varepsilon p') + [g]\underline{\nabla}(\bar{\chi}+\varepsilon\chi') = [2\Omega\varepsilon\nu/r_c]\underline{\nabla}\cdot\underline{\underline{\tau}} \qquad (2)$$

Equating the terms of order ε^0:

$$\frac{1}{\bar{\rho}}\underline{\nabla}\bar{p} + \underline{\nabla}\bar{\chi} = 0, \qquad (3)$$

which is the equation of hydrostatic equilibrium. We can simplify the remaining portion of (2) with the following definitions:

$$\delta \equiv 4\Omega^2 r_c/g \sim 10^{-2}$$

$$E \equiv \nu/2\Omega r_c^2 \sim 10^{-15}$$

Then

$$\delta(\bar{\rho}+\varepsilon\rho')\frac{\partial \underline{v}}{\partial t} + \delta\varepsilon(\bar{\rho}+\varepsilon\rho')\underline{v}\cdot\underline{\nabla}\underline{v} + \delta(\bar{\rho}+\varepsilon\rho')\hat{k}\times\underline{v} + \frac{\delta}{2}(\bar{\rho}+\varepsilon\rho')(\underline{k}\times\underline{\omega})\times\underline{r} + \\ + \underline{\nabla}p' + \rho'\underline{\nabla}\bar{\chi} + (\bar{\rho}+\varepsilon\rho')\underline{\nabla}\chi' = \delta E(\bar{\rho}+\varepsilon\rho')\underline{\nabla}\cdot\underline{\underline{\tau}} \qquad (4)$$

The order ε^0 term (E assumed higher order) becomes

$$\delta \frac{\partial \underline{v}}{\partial t} + \delta \hat{k} \times \underline{v} + \frac{\delta}{2}(\hat{k} \times \underline{\omega}) \times \underline{r} + \frac{1}{\bar{\rho}} \nabla p' + \frac{\rho'}{\bar{\rho}} \nabla \bar{\chi} + \nabla \chi' = 0 \qquad (5)$$

which is the Boussinesq equation of motion.

We will write all quantities as $\propto e^{i(m\varphi + st)}$

The higher order equation is

$$-\frac{\rho'}{\bar{\rho}} \nabla p' - \frac{\rho'}{\bar{\rho}} \nabla \bar{\chi} + \delta \bar{\rho}\, \underline{v} \cdot \underline{\nabla} \underline{v} = \frac{\delta E}{\varepsilon} \bar{\rho} \underline{\nabla} \cdot \underline{\tau} \qquad (6)$$

Equation (6) is important in solving for the time-average azimuthal velocity. The balance here is

$$\overline{v \cdot \nabla v} = E/\varepsilon \, \nabla^2 \bar{v} \qquad (6a)$$

For boundary conditions (values of h) in which there is a phase lag between the boundary response and the instantaneous response of the perfect fluid (signified by an imaginary part of h), there will be a correlation between velocity components and the left-hand side of (6a) will be a non-zero time average. If ϕ is the size of this correlation the magnitude of the mean flow $\bar{v}$ is

$$\bar{v} \sim \frac{\varepsilon \phi}{E}$$

so $\bar{v}$ can be quite large even for very small values of ϕ. It is always in the sense of a westward drift of the core material with respect to the mantle. The above balance may be adjusted somewhat by large-scale steady motions.

We can simplify Eq.(5) a bit by the introduction of an equation of state (a relation between p' and ρ'). We may write

$$\frac{1}{p} \frac{Dp}{Dt} = \frac{\gamma}{\rho} \frac{D\rho}{Dt} \qquad (7)$$

where γ is an adiabatic exponent. The basic state may be written as

$$\frac{1}{\bar{p}} \nabla \bar{p} = \frac{\gamma}{\bar{\rho}} \nabla \bar{\rho}. \qquad (8)$$

A rising parcel of core material, always in pressure equilibrium with the surrounding medium will become denser than the external matter if $\gamma > \gamma_1$, which is the criterion for stability. The equation of motion of such a parcel is

$$\ddot{r} + \frac{\gamma_1 - \gamma}{\gamma} \frac{\nabla \bar{p}}{\bar{\rho}} \nabla \bar{\chi}\, r = 0$$

so the buoyancy frequency is defined by

$$N^2 = \frac{\gamma_1 - \gamma}{\gamma} \frac{\nabla \bar{p}}{\bar{\rho}} \nabla \bar{\chi}.$$

The Boussinesq approximation is obtained for $\gamma \to \infty$ which however is not appropriate in the Earth's core where the ambient pressure is a reasonable fraction of the bulk modulus.

A reasonable approximation to the density run in the core is given by $\bar{\rho} = \rho_0 e^{-br^2}$ with $\rho_0 = 12.5 \text{ gm cm}^{-3}$ and $b = .2$ so that $\nabla \bar{\rho}/\bar{\rho} = -.2\, r$. We may similarly write $\bar{p} = p_0 e^{-ar^2}$ with $p_0 = 3.5 \times 10^{12}$ cgs and $a = .6$. Then $\gamma_1 \approx 3$. The value of γ depends on the temperature gradient in the core (and the Gruneisen parameter) and is a subject of some controversy as sited above. The resulting value of $\frac{\gamma_1 - \gamma}{\gamma}$ (via the Adams-Williamson relation) is $-\propto T \Delta\Gamma$ where $\Delta\Gamma$ is the difference between the real value of Gruneisen's parameter and the value which would make the core adiabatic (≈ 1). So $\frac{\gamma_1 - \gamma}{\gamma} \sim .1$.

We can non-dimensionalize N as

$$N^2 \Rightarrow \left[4\Omega^2\right] \frac{\cdot 02}{g} \nabla \bar{\chi}\, r \quad \text{so} \quad N \approx 2 \text{ (in units of } 2\Omega).$$

Also approximately $\nabla \chi \propto r$, so $N^2 \propto r^2$. (Indeed $N^2 \approx 0$ near the inner core boundary.)

In (5) we assume time dependences of the form e^{isct} for all quantities where $s = 1$ for K_2 tide, $\frac{1}{2}$ for K_1 tide, and $\approx .97$ for M_2 tide. Using (7) we write

$$\frac{\rho'}{\bar{\rho}} = \frac{1}{\gamma}\frac{p'}{\bar{p}} - \frac{\gamma-\gamma_1}{\gamma}\frac{\underline{V}}{is}\cdot\frac{\nabla\bar{p}}{\bar{p}} \tag{9}$$

The buoyancy term in (5) is then (with the help of (3))

$$-\frac{1}{\gamma}\frac{p'}{\bar{p}\rho}\nabla\bar{p} + \frac{\gamma_1-\gamma}{\gamma}\frac{V}{is}\cdot\frac{\nabla\bar{\rho}}{\bar{\rho}}\nabla\bar{\chi} = -\frac{\gamma_1}{\gamma}\frac{p'}{\bar{\rho}^2}\nabla\bar{\rho} + \frac{\gamma_1-\gamma}{\gamma}\frac{V\cdot\nabla\bar{\rho}}{is\,\bar{\rho}}\nabla\bar{\chi}$$

We are left with

$$is\underline{V} + \hat{K}\times\underline{V} + \tfrac{1}{2}(\hat{K}\times\underline{\omega})\times\underline{r} + \frac{1}{\delta}\nabla\left(\frac{p'}{\rho}+\chi'\right) + \frac{\gamma-\gamma_1}{\gamma\delta}\frac{p'}{\bar{\rho}^2}\nabla\bar{\rho} + \frac{N^2}{is}V_r\hat{r} = 0 \tag{10}$$

Writing $\bar{N}^2$ for N^2/r^2 and Φ for $\frac{1}{\delta}\left(\frac{p'}{\rho}+\chi'\right)$

$$is\underline{V} + \frac{\bar{N}^2}{is}(\underline{V}\cdot\underline{r})\underline{r} + \hat{K}\times\underline{V} + \tfrac{1}{2}(\hat{K}\times\underline{\omega})\times\underline{r} + \nabla\Phi - \bar{N}^2\left[\delta\Phi-\chi'\right]\underline{r} = 0 \tag{11}$$

The components in spherical coordinates are

$$\left(is + \frac{\bar{N}^2r^2}{is}\right)V_r - \sin\theta\, V_\varphi = -\frac{\partial\Phi}{\partial\theta} - \bar{N}^2 r\left[\delta\Phi-\chi'\right]$$

$$isV_\theta - \cos\theta V_\varphi = -\frac{1}{r}\frac{\partial\Phi}{\partial\theta} - \frac{\omega r}{2}\left[\sin\theta\cos(\theta-\alpha)\,e^{i(\varphi+t/2)} - \cos\theta\sin(\theta-\alpha)\right] \tag{12}$$

$$isV_\varphi + \cos\theta V_\theta + \sin\theta V_r = -\frac{1}{r\sin\theta}\frac{\partial\Phi}{\partial\varphi} - i\frac{\omega r}{2}\cos\theta\cos(\theta-\alpha)\,e^{i(\varphi+t/2)}$$

where $\hat{K} = \hat{r}\cos\theta - \hat{\theta}\sin\theta$; α is the angle between $\underline{\omega}$ and $\hat{K}$ and

$$\underline{\omega} = \omega\left[\hat{r}\cos(\theta-\alpha)e^{i(\varphi+t/2)} - \hat{\theta}\sin(\theta-\alpha) + i\hat{\varphi}\cos(\theta-\alpha)e^{i(\varphi+t/2)}\right]$$

Equations (12) give rise to another time-average azimuthal velocity forced by precession.

$$V_\varphi = 2\omega r\left[\cos\alpha\sin\theta\log\sin\theta + \sin\alpha\,(\cos\theta + \theta\sin\theta)\right] \text{ from}$$

$$\bar{\Phi} = \omega r^2\left[\cos\alpha\sin^2\theta\log\sin\theta + \sin\alpha\,(\sin\theta\cos\theta + \theta\sin^2\theta)\right]$$

The velocity is too small to account for the westward drift and of uncertain direction (due to the latitude dependence).

Solving for the velocity components (in the case $S \neq \frac{1}{2}$)

$$\left.\begin{aligned}\Delta &= is\left(1-s^2\right) + \frac{i\bar{N}^2r^2}{s}\left(s^2-\cos^2\theta\right)\\ \Delta V_r &= \left(-\frac{\partial\Phi}{\partial r} - \bar{N}^2r\left[\delta\Phi-\chi'\right]\right)\left(\cos^2\theta-s^2\right) - \sin\theta\left(\frac{is}{r\sin\theta}\frac{\partial\Phi}{\partial\varphi} - \frac{\cos\theta}{r}\frac{\partial\Phi}{\partial\theta}\right)\end{aligned}\right\} \tag{13}$$

$$\Delta V_\theta = \left(is + \frac{\bar N^2 r^2}{is}\right)\left(\frac{-\cos\theta}{r\sin\theta}\frac{\partial \bar\Phi}{\partial\varphi} - \frac{is}{r}\frac{\partial\bar\Phi}{\partial\theta}\right) + \sin\theta\left(\cos\theta\left[\frac{\partial\bar\Phi}{\partial r} + \bar N^2 r\left[\delta\bar\Phi - \chi'\right]\right] - \frac{\sin\theta}{r}\frac{\partial\bar\Phi}{\partial\theta}\right)$$

$$\Delta V_\varphi = \left(is + \frac{\bar N^2 r^2}{is}\right)\left(\frac{-is}{r\sin\theta}\frac{\partial\bar\Phi}{\partial\varphi} + \frac{\cos\theta}{r}\frac{\partial\bar\Phi}{\partial\theta}\right) + is\sin\theta\left(\frac{\partial\bar\Phi}{\partial r} + \bar N^2 r\left[\delta\bar\Phi - \chi'\right]\right) \qquad (13)$$

The $s = \frac{1}{2}$ equations also contain terms proportional to ω. These equations must be solved in conjunction with the continuity equation

$$\frac{1}{\rho}\frac{D\rho}{Dt} + \nabla\cdot V = \frac{1}{\gamma p}\frac{Dp}{Dt} + \nabla\cdot V = 0 \qquad (14)$$ which reduces to

$$\frac{is}{\gamma}\frac{\bar p}{\bar\rho}\left[\delta\bar\Phi - \chi'\right] + \frac{1}{\gamma}\frac{\nabla\bar p}{\bar p}V_r + \nabla\cdot V = 0. \qquad (15)$$

(In the Boussinesq approximation: $\gamma \to \infty$, this reduces to $\nabla\cdot V = 0$)

Also there is Poisson's equation for χ':

$$\nabla^2\chi' = \rho' \Rightarrow \nabla^2\chi' + \frac{1}{\gamma}\frac{\bar\rho^2}{\bar p}\chi' = \frac{\delta}{\gamma}\frac{\bar\rho^2}{\bar p}\bar\Phi - \frac{\gamma-1}{is\,r}\nabla\bar\rho\, V_r \qquad (16)$$

$\sim N^2\delta V_r$

This has the boundary conditions

$\chi' = (1+k_i)\psi(r_i)$ at boundaries $i = 1.2$ (k_i is another Love number of order unity). We may also restate the V_r boundary conditions which are

$V_r = -is\frac{h_i}{g_i}\psi(r_i) = -is\,h_i\frac{\Psi(r_i)}{r_i}$ at $i = 1.2$ since we are assuming Γ. We thus have two complicated coupled equations for the potentials $\bar\Phi$ and χ'.

(One substitutes from (13) to (15)).

In the case $\bar N = 0$, the continuity equation ($\nabla\cdot V$) results in a hyperbolic differential equation for the potential $\bar\Phi$, whereas the boundary conditions are those appropriate to an elliptic equation. The result of this is that the solution for $\bar\Phi$ does not have the same analytic form at all points. In particular we get the zones of strong shear evident in the experiments of Malkus and Suess (1970). The presence of the stratification renders the equation elliptic in at least part of the domain of interest. The hope is that the boundary layers are then mere Stokes layers which are stable at the relevant low Reynold's number of about 1. (See Davis 1975 and Robinson and McEwan 1975.) If this is the case we can obtain laminar solutions to the equations.

Note that in Eq.(13), the derivatives of $\bar\Phi$ do not contribute to V_r when $\bar\Phi$ is of the form $Ar^2\sin\theta\cos\theta$ (which is appropriate for the K_1 tide). Our equations are then approximately solved by the balance $\delta\bar\Phi \approx \chi'$ (though this is not an exact solution of (15)). Now $\chi' \approx (1+k)\Psi$ and $\Psi \approx 3r^2\sin\theta\cos\theta$. (The 3 comes from the normalization of the Legendre polynomials.) So A is given by

$$A \approx 3(1+k)/\delta \sim 10^3.$$

We see that the velocities in the meridional and azimuthal directions can be quite large (though this calls into question the stability of the Stokes layers which now have a Reynold's number $\sim 10^3$). So we have $V_\theta \sim 10^3$; $V_\varphi \sim 10^3$. The velocity fields are given by

$$V_\theta = -2iAr\sin(\varphi + t/2)$$

$$V_\varphi = 2Ar\cos\theta\sin(\varphi + t/2).$$

The streamlines look like large scale hurricanes on the planet.

We now turn to consideration of the magnetic field. The dynamo equation is

$$\frac{\partial B}{\partial t} - \lambda \nabla^2 B = \nabla \times (V \times B) \quad \text{where } \lambda = 1/4\pi\sigma \sim 10^4 \tag{21}$$

Non-dimensionalizing

$$\frac{\partial B}{\partial t} - \frac{\lambda}{2\Omega r_o^2} \nabla^2 B = \varepsilon \nabla \times (V \times B)$$

$$\frac{\partial B}{\partial t} - E_m \nabla^2 B = \varepsilon \nabla \times (V \times B) \quad \text{where the magnetic Ekman number}$$

$$E_m = \lambda / 2\Omega r_o^2 \sim 10^{-9}$$

We divide the magnetic field into two parts

$B = \bar{B} + B'$ where $\bar{B}$ is the time average. We do the same with $V = \bar{V} + V'$.

Then
$$\frac{\partial B'}{\partial t} = \varepsilon \nabla \times (\bar{V} \times B') + \varepsilon \nabla \times (V' \times \bar{B})$$

$$B' = \frac{\varepsilon}{1s} \nabla \times \left[\bar{V} \times B' + V' \times \bar{B}\right] \quad \text{and} \quad -\nabla^2 \bar{B} = \frac{\varepsilon}{E_m} \nabla \times (\overline{V' \times B'})$$

and
$$-\nabla^2 \bar{B} = R_m \nabla \times \left[\overline{V' \times \frac{\varepsilon}{1s} \nabla \times \left\{\bar{V} \times B' + V' \times \bar{B}\right\}}\right]$$

where the magnetic Reynolds number $R_m = \varepsilon / E_m \sim 30$

$$-\nabla^2 \bar{B} = + \frac{R_m \varepsilon}{s} \nabla \times \left\{\overline{V' \times \left(\frac{1}{\tau} \nabla \times (V' \times \bar{B})\right)}\right\} \quad \text{for } \bar{V} = 0. \tag{22}$$

We require $V' \sim 10^3$ for regeneration. This balance in magnitude of terms is not enough to insure regeneration, but it is a step in the right direction.

So we have shown that it is plausible that a magnetic field of the right form could be maintained by the oscillating tidal flows. Note that a toroidal field would undoubtedly arise from the advection of the poloidal field by a mean flow.

In conclusion, it seems a possibility that rapid time varying flows can be adequate to explain the Earth's long-term magnetic field. It has not conclusively been shown, however, that it is the laminar flow due to the tides which does this. It will be necessary to further investigate the instability of the boundary layers, and the possibility that the resultant internal waves generate a field in the manner shown above.

References

Bartels in Handbuch der Physik 1957 48: 734. Spinger, Berlin.
Bullard and Gellman 1954 Phil.Trans.Roy.Soc. 247: 213
Busse, GFD Lectures 1975
Chapman and Lindzen, Atmospheric Tides, 1970 Gordon and Breach.
Davis, GFD Lectures 1975
Gibson and Roberts 1969 in Application of Modern Physics to Earth and Planetary Interiors. S.K.Runcord, ed.
Higgins and Kennedy 1971 J.G.R. 76: 1870
Kennedy and Higgins 1973 J.G.R. 78: 900
Lewis, 1971 Earth Planet.Sci.Letters 11: 130
Munk and MacDonald 1960 The Rotation of the Earth, Cambridge Univ. Press.
Ness et al. 1975 Nature 255: 204
Robinson and McEwan 1975 JFM 68: 41
Stacey, 1969 Physics of the Earth, Wiley
Stacey, 1975 Nature 255: 44
Stevenson, 1974 Icarus 22: 403
Suess. 1970 J.G.R. 75: 6650.

THE INSTABILITY OF A BAROCLINIC BOUNDARY JET IN A ROTATING FLUID

Stephen Jones

Introduction

This study was motivated by certain observations made on an experimental investigation of geostrophic adjustment. (1,2). This consisted of a long, narrow tank mounted on a rotating turntable. The tank was divided into two sections by a barrier, one section (the longer one) consisting of a single layer of cool (saline) water, and the other section consisting of a thin layer of warm (fresh) dyed water.

After spin-up was complete, the barrier was removed and the lighter fluid began to move out from behind the position where the barrier had been, Rotational constraints forced the fluid to move towards the leading edge of the tank, where it formed a jet travelling along the side boundary. This jet became unstable in a number of instances, breaking away from the side boundary at regular intervals downstream and forming a number of eddies extending across the width of the tank.

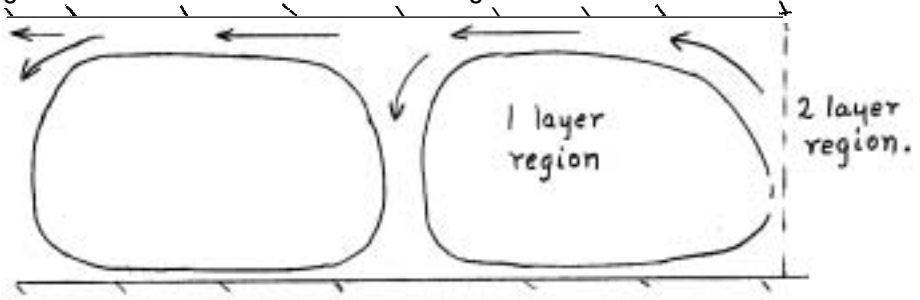

Fig.1 Plane sketch of observed boundary jet instability.

This instability is very striking and is relatively easy to observe in the laboratory. Consequently, it would be of great value to our understanding of the dynamics of rotating, stratified fluids to determine what type of instability is being observed. The question we would most like to answer is what type of instability is operating. Is it a geostrophic instability, or an instability of an (inviscid) ageostrophic nature, or is it a viscous-dominated instability?

Unfortunately, very little reliable quantitative data is available from which we can gain, via scaling arguments, some idea of the effect of viscosity on the instability. W. Facinelli (2) is doing experiments on the geostrophic adjustment problem in which the instability manifests itself, and it is hoped that these, and other experiments in the future, will provide the necessary data to gauge the effect of viscosity on the instability. Therefore, in this report, we shall neglect the effect of viscosity entirely and concentrate attention primarily on the stability, or otherwise, of the baroclinic boundary jet to geostrophic perturbations. Throughout, it will be assumed that the basic flow in the jet is geostrophic.

The Basic State

Before formulating the stability problem, we shall look at the form of the basic state in order to gain a better idea of how to set up the problem. We shall assume that the effect of the far side boundary is small, thereby picturing a side boundary jet in a semi-infinite fluid. The diagram represents a cross section of the fluid, showing two layers, the top (and lighter) layer being in motion, and the bottom one being static. The basic state is assumed to be independent of y, the downstream ordinate.

The momentum equations for the geostrophic jet reduce to the single equation

$$fV = g' h_x$$

where $g' = \frac{\Delta\rho}{\rho}$, $\Delta\rho$ being the density difference between the two layers, and ρ is the average density.

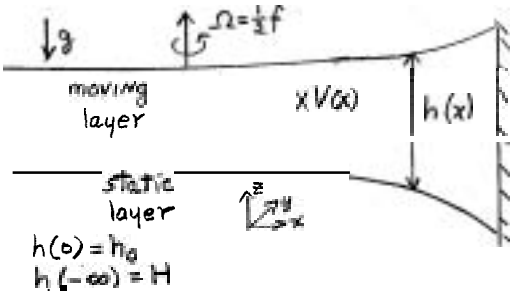

Fig.2. Cross section of boundary jet

If the mass flux

$$Q = \int_{-\infty}^{0} hV\,dx$$

is assumed constant, the geostrophic balance equation implies

$$\tfrac{1}{2} g' (h_0^2 - H^2) = fQ$$

In addition to the momentum equation, conservation of potential vorticity implies

$$\frac{f + V_x}{h} = \frac{f}{H}$$

Solving for h and V gives

$$h = H + \frac{Q}{fa^2} e^{x/a}$$

$$V = \frac{Q}{Ha} e^{x/a}$$

where $a = \frac{(g'H)^{1/2}}{f}$ is the radius of deformation.

If we perturb this basic state, whilst keeping the bottom layer at rest, it can be shown (3,4) that the necessary condition for unstable geostrophic disturbances is that the gradient of the basic potential vorticity must change sign somewhere in the region of interest. However, the basic potential vorticity gradient is zero everywhere, and therefore we conclude that the jet is stable to geostrophic disturbances which confine themselves to the upper layer.

The basic state derived above also presents some grave mathematical difficulties in that any stability analysis will consist of equations with exponentially varying coefficients. To simplify the analysis, we shall consider the simplest jet possible, i.e. a constant velocity jet confined to a distance L of the wall (by geostrophy, this implies that the layer thicknesses in the jet vary linearly).

Rayleigh Instability Criterion for two layers

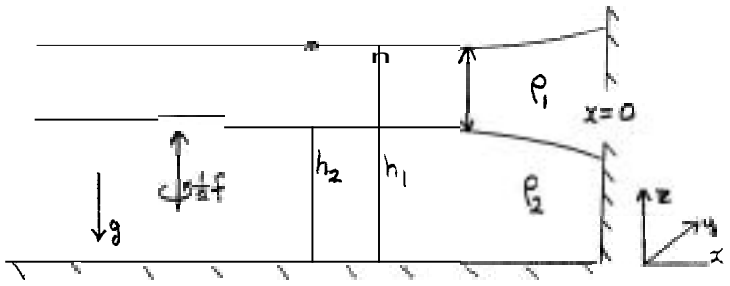

It is possible to derive a square-integrable condition for the stability of geostrophic disturbances in a two-layer system under certain conditions. A similar type of criterion was derived by Orlanski (5) for a related problem, therefore we shall only sketch an outline of the proof here.

Again we consider two semi-infinite layers of incompressible homogeneous fluid in a rotating coordinate system with constant Coriolis parameter f. The motion in both layers is hydrostatic and independent of vertical coordinate z, and satisfies conservation of potential vorticity:

$$\frac{d_1}{dt}\left\{\frac{\zeta_1 + f}{h_1 - h_2}\right\} = 0 \qquad (1)$$

$$\frac{d_2}{dt}\left\{\frac{\zeta_2+f}{h_2}\right\}=0 \tag{2}$$

where

$$\zeta_i = v_{ix}-u_{iy}$$

$$\frac{d_i}{dt} \equiv \frac{\partial}{\partial t}+u_i\frac{\partial}{\partial x}+v_i\frac{\partial}{\partial y}\Bigg\}\ i=1,2$$

and (u_i, v_i) are the velocities in the i^{th} layer.

We shall now expand the system about the basic state by setting

$$\begin{aligned}\zeta_i &= \zeta_{i0}+\zeta_i'\\ u_i &= u_i'\\ v_i &= v_{i0}+v_i'\\ h_1 &= h_{10}+h_1'\\ h_2 &= h_{20}+h_2'\\ h_1 &= h_{10}-h_2\end{aligned}$$

and linearizing. The equations then become, upon dropping primes

$$\left(\frac{\partial}{\partial t}+V_{10}\frac{\partial}{\partial y}\right)\left(\zeta_1-\pi_1 h\right)+h_0\frac{d\pi_1}{dx}u_1=0$$

$$\left(\frac{\partial}{\partial t}+V_{20}\frac{\partial}{\partial y}\right)\left(\zeta_2-\pi_2 h_2\right)+h_{20}\frac{d\pi_2}{dx}u_2=0$$

where

$$\pi_1=\frac{f+\zeta_{10}}{h_0}$$

$$\pi_2=\frac{f+\zeta_{20}}{h_{20}}$$

The quantities π_1 and π_2 are the basic potential vorticity of the top and bottom layers respectively.

If we assume that the disturbance is quasi-geostrophic, it follows that we can write

$$(u_i, v_i) = \frac{g}{f}(-p_{iy}, p_{ix})$$

where

$$p_1 = h_1$$

and

$$p_2 = \frac{\rho}{\rho_2}h_1+\frac{\Delta\rho}{\rho_2}h_2$$

In addition, we assume the solution takes the wave-like form

$$p_i = p_i(x)\exp\left\{il(y-ct)\right\}$$

The governing equations then become

$$\frac{d^2p_1}{dx^2}-\left(l^2+\frac{h_{10}}{V_1-c}\frac{d\pi_1}{dx}\right)p_1+\frac{f}{g'}\pi_1(p_2-p_1)=0 \tag{3}$$

$$\frac{d^2p_2}{dx^2}-\left(l^2+\frac{h_{20}}{V_2-c}\frac{d\pi_2}{dx}\right)p_2-\frac{f}{g'}\pi_2\left(p_2-\frac{\rho}{\rho_2}p_1\right)=0 \tag{4}$$

where

$$g'=\frac{\Delta\rho}{\rho_2}g$$

We are interested in the case where $V_{20}=0$ in which case

$$\Pi_1 = \frac{f + V_{10x}}{h_0}, \quad \Pi_2 = \frac{f}{h_{20}}$$

The basic state satisfies the geosfrophic balance equations

$$V_{10} = \frac{g}{f} h_{10x} = \frac{g}{f}(h_{0x} + h_{20x})$$

and

$$0 = \frac{g}{f}\left(\frac{\rho}{\rho_2} h_{10x} + \frac{\Delta\rho}{\rho_2} h_{20x}\right) = \frac{g}{f}\left(\frac{\rho}{\rho_2} h_{0x} + h_{20x}\right)$$

If we scale the horizontal length scale by L, the velocity scale by V, and define

$$\blacksquare = L\eta$$

$R_o = \frac{V}{fL}$, a Rossby number

$R_i = \frac{g' H_0}{V^2}$, a Richardson number

$\mu = \ell L$

$c = V c_0$

we can write

$$V_{10} = V h_\eta$$

$$h_0 = H_0\left(1 + \frac{h}{R_o R_i}\right)$$

$$h_{20} = H_2\left(1 - \frac{\rho}{\rho_2}\frac{H_0}{H_{20}}\frac{h}{R_o R_i}\right)$$

where H_0, H_{20} are the mean depths of the top and bottom layers respectively. It now follows that

$$\Pi_1 = \frac{f}{H_0}\left(\frac{1 + R_o h_{\eta\eta}}{1 + h/R_o R_i}\right)$$

$$\Pi_2 = \frac{H_{20}}{}\left(1 - \frac{\rho}{\rho_2}\frac{H_0}{H_{20}}\frac{h}{R_o R_i}\right)^{-1}$$

$$* + - \left[* \frac{}{R_i} - \frac{(R_o^2 R_i)^{-1} h_\eta (1 + R_o h_\eta)}{(1 + h/R_o R_i)^2} \right\}$$

and

$$\frac{d\Pi_2}{dx} = \frac{f}{H_{20} L} R_o \left\{ \frac{\frac{H_2}{H_{20}}\frac{\rho}{\rho_2}(R_o^2 R_i)^{-1} h_\eta}{\left(1 - \frac{\rho}{\rho_2}\frac{H_0}{H_{20}} h/R_o R_i\right)^2} \right\}$$

and the equations become

$$\frac{d^2 p_1}{d\eta^2} - \left[\mu^2 + \frac{1}{h_\eta - c_0}\left\{h_{\eta\eta\eta} - \frac{1}{R} h_\eta \left(\frac{1 + R_o h_{\eta\eta}}{1 + \frac{R_o}{R} h}\right)\right\}\right] p_1 = \frac{1}{R}\left[\frac{1 + R_o h_{\eta\eta}}{1 + R_o/R\, h}\right](p_1 - p_2) \qquad (5)$$

$$\frac{d^2 p_2}{d\eta^2} - \left[\mu^2 - \frac{1}{c_0}\frac{\rho}{\rho_2}\frac{H_0}{H_{20} R}\frac{h_\eta}{1 - \frac{\rho}{\rho_2}\frac{H_0}{H_{20}}\frac{R_o}{R} h}\right] p_2 = + \frac{H_0}{H_{20}}\cdot\frac{1}{R}\left(\frac{1}{1 - \frac{\rho}{\rho_2}\frac{H_0}{H_{20}}\frac{R_o}{R} h}\right)\left(p_2 - \frac{\rho_1}{\rho_2} p_1\right) \qquad (6)$$

where $$R = R_0^2 R_i = \frac{g' H_0}{f^2 L^2}$$

If we now assume $R_0 << R$, and approximate $\frac{\rho_1}{\rho_2}$ by unity, the equations can be approximated by

$$\frac{d^2 p_1}{d\eta^2} - \left[\mu^2 + \frac{h_{\eta\eta\eta} - R^{-1} h_\eta}{h_\eta - c_0}\right] p_1 = R^{-1}(p_1 - p_2) \qquad (7)$$

and

$$\frac{d^2 p_2}{d\eta^2} - \left[\mu^2 - \frac{1}{c_0}\frac{H_0}{H_{20}} R^{-1} h_\eta\right] p_2 = \frac{H_0}{H_{20}} R^{-1}(p_1 - p_2) \qquad (8)$$

Note that in deriving Eqs.(7) and (8), R_0 is taken to be very small at the outset, because we are looking at geostrophic disturbances.

If we multiply (7) by $H_0 p_1^*$, and (8) by $H_{20} p_2^*$, add the resulting equations and integrate over η, using the boundary conditions that p_1, p_2 vanish at $\eta = -\infty$ and $\eta = 0$, we arrive at the integral constraint

$$-\int_{-\infty}^{0}\left(H_0\left|\frac{dp_1}{d\eta}\right|^2 + H_{20}\left|\frac{dp_2}{d\eta}\right|^2\right)d\eta$$

$$-\mu^2\int_{-\infty}^{0}\left(H_0|p_1|^2 + H_{20}|p_2|^2\right)d\eta$$

$$-H_0\int_{-\infty}^{0}\left\{\frac{h_{\eta\eta\eta} - R^{-1}h_\eta}{h_\eta - c_0}|p_1|^2 - \frac{R^{-1}h_\eta}{c_0}|p_2|^2\right\}d\eta$$

$$= H_0 R^{-1}\int_{-\infty}^{0}\left\{|p_1|^2 + |p_2|^2 - (p_1^* p_2 + p_2^* p_1)\right\}d\eta$$

Writing $c_c = c_r + i c_i$, and taking the imaginary part of the integral constraint yields

$$c_i\int_{-\infty}^{0}\left[\frac{h_{\eta\eta\eta} - R^{-1}h_\eta}{|h_\eta - c_0|^2}|p_1|^2 + \frac{R^{-1}h_\eta}{|c_0|^2}|p_2|^2\right]d\eta = 0$$

It follows that if c_i is to be non-zero, we require the quantities $(h_{\eta\eta\eta} - R^{-1} h_\eta)$ and $R^{-1} h_\eta$ to have opposite signs in the region of integration. Therefore, the necessary condition for instability if that the interface displacement must be such as to allow

$$h_{\eta\eta\eta} - R^{-1} h_\eta \gtrless 0 \quad \text{and} \quad h_\eta \lessgtr 0$$

Somewhere in the range $-\infty < \eta \leq 0$. It should be noted that this criterion is similar to that obtained by Orlanski (5).

For the simple case of a finite region (the boundary jet) near the wall, where h is a linear function of η, this condition is satisfied. Therefore, such a simple jet may be unstable to quasi-geostrophic disturbances; the next step should be to determine if this is indeed so, and to see if any such instabilities, if they exist, can help explain the observed instability in the boundary jet.

The Constant Velocity Boundary Jet

In the laboratory experiments, the lighter fluid in the jet was initially (before it became unstable) confined to a layer near the wall, while the fluid in the interior of the tank was homogeneous throughout its depth. This suggests that the interface between the lighter and heavier fluid hits the surface at the edge of the jet,

Such a system is similar to Orlanski's polar front model (6) in which he investigated the stability of an idealized front, represented by the interface between two fluids of slightly different density, In the basic equilibrium state, the front (or interface) hits the top and bottom boundaries of the fluid; the main difference between Orlanski's model and the above picture of the jet, is that the interface associated with the jet does not meet the bottom boundary. Thus, although the formulation of the stability problem associated with such a jet will be similar to Orlanski's formulation, the two problems should be sufficiently different as to require a separate treatment for the jet. Unfortunately, the vanishing of the upper layer thickness at the edge of the jet presents some difficulties which we should like to avoid, if possible, at this stage,

Therefore, we shall first look at the stability of a baroclinic jet in which the upper layer thickness is always finite, We shall also assume that the motion of the free surface will have little effect on the stability of the jet, and impose a rigid lid on the system, while still allowing pressure differences along the upper boundary of the fluid.

Now the jet is bounded on one side by a rigid boundary (the side wall) and on the other side by a free boundary, To simplify the mathematics, we shall replace this free side boundary by a rigid boundary; the motion behind this lies in the result Orlanski achieved for very long waves (quasi-geostrophic disturbances?) in which the growth rate was found to follow a curve very close to that derived by Eady (7) for his continuously stratified, baroclinic, quasi-geostrophic model. This seemed to suggest that the same growth rate is obtained regardless of whether the side boundaries are free or rigid. In addition, following Orlanski, we shall formulate the problem for general ageostrophic disturbances; we shall make the geostrophic assumption further on in the problem,

The constant velocity boundary jet with rigid lid.

A. Ageostrophic formulation with rigid side boundaries.

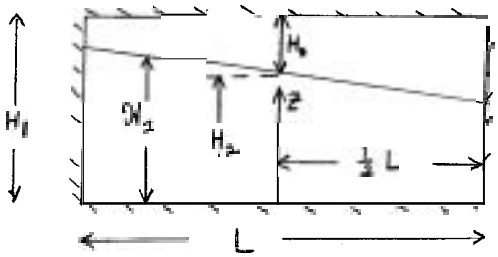

Fig.3 Rigid Side Boundary Model,

We consider two layers of incompressible fluid in a rotating coordinate system with constant Coriolis parameter f. The motion in each layer is hydrostatic and independent of the vertical coordinate z, and the two fluids are bounded above and below by rigid horizontal planes at $z = 0$ and $z = H_1$, and to the side by rigid vertical planes at $x = \pm \frac{1}{2}L$. In the equilibrium state, the upper layer is in motion with velocity V, and the lower layer is at rest; the depths of the upper and lower layer at the mid-point of the jet are H_0 and H_2 respectively. It can be easily shown that the height of the interface $\mathcal{H}_2$ in the equilibrium state is

$$\mathcal{H}_2 = H_2 - \frac{\rho f V}{(\rho_2 - \rho_1)g} x \qquad \text{(A-1)}$$

We are interested in the perturbation to this equilibrium state. Let $v_j' = (u_j', v_j')$ represent the horizontal perturbation velocity in the upper layer $(j=1)$ and the lower layer $(j=2)$. The perturbation pressures p' and p^2 are given at $z=0$ and $z=H_1$ respectively. The equations governing this model, which satisfy the dynamic and kinematic conditions of $z=0$, $\mathcal{H}_2$ and H_1 are, after linearization, as follows:

$$\frac{\partial u_1'}{\partial t} + V\frac{\partial u_1'}{\partial y} - f v_1' = -\frac{1}{\rho_1} p_{1x}' \tag{A-2}$$

$$\frac{\partial v_1'}{\partial t} + V\frac{\partial v_1'}{\partial y} + f u_1' = -\frac{1}{\rho_1} p_{1y}' \tag{A-3}$$

$$\frac{\partial u_2'}{\partial t} - f v_2' = -\frac{1}{\rho_2} p_{2x}' \tag{A-4}$$

$$\frac{\partial v_2'}{\partial t} + f u_2' = -\frac{1}{\rho_2} p_{2y}' \tag{A-5}$$

$$\left(\frac{\partial}{\partial t} + V\frac{\partial}{\partial y}\right) h_2' + \mathcal{H}_{2x} u_1' - (H_1 - \mathcal{H}_2)(u_{1x}' + v_{1y}') = 0 \tag{A-6}$$

$$\frac{\partial h_2'}{\partial t} + \mathcal{H}_{2x} u_2' - \mathcal{H}_2 (u_{2x}' + v_{2y}') = 0 \tag{A-7}$$

$$p_2' - p_1' = (\rho_2 - \rho_1) g h_2' \tag{A-8}$$

where h_2' is the perturbation to $\mathcal{H}_2$, the height of the interface.

If we substitute

$$(u_i', v_i', \ , h_2') = (u_i, v_i, p_i, h_2) e^{i\ell(y-ct)}$$

into the above equations, then Eqs. (A-2) - (A-5) allow the velocity fields to be expressed in terms of the pressure fields, i.e.,

$$u_1 = -\frac{i\ell\left[f p_1 + (V-c)\frac{dp_1}{dx}\right]}{\rho_1\left[f^2 - \ell^2(V-c)^2\right]} \tag{A-9}$$

$$v_1 = \frac{f\frac{dp_1}{dx} + \ell^2(V-c)p_1}{\rho_1\left[f^2 - \ell^2(V-c)^2\right]} \tag{A-10}$$

$$u_2 = -\frac{i\ell\left[f p_2 - c\frac{dp_2}{dx}\right]}{\rho_2\left[f^2 - \ell^2 c^2\right]} \tag{A-11}$$

$$v_2 = \frac{f\frac{dp_2}{dx} - \ell^2 c p_2}{\rho_2\left[f^2 - \ell^2 c^2\right]} \tag{A-12}$$

It then follows that Eqs. (A-6) and (A-7) yield the two coupled equations

$$\frac{il(V-c)}{(\rho_2-\rho_1)g}(p_2-p_1)-\frac{il\mathcal{H}_{2x}\left[f p_1+(V-c)\frac{dp_1}{dx}\right]}{\rho_1\left[f^2-l^2(V-c)^2\right]}+\frac{il(V-c)(H_1-\mathcal{H}_2)\left(\frac{d^2p_1}{dx^2}-l^2p_1\right)}{\rho_1\left[f^2-l^2(V-c)^2\right]}=0 \qquad \text{(A-13)}$$

and

$$-\frac{ilc}{(\rho_2-\rho_1)g}(p_2-p_1)-\frac{il\mathcal{H}_{2x}\left[f p_2-c\frac{dp_2}{dx}\right]}{\rho_2\left[f^2-l^2c^2\right]}+\frac{ilc\,\mathcal{H}_2\left(\frac{d^2p_2}{dx^2}-l^2p_2\right)}{\rho_2\left[f^2-l^2c^2\right]}=0 \qquad \text{(A-14)}$$

We can non-dimensionalize the coefficients of these equations by defining

$$x=\tfrac{1}{2}L\eta \qquad \text{(A-15)}$$

$$c=\tfrac{1}{2}V(\tau+1) \qquad \text{(A-16)}$$

$$R_0=\frac{Vl}{2f} \qquad \text{(A-17)}$$

$$F_1=\frac{\rho_1 f^2L^2}{2(\rho_2-\rho_1)gH_0} \qquad \text{(A-18)}$$

$$F_2=\frac{\rho f^2L^2}{2(\rho_2-\rho_1)gH_2} \qquad \text{(A-19)}$$

$$R=\frac{fL}{V} \qquad \text{(A-20)}$$

Then Eqs. (A-13) and (A-14) become

$$\frac{d^2p_1}{d\eta^2}-\left[\frac{F_1}{\tau-1}+R_0^2R^2\right]p_1+F_1R^{-1}\left\{\frac{d}{d\eta}\left(\eta\frac{dp_1}{d\eta}\right)-R_0^2R^2\eta p_1\right\}=\tfrac{1}{2}F_1\left(1-R_0^2(\tau-1)^2\right)(p_1-p_2) \qquad \text{(A-22)}$$

and

$$\frac{d^2p_2}{d\eta^2}+\left[\frac{F_2}{\tau+1}-R_0^2R^2\right]p_2-F_2R^{-1}\left\{\frac{d}{d\eta}\left(\eta\frac{dp_2}{d\eta}\right)-R_0^2R^2\eta p_2\right\}=-\tfrac{1}{2}F_2\left(1-R_0^2(\tau+1)^2\right)(p_1-p_2) \qquad \text{(A-23)}$$

where we have approximated $\frac{\rho_1}{\rho_2}$ by unity in the second equation. It should be noted that setting $F_1=F_2$ and $F_1R^{-1}=1$ in these equations gives Orlanski's equations, with R being Orlanski's Richardson Number.

Now, the boundary conditions on these equations are that there be no normal motion at the side boundaries, i.e., u_1, u_2 vanish at $x=\pm\frac{1}{2}L$. In non-dimensional terms, these become

$$\frac{dp_1}{d\eta}=\frac{R}{\tau-1}p_1 \qquad \text{at} \qquad \eta=\pm1 \qquad \text{(A-24)}$$

$$\frac{dp_2}{d\eta}=\frac{R}{\tau+1}p_2 \qquad \text{at} \qquad \eta=\pm1 \qquad \text{(A-25)}$$

These equations describe ageostrophic disturbances in general, the ageostrophy coming in with the terms in curly brackets, We are interested in the quasi-geostrophic regime where any ageostrophic effects can be considered small, and shall expand the solution and its eigenvalue τ about the quasi-geostrophic state in terms of some ageostrophic parameter. To set up this perturbation scheme, we define

$$F^2=F_1F_2$$

$$\epsilon=F^2R^{-1}$$

$$R_0 = T\epsilon$$

and

$$R_0 R = K$$

where K is the non-dimensional downstream wave number of the disturbance, such that

$$K = \tfrac{1}{2}\ell L$$

The system of equations and boundary conditions then become

$$\frac{d^2p_1}{d\eta^2} - \left[\frac{F_1}{\tau-1} + K^2\right]p_1 - \tfrac{1}{2}F_1\left[1 - T^2(\tau-1)^2\epsilon^2\right](p_1-p_2) + \frac{\epsilon}{F_2}\left\{\frac{d}{d\eta}\left(\eta\frac{dp_1}{d\eta}\right) - K^2\eta p_1\right\} = 0 \qquad \text{(A-26)}$$

$$\frac{d^2p_2}{d\eta^2} - \left[K^2 - \frac{F_2}{\tau+1}\right]p_2 - \tfrac{1}{2}F_2\left[1 - T^2(\tau+1)^2\epsilon^2\right](p_2-p_1) - \frac{\epsilon}{F_1}\left\{\frac{d}{d\eta}\left(\eta\frac{dp_2}{d\eta}\right) - K^2\eta p_2\right\} = 0 \qquad \text{(A-27)}$$

where

$$\epsilon\frac{dp_1}{d\eta} = \frac{F^2}{\tau-1}p_1 \qquad \text{at } \eta = \pm 1 \qquad \text{(A-28)}$$

$$\epsilon\frac{dp_2}{d\eta} = \frac{F^2}{\tau+1}p_2 \qquad \text{at } \eta = \pm 1 \qquad \text{(A-29)}$$

We now make an expansion in ϵ as follows:

$$p_1 = p_1^{(0)} + \epsilon p_1^{(1)} + \epsilon^2 p_1^{(2)} + \ldots$$

$$p_2 = p_2^{(0)} + \epsilon p_2^{(1)} + \epsilon^2 p_2^{(2)} + \ldots$$

$$\tau = \tau^{(0)} + \epsilon\tau^{(1)} + \epsilon^2\tau^{(2)} + \ldots$$

We can now write down the n^{th} order problem in metric form

$$\underline{\underline{\mathcal{L}}}\,\underline{p}^{(n)} = \underline{f}^{(n)}, \qquad n = 0, 1, 2, \ldots \qquad \text{(A-30)}$$

with boundary conditions

$$\underline{p}^{(n)} = \underline{g}^{(n)}, \qquad n = 0, 1, 2, \ldots \qquad \text{(A-31)}$$

where

$$\underline{\underline{\mathcal{L}}} = \begin{pmatrix} \frac{d^2}{d\eta^2} - \left[K^2 + \frac{1}{2}F_1\frac{\tau^{(0)}+1}{\tau^{(0)}-1}\right] & \frac{1}{2}F_1 \\ \frac{1}{2}F_2 & \frac{d^2}{d\eta^2} - \left[K^2 + \frac{1}{2}F_2\frac{\tau^{(0)}-1}{\tau^{(0)}+1}\right] \end{pmatrix} \qquad \text{(A-32)}$$

$$\underline{p}^{(n)} = \begin{pmatrix} p_1^{(n)} \\ p_2^{(n)} \end{pmatrix}$$

and $\underline{f}^{(n)}$, $\underline{g}^{(n)}$ are functions of $\underline{p}^{(n-1)}, \underline{p}^{(n-2)}, \ldots \underline{p}^{(0)}$.

The Zeroth Order Problem

The zeroth order system is simply the homogeneous problem

$$\frac{d^2p_1^{(0)}}{d\eta^2} - \left[K^2 + \tfrac{1}{2}F_1\frac{\tau^{(0)}+1}{\tau^{(0)}-1}\right]p_1^{(0)} + \tfrac{1}{2}F_1p_2^{(0)} = 0 \qquad \text{(A-33)}$$

$$\frac{d^2 P_2^{(0)}}{d\eta^2} - \left[K^2 + \tfrac{1}{2} F_2 \frac{\tau^{(0)}-1}{\tau^{(0)}+1}\right] P_2^{(0)} + \tfrac{1}{2} F_1 P_1^{(0)} = 0 \qquad \text{(A-34)}$$

with boundary conditions

$$P_1^{(0)} = 0 \qquad \text{at} \quad \eta = \pm 1 \qquad \text{(A-35)}$$

$$P_2^{(0)} = 0 \qquad \text{at} \quad \eta = \pm 1 \qquad \text{(A-36)}$$

The boundary conditions imply a solution of the form

$$P^{(0)} = R_e \left\{ \begin{pmatrix} 1 \\ \beta \end{pmatrix} A \cdot \sin \pi \eta \right\} \qquad \text{(A-37)}$$

Substituting (A-37) into (A-33) and (A-34) gives

$$\begin{pmatrix} -\{\pi^2 + K^2 + \frac{1}{2} F_1 \frac{\tau^{(0)}+1}{\tau^{(0)}-1}\} & \frac{1}{2} F_1 \\ \frac{1}{2} F_2 & -\{\pi^2 + K^2 + \frac{1}{2} F_2 \frac{\tau^{(0)}-1}{\tau^{(0)}+1}\} \end{pmatrix} \begin{pmatrix} 1 \\ \beta \end{pmatrix} = 0$$

For a non-trivial solution, the determinant of the coefficients must vanish, and this result in the following equation for $\tau^{(0)}$

$$(F_1 + F_2 + 2K_0^2)\tau^{(0)2} - 2(F_2 - F_1)\tau^{(0)} + (F_1 + F_2 - 2K_0^2) = 0$$

with solution

$$\tau^{(0)} = \frac{(F_2 - F_1) \pm 2\sqrt{(K_0^4 - F^2)}}{F_1 + F_2 + 2K_0^2} \qquad \text{(A-38)}$$

and

$$\beta = \frac{2K_0^2}{F_1} + \frac{\tau^{(0)}+1}{\tau^{(0)}-1} \qquad \text{(A-39)}$$

It can be seen that instability is assured for all non-zero currents when F exceeds the critical value

$$F_c = K_0^2 = K^2 + \pi^2$$

This is a similar result to that found by Pedlosky (8) for the equal depth layer case.

For unstable disturbances, it can be easily shown that the maximum growth rate occurs at some small, but finite value of K. The small ageostrophy of the flow will presumably add a correction to τ, and hence the growth rate kc_i. This will then shift the critical value of the wave number K away from the geostrophic value. It was decided to take the expansion to higher order in ϵ in order to determine the first non-trivial correction to τ.

However, before this had progressed very far, an experiment was performed by W. Facinelli in the basement of Walsh Cottage at the Woods Hole Oceanographic Institution in which this instability was observed, and some crude measurements were made of the relevant parameters. These were

$$\frac{\Delta\rho}{\rho} \simeq 0.005, \qquad H_0 = 3/4 \text{ cm}, \qquad H_2 = 11\tfrac{1}{2} \text{ cm}, \qquad f = 1 \text{ rd.s}^{-1},$$

and the critical downstream wavelength of the instability was approximately 15 cm. The width of the boundary jet was approximately 2 - 3 cm. For these values

$$F = \sqrt{F_1 F_2} = \frac{f^2 L^2}{2g'\sqrt{H_0 H_2}} \sim \frac{1}{4} < \pi^2$$

The conclusion is that such a jet is stable to geostrophic disturbances; this suggests either that the instability is not a geostrophic instability, or the

rigid side boundaries are too great a constraint, and need to be relaxed. It will be seen later that this second possibility is probably correct.

The above results indicate that the ageostrophic perturbation problem for rigid side boundaries is irrelevant to the boundary jet instability we are interested in. However, an outline of the perturbation analysis is in order, because it could be relevant to larger scale problems.

Formulation of the integral constraint for the n^{th} order problem

The first and higher order systems in ϵ are in general inhomogeneous, and the possibility exists of secularities occurring. Therefore we must seek an integral condition on the n^{th} order system in order to allow a solution to exist.

It can be shown that the corresponding homogeneous adjoint problem associated with (A-30) and (A-31) is

$$\underline{\underline{\mathcal{L}}}^{\dagger}\,\underline{\Psi} = 0 \qquad \text{(A-40)}$$

with boundary conditions

$$\Psi = 0 \qquad \text{at } \eta = \pm 1 \qquad \text{(A-41)}$$

where

$$\underline{\underline{\mathcal{L}}}^{\dagger} = \begin{pmatrix} \mathcal{L}_{11}^{*} & \mathcal{L}_{21}^{*} \\ \mathcal{L}_{12}^{*} & \mathcal{L}_{22}^{*} \end{pmatrix}$$

If we define the scalar product of two vectors $\underline{a}$ and $\underline{b}$ as follows:

$$\langle \underline{a}, \underline{b} \rangle = a_1^{*} b_1 + a_2^{*} b_2$$

then, starting from the integral equation

$$\int_{-1}^{1} \langle \underline{P}^{(n)}, \underline{\underline{\mathcal{L}}}^{\dagger}\,\underline{\Psi} \rangle \, d\eta = 0$$

integrating by parts, and using the boundary condition on $\underline{\Psi}$, $\underline{P}^{(n)}$ we arrive at the required integral condition that (A-30), (A-31) possess a solution, i.e.,

$$\int_{-1}^{1} \langle \underline{\Psi}, \underline{\underline{\mathcal{L}}}\,\underline{P}^{(n)} \rangle \, d\eta + \left[\left\langle \frac{d\underline{\Psi}}{d\eta}, \underline{P}^{(n)} \right\rangle \right]_{-1}^{1} = 0 \qquad \text{(A-42)}$$

Since $\underline{\underline{\mathcal{L}}}\,\underline{P}^{(n)}$ and $\underline{P}^{(n)}|_{\eta=\pm 1}$ are known, it remains only to specify $\underline{\Psi}$. It can be easily shown that

$$\underline{\Psi} = \left(\frac{1}{\gamma^{*}}\right) \sin \pi \eta \qquad \text{(A-43)}$$

where

$$\gamma = \frac{F_1}{F_2}\,\beta \qquad \text{(A-44)}$$

Equation (A-42), when expanded out, can be easily seen to be an equation determining $\tau^{(n)}$, the n^{th} order correction to τ.

The first order problem

The first order system takes the form

$$\frac{d^2 p_1^{(1)}}{d\eta^2} - \left[K^2 + \tfrac{1}{2} F_1 \frac{\tau^{(0)}+1}{\tau^{(0)}-1}\right] p_1^{(1)} + \tfrac{1}{2} F_1 p_2^{(1)} = -\left\{ \frac{1}{F_2} \frac{d}{d\eta}\left(\eta \frac{dp_1^{(0)}}{d\eta}\right) - \frac{K^2}{F_2}\eta p_1^{(0)} + \frac{F_1 \tau^{(1)}}{(\tau^{(0)}-1)^2} p_1^{(0)} \right\}$$

$$\frac{d^2 p_2^{(1)}}{d\eta^2} - \left[K^2 + \tfrac{1}{2} F_2 \frac{\tau^{(0)}-1}{\tau^{(0)}+1}\right] p_2^{(1)} + \tfrac{1}{2} F_2 p_1^{(1)} = \left\{ \frac{1}{F_1} \frac{d}{d\eta}\left(\eta \frac{dp_2^{(0)}}{d\eta}\right) - \frac{K^2}{F_1}\eta p_2^{(0)} + \frac{F_2 \tau^{(1)}}{(\tau^{(0)}+1)^2} p_2^{(0)} \right\}$$

with boundary conditions

$$p_1^{(1)} = \frac{\tau^{(0)}-1}{F^2} \frac{dp_1^{(0)}}{d\eta} \qquad \text{at } \eta = \pm 1$$

$$P_2^{(1)} = \frac{\tau^{(0)}+1}{F^2}\frac{dP_2^{(0)}}{d\eta} \qquad \text{at} \quad \eta = \pm 1$$

The integral constraint, with $\eta = 1$, yields the result

$$\tau^{(1)} = 0$$

Therefore, we need to go to the second order problem to calculate the lowest order correction to τ.

It is possible to show, after a lot of algebra, that the solution to the first order system is

$$\begin{pmatrix} P_1^{(1)} \\ P_2^{(1)} \end{pmatrix} = \begin{pmatrix} 1 \\ \beta \end{pmatrix} B \sin \pi\eta + \begin{pmatrix} d_1 \\ \beta d_1 - t_1 \end{pmatrix} \cos \pi\eta + \begin{pmatrix} 1 \\ \mu \end{pmatrix} s_1 \cosh K\eta + \begin{pmatrix} b_1 \\ b_2 \end{pmatrix} \eta \sin \pi\eta + \begin{pmatrix} 1 \\ \beta \end{pmatrix} f_1 \eta^2 \cos \pi\eta \qquad \text{(A-45)}$$

where

$$f_1 = \frac{A}{8\pi}\left(\beta - \frac{1}{\beta}\right)$$

$$t_1 = -\frac{\pi\beta(F_1+F_2)A}{F^2 K_0^2}$$

$$\mu = -\frac{F_2}{F_1\beta}$$

$$s_1 = \frac{t_1 + \frac{2\pi\beta A}{F^2}}{(\beta-\mu)\cosh K}$$

$$d_1 = \frac{\pi\tau^{(0)}A}{F^2} - f_1 + \frac{t_1 + \frac{(\beta+\mu)\pi A}{F^2}}{\beta-\mu}$$

$$b_1 = \left[\frac{(\beta^2-1)(2\pi^2-K_0^2)}{8\pi^2\beta K_0^2} - \frac{\beta(F_1+F_2)}{2F_2K_0^2}\right]A$$

$$b_2 = \left[\frac{(\beta^2-1)(2\pi^2-K_0^2)}{8\pi^2 K_0^2} + \frac{(F_1+F_2)}{2F_1K_0^2}\right]$$

and B is an arbitrary constant.

The Second Order System

The second order system takes the form

$$\frac{d^2P_1^{(2)}}{d\eta^2} - \left[K^2 + \tfrac{1}{2}F_1\frac{\tau^{(0)}+1}{\tau^{(0)}-1}\right]P_1^{(2)} + \tfrac{1}{2}F_1P_2^{(2)} = -\left\{\frac{1}{F_2}\frac{d}{d\eta}\left(\eta\frac{dP_1^{(1)}}{d\eta}\right) - \frac{K^2}{F_2}\eta P_1^{(1)} + \frac{F_1\tau^{(2)}}{(\tau^{(0)}-1)^2}P_1^{(0)} + \tfrac{1}{2}F_1T^2(\tau^{(0)}-1)^2(P_1^{(0)}-P_2^{(0)})\right\}$$

$$\frac{d^2P_2^{(2)}}{d\eta^2} - \left[K^2 + \tfrac{1}{2}F_1\frac{\tau^{(0)}-1}{\tau^{(0)}+1}\right]P_2^{(2)} + \tfrac{1}{2}F_2P_1^{(2)} = \left\{\frac{1}{F_1}\frac{d}{d\eta}\left(\eta\frac{dP_2^{(1)}}{d\eta}\right) - \frac{K^2}{F_1}\eta P_2^{(1)} + \frac{F_2\tau^{(2)}}{(\tau^{(0)}+1)^2}P_2^{(0)} + \tfrac{1}{2}F_2T^2(\tau^{(0)}+1)^2(P_1^{(0)}-P_2^{(0)})\right\}$$

and the boundary conditions are

$$P_1^{(2)} = \frac{\tau^{(0)}-1}{F^2}\frac{dP_1^{(0)}}{d\eta} \qquad \text{at} \quad \eta = \pm 1$$

$$P_2^{(2)} = \frac{\tau^{(0)}+1}{F^2}\frac{dP_2^{(0)}}{d\eta} \qquad \text{at} \quad \eta = \pm 1$$

The integral constraint on this system gives the following expression for $\tau^{(2)}$:

$$F_1\left[\frac{\beta^2}{(\tau^{(0)}+1)^2}-\frac{1}{(\tau^{(0)}-1)^2}\right]A\tau^{(2)}=\frac{1}{2}F_1(\beta-1)T^2A\left[\beta(\tau^{(0)}+1)^2-(\tau^{(0)}-1)^2\right]+\frac{(\beta^2-1)}{F_2}\left[(2\pi^2-K_0^2)\frac{d_1}{2\pi}+\right.$$

$$\left.+\frac{20\pi^4-6\pi^2K_0^2-24\pi^2+9K_0^2}{12\pi^3}f_1\right]+\frac{\beta b_2-b_1}{F_2}\left[\frac{3\pi^2+2\pi^2K_0^2-3K_0^2}{6\pi^2}\right]-(2\pi^2-K_0^2)\frac{\beta t_1}{2\pi F_2}+$$

$$+\frac{2\pi K s_1}{K_0^2}\left(\frac{F_1+F_2}{F_2}\right)\left(1+\frac{4K^2}{K_0^2}\right)\sinh K-4\pi s_1\left(\frac{F_1+F_2}{F_2}\right)\frac{K^2}{K_0^2}\cosh K-\frac{4\pi K s_1}{)=,}\sinh |<-$$

$$-\frac{2\pi^2}{F^2}\left[(\tau^{(0)}-1)b_1+\frac{F_1b}{F_2}(\tau^{(0)}+1)b_2\right]-\frac{4\pi f_1}{F^2}\left[\tau^{(0)}-1+\frac{F_1}{F_2}\beta^2(\tau^{(0)}+1)\right] \qquad \text{(A-46)}$$

B. Geostrophic formulation with rigid-free side boundaries.

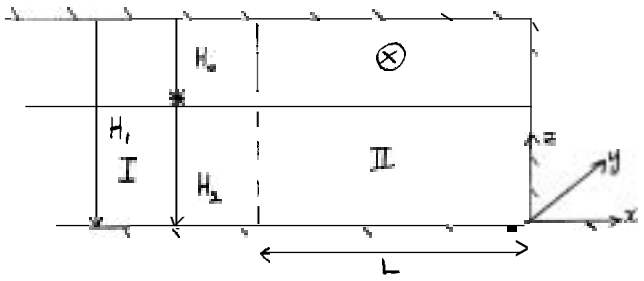

Fig.4 Rigid-free side boundary model.

We consider much the same kind of model as in A, with the following modifications. The origin has been shifted to the right boundary which remains a rigid boundary, and the left boundary at x = -L has been replaced by a free boundary, with fluid extending to the left of this. This relaxation of the left-side boundary follows from the possibility arising out of the previous section that a rigid left-hand boundary stabilizes the geostrophic disturbances we are interested in. The mean depths H_0 and H_2 are taken to be the equilibrium depths of the layers to the left of the free boundary at $x = -L$, i.e. outside the jet. As in section A, in the region $-L \leq x \leq 0$, the upper layer is in motion at velocity V and the lower layer is at rest. From the outset, we shall be considering geostrophic disturbances, and variations in the interface height in the equilibrium state will be considered small.

If we set

$$P_1 = \Psi_1 \qquad \text{(B-1)}$$

$$P_2 = \Psi_2 \qquad \text{(B-2)}$$

it can be easily shown that

$$\left(\frac{\partial}{\partial t}+V\frac{\partial}{\partial x}\right)\left[\nabla^2\Psi_1+\frac{\rho_1 f^2}{(\rho_2-\rho_1)gH_0}(\Psi_2-\Psi_1)\right]+\frac{\rho f^2 V}{(\rho_2-\rho)gH_0}\Psi_{1y}=0 \qquad \text{(B-3)}$$

and

$$\frac{\partial}{\partial t}\left[\nabla^2\Psi_2-\frac{\rho_1 f^2}{(\rho_2-\rho_1)gH_2}(\Psi_2-\Psi_1)\right]-\frac{\rho_1 f^2}{(\rho_2-\rho_1)gH_2}\Psi_{2y}=0 \qquad \text{(B-4)}$$

Note that in the region $x < -L$, $V = 0$.

Now we can set

$$= \phi_i \exp\{il(y-ct)\}$$

and the equations become

$$\frac{d^2\phi_1}{dx^2} - \ell^2\phi_1 + \frac{\rho_1 f^2}{(\rho_2-\rho_1)gH_0}\,\frac{V}{V-c}\,\phi_1 + \frac{\rho_1 f^2}{(\rho_2-\rho_1)gH_0}(\phi_2-\phi_1) = 0$$

$$\frac{d^2\phi_2}{dx^2} - \ell^2\phi_2 + \frac{\rho_1 f^2}{(\rho_2-\rho_1)gH_2}\,\frac{V}{c}\,\phi_2 + \frac{\rho_2 f^2}{(\rho_2-\rho_1)gH_2}(\phi_1-\phi_2) = 0$$

We can non-dimensionalize these equations to some extent by defining

$$x = L\eta$$
$$k = \ell L$$
$$F_1 = \frac{\rho_1 f^2 L^2}{(\rho_2-\rho_1)gH_0}$$
$$F_2 = \frac{\rho_2 f^2 L^2}{(\rho_2-\rho_1)gH_2}$$

thus yielding the following set of equations

$$\frac{d^2\phi_1}{d\eta^2} - \left(k^2 - F_1\frac{c}{V-c}\right)\phi_1 + F_1\phi_2 = 0 \qquad \text{(B-5)}$$

$$\frac{d^2\phi_2}{d\eta^2} - \left(k^2 - F_2\frac{V-c}{c}\right)\phi_2 + F_2\phi_1 = 0 \qquad \text{(B-6)}$$

where we have made the approximation $\frac{\rho_1}{\rho_2} \simeq 1$.

The boundary conditions on these equations require (i) the velocities to be continuous across the free side boundary, (ii) the normal velocity to vanish at the rigid side boundary, and (iii) the velocities to vanish very far away, i.e.,

$\phi_i,\ \phi_{i\eta}$ continuous at $\eta = -1,\ i = 1, 2$ (B-7)

$\phi_i = 0$ at $\eta = 0,\ i = 1, 2$ (B-8)

$\phi_i,\ \phi_{i\eta} = 0$ at $\eta = -\infty,\ i = 1, 2$ (B-9)

Region I: $\eta < -1,\ V = 0$

$$\frac{d^2\phi_1}{d\eta^2} - (k^2 + F_1)\phi_1 + F_1\phi_2 = 0$$
$$\frac{d^2\phi_2}{d\eta^2} - (k^2 + F_2)\phi_2 + F_2\phi_1 = 0$$

We set

$$\begin{pmatrix}\phi_1\\ \phi_2\end{pmatrix} = \begin{pmatrix}a_1\\ a_2\end{pmatrix}e^{\lambda\eta}$$

$$\therefore \begin{vmatrix}\lambda^2 - k^2 - F_1 & F_1\\ F_2 & \lambda^2 - k^2 - F_2\end{vmatrix} = 0$$

for a non-trivial solution to exist.

The solution of this equation is

$$\lambda^2 = k^2,\ F_1 + F_2 + k^2$$

For the solution $\lambda_1 = k$, we have $a_2 = a_1$

and for $\lambda_2 = \sqrt{(F_1 + F_2 + k_2)}$ we have $a_2 = -\frac{F_2}{F_1} a_1$

The boundary condition (B-9) implies that the solution in Region I is

$$\begin{pmatrix} \phi_1 \\ \phi_2 \end{pmatrix}_I = \begin{pmatrix} A_1 \\ A_1 \end{pmatrix} e^{\lambda_1(\eta+1)} + \begin{pmatrix} A_2 \\ -\frac{F_2}{F_1} \end{pmatrix} e^{\lambda_2(\eta+1)} \qquad \text{(B-10)}$$

Region II: $-1 < \eta \leq 0$, V = constant

$$\therefore \quad \frac{d^2\phi_1}{d\eta^2} - \left(\ell^2 - F_1 \frac{c}{V-c}\right)\phi_1 + F_1 \phi_2 = 0$$

$$\frac{d^2\phi_2}{d\eta^2} - \left(\ell^2 - F_2 \frac{V-c}{c}\right)\phi_2 + F_2 \phi_1 = 0$$

We set

$$\begin{pmatrix} \phi_1 \\ \phi_2 \end{pmatrix} = \begin{pmatrix} a_1 \\ a_2 \end{pmatrix} e^{\mu\eta}$$

Then, for a non-trivial solution, we require

$$\begin{vmatrix} \mu^2 - k^2 - F_1 \frac{c}{V-c} & F_1 \\ F_2 & \mu^2 - k^2 - F_2 \frac{V-c}{c} \end{vmatrix} = 0$$

The solution of this equation is

$$\mu^2 = k^2, \; k^2 - F_1 \frac{c}{V-c} - F_2 \frac{V-c}{c}$$

For the solution $\mu = \mu_1 = k$, we have

$$a_2 = -\frac{c}{V-c} a_1$$

and for $\mu = \mu_2 = i\sqrt{\left(F_1 \frac{c}{V-c} + F_2 \frac{V-c}{c} - k^2\right)}$

$$a_2 = \frac{F_1}{c} a_1$$

The solution for ϕ_1, ϕ_2 can be written

$$\begin{pmatrix} \phi_1 \\ \phi_2 \end{pmatrix}_{II} = \begin{pmatrix} 1 \\ -\frac{c}{V-c} \end{pmatrix} B_1 \sinh \mu_1 \eta + \begin{pmatrix} 1 \\ -\frac{c}{V-c} \end{pmatrix} B_3 \cosh \mu_1 \eta + \begin{pmatrix} 1 \\ \frac{F_2}{F_1}\frac{V-c}{c} \end{pmatrix} B_2 \sin \mu_2 \eta + \begin{pmatrix} 1 \\ \frac{F_2}{F_1}\frac{V-c}{c} \end{pmatrix} B_4 \cos \mu_2 \eta$$

The boundary condition (B-8) implies that $B_3 = B_4 = 0$ except when

$$F_1 \frac{c}{V-c} + F_2 \frac{V-c}{c} = 0, \quad \text{in which case } B_4 = -B_3.$$

However, in this case $\mu_2 = i\mu_1$. Therefore, without loss of generality we shall take $B_3 = B_4 = 0$, and

$$\therefore \begin{pmatrix} \phi_1 \\ \phi_2 \end{pmatrix}_{II} = \begin{pmatrix} 1 \\ -\frac{c}{V-c} \end{pmatrix} B_1 \sinh \mu_1 \eta + \begin{pmatrix} 1 \\ \frac{F_2}{F_1}\frac{V-c}{c} \end{pmatrix} B_2 \sin \mu_2 \eta \qquad \text{(B-11)}$$

provided $\mu_2 \neq i\mu_1$. (see later).

We now match the solutions at $\eta = -1$; this yields the set of four equations:

$$A_1 + A_2 + B_1 \sinh \mu_1 + B_2 \sin \mu_2 = 0$$

$$A_1 - \frac{F_2}{F_1} A_2 - \frac{c}{V-c} B_1 \sinh \mu_1 + \frac{F_2}{F_1} \frac{V-c}{c} B_2 \sin \mu_2 = 0$$

$$\lambda_1 A_1 + \lambda_2 A_2 - \mu_1 B_1 \cosh \mu_1 - \mu_2 B_2 \cos \mu_2 = 0$$

$$\lambda_1 A_1 - \frac{F_2}{F_1} \lambda_2 A_2 + \frac{\mu_1 c}{V-c} B_1 \cosh \mu_1 - \frac{F_2}{F_1} \mu_2 \frac{V-c}{c} B_2 \cos \mu_2 = 0$$

A non-trivial solution exists if the determinant of the coefficients vanishes. If we define the following

$$\beta = \frac{F_2}{F_1}$$
$$S(\mu_1) = \sinh \mu_1$$
$$S(\mu_2) = \sin \mu_2$$
$$C(\mu_1) = \cosh \mu_1$$
$$C(\mu_2) = \cos \mu_2$$

this condition becomes

$$(1+\beta)\left\{\beta \frac{V}{c}\left[\mu_1\mu_2 C(\mu_1) C(\mu_2) + \mu_1\lambda_1 C(\mu_1) S(\mu_2) + \lambda_2\mu_2 S(\mu_1) C(\mu_2) + \lambda_1\lambda_2 S(\mu_1) S(\mu_2)\right] - \right.$$
$$\left. - \left(\beta - \frac{c}{V-c}\right)\left[\mu_1\mu_2 C(\mu_1) C(\mu_2) + \mu_1\lambda_2 C(\mu_1) S(\mu_2) + \lambda_1\mu_2 S(\mu_1) C(\mu_2) + \lambda_1\lambda_2 S(\mu_1) S(\mu_2)\right]\right\} +$$
$$+ \beta\left(\beta \frac{V}{c} - \frac{V}{V-c}\right)\left[\mu_2(\lambda_1 - \lambda_2) S(\mu_1) C(\mu_2) - \mu_1(\lambda_1 - \lambda_2) S(\mu_2) C(\mu_1)\right] = 0 \qquad \text{(B-12)}$$

In analogy with the corresponding problem with rigid side walls, where a sine function was fitted into the jet region so that it vanished at both boundaries, we can put

$$\mu_2 = 2\pi$$

thereby implying

$$F_1 \frac{c}{V-c} + F_2 \frac{V-c}{c} = k^2 + 4\pi^2$$

and $C(\mu_2) = 1 \quad S(\mu_2) = 0$

If we substitute these values into (B-12) we should obtain some condition for the "free-rigid side boundary" problem to have the same structure as the "rigid-rigid side boundary" problem. This results in

$$2\pi k\left[\beta(1+\beta)\frac{V}{c} C(\mu_1) - (1+\beta)\left(\beta - \frac{c}{V-c}\right)\left(C(\mu_1) + S(\mu_1)\right) + \beta\left(\beta \frac{V}{c} - \frac{V}{V-c}\right) S(\mu_1)\right] +$$
$$+ 2\pi\lambda_2 S(\mu_1)\left(\beta \frac{V}{c} + \frac{\beta V}{V-c}\right) = 0$$

Since $S(\mu_1) = \sinh \mu_1 = \sinh k = k + \frac{1}{6}k^3 + \ldots$ it follows that one root of this equation is $k = 0$.

This suggests that the "free-rigid side boundary" problem may have the same structure as the "rigid-rigid side boundary" problem if the downstream wavelength is zero, Therefore, it is not altogether surprising that Orlandki derived a growth rated curve for very long downstream wavelengths very close to the one Eady calculated. It also points to the error in our intuition in assuming that the "rigid-rigid" side

boundary problem could illuminate the nature of the boundary jet instability observed; rather, placing two rigid side boundaries on the jet appears to place too great a constraint on geostrophic disturbances.

We shall now redefine

$$\mu = \mu_2 = F_1 \frac{c}{V-c} + F_2 \frac{V-c}{c} - k^2$$
$$\lambda = \lambda_2 = \sqrt{(F_1 + F_2 + k^2)}$$

and, using $\mu_1 = \lambda_1 = k$, Eq.(B-12) can be rewritten

$$(1+\beta)\left\{\beta \frac{V}{c}\left[k\mu C(k)C(\mu) + k^2 C(k)S(\mu) + \lambda\mu S(k)C(\mu) + k\lambda S(k)S(\mu)\right] - \right.$$
$$\left. - \left(\beta - \frac{c}{V-c}\right)\left[k\mu C(k)C(\mu) + k\lambda C(k)S(\mu) + k\mu S(k)C(\mu) + k\lambda S(k)S(\mu)\right]\right\} +$$
$$+ \beta\left(\beta\frac{V}{c} - \frac{V}{V-c}\right)\left[\mu(k-\lambda)S(k)C(\mu) - k(k-\lambda)S(\mu)C(k)\right] = 0 \qquad \text{(B-13)}$$

where

$$C(k) = \cosh k, \; S(k) = \sinh k$$
$$C(\mu) = \cos\mu, \; S(\mu) = \sin\mu$$

We now assume that $|\mu|$ is small; the motivation behind this is that $\mu = 2\pi$, i.e. $O(1)$, leads to stability for the laboratory scales considered. With this assumption, we can approximate

$$C(\mu) \approx 1$$
$$S(\mu) \approx \mu$$

and Eq.(B- 13) becomes

$$\mu\left\{k(1+\beta)\left(\beta\frac{V-c}{c} + \frac{c}{V-c}\right)\left(C(k) + \lambda S(k)\right) + \frac{\beta V^2}{c(V-c)}\left(k^2 C(k) + \lambda S(k)\right) - \right.$$
$$\left. - k\left(2\beta - \left[\frac{c}{V-c} + \beta^2\frac{V-c}{c}\right]\right)\left(\lambda C(k) + S(k)\right)\right\} = 0 \qquad \text{(B-14)}$$

We shall treat the two solutions to this equation separately.

Case 1.

Here we have $\mu = 0$ which can be rewritten as

$$\left(F_1 + F_2 + k^2\right)c^2 - \left(2F_2 + k^2\right)Vc + F_2 V^2 = 0$$

The solution of this eauation is

$$c = V\left[\frac{2F_2 + k^2}{2(F_1 + F_2 + k^2)} \pm \frac{\sqrt{(k^4 - 4F_1F_2)}}{2(F_1 + F_2 + k^2)}\right] \qquad \text{(B-15)}$$

This mode possesses unstable solutions provided

$$4F_1F_2 > k^4 \qquad \text{(B-16)}$$

which states that the jet is unstable to long wavelengths, a conclusion which we expect physically.

If condition (B-16) is satisfied, the growth rate is

$$kc_i = \frac{Vk\sqrt{(4F_1F_2 - k^4)}}{2(k^2 + F_1 + F_2)} \qquad \text{(B-17)}$$

Case 2.

Here, the quantity in curly brackets in Eq. (B-14) is equal to zero; this can be rewritten

$$Ac^2 - 2BVc + Dc^2 = 0$$

where

$$A = k(1+\lambda)(1+\beta)^2(C(k)+S(k))$$

$$B = \beta k(1+\lambda)(1+\beta)(C(k)+S(k))$$

$$D = \beta\left[(k+\beta k+k^2+\beta k\lambda)C(k)+(k\lambda+\beta k\lambda+\lambda+k\beta)S(k)\right]$$

The solution of this equation is

$$c = \left(\frac{\beta}{1+\beta} \pm \frac{i\beta^{1/2}}{(1+\beta)}\sqrt{\frac{(1+k)(C(k)+\lambda\frac{S(k)}{k})}{(1+\lambda)(C(k)+S(k))}}\right)V$$

It is apparent that this mode is always unstable; the corresponding growth rate is

$$k c_i = \frac{\beta^{1/2}Vk}{1+\beta}\sqrt{\frac{(1+k)(C(k)+\lambda\frac{S(k)}{k})}{(1+\lambda)(C(k)+S(k))}} \qquad \text{(B-18)}$$

The quantity under the square root sign is very close to unity for all values of k, and consequently, this branch implies a growth rate which increases linearly with k. This branch appears to be an unphysical one. Indeed, if we approximate

$$c = \left(\frac{\beta}{1+\beta} + \frac{i\sqrt{\beta}}{1+\beta}\right)V$$

it follows that

$$F_1\frac{c}{V-c} + F_2\frac{V-c}{c} = 0$$

This means that $\mu_2 = i\mu_1$. It will now be shown that this leads to a trivial result. When $\mu_2 = i\mu_1$, B_1 and B_2 are not independent, and the solution in Region II is not given by (B-11); instead it is

$$\begin{pmatrix}\phi_1\\ \phi_2\end{pmatrix}_{II} = \begin{pmatrix}1\\ -\frac{c}{V-c}\end{pmatrix}B_1\sinh K\eta + \begin{pmatrix}1\\ -\frac{c}{V-c}\end{pmatrix}B_3\cosh K\eta$$

Matching the solutions at $\eta = -1$ gives

$$A_1 + A_2 + B_1\sinh K - B_3\cosh K = 0 \qquad \text{(B-19)}$$

$$A_1 - \beta A_2 - \frac{c}{V-c}B_1\sinh K + \frac{c}{V-c}B_3\cosh K = 0 \qquad \text{(B-20)}$$

$$\lambda_1 A_1 + \lambda_2 A_2 - KB_1\cosh K + K\sinh K B_3 = 0 \qquad \text{(B-21)}$$

$$\lambda_1 A_1 - \beta\lambda_2 A_2 + \frac{cK}{V-c}B_1\cosh K - \frac{cK}{V-c}B_3\sinh K = 0 \qquad \text{(B-22)}$$

Eliminating B_1 and B_3 from Eqs. (B-19) and (B-20) yields

$$\frac{V}{V-c}A_1 + \left(\frac{c}{V-c} - \beta\right)A_2 = 0$$

Similarly, (B-21) and (B-22) give

$$\lambda_1\frac{V}{V-c}A_1 + \lambda_2\left(\frac{c}{V-c} - \beta\right)A_2 = 0$$

from which we have $A_1 = A_2 = 0$. Equations (B-19) and (B-21) then imply $B_1 = 0 = B_3$.

Therefore it appears that this second branch, with growth rate given by (B-18), is very close to a trivial solution to the system. At first it was thought that this suggested that the mode of physical interest is the first case. More will be said about this in the next section.

The Growth Rate.

We have seen that the growth rate of unstable geostrophic disturbances in case (i) is given by

$$kc_i = \frac{Vk\sqrt{(4F_1F_2 - k^4)}}{2(F_1 + F_2 + k^2)}$$

We now seek the value of k at which this attains a maximum; this critical value of k satisfies the equation

$$k^6 + 3(F_1+F_2)k^4 + 4F_1F_2k^2 - 4F_1F_2(F_1+F_2) = 0 \qquad \text{(B-23)}$$

For the experimental observations quoted above, ($f = 1\ s^{-1}$, $\quad = 0.005$, H_0 = 3/4 cm, H_2 = 11½ cm, $L \approx 2$ cm.) the values of F_1 and F_2 are

$$F_1 \simeq 1, \quad F_2 \simeq 1/16$$

and (B-23) can be approximated by

$$4k^6 + 12k^4 + k^2 - 1 = 0$$

An approximate solution to this equation is $k^2 \simeq 1/4$. Therefore, the critical value of the downstream wavelength is approximately 24 cm, which compares well with the observed wavelength of 15 cm, considering the crudeness of the experiment and the measurements.

We can understand physically why (i) the disturbance seeks a large, but finite downstream wavelength, and (ii) it is more likely to be stable with two rigid side boundaries than with one rigid side boundary, for the following reasons: It is a well-known result in theoretical physical oceanography that the relative proportion of available potential energy to kinetic energy in a rotating, stratified flow depends on the ratio of the length scale of the flow to the internal radius of deformation; for a given amount of kinetic energy in the flow, larger scale flows possess more available potential energy than small scale flows. Now in the baroclinic boundary jet, the system is expected to seek a mode with as large a levelling off in the interface as is physically possible, i.e., a disturbance flow possessing a lot of available potential energy. Therefore, the system will favour large scale flows over small scale flows. Contrariwise, the system would not be expected to favour flows of too great a scale, because the kinetic energy would become trivial in the limit of infinite scale. Therefore, there must be a finite, optimum length scale at which the disturbance manifests itself.

In the case of a jet with two rigid side boundaries, if the width of the jet is small enough, the disturbances will be attempting to assume a length scale considerably larger than the width of the jet, but will be "seeing" the constraining second rigid wall far too soon. Consequently, they are much more likely to be damped than if this rigid barrier were not there, i.e., the "interior" side boundary was free.

Now although growth rate in case (i) gave a critical wavelength which agreed remarkably with experiment, the solution $\mu = 0$ gives rise to some grave difficulties. At a late date in the program, it was noticed by the author that the exact root $\mu = 0$

presents the following difficulty: in the solution (B-11), the second term is trivial and the set of equations in A_1, A_2, and B_1 may be inconsistent. This difficulty had not been resolved at the time of writing. It is thought that a closer look at the original condition (B-13) may be in order. In addition, the difficulty previously mentioned with the case (ii) may not be as bad as it looked at first: the c_i of case (ii) is not exactly equal to $\frac{1}{2}\sqrt{\beta}\, V/(1+\beta)$, and the solution may approach the trivial solution but never actually reach it. One suggested approach is to set $\mu = \epsilon(k)$ where ϵ is small, and solve for ϵ. If these approaches do not resolve the difficulty, it may be that the problem has been ill-posed.

Conclusions and suggestions for future work

This project contains both success and failure. We have attempted the study of the stability of a baroclinic boundary jet in a rotating fluid. Experiment teaches that such a jet is unstable under cetain circumstances. Assuming the jet is geostrophic, one-dimensional and confined to the upper layer, the Rayleigh criterion for rotating, geostrophic flows implies

(i) if geostrophic disturbances are confined to the upper layer, the jet is always stable provided the basic potential vorticity gradient does not change sign and (ii) for a jet that is wide enough and slow enough, geostrophic disturbances (in both layers) may be unstable if the non-dimensional displacement h of the interface is such that $h_{\eta\eta\eta} - R^{-1} h_\eta$ and h_η have opposite signs somewhere.

The stability of a constant velocity boundary jet with a free interior side boundary has two branches. One branch, case (1), was found to give an instability for small enough k, the downstream wavenumber, and possesses a growth rate,

$$\frac{Vk\sqrt{(4F_1F_2 - k^4)}}{2(F_1 + F_2 + k^2)}$$

The critical wavenumber k_c was found to agree fairly well with an observed value in the laboratory. However, this branch, defined by $\mu = 0$, leads to an inconsistency in the original condition equation, probably leading to trivial result.

The second branch looks, in the light of this, to be the only non-trivial branch. To first order, it gives a growth rate which grows linearly with k; this soon breaks down as $k \to 1$ and the original assumption $|\mu|$ small is violated. A much closer look at this branch is in order.

The above difficulties are somewhat disconcerting, since on physical grounds, we can expect a geostrophic instability at a wavelength somewhat larger than the width of the jet. No definite conclusions can be made regarding the stability of the jet to geostrophic disturbance until these difficulties are clarified.

In future work, of first priority is the clarification of the above difficulties. After this, it would be desirable to investigate the effect of ageostrophy on the instability. Also, some quantitative statement of the stabilizing or destabilizing effect of viscosity would be very desirable.

Acknowledgments

I would like to thank Drs. George Veronis and Melvin Stern for suggesting this problem to me, and to them and Drs. Joseph Pedlosky and Stephen Davis for their many helpful discussions. I would also like to extend thanks to the National Science Foundation for their financial support during an active and stimulating summer.

References

(1) Saunders, K.D. 1971 "On the formation of the North Atlantic Bottom Water" in G.F.D. Fellowship Lectures, Vol.II: 61-71.

(2) Facinelli, W. 1975 "Geostrophic adjustment: theory and experiment" in G.F.D. Fellowship Lectures, Vol.II.
(3) Pedlosky, Joseph 1964 "The stability of currents in the atmosphere and ocean, Part I", J.Atmos.Sci., 21: 201-219.
(4) Pedlosky, Joseph 1964 "The stability of currents in the atmosphere and ocean, Part II", J.Atmos.Sci., 21: 201-219.
(5) Orlanski, I. 1969 "The influence of bottom topography on the stability of jets in a baroclinic fluid". J.Atmos.Sci., 26: 1216-1232.
(6) Orlanski, I. 1968 "Instability of frontal waves". J.Atmos.Sci., 25: 178-200.
(7) Eady, E. 1949 "Long waves and cyclone waves". Tellus 1: 33-52.
(8) Pedlosky, J. 1970 "Finite Amplitude Baroclinic Waves". J.Atmos.Sci. 27: 15-30.

Footnote: During the lecture on this problem at Walsh Cottage, it was pointed out by Joseph Pedlosky that the free boundary condition in the free rigid side boundary problem is incorrect in the sense that there is a discontinuity in the streamlines. The proper boundary condition can be obtained by integrating the equations across the jump in V, thereby giving some kind of jump condition across the free boundary.

CONVECTION WAVES

Mark Koenigsberg

1. Introduction

The surface of the earth is in continual motion, and over millions of years, the pattern of continent and ocean has been gradually changing. This movement of continents, and the formation and destruction of oceanic plates is the surface expression of convection in the mantle. The nature of this convection is insufficiently understood. Classical theories of convection in a layer of fluid heated from below or within have been applied, but little insight has been gained in understanding the particular nature of the convection occurring in the earth. It is the purpose of this paper to modify the classical theory of convection in a way suggested by the pattern of motion on the earth and to explore the consequences of the theory.

Consider an infinite homogeneous fluid confined between two horizontal planes. Let the fluid be Boussinesq, and appropriate for the earth, let the fluid be characterized by an infinite Prandtl number. As a basic state there will be motionless conduction that is supplied heat from below when the heat flux through the layer exceeds a certain critical value, steady cellular motion replaces the conductive state. The numerical value of the critical heat flux depends on the type of boundary conditions imposed on the velocity and temperature above and below the fluid. In what follows, there will be a stress-free, isothermal bottom boundary. The top boundary will also be stress free. However, the condition on the temperature of the top boundary will be altered in a way that may be representative of the earth.

Continental material has a much greater concentration of radioactivity than either oceanic basalt or mantle rock. This excess heat source produces horizontal gradients of temperature that lead to motion. But, interestingly, the consequent motion changes the distribution of the variable heating, so that a feedback mechanism between the temperature on the upper boundary and the interior motion is created. This interaction of a movable heat source and the motion it produces was analyzed by Howard, Malkus, Whitehead (1970), and Whitehead (1972). They found that a floating heater can propel itself through a fluid if its heating is sufficiently great, and

they suggested this mechanism as an explanation for continental drift. Their analysis involved a discrete non-deformable heater, and the drift was produced by a nonlinear self-interaction of the heat source.

As a natural extension of the problem of a single heat source, we will consider an initially uniform distribution of heat source that is floating on the upper surface of a motionless fluid which is heated from below. The question is asked in what manner would such an initial state become unstable. It will be found that when convection sets in, a horizontally varying distribution of heat source results. If the floating heat source has a sufficiently large heat flux, the entire convective pattern, including the differentiated heat source, will drift along with the wave. The convection will appear stationary in a frame moving along with the wave, and the upwellings and downwellings will tilt in the direction of motion. The physical basis of this phenomenon is the interaction of the surface heating and the heating from below. The heat flux entering from the bottom of the fluid is responsible for differentiating the heat source, and the surface heating leads to the drift of the entire convective field. This drift that is produced is the result of linear interactions between heat source elements at different parts of the fluid.

It should be noted that the continents can act as an insulating shield to the heat coming from below, as well as provide radioactive generation of heat. This mechanism was suggested by Elder (1967). The effect is similar to the continents acting as heat sources and will be considered as such.

In Section II, both the equations of motion of the fluid and of the heat source will be presented. Then, the boundary condition describing the heat source modification of the temperature will be derived, and its physical implications will be discussed. The boundary condition that will be analyzed will be seen to be only a particular example of a more general class of problems that possess similar interesting features. Section III will be devoted to the linear problem. The influence of the modified boundary condition will be taken as small so that to lowest order, the problem will be identical to the one analyzed by Rayleigh. The second order solution will modify the spatial structure of the first order solution, and if the heat source is sufficiently great, the complete solution will move with time. Section IV will present the results of solving the complete linear problem by the method of Fourier Series. It will be valid for all ranges of the parameters and reproduces the results obtained by the perturbation method. In Section V, preliminary nonlinear results will be obtained. By means of power integrals that result from the full nonlinear equations of motion, it will be shown that travelling wave solutions have a greater heat flux than the standing wave solutions. So, there is a nonlinear mechanism for selecting which of the two types of time-dependent solutions will be preferred in finite amplitude. Finally in Section VI, there is a general discussion of this type of convection and how it may relate to continental drift on the earth.

II. The Equations of Motion and the Heat Source-Temperature Boundary Condition.

Because continental material is so much lighter than surrounding material, it is located near the upper surface of the earth, and its motion is confined primarily to the horizontal direction. So, let there be an initial horizontally uniform distribution of heat source located at the upper surface of a fluid. Let it be localized in the vertical at one depth so that its dependence on depth is a delta function. Also consider a layer of material lying above the heat source. The upper layer, which will not be allowed to convect will serve as the earth's thermal boundary layer - the lithosphere. The layer below the heat source serves as the earth's aesthenosphere. The upper surface of the fluid at $z = d$ will be taken as stress-free for mathematical convenience.

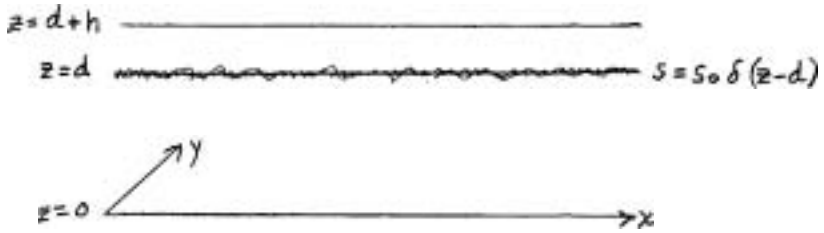

The motion of the heat source will be due to advection by the fluid below and diffusion of the heat source away from large concentrations. The equation of conservation of the heat source is

$$\frac{\partial S}{\partial t} + \frac{\partial}{\partial x}(uS) + \frac{\partial}{\partial y}(vS) = K_S\left(\frac{\partial^2}{\partial x^2} + \frac{\partial^2}{\partial y^2}\right)S. \tag{1}$$

The heat source is subject to movement by only the horizontal velocity field. Since the total velocity field for a Boussinesq fluid has zero divergence,

$$\frac{\partial u}{\partial x} + \frac{\partial v}{\partial y} + \frac{\partial w}{\partial z} = 0, \tag{2}$$

the heat source is advected by an equivalent velocity field with a non-zero divergence. This will tend to produce concentrations of heat source over downwellings and depletions of heat source over upwellings.

The fluid under a concentration of heat source will get hotter and the fluid under a depletion of heat source will get cooler. This, however, is contrary to the sense of the temperature perturbation that created the upwelling and downwelling in the first place. It is immediately apparent that the critical Rayleigh number for the onset of convection will be elevated as a result. In addition, however, there is created a mechanism for the possible oscillation of the temperature and velocity fields in the fluid. First, a downwelling occurs where there is a negative temperature perturbation and this concentrates the heat source thereby producing an excess temperature. The fluid can now become hotter where it was colder, so that a standing oscillation or travelling wave can result.

The equation describing the evolution of temperature is

$$\frac{\partial T}{\partial t} + \underline{u}\cdot\nabla T = K_T\nabla^2 T + S\delta(z-d), \tag{3}$$

where K_T is the coefficient of thermal diffusivity. The Navier-Stokes equations in an infinite Prandtl number Boussinesq fluid are

$$0 = -\nabla P + \alpha g T\hat{k} + \nu\nabla^2\underline{u}, \tag{4}$$

where α is the thermal expansion coefficient, ν is the kinematic viscosity, and $\hat{k}$ the unit vector in the vertical direction. We are considering a motionless basic state with an imposed temperature gradient of $-\frac{\Delta T}{d}$, and a uniform heat source S_0. The equations governing perturbations away from this solution are

$$\frac{\partial S}{\partial t} - S_0\frac{\partial w}{\partial z} = K_S\nabla_H^2 S \qquad z = d \tag{5}$$

$$\frac{\partial\theta}{\partial t} - \frac{\Delta T}{d}w + \underline{u}\cdot\nabla\theta = K_T\nabla^2\theta + S\delta(z-d) \tag{6}$$

$$0 = -\nabla P + \alpha g\theta\hat{k} + \nu\nabla^2\underline{u} \tag{7}$$

$$\nabla\cdot\underline{u} = 0 \tag{8}$$

If the temperature equation (6) is integrated across the heat source interface, there results,

$$K_T\left[\frac{\partial\theta}{\partial z}(z=d+)-\frac{\partial\theta}{\partial z}(z=d-)\right]+S=0 \tag{9}$$

The upper boundary at $z=d+h$ is maintained at 0°C by the ocean so that $\theta(z=d+h)=0$. Since h is much less than d, the temperature profile in the upper layer will always be linear with depth.

$$\frac{\partial\theta}{\partial z}(z=d+)=-\frac{\theta}{h}\,. \tag{10}$$

The boundary condition for the temperature at $z=d$ now becomes,

$$\theta=\frac{h}{K_T}\left(S-K_T\frac{\partial\theta}{\partial z}\right),\quad z=d\,. \tag{11}$$

For convenience, the equations of motion are non-dimensionalized with the following scales.

distance : d

velocity : K_T/d

time : d^2/K_T

temperature: $\frac{K\nu}{\alpha g\Delta T d^3}$

heat source: S_0

Analysis will be restricted to two-dimensional motion, so a stream function ψ is introduced to satisfy the continuity equation (8).

$$u=\psi_z\,,\quad w=-\psi_x\,.$$

Taking $\hat{k}\cdot\nabla\times\nabla\times$(Eq. 7), the full nonlinear problem can be written as follows:

$$\theta_t+R\psi_x=\nabla^2\theta-(\psi_z\theta_x-\psi_x\theta_z) \tag{12}$$

$$\nabla^4\psi=\theta_x \tag{13}$$

$$\psi=\psi_{zz}=\theta=0,\quad z=0 \tag{14}$$

$$\psi=\psi_{zz}=0,\quad S_t+\psi_x S_z=\sigma S_{xx}-(\psi_z S)_x\,,\quad \theta=\ell(\eta RS-\theta_z)\qquad z=1 \tag{15}$$

where $R=\frac{\alpha g\Delta T d^3}{K_T\nu}$ is the Rayleigh number, $\eta=\frac{S_0 d}{K_T\Delta T}$ is the ratio of the surface heat source flux to the heat flux entering the fluid from below, $\sigma=\frac{K_S}{K_T}$, and $\ell=h/d$.

In this model the effect of heating due to the continents is localized at a specific depth, and for convenience, is treated as a boundary condition. A distribution with depth of the heat source can easily be incorporated. For instance, consider a heating source whose vertical structure is maintained on a time scale shorter than the convective time scale, by erosional processes at the surface of the earth and chemical processes beneath the surface. The magnitude of heat source concentration would be a function of only time and horizontal position, producing results similar to that presented above. In this way the heat source can provide its own heating from below and an external supply of heat would be unnecessary. As a further generalization, the vertical structure of the heat source can be left as unspecified. All that is required to produce effects similar to those dealt with in

this paper, is that there be produced an agglomeration of heat source in regions of downwelling. It is emphasized that the model studied herein is chosen to closely depict the situation on the earth and to be simple enough to facilitate the demonstration of the interesting phenomenon.

III. Linear Problem - Perturbation Solution

A convective mode that can migrate with time is produced by the above feedback boundary condition between heat source and temperature (15). The heat source is advected by the fluid thereby modifying the temperature structure. The $(\ell\eta RS)$ term is the one that yields the interesting effect. The $(-\ell\theta_z)$ merely represents the boundary condition for a fluid with a boundary of finite conductivity. Its effect is to slightly lower the critical Rayleigh number at which convection occurs, and to increase the preferred scale of motion. This conduction term does not alter the time dependence of the conduction-convection transition. For this reason and mathematical clarity, the $(-\ell\theta_z)$ term will be neglected. Indeed this approximation is valid in the limit $\ell \to 0$, $\ell\eta$ = finite. In this section, the analysis will be carried out by means of an expansion in $\ell\eta$. As $\ell\eta$ goes to zero, the classical problem treated by Rayleigh is produced. In Section IV, the problem for arbitrary $\ell\eta$ will be solved. The full problem with the complete boundary condition (15) will not be done at this time.

The equations to be solved are:

$$\theta_t + R\psi_x = \nabla^2\theta - (\psi_z\theta_x - \psi_x\theta_z) \tag{16}$$

$$\nabla^4\psi = \theta_x \tag{17}$$

$$\psi = \psi_{zz} = \theta = 0, \quad z = 0 \tag{18}$$

$$\psi = \psi_{zz} = 0, \quad S_t + \psi_{xz} = \sigma S_{xx} - (\psi_z S)_x, \quad \theta = \ell\eta RS, \quad z = 1 \tag{19}$$

The heat source variable, S, can be eliminated from the upper surface boundary condition, so that condition (19) becomes

$$\theta_t + \ell\eta R\psi_{xz} = \sigma\theta_{xx} - (\psi_z\theta)_x, \quad z = 1. \tag{20}$$

The problem represented by (16 - 20) is nonlinear. The linear problem is obtained by dropping the nonlinear terms.

$$\psi = \psi_{zz} = 0, \quad \theta_t - \sigma\theta_{xx} = -\ell\eta R\psi_{xz}$$

$$Q_t + R\psi_x = \nabla^2\theta$$
$$\nabla^4\psi = \theta_x$$

$$\psi = \psi_{zz} = \theta = 0$$

Solutions of these equations are sought in the form

$$(\psi, \theta) = Re\left[e^{i(ax+\omega t)}\psi(z), \theta(z)\right],$$

where $\psi(z)$ and $\theta(z)$ can be complex functions of z. The system of equations now is

$$i\omega\theta + R\psi_x = \nabla^2\theta \tag{21}$$

$$\nabla^4\psi = \theta_x \tag{22}$$

$$\psi = \psi_{zz} = \theta = 0 , \qquad z = 0 \tag{23}$$

$$\psi = \psi_{zz} = 0 , \quad \theta = -\frac{\ell_\eta R(-i\omega + \sigma a^2)}{\omega^2 + \sigma^2 a^4} \psi_{xz} , \quad z = 1 . \tag{24}$$

As ℓ_η approaches zero, the boundary condition on temperature reduces to an isothermal condition $\theta = 0$, $z = 1$. Since the modified boundary condition will be treated as small, the solution of the linear problem is obtained by consecutively taking into account higher order corrections to the boundary conditions. For $\ell_\eta = 0$, the convection is steady and the solution can be written as

$$\psi_0 = e^{i(ax + \omega t)} \sin \pi z \tag{25}$$

$$\theta_0 = -\frac{i(a^2 + \pi^2)^2}{a} e^{i(ax + \omega t)} \sin \pi z , \tag{26}$$

where the subscript corresponds to the order of the modified boundary condition. This problem is self-adjoint and requires that

$$R_0 = \frac{(a^2 + \pi^2)^3}{a^2}$$

The minimum value of which

$$R_{min} = \frac{27}{4} \pi^4$$

is attained at

$$a^2 = \frac{\pi^2}{2}$$

There is no time dependence to this order, so that

$$\omega_0 = 0$$

However the time dependence is included in (25) and (26) so that higher order corrections can later be incorporated.

Now consider the first order correction due to the modified boundary condition.

$$i\omega_1 \theta_0 + R_0 \psi_{1x} = \nabla^2 \theta_1 - R_1 \psi_{0x} \tag{27}$$

$$\nabla^4 \psi_1 = \theta_{1x} \tag{28}$$

$$\psi_1 = \psi_{1zz} = \theta_1 = 0 , \qquad z = 0 \tag{29}$$

$$\psi_1 = \psi_{1zz} = 0 , \quad \theta_1 = -\frac{\ell_\eta R_0 (-i\omega_1 + \sigma a^2)}{\omega_1^2 + \sigma^2 a^4} \psi_{0xz} , \quad z = 1 \tag{30}$$

This linear inhomogeneous problem for ψ_1, θ_1 has the same linear operator as the previous order problem, so if solutions are to exist at this order a certain solvability condition must be satisfied. The inhomogeneous terms that appear in the above equations together with the terms resulting from the boundary conditions must be orthogonal to the adjoint solution of the first order problem. This requires

$$i\omega_1 \langle \theta_0^* \theta_0 \rangle + R_1 \langle \theta_0^* \psi_{0x} \rangle = -\overline{\theta_{0z}^* \theta_1} \quad (z = 1) , \tag{31}$$

where $\langle \cdot \rangle$ and $\overline{\cdot}$ denote a volume average and horizontal average, respectively, and $*$ denotes the complex conjugate. The third term arises from the modified boundary condition. The boundary condition on θ_1 can be substituted from (30) to obtain,

$$i\omega_1 \langle \theta_0^* \theta_0 \rangle + R_1 \langle \theta_0^* \psi_{0x} \rangle = \frac{\ell_\eta R_0}{\omega_1^2 + \sigma^2 a^4} \left(-i\omega_1 + \sigma a^2\right) \overline{\theta_{0z}^* \psi_{0xz}} \quad (z = 1) . \tag{32}$$

This expression can be evaluated using the zeroth order solutions (25 - 26), yielding a real and an imaginary condition. The imaginary condition is:

$$\omega_1\left[(\omega_1^2+\sigma^2a^4)-\frac{2\ell\eta R_0a^2\pi^2}{(a^2+\pi^2)^2}\right]=0 \qquad (33)$$

The real condition is:

$$R_1=\frac{2\ell\eta R_0\sigma a^2\pi^2}{\omega_1^2+\sigma^2a^4} \qquad (34)$$

Condition (33) has two alternatives:

$$\omega_1=0 \quad \text{or} \quad \omega_1^2+\sigma^2a^4=\frac{2\ell\eta R_0a^2\pi^2}{(a^2+\pi^2)^2} \qquad (35)$$

If $\omega_1=0$ then $R_1=\dfrac{2\ell\eta R_0\pi^2}{\sigma a^2}$

If $\omega_1\neq0$ then $R_1=\sigma(a^2+\pi^2)^2$

The solvability condition at this order determines the time dependence of the previous order solution. The time dependent solution cannot exist unless $\ell\eta$ is sufficiently great to overcome the effect of a non-zero σ. Also, if the time dependent solution can exist, it will have a lower Rayleigh number than the steady solution. This is because the build-up of heat source is always out of phase with the downwelling, and rather than forestall convection, the phase shift allows a time dependence. The difference between the two cases is accentuated for $\sigma=0$, in which case

$$\omega_1=\frac{\pi a}{(a^2+\pi^2)}(2\ell\eta R_0)^{1/2},\quad R_1=0 \qquad (36)$$

This indicates the importance of the parameter $(\ell\eta)^{1/2}$, and if higher order corrections are desired, the frequency should be expanded in one-half powers of $\ell\eta$. Since the frequency appears in the boundary condition as $\frac{\ell\eta}{\omega}$ (for $\sigma=0$), the function can be evaluated at the most unstable wavelength $a^2=\pi^2/2$.

$$\omega_1=\sqrt{3}\,\pi^2(\ell\eta)^{1/2}. \qquad (37)$$

Now that ω_1 and R_1 are known, the ψ_1 and θ_1 fields can be calculated. Eliminating θ_1 from the problem gives an equation for ψ_1 for the case $\omega_1\neq0, \sigma=0$.

$$\nabla^6\psi_1-R_0\psi_{1xx}=i\,\omega_1(a^2+\pi^2)^2e^{i(ax+\omega t)}\sin\pi z \qquad (38)$$

$$\psi_1=\psi_{1zz}=\psi_{1zzzz}=0,\quad z=0 \qquad (39)$$

$$\psi_1=\psi_{1zz}=0,\quad \psi_{1zzzz}=-\frac{i\ell\eta R_0a^2}{\omega_1}\psi_{0z},\quad z=1. \qquad (40)$$

It can be seen that ψ_1 will be proportional to $\sin(ax+\omega t)$ whereas ψ_0 is proportional to $\cos(ax+\omega t)$. The effect of the non-zero frequency ω_1, is to produce this out-of-phase solution. The vertical structure of the zeroth order solution is unchanged at this order. If either $\sigma\neq0$ or the $(-\ell\theta_z)$ boundary term is included in the analysis, there will be a correction to the vertical structure of the zeroth order solution. The solution can be written as the sum of a particular and a homogeneous solution.

$$\psi_1=\sin(ax+\omega t)\left[\frac{\omega_1}{6\pi}z\cos\pi z+2\,\mathrm{Re}(A\sinh qz)\right] \qquad (41)$$

where

$$A = A_1 + i A_2$$

$$q = q_1 + i q_2$$

$$q_1 = \frac{a}{\sqrt{2}} \left(\sqrt{1 + \tau + \tau^2} + \left(1 + \frac{\tau}{2}\right) \right)^{1/2}$$

$$q_2 = \frac{a}{\sqrt{2}} \left(\sqrt{1 + \tau + \tau^2} - \left(1 + \frac{\tau}{2}\right) \right)^{1/2}$$

$$\tau = \left(\frac{R}{a^4}\right)^{1/3}$$

The boundary conditions $\psi_1 = \psi_{1zz} = \psi_{1zzzz} = 0$ are identically satisfied by (41). Applying the boundary conditions at $z = 1$ gives,

$$-\frac{4\pi}{6} + 2\,\mathrm{Re}\,(A \sinh q) = 0 \tag{42}$$

$$\frac{\omega_1 \pi}{6} + 2\,\mathrm{Re}\,(A q^2 \sinh q) = 0 \tag{43}$$

$$-\frac{\omega_1 \pi^2}{6} + 2\,\mathrm{Re}\,(A q^4 \sinh q) = -\frac{\ell \eta R_0 \pi a^2}{\omega_1} \tag{44}$$

These three boundary conditions must be satisfied by the three parameters A_1, A_2, ω_1. The value of ω_1 was chosen such that a solution is guaranteed to exist, so the third boundary condition (44) can be considered redundant. After some algebra there is obtained:

$$A_1 = \frac{\omega_1 \left[\left((a^2 + \pi^2) + \frac{a^2 \tau}{2} \right) \cosh q_1 \sin q_2 + \frac{\sqrt{3}}{2} a^2 \tau \sinh q_1 \cos q_2 \right]}{6 \pi a^2 \sqrt{3} \tau (\sinh^2 q_1 + \sin^2 q_2)} \tag{45}$$

$$A_2 = \frac{\omega_1 \left[\left((a^2 + \pi^2) + \frac{a^2 \tau}{2} \right) \sinh q_1 \cos q_2 - \frac{\sqrt{3}}{2} a^2 \tau \cosh q_1 \sin q_2 \right]}{6 \pi a^2 \sqrt{3} \tau (\sinh^2 q_1 + \sin^2 q_2)} \tag{46}$$

The solution for ψ is now

$$\psi = \cos(ax + \omega t) \sin \pi z + \sin(ax + \omega t) \left[\frac{\omega}{6\pi} z \cos \pi z + 2 A_1 \sinh q_1 z \cos q_2 z - 2 A_2 \cosh q_1 z \sin q_2 z \right] \tag{47}$$

The solution for θ is obtained in an identical manner.

$$\theta = \frac{(a^2 + \pi^2)^2}{a} \sin(ax + \omega t) \sin \pi z + \cos(ax + \omega t) \left[\frac{-\omega_1 (a^2 + \pi^2)^2}{6 \pi a} z \cos \pi z + 2 B_1 \sinh q_1 z \cos q_2 z - 2 B_2 \cosh q_1 z \sin q_2 z \right] \tag{48}$$

where

$$B_1 = \frac{-\omega_1 (a^2 + \pi^2)^2 \left[\left((a^2 + \pi^2) + \frac{a^2 \tau}{2} \right) \cosh q_1 \sin q_2 + \frac{\sqrt{3}}{2} a^2 (\sinh q_1 \cos q_2 \right]}{6 \pi a^3 \sqrt{3} \tau (\sinh^2 q_1 + \sin^2 q_2)} + \frac{\pi \ell \eta R_0 a \left(\sinh q_1 \cos q_2 + \frac{1}{\sqrt{3}} \cosh q_1 \sin q_2 \right)}{2 \omega_1 (\sinh^2 q_1 + \sin^2 q_2)} \tag{49}$$

$$B_2 = \frac{-\omega_1 (a^2 + \pi^2)^2 \left[\left((a^2 + \pi^2) + \frac{a^2 \tau}{2} \right) \sinh q_1 \cos q_2 - \frac{\sqrt{3}}{2} a^2 \tau \cosh q_1 \sin q_2 \right]}{6 \pi a^3 \sqrt{3} \tau (\sinh^2 q_1 + \sin^2 q_2)} + \frac{\pi \ell \eta R_0 a \left(\frac{1}{\sqrt{3}} \sinh q_1 \cos q_2 \sin q_2 \right)}{2 \omega_1 (\sinh^2 q_1 + \sin^2 q_2)} \tag{50}$$

The expressions A_1, A_2, B_1, B_2 evaluated at $a^2 = \pi^2/2$ are

$$A_1 = .0308\,(\ell\eta)^{1/2}$$
$$A_2 = -.0211\,(\ell\eta)^{1/2}$$
$$B_1 = -.296\,(\ell\eta)^{1/2}$$
$$B_2 = -3/67\,(\ell\eta)^{1/2}$$

so that the solution is

$$\psi = \cos(ax+\omega t)\sin\pi z + (\ell\eta)^{1/2}\sin(ax+\omega t)\left[.908 z\cos\pi z + .0616\sinh 3.88 z\cos 1.65 z + \right.$$
$$\left. + .0422\cosh 3.88 z\sin 1.65 z\right] \qquad (51)$$

$$\theta = 99.4\sin(ax+\omega t)\left[90.0 z\cos\pi z - .592\sinh 3.88 z\cos 1.65 z + \right.$$
$$\left. + 2.34\cosh 3.88 z\sin 1.65 z\right] \qquad (52)$$

To see the effects of the out-of-phase solutions, contour maps of ψ and θ are presented below for $(\ell\eta)^{1/2} = 0$ and 1 for the travelling wave solution.

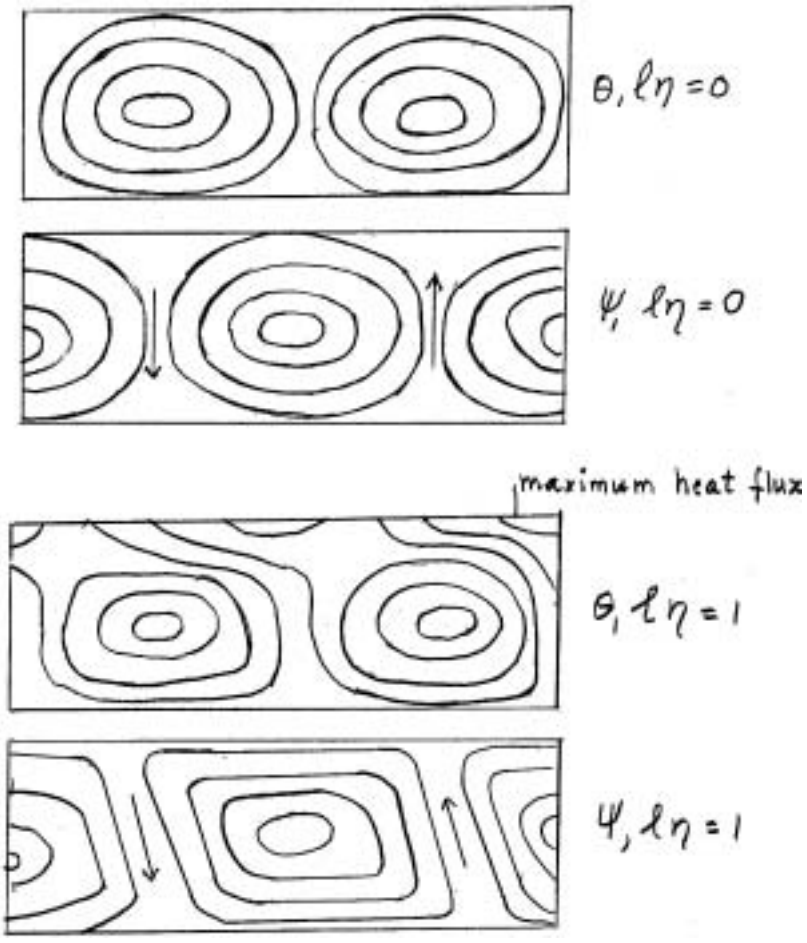

It is seen that for $\ell_\eta \neq 0$, the streamlines tilt in the direction of motion of the wave and that the isotherms penetrate to the surface. The heat source concentration for $\sigma = 0$ is maximum where the horizontal velocity is maximum in the propagation direction at the surface, and a minimum where the horizontal velocity is minimum in the propagation direction. Since the boundary condition used is $\Theta = \ell_\eta R S$, the hottest part of the fluid at the surface is in phase with the heat source. The maximum of the heat flux leaving the fluid is pushed from directly over the upwelling to a region behind the upwelling.

The contours for the standing wave would show the magnitude of convection periodically stopping and growing. Also, the direction of the tilt of the cells oscillates as the magnitude of convection goes up and down. The contours for the steady convection show the heat source located directly over the downwellings, and as a result the isotherms and streamlines are pushed away from the upper surface.

IV. Linear Problem - Fourier Series Solution

The complete linear problem as represented by (21-24) can be solved by expanding the unknown functions in terms of a $\sin \pi z$ series. This method can be used to solve general convection problems with complicated boundary conditions (see Jeffreys and Jeffreys, 1946, p.442). The result for $\sigma \neq 0$ is given by the following two summation conditions.

$$\omega^2 \left[\sum_{n=1}^{\infty} \frac{n^2\left((n^2\pi^2+a^2)^3 - Ra^2\right)}{D} + a^2 \sum_{n=1}^{\infty} \frac{n^2(n^2\pi^2+a^2)^2}{D} \right] = 0 \tag{53}$$

$$(\omega^2+\sigma^2a^4)\left[\frac{1}{2\ell_\eta Ra^2\pi^2} + \frac{1}{\sigma a^2} \sum_{n=1}^{\infty} \frac{n^2\left((n^2\pi^2+a^2)^3 - Ra^2\right)}{D} \right] = 0 \tag{54}$$

where $$D = \left((n^2\pi^2+a^2)^3 - Ra^2\right)^2 + \omega^2(n^2\pi^2+a^2)^4.$$

These two summations can be solved simultaneously for R and ω in terms of a and σ, and the minimum value of R as a function of a can be determined. As an approximation, consider only the $n=1$ term. For the case $\omega = 0$,

$$R = \frac{(a^2+\pi^2)^3}{a^2} + \frac{2\ell_\eta R\pi^2}{\sigma a^2} \tag{55}$$

For the case $\omega \neq 0$,

$$\omega^2+\sigma^2a^4 = \frac{2\ell_\eta Ra^2\pi^2}{(a^2+\pi^2)} \tag{56}$$

$$R = \frac{(a^2+\pi^2)^3}{a^2} + \sigma(a^2+\pi^2)^2. \tag{57}$$

This reproduces the results obtained in Section III. Also, this method can be used to solve the problem with $(-\ell\theta_z)$ included in the boundary condition on temperature.

V. Nonlinear Theory

It was shown that if the surface heat source is allowed to diffuse, two different modes are possible: stationary convection and time dependent convection. The time dependent convection can exist at a lower Rayleigh number than the steady convection, so linear theory says the time dependent solution will occur first. The subcritical structure for these solutions has not been fully studied. But since the

difference in Rayleigh numbers for the two types of solution can be made larger as $\sigma \to 0$, it is believed that there is a parameter range where the time dependent convection will be preferred in finite amplitude. The planform that will occur will also be determined by nonlinear interactions.

There remains the question as to whether a standing or travelling wave will be the preferred form of time dependent convection in finite amplitude. It will be demonstrated that (with the neglect of the possibility of subcritical instabilities) in the limit of vanishing $\ell\eta$, the travelling mode has a greater heat flux than the standing mode. Since solutions of the Rayleigh problem with maximum heat flux are preferred up to order ϵ^2, and we are considering $\ell\eta \to 0$, it is expected that the travelling convective mode will be the most stable and therefore most preferred solution.

First, the travelling wave solution will be examined. The travelling wave appears steady in a frame moving with $U = a\omega$, so in what follows, horizontal averages are identical to time averages. Write,

$$\theta = A\cos(ax+\omega t)\sin\pi z \tag{58}$$

$$W = B\cos(ax+\omega t)\sin\pi z \tag{59}$$

$$u = \frac{-\pi}{a} B\sin(ax+\omega t)\cos\pi z \tag{60}$$

The value of $(\ell\eta)$ is thought of as being small so that only the zeroth order solution is considered. However both the amplitude and time dependence of this solution is taken into account.

Take the horizontal average of the full temperature equation,

$$\overline{T}_t = \overline{T}_{zz} - (\overline{\omega\theta})_z. \tag{61}$$

If $(\overline{\omega\theta})_z$ is computed using (58-60), there results,

$$\overline{T}_t = \overline{T}_{zz} - \frac{\pi}{2} AB\sin 2\pi z. \tag{62}$$

The solution of (62) is

$$-\beta \equiv \overline{T}_z = -R - \frac{AB}{4}\cos 2\pi z. \tag{63}$$

The power integrals for the full nonlinear equations are derived by multiplying Eq.(4) by $\underline{u}$ and Eq.(12) by θ and then integrating over volume and one period in time.

$$\{\theta W\} = -\{\underline{u}\cdot\nabla^2\underline{u}\} \tag{64}$$

$$\{\beta\theta W\} = -\{\theta\nabla^2\theta\} \tag{65}$$

where $\{\ \}$ is an average in space and time. Substituting (58-60, 63) in relations (64-65) produces the following relations between the amplitudes A, B:

$$AB = \frac{(a^2+\pi^2)^2}{a^2} B^2 \tag{66}$$

$$AB\left(R - \frac{AB}{8}\right) = A^2(a^2+\pi^2) \tag{67}$$

The heat flux through the layer is from (63).

$$H = R + \frac{AB}{4} \tag{68}$$

With (68), Eq.(67) becomes

$$AB\left(H - \frac{3AB}{8}\right) = A^2(a^2 + \pi^2) \tag{69}$$

Now (66) and (69) can be combined to yield

$$AB = \frac{8}{3}\left(H - \frac{(a^2+\pi^2)^3}{a^2}\right) \tag{70}$$

The maximum heat flux is attained at $a^2 = \pi^2/2$ in which case (68) and (70) give

$$\text{Nusselt number} = \frac{H}{R} = 3 - \frac{2R_c}{R} \quad \text{for the travelling mode} \tag{71}$$

When $R = R_c$ the Nusselt number is one and when $R \to \infty$ the heat flux increases as $3R$.

Similar calculations can be done for the standing wave case. Consider

$$\theta = \sqrt{2}\, A' \cos \omega t \cos ax \sin \pi z \tag{72}$$

$$w = \sqrt{2}\, B' \cos \omega t \cos ax \sin \pi z \tag{73}$$

$$u = \frac{-\pi}{a}\sqrt{2}\, B' \sin \omega t \sin ax \cos \pi z \tag{74}$$

The factor of $\sqrt{2}$ appears so there is the same amount of energy in both the travelling and standing waves. The equation for the mean temperature is

$$\overline{T}_t = T_{zz} - \frac{\pi}{2} A'B'(1 + \cos 2\omega t) \sin 2\pi z \tag{75}$$

Comparison of (75) with (62) shows that the time average of $\overline{T}_t$ for the standing wave is the same as the time independent $\overline{T}_z$ for the travelling wave. The solution of (75) is

$$-\beta \equiv \overline{T}_z = -R - \frac{A'B'}{4}\cos 2\pi z \left[1 + \frac{\cos(2\omega t - \phi)}{\left(1 + \left(\frac{\omega}{2\pi^2}\right)^2\right)^{1/2}}\right] \tag{76}$$

where

$$\tan \phi = \frac{\omega}{2\pi^2}.$$

If relations (72-74, 76) are substituted in (64-65), and the same manipulations are carried out as for the travelling wave, there results,

$$\left\{\text{Nusselt}\right\}\left(1 + \frac{1}{\left(1 + \left(\frac{\omega}{2\pi^2}\right)^2\right)^{1/2}}\right) = 3\left(1 + \frac{1/6}{\left(1 + \left(\frac{\omega}{2\pi^2}\right)^2\right)^{1/2}}\right) - \frac{2R_c}{R} \tag{77}$$

Relation (77) differs from (71) because the standing wave convects a time varying mean temperature gradient, whereas the travelling wave convects a time independent mean temperature gradient. As $\omega \to 0$ (77) reduces to

$$\left\{\text{Nusselt}\right\} = \frac{7}{3} - \frac{4}{3}\frac{R_c}{R} \quad \text{for the standing mode.} \tag{78}$$

The maximum time averaged heat flux obtained by convection with one vertical mode, in the limit $(\ell_\eta) \to 0$, $\omega \to 0$, is reduced for the standing wave solution.

VI. Discussion

The main emphasis of this paper has been the appearance of a travelling convective solution in a convection problem that classically has time independent solutions. The modification was obtained by abstracting a situation that possibly exists on the earth. If the heating associated with the continents is important dynamically, the continental drift that is observed may be a manifestation of time dependent convective solutions as discussed above. Of course, the motion on the earth is not one sole travelling or standing convective wave. Due to the variation of various parameters and different initial conditions, different parts of the earth's surface can be the realization of different solutions. A great deal of chemistry that may be important has been ignored, so exact correlations with the earth are impossible. Since some of the heat produced by the differentiated heat source is convected downwards it is not unreasonable to expect motion on the earth's surface even where there is no continental material nearby.

It is interesting to compute the velocity of drift from Eq.(35). Using a value for γ of 1, and a value of ℓ of $1/10$, and a value of σ of 1, the value of the drift velocity is the same order of magnitude as the convective velocity.

One of the puzzling features of continental drift is the asymmetry of the downwelling regions. It is seen that in the above model, because of the drift of the motion, the convection cells are tilted in the direction of motion. As a result, both the upwellings and downwellings are rendered asymmetric. The concentration of heaf source is located just behind the downwelling region which penetrates beneath the "continental area". It is possible that the asymmetry of the downwellings in the earth reflect the fact that the convective motion as a whole is drifting. The direction of the downwelling should point opposite to the direction of the propagation of the wave. By further studying this and similar models greater understanding of the convection in the earth may be achieved.

I would like to extend special thanks to Dr. Willem Malkus and Dr. John Whitehead for encouragement and assistance in this study.

References

Elder, J. 1967 Convective self-propulsion of continents. Nature 214:657-660, 750.

Howard, L. N., W.V.R.Malkus and J.A.Whitehead 1970 Self-convection of floating heat sources: A model for continental drift. Geophysical Fluid Dynamics, I: 123-242.

Jeffreys and Jeffreys 1946 Methods of Mathematical Physics, Cambridge University Press.

Whitehead, J.A. 1972 Moving heaters as a model of continental drift. Physics of the Earth and Planetary Interiors 5: 199-212.

PLATE MOTION AND THERMAL INSTABILITY IN THE ASTHENOSPHERE

H. Jay Melosh

Introduction

This paper investigates the effect of a strongly temperature-dependent stress-strain relation on the thermal structure of the asthenosphere. Laboratory measurements and theoretical considerations concur in predicting that the stress-strain relation for a hot crystalline material such as olivine (which is probably a major constituent of the earth's mantle) is of the form

$$\dot{\epsilon}_{ij} = B\sigma^{n-1}\sigma_{ij}\, e^{\frac{-E^* + PV^*}{RT}} \qquad (1)$$

Where $\dot{\epsilon}_{ij}$ is the strain rate tensor, σ_{ij} is the deviatoric stress, $\sigma = \sqrt{\frac{1}{2} T_r(\sigma_{ij}\sigma_{jk})}$ is the second invarient of σ_{ij}, and B is a constant. In the exponential, E^* and V^* are activation energy and volume, respectively. P is pressure and T is the absolute temperature.

Equation (1) displays the exponential temperature dependence of $\dot{\epsilon}_{ij}$. As the temperature increases, $\dot{\epsilon}_{ij}$ increases so that a hot crystalline solid flows more readily as its melting point is approached. Equation (1) does not apply above the solidus temperature. Note that increasing pressure tends to decrease $\dot{\epsilon}_{ij}$, so that temperature and pressure work against one another. This conflict between P and T yields the rheological stratification of the earth which is responsible for plate tectonics. Near earth's surface P and T are low and the material of the crust is far below its melting point, so that the crust and uppermost mantle respond to stresses as elastic solids. This portion of the earth is the lithosphere. As we descend further into the earth both P and T rise, but the T rise is more significant. Eventually $\dot{\epsilon}_{ij}$ reaches a maximum for given σ_{ij}. At greater depths T increases more slowly and the P effect takes over. The region containing the maximum $\dot{\epsilon}_{ij}$ is known as the asthenosphere and the mantle material is most fluid in this region. It lies at depths ranging from 100 to 200 km, depending upon the locality.

This picture of the upper mantle, which allows the rigid lithospheric plates to slide over the fluid asthenosphere, involves a fundamental instability stemming from the temperature dependence of Eq.(1). The 50-100 km thick lithospheric plate is an excellent insulator, having a thermal time constant of the order of 100 Myr. On the other hand, shearing of the asthenosphere generates heat in the amount $\sigma_{xz}\dot{\epsilon}_{xz}$ erg/cm^3 - sec. If this heat is not conducted away through the lithosphere, the temperature in the asthenosphere must rise. But then $\dot{\epsilon}_{xz}$ increases (σ_{xz} held constant), the heat generation increases still more, and thermal runaway occurs, ceasing only when σ_{xz} is relieved or when temperatures reach the solidus and Eq.(1) no longer applies. This phenomenon was first studied by I.J.Grundfest[a] who was investigating the sudden (explosive) failure of rocket engines.

The purpose of this paper is to investigate the significance of this instability for plate motions. We shall see that shear heating of the type described above is not an important factor in determining the thermal structure of the asthenosphere under normal conditions. If, however, the applied shear stress exceeds a critical value (σ_c) then thermal runaway becomes inevitable and the mantle must adjust somehow, either by reducing the shear stress or by generating a large amount of melt in the asthenosphere. This critical stress σ_c is associated with a critical velocity v_c, which likewise represents an upper limit to the velocity at which a plate can move without causing thermal runaway. If v_c is assumed to exceed 10 cm/year (the velocity of the fastest observed plates), then σ_c cannot exceed a few

tens of bars. The stresses required to move lithospheric plates over the asthenosphere are thus remarkably small.

These conclusions are in strong conflict with those of C. Froidevaux and C. Schubert[2] who studied a similar problem numerically. These authors found that the thermal structure of the asthenosphere is strongly controlled by the velocity of the plate, and that there is no upper limit to the plate velocity. We shall show that this disagreement is due to the existence of two sets of solutions to the equations, and that Froidevaux and Schubert's choice of initial conditions was such as to put them onto the "unphysical" branch of solutions. This branch has the property that a decrease of shear stress leads to higher plate velocity (a fact noted by Froidevaux and Schubert), with the logical consequence that reduction of the shear stress to zero implies infinite plate velocity! It is this property which leads us to call this set of solutions "unphysical".

The present approach is analytical, and we shall use several approximations in order to make the problem tractible. We can show, a posteriori, that these approximations are excellent, and that the results obtained are good to 10% or better. Our approach is to study the idealized problem of an infinite half-space of material governed by Eq. (1). We apply a shear stress σ_{xz} to the half-space and seek the distribution of temperature with depth, $T(z)$. The problem is simplified by seeking only steady solutions, $\frac{\partial T}{\partial t} = 0$ (the question of time scales will be discussed later). In all of this work we ignore the advective transfer of heat. In the real earth it is possible that the asthenosphere could be cooled by convection in the mantle below (although this is contrary to the usual picture of a monotonic increase of temperature with depth). Such cooling of the asthenosphere is unlikely to be so efficient as to cause much modification of the model parameters, and we thus neglect it for the present.

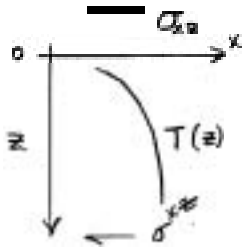

Fig. 1
coordinates

Neglecting advection, the relevant equations are

$$\frac{\partial T}{\partial t} = \frac{K}{\rho c_p}\frac{\partial^2 T}{\partial z^2} + \frac{2\beta\sigma_{xz}^{n+1}}{\rho c_p} e^{-\frac{E^* + PV^*}{RT(z,t)}} + \frac{H}{\rho c_p} \qquad (2)$$

heat conduction — shear heating — volumetric heat production

where K is the thermal conductivity, ρ is density, and c_p is the heat capacity of the mantle material. H is a volumetric heat production, and must be included to produce a zone of maximum $\dot{\epsilon}_{ij}$, hence a zone at depth where shearing takes place. H need not represent an actual radiogenic heat production - it may simply be taken as an empirical parameter describing the curvature of $T(z)$ vs. z.

Equation (2) cannot be solved analytically even for the case where $\frac{\partial T}{\partial t}(z,t) = 0$.

The main difficulty is the $1/RT(z)$ factor in the exponential. Our first approximation is thus to expand this term about some temperature T_s, which will be taken to be the temperature in the zone of most intense shearing. We shall show later that this yields an excellent approximation, since the shear heating term is large only in this zone. We thus write

$$Be^{-\frac{E^*+PV^*}{RT(z)}} \simeq ce^{\frac{T}{T^*}-z} \tag{3}$$

where

$$C \equiv Be^{-\frac{2E^*+P_0V^*}{RT_0}} \tag{4}$$

$$T_s \equiv \frac{RT_0^2}{E^*} \tag{5}$$

$$z_m \equiv \frac{RT_0}{\rho g V^*} \tag{6}$$

P_0 is the pressure at the surface of the earth, and we shall set it equal to zero for our purposes. We introduce a dimensionless rheological potential temperature

$$f(z) \equiv \frac{T(z)}{T_s} - \frac{z}{z_m} \tag{7}$$

Equation (2) becomes

$$0 = \frac{d^2f(z)}{dz^2} + pe^{f(z)} + q_0 \tag{8}$$

where

$$p \equiv \frac{2C\sigma_{xz}^{n+1}}{T_s K} \tag{9}$$

$$q_0 \equiv \frac{H}{KT_s} \tag{10}$$

The parameter p describes the effect of shear stress, while q_0 prescribes a curvature (hence a maximum) for $f(z)$, even in the absence of shear stress. f combines both temperature and pressure effects on $\dot{\epsilon}_{ij}$, such that when $f(z)$ reaches a maximum, $\dot{\epsilon}_{ij}$ is maximum also (σ_{ij} fixed).

Equation (8) is the master equation for the remainder of this work. In the next section we find solutions of Eq. (8) in terms of a non-elementary integral, and examine several special cases of the solution. We then use several approximations to this integral to solve the general problem in regions of geologic interest. These approximate solutions are applied to a model of plate motions, and important deductions about the stress-velocity relation for plates are obtained. Finally, we present several numerical models for the earth, and show that the stresses responsible for plate motions can be no lorger than a few tens of bars. A discussion of time scales shows that, while it is not certain that a steady state has been attained in the earth, the critical stress cannot be exceeded by a large amount (by a factor of two or more) without thermal runaway occurring on a very short timescale (a few tens of Myr). Thus, the relation between stress and velocity deduced from the steady state assumption is probably not far from the correct relation.

The Mathematical Problem

Equation (8) can be reduced to a first order differential equation by use of the integrating factor $\frac{df}{dz}$. The result is

$$\frac{df}{dz} = \pm\sqrt{2\{p(e^{f_m} - e^{f(z)}) + q_0(f_m - f(z))\}} \tag{11}$$

The constant has been determined by requiring that $\frac{df}{dz}=0$ when $f=f_m$, the maximum potential temperature. If the maximum $f(?)$occurs at $z=z_m$, then the solution can be written

$$z-z_m = \pm\sqrt{\frac{f_m-f(z)}{2q}}\; I\left(\frac{p e^{f_m}}{q(f_m-f(z))},\; f_m-f(z)\right) \tag{12}$$

where $I(\alpha,\beta)$ is a non-elementary integral

$$I(\alpha,\beta) \equiv \int_0^1 \frac{d\zeta}{\sqrt{\zeta+\alpha(1-e^{-\beta\zeta})}} \tag{13}$$

The properties of $I(\alpha,\beta)$ are described in Appendix I.

Equation (12) implicitly determines $f(z)$ in terms of the two arbitrary constants $\$$ and $+$. If these constants were known then our task would be complete, However, in the geological problem, we must consider these constants to be the result of applying other boundary conditions. In particular, we shall specify the surface temperature $T(o)$ (hence $f(o)$, and the heat flux (hence $\frac{df}{dz}$) at some depth z_b which lies far below the depth of significant shearing. We then ask what are the values of f_m and z_m for given p, q, and fixed $f(o)$, $\left.\frac{df}{dz}\right|_{z_b}$. In this way we shall find that solutions exist only for a finite range of p.

Let us look at two special cases of the solution (12):

(1) $p=0$ case (no shear stress)

This is the case of pure conduction, given $f(o)$ and $\left.\frac{df}{dz}\right|_{z_b}$. Since $I(0,\beta)=2$, Eq. (12) yields

$$f_m^\circ - f(z) = \frac{q}{2}\left(z-z_m^\circ\right)^2 \tag{14}$$

this is exactly the form expected for pure conduction. If we define $\left.\frac{df}{dz}\right|_{z_b} = -b$, then the boundary conditions imply

$$z_m^\circ = z_b - \frac{b}{q} \tag{15}$$

$$f_m^\circ = f(o) + \frac{q}{2}\left(z_m^\circ\right)^2 \tag{16}$$

The superscripts on z_m° and f_m° are to indicate that they are solutions to the $p=0$ (no shear stress) problem.

Note that $\left.\frac{df}{dz}\right|_{z_b}$ must be negative in order for a maximum in $f(z)$ to occur $\left(\left.\frac{df}{dz}\right|_o > 0\right)$. However, this does not imply $\left.\frac{dT}{dz}\right|_{z_b} < 0$ as Eq. (7) shows. We merely require

$$\left.\frac{dT}{dz}\right|_{z_b} > 0 \;\Rightarrow\; \left.\frac{df}{dz}\right|_{z_b} > -\frac{1}{z_*} \quad \text{or} \quad b < \frac{1}{z_*} \tag{17}$$

The maximum in $f(z)$ occurs when $\left.\frac{dT}{dz}\right|_{z_m} = \frac{T_*}{z_*}$. Thus the condition for a zone of maximum fluidity to exist is simply

$$\left.\frac{dT}{dz}\right|_{z=0} > \frac{T_*}{z_*} > \left.\frac{dT}{dz}\right|_{z_b} \tag{18}$$

In the earth $\left.\frac{dt}{dz}\right|_{z=0} \simeq 13 - 20^\circ C/km$, while at great depth $\left.\frac{dT}{dz}\right|_{z_b}$ is near the adiabatic gradient, .3 - $1^\circ C/km$. It is readily found that $T_*/z_* \simeq 1\text{-}4^\circ C$, so that a zone of maximum fluidity must exist between the surface and the region of adiabatic temperature gradient,

(2) $q_0 = 0$ case (no heat generation)

In this case $\alpha \to \infty$ and Eq.(12) can be integrated exactly. Solving the result for $f(z)$ we obtain the exact solution

$$f_m - f(z) = 2 \ln \left\{ \cosh \left[\sqrt{\frac{p e^{f_m}}{2}} (z - z_m) \right] \right\} \tag{19}$$

If $z_b >> z_m$, then $\left.\frac{df}{dz}\right|_{z_b} = -b$ determines f_m;

$$f_m = \ln \frac{b^2}{2p} \tag{20}$$

from which z_m can be determined if $f(0)$ is fixed;

$$z_m = \pm \frac{z}{b} \cosh^{-1} \left\{ \sqrt{\frac{b^2}{2p}}\, e^{-f(0)/2} \right\} \tag{21}$$

There are two sets of solutions, one set corresponding to $z_m > 0$ (shearing zone lies within the mantle), the other corresponding to $z_m < 0$ (shearing zone above surface - no maximum $f(z)$ occurs within the mantle). Since the argument of $\cosh^{-1}$ must be greater than 1 for a solution to exist, we find an upper limit p_c on p :

$$p \le p_c \equiv \frac{b^2}{2} e^{-f(0)} \tag{22}$$

In other words,

$$\sigma_{xz} \le \sigma_c = \left[\frac{K T_* b^2}{4C}\, e^{-T(0)/T_*} \right]^{\frac{1}{n+1}} \tag{23}$$

The corresponding velocity can be determined by substituting $f(z)$ in Eq.(1) and integrating from $z = \infty$ to $z = 0$. The resulting differential velocity can be expressed as

$$\frac{v}{v_c} = \frac{\sigma_c}{\sigma_{xz}} \left\{ 1 \pm \sqrt{1 - \left(\frac{\sigma_{xz}}{\sigma_c} \right)^{n+1}} \right\} \tag{24}$$

where

$$v_c = \frac{K T_* b}{\sigma_c} \tag{25}$$

The two solutions in Eq.(24) correspond to the two sets of solutions in Eq.(21). Most of the differential velocity between the bottom of the shear zone ($z \to \infty$) and the top of the shear zone ($a \to -\infty$) occurs in a thin layer of width $w = 4/b$ centered about $z = z_m$. In the case $z_m < 0$, the surface velocity v is a small fraction of the velocity for $z_m > 0$, since the zone of maximum shear does not occur in the mantle.

The branch of solutions for $z_m > 0$ corresponds to the (+) sign in Eqs.(21) and (24). Equation (24) shows that as $\sigma_{xz} \to 0$, $v/v_c \to \infty$ with $\sigma_{xz} v \approx$ constant for $\sigma_{xz} << \sigma_c$. This state of affairs, in which a decrease in shear stress leads to an increase in velocity is physically absurd, and we label this set of solutions the "unphysical" set. All solutions with $v/v_c > 1$ belong to this set.

The $z_m < 0$ branch of solutions if "physical" in the sense that as $\sigma_{xz} \to 0$, $v/v_c \to (\sigma_{xz}/\sigma_c)^n$ which is the correct limit for low shear stress where the thermal structure of the mantle is not affected by shear heating. All physical solutions have $v/v_c \le 1$.

These two sets of solutions coincide for $\sigma = \sigma_c$. To interpret the unphysical set of solutions, note that as $\sigma \to 0$, $z_m \to \infty$ for this set. In this case $\frac{df}{dz} > 0$ from the surface down to z_m, so that the fluidity of the mantle increases downward until either z_m or the solidus temperature is reached. These solutions thus correspond to a mantle which overlies a fluid stratum, and in which the fluidity increases monotomically with distance down to the stratum. Such a mantle has no

asthenosphere. Shear stress applied to this mantle would actually result in motfon over the fluid substratum rather than in a zone of shearing within the much less fluid mantle, so that such solutions are mathematical fictions (i.e., they imply a violation of the approximations which led to Eq.(8)). It is thus highly unlikely that this set of solutions has any relevance to the real earth.

The physical set of solutions has $\frac{df}{dz} \leq 0$, so that the fluidity of the mantle decreases with depth. In this case shearing is confined to the upper layers of the mantle, and solutions for $p \to 0$ do not violate our initial approximations. As p increases toward p_c, z_m approaches $z = 0$, reaching it when $p = p_c$.

Both sets of solutions are plotted in Fig.2.

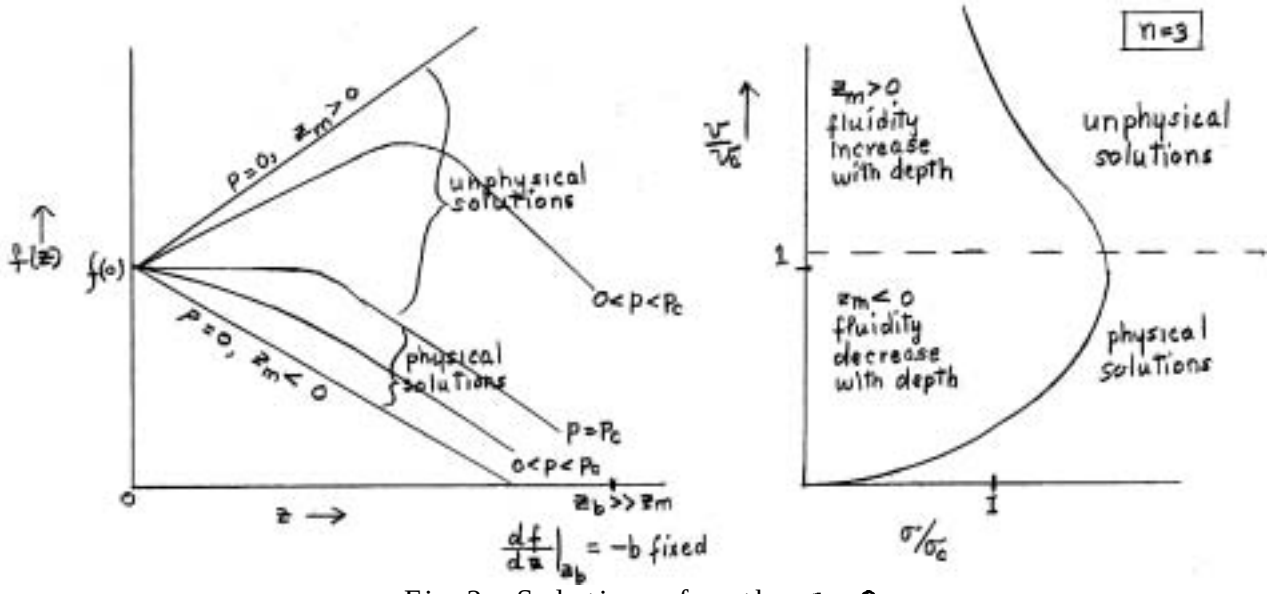

Fig.2 Solutions for the $q_0 = 0$ case

Neither of these two sets of solutions correspond very well to the earth's mantle. The trouble with the $q_0 = 0$ case is that $\frac{df}{dz}$ is constant in the absence of shear stress, so that the fluidity of the mantle must either increase continuously with depth (unphysical solutions), or decrease continuously with depth (physical solutions). In the latter case, the maximum fluidity occurs at the surface.

Current ideas, however, require a zone of maximum fluidity at some finite depth (100-200 km). We are thus led to consider cases where $q_0 \neq 0$. The solution for pure conduction has made it plain that $f(z)$ may have a maximum f_m^0 at depth z_m^0 when $p = 0$. We thus expect shearing at small p to begin in this region, which lies at a controlled depth below the surface. We can examine solutions for larger p to see how more intense shearing modifies f_m and z_m from the conduction solution.

Specification of $\frac{df}{dz}\Big|_{z_b} = -b$ for $z_b >> z_m$ allows us to neglect $pe^{f(z_b)}$ in Eq. (11) which thus yields

$$f_m - f(z_b) = \frac{b^2 - 2pe^{f_m}}{2q_0} \tag{26}$$

We determine $z_b - z_m$ from (12), using (26) to eliminate $f(z_b)$:

$$z_b - z_m = \sqrt{\frac{b^2 - 2pe^{f_m}}{2q_0}}\; I\left(\frac{2pe^{f_m}}{b^2 - 2pe^{f_m}},\ \frac{b^2 - 2pe^{f_m}}{2q_0}\right) \tag{27}$$

We can always choose z_b sufficiently deep so that $b^2 >> 2pe^{f_m}$, and (27) becomes

$$z_b - z_m \cong \frac{b}{q_0} - \sqrt{\frac{\pi}{2q_0}}\,\frac{pe^{f_m}}{q_0(f_m - f(0))} \tag{28}$$

Above z_m we use Eq.(12) again to relate z_m to $f(0)$:

$$z_m = \sqrt{\frac{f_m - f(0)}{2q}}\, I\left(\frac{p e^{f_m}}{q(f_m - f(0))}, f_m - f(0)\right) \tag{29}$$

Thus, the problem is to use Eqs.(27) and (29) to determine z_m, f_m in terms of $f(0)$, $\left.\frac{df}{dz}\right|_{z_b} = -b$ for given p, q. Once f_m, z_m are known, v can be determined by equating the surface heat flux to the energy dissipated by shear heating, σv, plus the heat flowing into the bottom at z_b and the heat generated by the q_b term in (8). Since all quantities are known except v, we find:

$$v = \frac{kT_a}{\sigma_{xz}}\left\{\sqrt{2\left[p(e^{f_m} - e^{f(0)}) + q(f_m - f(0)\right]} - q_b\left(z_b - \frac{b}{q}\right)\right\} \tag{30}$$

Equations (27) and (29) are too complex to be solved analytically without approximations. Equation (28) is a valid approximation to (27) in all cases, whereas (29) can be well-approximated in two regions. For simplicity we adopt nondimensional variables:

$$\mu = \frac{q z_b - b}{\sqrt{2q}} \tag{31}$$

$$\rho = \frac{p e^{f(0)}}{q} \tag{32}$$

$$\eta = \sqrt{f_m - f(0)} \tag{33}$$

In terms of these variables Eqs.(28) and (29) become

$$\sqrt{2q}\, z_m \cong 2\mu + \sqrt{\pi}\,\rho e^{\eta^2} \tag{34}$$

$$\sqrt{2q}\, z_m = \eta I\left(\frac{\rho e^{\eta^2}}{\eta^2}; \eta^2\right) \tag{35}$$

The two cases are

a) $f_m - f(0) = \eta^2 >> 1$

Equation (35) is, for $\frac{\rho e^{\eta^2}}{\eta^2} << 1$ (which we shall demonstrate is the case).

$$\sqrt{2q}\, z_m \simeq 2\eta - \sqrt{\pi}\left(1 - \frac{1}{\sqrt{\pi}\,\eta}\right)\rho e^{\eta^2} \tag{36}$$

Combining (36) and (34), and realizing that $\eta \simeq \mu$, we obtain

$$\eta - \mu = \sqrt{\pi}\left(1 - \frac{1}{2\sqrt{\pi}\mu}\right)\rho e^{\eta^2} \tag{37}$$

In general this must be solved iteratively for η ; however, it is easy to show that solutions exist only for $\rho < \rho_c$ where

$$\eta_c = \frac{\mu + \sqrt{\mu^2 + 2}}{2} \tag{38}$$

$$\rho_c = \frac{1}{\left(2\sqrt{\pi} - \frac{1}{\mu}\right)}\,\frac{e^{-\eta_c^2}}{\eta_c} \tag{39}$$

for $\rho = 0$, $\eta = \mu$ and we recover the conductive solution. For large μ, $\eta_c \simeq \mu + \frac{1}{2\mu}$ so that η_c and μ differ only slightly, as previously assumed (if μ is not $>> 1$ then η^2 is not $>> 1$ and the entire approximation fails, so this result is consistent). Moreover,

$$\frac{\rho e^{\eta^2}}{\eta^2} < \frac{\rho_c e^{\eta_c^2}}{\eta_c^2} = \frac{1}{2\sqrt{\pi}\,\eta_c^2} << 1 \tag{40}$$

Thus, this approximation is self-consistent for $\mu >> 1$. In practice, it works

well for $\mu \geq 2$. This condition will hold for nearly all earth models of interest, so this solution is very useful.

b) $$f_m - f(0) = \eta^2 << 1$$

Equation (35) is well approximated by

$$\sqrt{2q}\, z_m \simeq \frac{2\eta}{\sqrt{1+\rho e^{\eta^2}}} \tag{41}$$

which, together with (34) yields

$$2\mu + \sqrt{\pi}\,\rho e^{\eta^2} \cong \frac{1+2\rho e^{\eta^2}}{\sqrt{\quad}} \tag{42}$$

this equation is readily solved only for $\mu = 0$, in which case

$$\begin{aligned} \rho_c &= .292 \\ \eta_c^2 &= .111 \end{aligned} \tag{43}$$

Thus, $\eta_c^2 << 1$ as required. Again, ρ and η must be determined by iteration for $\rho < \rho_c$.

Once and are determined, all quantities of interest can be expressed in terms of them:

$$z_m \cong z_m^0 + \sqrt{\frac{\pi}{2q}}\,\rho e^{\eta^2} \tag{44}$$

$$f_m = f_m^0 + (\eta^2 - \mu^2) \tag{45}$$

$$\frac{\sigma_{xz}}{\sigma_c} = \left(\frac{\rho}{\rho_c}\right)^{\frac{1}{n+1}} \tag{46}$$

$$\frac{v}{v_c} = \frac{\sigma_c}{\sigma}\left\{\frac{\sqrt{\rho e^{\eta^2}(1-e^{\eta^2})+\eta^2} - \mu}{\sqrt{\rho_c e^{\eta_c^2}(1-e^{\eta_c^2})+\eta_c^2} - \mu}\right\} \tag{47}$$

where

$$\sigma_c = \left\{\frac{q^n K T_*}{2c}\, e^{-f(0)}\, \rho_c\right\}^{\frac{1}{n+1}} \tag{48}$$

$$v_c = \frac{\sqrt{2q}\, K T_*}{\sigma_c}\left\{\sqrt{\rho_c e^{\eta_c^2}(1-e^{-\eta_c^2})+\eta_c^2} - \mu\right\} \tag{49}$$

Furthermore, by expanding $I(\alpha, b)$ about z_m to get $f(z)$ near f_m, then integrating $\dot{e}_{ij}$ in that region, we find that $v(z)$ behaves like an error function near f_m, and is appreciable only over a zone of total width

$$w \equiv \sqrt{\frac{2\pi}{2\rho e^{f_m} + q}} \tag{50}$$

which is valid for $\rho \frac{e^{f_m}}{q} << 1$ (as it is in all cases). As $\rho \to 0$, we define the width $w^0 = \sqrt{2\pi/q}$ in time of which

$$\mu = \sqrt{\pi}\,\frac{z_m^0}{w^0} \tag{51}$$

Thus, $\mu >> 1$ implies that the width of the zone of shearing is much less than its depth. In the $\mu = 0$ case, $z_m^0 = 0$ and the region of maximum fluidity lies at the surface when $\rho \to 0$. The most striking conclusion to be drawn from these equations is that even at $\rho = \rho_c$ the thermal structure of the asthenosphere is only slightly different from the $\rho = 0$ case. Thus,

$$z_m^c - z_m^o \simeq \frac{\rho_c e^{\eta_c^2}}{2} W^o \qquad (52)$$

$$f_m^c - f_m^o \simeq \eta_c^2 - \mu^2 \cong 1 + \frac{1}{4\mu^2} + \cdots \quad \mu >> 1 \qquad (53)$$

Since $\rho_c e^{\eta_c^2} << 1$ for all μ, and likewise $\eta_c^2 - \mu^2 \leq 1$ for all μ, we see that the depth of the zone of maximum shearing increases by only a small fraction of its width (.26 for $\mu = 0$, decreasing to .03 for $\mu = 5$. The maximum $f_m^c - f_m^o \leq 1$ so that the temperature difference between the state with $\rho = \rho_c$ and that with $\rho = 0$ is at most T_* - a matter of 20 - 80°C for estimated mantle parameters.

Thus, as long as $\sigma < \sigma_c$ (hence $v < v_c$) shear heating has no profound influence on the temperature structure of the mantle. It is only when $\sigma > \sigma_c$ or $v > v_c$ that effects of shear heating can become appreciable.

To make this point clear, and to demonstrate some solutions to Eqs.(37) and (42), we plot v/v_c versus σ/σ_c for $\eta = 3$ in Fig.3. We again see that there are two sets of solutions to Eqs.(37) and (42), one set (the "unphysical" set) with $v > v_c$, $\frac{\partial v}{\partial \sigma} < 0$, while the other set (the "physical" set) has $v < v_c$, $\frac{\partial v}{\partial \sigma} > 0$. Only the physical set is connected to the $\sigma = 0$ conduction solution through a continuous sequence of states with increasing σ. The physical and unphysical sets of solutions coincide at $\sigma = \sigma_c$. The unphysical set of solutions (which have large $\eta > \eta_c$) do imply profound alterations of the mantle's thermal structure, with $\eta \to \infty$ as $\sigma \to 0$. As before, however, the $\frac{\partial v}{\partial \sigma} < 0$ property has the absurd implication that $v \to \infty$ as $\sigma \to 0$, so that we reject the physical existence of such solutions. Only the "physical" set of solutions yields the expected $v \sim \sigma_{xz}^n$ dependence of velocity on shear stress for $\sigma_{xz} << \sigma_c$.

In fact, for $\sigma_{xz} \ll \sigma_c$, $\eta \simeq \mu + \left(\sqrt{\pi} - \frac{1}{2\mu}\right) e^{\mu^2} \rho$ ... when $\mu >> 1$. Substitution gives the expected result $v \cong 2Be^{-\frac{E^* + PV^*}{RT_m}} \sigma_{xz}^n W_o$, but only for the physical set of solutions).

We thus conclude that only the "physical" set of solutions may be applied to the earth's mantle, hence $v \leq v_c$ in all cases. These solutions do not involve significant changes in the thermal structure of the mantle, even when $\sigma = \sigma_c$. If $\sigma > \sigma_c$, however, no steady solutions exist and the temperatures in the zone of most intense shearing must rise until new cooling mechanisms or physical processes come into play. The actual values of σ_c and v_c are thus of fundamental importance for plate tectonics, since they mark the boundary between a regime of simple shearing without marked thermal disturbance and a regime where shear heating must dominate the thermal structure of the mantle.

Application to Plate Motion

The previous section has shown us the importance of the critical shear stress σ_c and critical velocity v_c to plate motion. The numerical values of these two quantities decide the nature of the asthenosphere; if $\sigma_{xz} \leq \sigma_c$ shear heating has little influence on the thermal structure of the asthenosphere, whereas if $\sigma_{xz} > \sigma_c$ the entire structure of the asthenosphere must alter in order to avoid thermal runaway.

It is a straightforward exercise to devise model mantles for given values of $T(o)$, $\left.\frac{dT}{dz}\right|_{z_b}$ and heat production H. Assigning laboratory values to the constants in Eq.(1), the equations given in the last section suffice to determine z_m, W, v_c, σ_c, etc. for each of these models. The detailed description of six models is given in Appendix II, where the thermal structure of the models is described in some detail. One clear result of this model building is that $\mu >> 1$ in all geologically

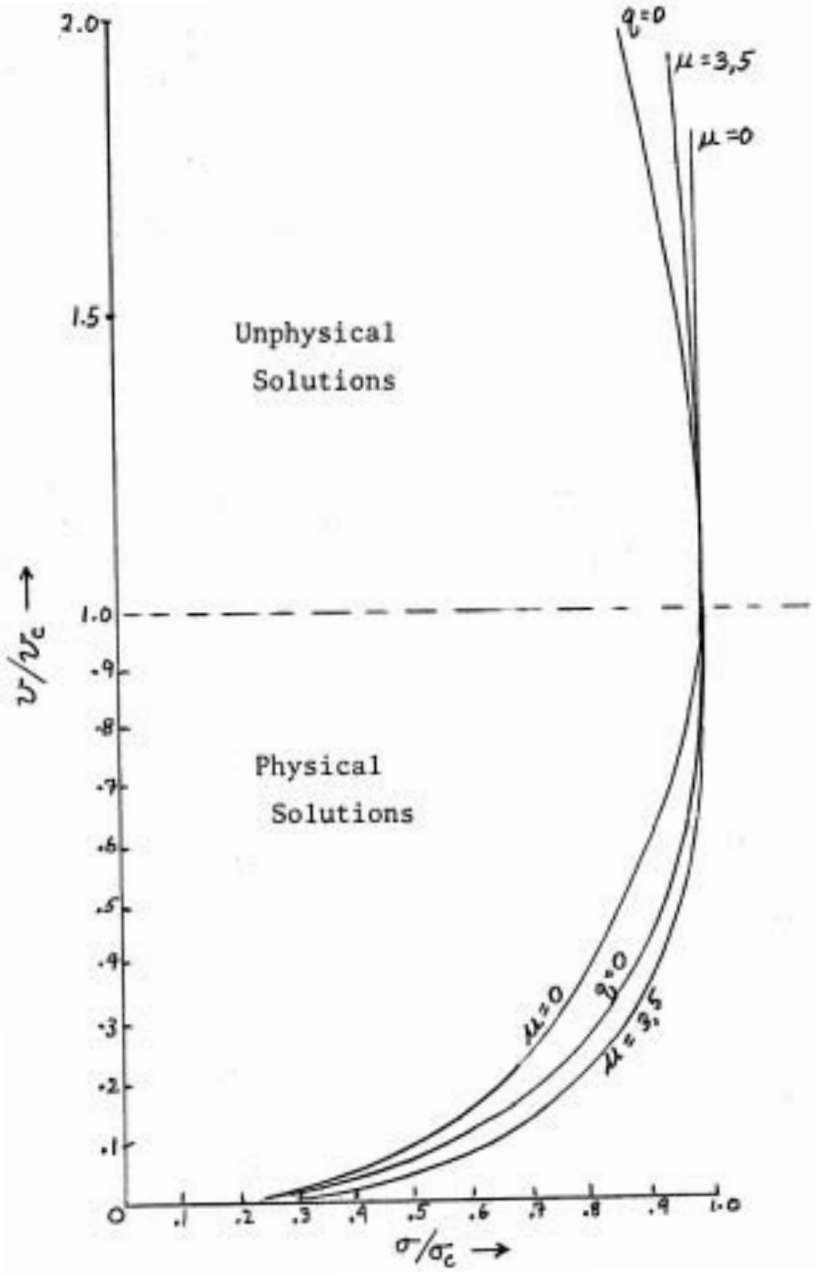

Fig.3 Shear stress - velocity relation for various thermal models of the asthenosphere. Curves are included for μ = 0, 3, 5 as well as for the exact $q = 0$ solution.

reasonable models. (This is almost obvious, since $\mu=0$ implies $z_m^{\circ} = 0$ yet we do not want to attribute the maximum fluidity zone of the upper mantle to the surface. We must thus require $\mu \neq 0$, and we will nearly always find $\mu > 1$.)

Even in the case that $\mu >> 1$, the equations for σ_t and v_t are complicated, and their relations to each other and to the other important parameters is obscure. It is therefore useful to derive crude approximate expressions for σ_t and v_t, accurate to 20% or so, which express the dominant relationships. Such expressions

are the only ones likely to be useful in evaluating geological data, since the various input parameters cannot be measured with any great precision.

Table I.B. indicates a sort of inverse relationship between σ_c and v_c. If σ_c is large, v_c is small, and vice versa. This suggests that $\sigma_c v_c$ may not be as dependent upon the input parameters as σ_c and v_c above. This suggestion is borne out in Eq. (49), where we see that

$$v_c \sigma_c = \sqrt{2g}\, K T_* \left\{ \sqrt{\rho_c e^{\eta_c^2}(1 - e^{-\eta_c^2}) + \eta_c^2} - \mu \right\} \tag{54}$$

using Eq. (39) for ρ_c, and expanding Eq. (38) for η_c when $\mu \gg 1$, we find that

$$v_c \sigma_c \simeq \frac{\sqrt{2g}\, K T_*}{2\mu} \tag{55}$$

which is valid to ca. 5% for $\mu \geq 4$. Noting that $\mu = \sqrt{\frac{3}{4}}\, z_m^*$, we obtain the useful formula

$$v_c \sigma_c \simeq \frac{K T_*}{z_m^*} \tag{56}$$

Since we can estimate a lower bound on v_c for the earth, $v_c \geq 10$ cm/yr (supposing that the fastest observed plate motions are below the critical velocity), we obtain an upper bound on the shear stress responsible:

$$\sigma_c \text{ (bar)} \leq 104 \frac{T_* (^\circ K)}{z_m^* (km)\, v_c (cm/yr)} \tag{57}$$

(where we have put $K = .008$ cal/cm^2-sec-$^\circ$k). Taking $v_c \geq$ cm/yr, $T_* = 50^\circ$k, and $z_m^* = 100$ km, we obtain a strict upper limit

$$\sigma_c \leq 5.2 \text{ bar} \tag{58}$$

Depending on the model chosen, T_* and z_m^* may each be varied by as much as a factor of 2, (although larger z_m, by requiring larger $T(z_m)$ implies larger T_*, so that T_*/z_m does not vary as much as each individually). Such variation from model to model, however, does not alter the basic conclusion that the shear stress acting on the lithospheric plates must be less than a few tens of bars in order to avoid thermal instability.

The product $v_c \sigma_c$ is not sensitive to the theological parameters of the mantle in any direct way. The value of σ_c (hence v_c) above is, however, much more dependent upon these parameters. This dependence can be readily seen by substituting Eq. (39) into Eq. (48), expanding η_c in terms of μ, and keeping only the leading terms for $\mu \gg 1$. Note that $e^{-\eta_c^2} = e^{f z_m^* - f(0)} \simeq e^{f z_m^* - f(0)}$ to a factor e). The error by a factor e is reduced in taking the $1/(1+n)$ root of e. Rearranging, we obtain the simplified expression

$$\sigma_c \simeq \left[\frac{\frac{K T_*}{W^* z_m^*}}{2Be^{-\frac{E^* + PV^*}{RT(z_m)}}} \right]^{\frac{1}{n+1}} \tag{59}$$

where the denominator $Be^{-\frac{E^*+PV^*}{RT(z_m)}}$ is just the coefficient relating $\dot{\epsilon}_{ij}$ and $\sigma^{n-1}\sigma_{ij}$ in Eq. (1) for the temperature and pressure prevailing in the zone of shearing. This expression is good to about 30% or better for $\mu \geq 4$ and $n = 3$. We see that the major uncertainty in evaluating this expression for a given earth model is the value of the denominator, which can change by an order of magnitude for a change of 100°k in $T(z_m)$.

Finally, it is useful to define an effective viscosity ν_c for the shear zone at a stress σ_c. By definition,

$$\nu_c \equiv \frac{\sigma_c}{v_c} w^o \tag{60}$$

hence, using (56) and (59), we obtain

$$\nu_c \simeq \frac{}{kT_*} \left(18\, e^{-\frac{E^*+pV^*}{RT(cm)}}\right)^{-\frac{2}{n+1}} \tag{61}$$

This equation is valid to only about 40% for $\mu \gtrsim 4$, $n = 3$; however, it is useful for a rough first approximation.

The Question of Time Scale

Although the time dependent version of Eq.(2) is too complex to solve analytically, we can get a rough idea of the time scales involved by means of the Grundfest parameter G. I.J.Grundfest[1] defined a dimensionless ratio of the two time scales relevant to the thermal instability question: the time for thermal conduction t_c, and the time for the temperature to diverge for zero thermal conductivity, t_∞. Thus,

$$G \equiv \frac{t_c}{t_\infty} \tag{62}$$

If $G \geq 1$ then $t_\infty \leq t_c$ and the temperature rises uncontrollably until new cooling mechanisms come into play. If $G \leq 1$, then conduction suffices to remove the heat generated, and steady solutions to the temperature field exist.

The thermal conduction time scale can be estimated by the usual means, and we find

$$t_c = \frac{z_m^2}{k/\rho c_p} \tag{63}$$

where the distance scale is taken to be z_m, the depth to the zone of heat production.*

To estimate the time scale for thermal runaway, we must use Eq.(2), neglecting the conduction term. Let the initial temperature correspond to a steady state characterized by stress parameter p_0. To this steady state temperature $T^o(p^o, z)$ add a small time dependent part $\theta(z,t)$. Suppose that p_0 is suddenly changed to p. Then the time evolution of $T(z,t) = T^o(p,z) + \theta(t,z)$ is given by:

$$\frac{\partial \theta}{\partial t} = \frac{kT_*}{\rho c_p} e^{\frac{T^o}{T_*} - \frac{z}{z_m}} \left(p e^{\frac{\theta}{T_*}} - p^o\right) \tag{64}$$

This equation is very difficult to integrate unless $p^o = 0$. For small θ, $\theta << T_*$, the temperature behaves like

$$\frac{\partial \theta}{\partial t} \simeq \frac{kT_*}{\rho c_p} e^{f^o} \left[(p - p^o) + \frac{p\theta}{T_*}\right] \tag{65}$$

where we have written $\frac{T^o}{T_*} - \frac{z}{z_m} \equiv f^o(z)$. Upon integration, with $\theta(z,0) = 0$,

$$\frac{\theta(t,z)}{T_*} = \frac{p - p^o}{p}\left[e^{p\frac{kT_*}{\rho c_p} e^{f^o} t} - 1\right] \tag{66}$$

The time scale over which θ changes by T_* is thus of order

$$t_\infty = \frac{\rho c_p}{kT_*} \frac{e^{-f^o}}{\delta p} \tag{67}$$

This is also the time required for θ to diverge if $p^o = 0$ in Eq.(64), so that it is the appropriate time scale. Note that as δp becomes larger, the temperature diverges more rapidly (t_∞ decreases).

The Grundfest parameter is thus

$$G = z_m^2 \delta p e^{f^\circ(z)} \tag{68}$$

It is easy to check that for $\delta p = p_c$ (the largest p allowing steady solutions), and $e^{f^\circ(z)} = e^{f_m^c}$, we obtain $G \simeq \mu / e\sqrt{\pi}\,(f_m \mu \gg 1)$. Our results are thus consistent with Grundfest's reasoning, since we find no steady solutions for $G \gtrsim 1$. Narrowing the shear zone adds stability in the sense that steady solutions exist for larger G as μ increases. Note that for the unphysical solutions pe^{f° is generally larger than $p_c e^{f_m^c}$, so that $G > 1$ for all such solutions. The physical solutions have pe^{f° less than $p_c e^{f_m^c}$, so that $G \lesssim 1$ in the physical region.

Equation (66) provides even more evidence for the non-existence of the unphysical solutions. This equation shows that a sudden increase of p invariably causes the temperature to rise at all depths (for either set of solutions). This temperature change is in the right direction to get to the larger p steady state temperature distribution for the physical solutions. The unphysical solutions, however, require that an increase of p yields lower temperatures at all depths (see, e.g. Fig.2). Thus, if the mantle were in a state described by an unphysical solution, and the stress were suddenly changed, the temperatures would rise, moving away from the steady state solution for the new stress. It is thus plausible that the new steady state is unattainable. A preliminary linear stability analysis for the unphysical solutions shows that they may be marginally stable to infinitesimal slow temperature perturbations for stresses close to the critical stress. It seems unlikely that they are stable for finite amplitude perturbations, but this work is still in progress.

In any case, it is clear that the time required to reach a steady state solution is of the order of the thermal conduction time constant t_c. This is supported by the numerical calculations of I.J.Grundfest[1] and of N. Fijii and S. Uyeda, where steady states were attained after a time t_c had elapsed (when steady states were possible). This time constant depends upon the depth of the zone of most intense shearing. Sample values for depths of geophysical interest are given in Table I (where we have taken k = .008 cal/cm^2-sec-$^\circ$k).

Table I

Depth of Shear Zone	Thermal Time Constant
z_m	t_c
30 km	36 Myr
50	99
70	194
100	400
150	890

Time constants of the order of 100 Myr are thus to be expected in the earth. Since much of the ocean floor is younger than this, it is not necessary that the actual temperature profile of the earth follows one of the steady state profiles derived in this paper. However, if the stresses acting on the lithospheric plates of the earth were much in excess of the critical stress, thermal runaway could occur on a much shorter time scale than t_c. In fact, since $t_\infty \sim 1/p$ or $t_\infty \sim 1/\sigma^{n+1}$, we can conclude that thermal runaway occurs on a time scale of roughly

$$t_{runaway} \approx t_c \left(\frac{\sigma_c}{\sigma}\right)^{n+1} \qquad (69)$$

Thus for $n=3$, applying a stress $\sigma = 2\sigma_c$, thermal runaway is reached in $t_c/16$, or about 5 Myr. If the possibility of thermal runaway is excluded in the earth, then Stresses must be close to σ_c, even though a steady state has not been attained. Hence, even in this case σ_c (and v_c) play an important role in marking the boundaries between different regimes of plate motion.

Conclusion

We have examined the equations describing the motion of the lithosphere over the asthenosphere when shear heating is taken into account. There are two classes of steady solution, which we have labeled the "physical" and the "unphysical" solutions. The physical solutions exhibit a stress-strain relation which at low stress is similar to that for no-shear heating, but which deviates from the low stress solution as a critical stress σ_c is approached. There are no steady solutions of any kind for stresses greater than σ_c. The velocity corresponding to σ_c is finite, and has a value v_c. The velocity of the plate is less than v_c for all physical solutions.

The unphysical solutions all have velocities greater than v_c, ranging from v_c (at $\sigma_{x_2} = \sigma_c$) to ∞ (at $\sigma_{x_2} = 0$). Velocity and stress are inversely related for these solutions, $v\sigma_{x_2} \approx$ constant, which leads to rather bizarre mechanical behavior. Such solutions appear to be unstable (or only marginally stable in certain special circumstances), and so are unlikely to be of any importance to the earth.

The physical solutions imply only slight modifications of the thermal structure of the mantle, even for $\sigma_{x_2} = \sigma_c$. Thus, as long as $\sigma_{x_2} \leq \sigma_c$, the heat generated by shearing can be neglected. However, if σ_{x_2} exceeds σ_c, the temperature must inevitably rise until new physical processes come into play.

These new processes include the production of large amounts of melt in the asthenosphere (which modifies the stress-strain relation) and relaxation of the applied stress. O.L.Anderson and P.C.Perkins[4] have suggested the association of thermal runaway with volcanism. This process could lead to cooling of the asthenosphere by the extension of basalt, and a new sort of steady solution might be attained by this means. In any case, if $\sigma_{x_2} > \sigma_c$ the physics of the asthenosphere must be dominated by the need to get rid of the excess heat developed by shearing.

Assuming that the present plates are moving at velocities less than v_c, we obtain a strict upper limit on σ_c of a few tens of bars. The stresses driving the plates must then be very small (corresponding to viscosities of ca. 10^{19} poise in the asthenosphere). The actual stresses in the earth might be somewhat higher than σ_c, since the time required to reach a steady state is of order 100 Myr. However, if the stresses are more than a few times σ_c, thermal runaway occurs on time scales of order 10 Myr or less, and the thermal structure of the asthenosphere must be dominated by the need to avoid this divergence.

The parameters σ_c and v_c thus mark the boundaries of a regime of plate motion in which there is little shear heating of the asthenosphere. If stresses or velocities greatly exceed these critical values, then an entirely new physics must come into play in order to dissipate the excessive amounts of heat generated.

Table II

Model Mantles

A. Model Input Parameters

Model #	Surface Temp. Gradient Q/k	Adiabatic Temp. Gradient γ	Depth to top of transition zone z_e	Depth to bottom of transition zone z_a	Rheological scale weight ζ
1	13°C/km	.3°C/km	100 km	200 km	1500 km
2	13	.3	100	200	500
3	13	.3	50	200	1500
4	13	.3	50	200	500
5	20	.3	50	100	1500
6	20	.3	50	100	500

We have taken $T(o) = 0°C$ for all models. The stress-strain relation is assumed to be of the form

$$\dot{\epsilon}_{ij} = 4.2 \times 10^{-16} \sigma^3 e^{-\frac{E^* + PV^*}{RT}}$$

where E^* = 125 k cal/mole, and V^* = 11.9 cm^3/mole (ζ = 1500 km) or 35.6 cm^3/mole (ζ = 500 km). The thermal conductivity k = .008 $cal/cm^2\text{-sec-}^oK$.

B. Model Rheological Results

Model #	Depth of shear zone z_m^o	Width of shear zone w^o	Temp. in shear zone $T(z_m)$	Temp. parameter T_*	$\frac{dT}{dz}$ at z_m T_*/z_*	Critical stress σ_c	Critical velocity v_c	Effective viscosity at σ_c, v_c
1	190 km	63 km	2229°k	79.1°k	1.5 °K/km	.33 bar	140 cm/yr	5×10^{17} poise
2	168	61	2163	74.5	4.3	1.8	26	1×10^{19}
3	184	63	1831	53.4	1.0	1.4	23	1×10^{19}
4	157	61	1766	49.7	3.5	12.	3.0	8×10^{20}
5	98	28	1778	50.3	1.2	1.5	38	4×10^{18}
6	92	28	1764	49.5	3.5	4.7	12	4×10^{19}

Appendix I: The structure of $I(\alpha,(3)$.

Definition

$$I(\alpha,\beta) \equiv \int_0^1 \frac{d\zeta}{\sqrt{3+\alpha[1-e^{-\beta\zeta}]}}$$

In general, $0 \le I(\alpha,\beta) \le 2$ for all $\alpha \ge 0, \beta \ge 0$.

A plot of $I(\alpha,\beta)$:

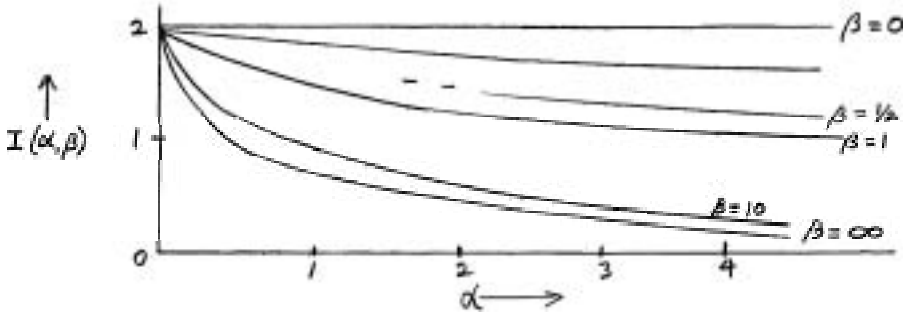

Approximations to $I(\alpha,\beta)$:

$$I(\alpha,0) = 2$$

$$I(\alpha,\beta \ll 1) \simeq \frac{2}{\sqrt{1+\alpha\beta}}$$

$$I(\alpha,\beta \gg 1) \simeq 2(\sqrt{1+\alpha}-\sqrt{\alpha}) + \frac{1}{\beta}\frac{2\beta n^2}{\sqrt{\alpha}}$$

$$I(\alpha,\infty) = 2(\sqrt{1+\alpha}-\sqrt{\alpha})$$

$$I(0,\beta) = 2$$

$$I(\alpha \ll 1,\beta) \cong 2+\alpha\left[1-e^{-\beta}-\sqrt{\pi\beta}\,erf\sqrt{\beta}\right]$$

$$I(\alpha \gg 1,\beta) \cong \frac{2}{\beta\sqrt{\alpha}}\cosh^{-1}e^{\beta/2}$$

$$I(\alpha \gg 1,\infty) \equiv \frac{1}{\sqrt{\alpha}}$$

Appendix II: The construction of rheological models of the earth.

In this section we show how to determine the parameters $\bar{z}_m^n$, μ, etc. which are needed to calculate the σ_{x_2} vs v relation for plates. Given these parameters, we can use the equations of the second section of this paper to compute such quantities as $v(\sigma_{x_2})$, v_c, and σ_c. It is possible to simply specify these parameters, and assume that the thermal structure of the upper mantle is such as to realize them. However, it is useful to see what values for $\bar{z}_m^n$, μ, etc. plausible thermal models yield, and that will be our motivation in the following work.

It is quickly found that thermal models with constant heat generation q do not yield a good representation of conditions probably existing in the asthenosphere. At great depths the temperature gradient is probably near the adiabatic gradient, whereas near the surface the temperature increases with depth at a higher rate. We

thus approach the problem by assuming a linear temperature gradient ($q = 0$) down to a depth z_ℓ. The gradient is Q_s/k, where Q_s is the surface heat flux. Between depths z_ℓ and z_a is a transition zone where $q \neq 0$. At depths greater than z_a the temperature gradient is again linear ($q = 0$), and is equal to the adiabatic gradient γ. In the transition zone q is determined by requiring that the temperature profile is continuous, and has a continuous first derivative. The heat production q is thus ficticious, and we only use it to enforce the curvature of the temperature profile, and thus to localize the shear zone. The value of q is

$$q = \frac{1}{T_*}\left(\frac{Q}{k} - \gamma\right)\left(\frac{z_a - z_\ell}{z_a - z_\ell}\right) \qquad (A.1)$$

hence from $w^0 = \sqrt{2\pi/q}$,

$$w^0 = \sqrt{\frac{2\pi\, T_a (z_a - z_\ell)}{Q/k - \gamma}} \qquad (A.2)$$

The temperature profile in this model is given by

$$T(z) = \left[T(0) - \left(\frac{Q}{k} - \gamma\right)\frac{z_\ell^2/2}{z_a - z_\ell}\right] + \left[\frac{\frac{Q}{k} z_a - \gamma z_\ell}{z_a - z_\ell}\right] z - \frac{\left(\frac{Q}{k} - \gamma\right)}{2(z_a - z_\ell)} z^2 \qquad (A.3)$$

The upper zone with $q = 0$ has no effect on the boundary conditions of the problem except to change the apparent temperature at $z = 0$ from $T(0)$ to $T_{eff}(0)$, where

$$T_{eff}(0) = T(0) - \left(\frac{Q}{k} - \gamma\right)\frac{z_\ell^2/2}{z_a - z_\ell} \qquad (A.4)$$

$T_{eff}(0)$ may be negative. Except for this change, the calculation of the thermal structure of the shear zone goes through as before. We define parameters B, C by means of

$$T(z) = T_{eff}(0) + Bz - Cz^2 \qquad (A.5)$$

The zone of initial shearing is located where

$$\left.\frac{dT}{da}\right|_{z_m} = \frac{T_*}{z_*} = \frac{\rho g V^*}{E^*} T(z_m) = \frac{T(z_m)}{\zeta} \qquad (A.6)$$

where $\zeta = E^*/\rho g V^*$ is a sort of rheological scale height. Since V^* is very poorly known, we perform the model calculations for

$$\zeta = 1500 \text{ km} \quad (E^* = 125 \text{ K cal/mole}, V^* = 11.9 \text{ cm}^3/\text{mole})$$

and $$\zeta = 500 \text{ km} \quad (E^* = 125 \text{ K cal/mole}, V^* = 35.6 \text{ cm}^3/\text{mole}).$$

Equation (A.6) yields a quadratic equation for z_m,

$$z_m = \frac{B + 2C - \sqrt{(B + 2C)^2 - 4C\left(T_{eff}(0) - \zeta B\right)}}{2C} \qquad (A.7)$$

once z_m is determined, $T(z_m)$ is computed from (A. 5). This allows T_*/z_*, T_*, w^0, and $\mu = \sqrt{\pi}\, z_m^*/w_0$ to be found. The equations of the second section can then be used to determine σ_c and v_c. The $v(\sigma_{xz})$ relation can be calculated by iteration the appropriate equations.

This labor has been performed for six thermal models of the earth, and the results appear in Table II. The results clearly show the rough inverse relation of v_c and σ_c, and all but Model 4 yield v_c compatable with present plate velocities, All models indicate that the shear stress required to maintain the plate motions is very small (ten bars or less). The data on the stress-strain relation is derived from the laboratory data of D.L.Kohlstedt and C.Goetze.[27] The results of the models

The results of the models are unfortunately quite sensitive to this poorly-known stress-strain relation.

Many different thermal models are possible, so that Table II only provides a small sampling. The rough formulae for σ_c and v_c in section 3 are thus likely to be of more value than the detailed models considered here. It is, however, comforting to see that many models exist which give results consistent with what appears to be occurring in the earth.

References

1. Grundfest, I. J. 1963 "Thermal feedback in liquid flow: plane shear at constant stress". Trans.Soc.Rheol. 7: 195-207.
2. Froidevaux, D. and G. Schubert 1975 "Plate motion and structure of the continental asthenosphere: a realistic model of the upper mantle". J.Geophys. Res. 80: 2553-2564.
3. Fijii, N. and S. Uyeda 1974 "Thermal Instabilities during flow of Magna in Volcanic Conduits" J.Geophys.Res. 79: 3367-3369.
4. Anderson, O.N. and P.C.Perkins 1974 "Runaway temperature in the asthenosphere resulting from viscous heating" J.Geophys.Res. 79: 2136-2138.
5. Kohlstedt, D.L. and C.Goetze 1974 "Low Stress, High Temperature Creep in Olivine Single Crystals" J.Geophys.Res. 79: 2045-2051.

THE DEVELOPMENT OF THE THERMAL STRACTURE OF THE PLATES

Barry Parsons

1. Introduction

The depth of the oceans, and also the heat flow measured at the ocean floor, behaves in a very simple way when considered as a function of the age of the ocean floor. For instance, the depth is observed to initiallyincrease linearly as $\sqrt{t}$, where t is the age of the ocean floor, but for ages greater than 60 my. This relationship breaks down and as the age increases further, the rate of increase in depth continues to diminish. An example of this behavior, taken from Parsons and Sclater (1975), is shown in Fig.1. Although heat flow measurements are somewhat suspect in regions near ridge crests, in older, generally well-sedimented areas, they are more reliable and in these areas also show a tendency to approach a constant value for large ages. A thermal model for the plates put forward by McKenzie in 1967 (Fig.2) has since been found to describe the variations in heat flow and depth reasonably well. The depth data can certainly discriminate between this and other models that have been proposed. This model is certainly simple in its construction, and the ease with which resulting properties can be calculated. However given that it describes the data well, one might expect the actual thermal structure of the plates to be closely similar to that of the model, and in that case it is not so obvious how such a picture is physically maintained. As an example, in the older ocean basins, where on the basis of the flattening in the heat flow and depths a close approach to thermal equilibrium seems to be indicated, the thermal model implies a constant supply of heat flux at the base of the plate. Because it does not seem possible to supply this heat by conduction without implying temperatures well in excess of the melting point in the upper mantle, convection on a smaller horizontal

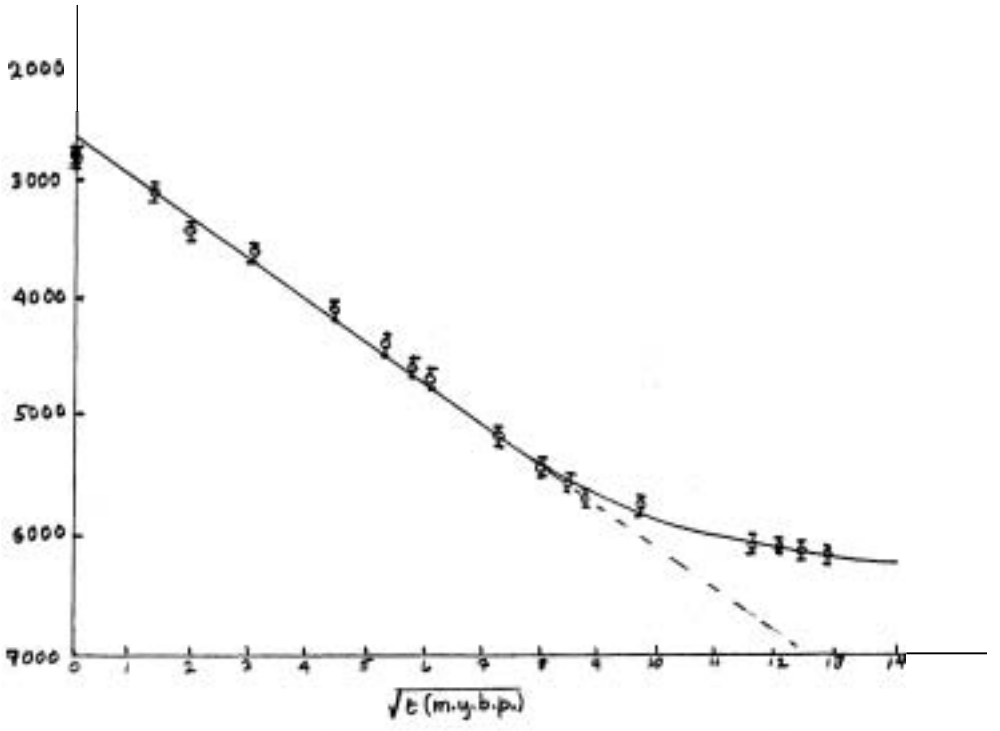

Fig.1 Plot of the mean depth in metres versus the square root of the age in million years (m.y.) for the North Pacific.

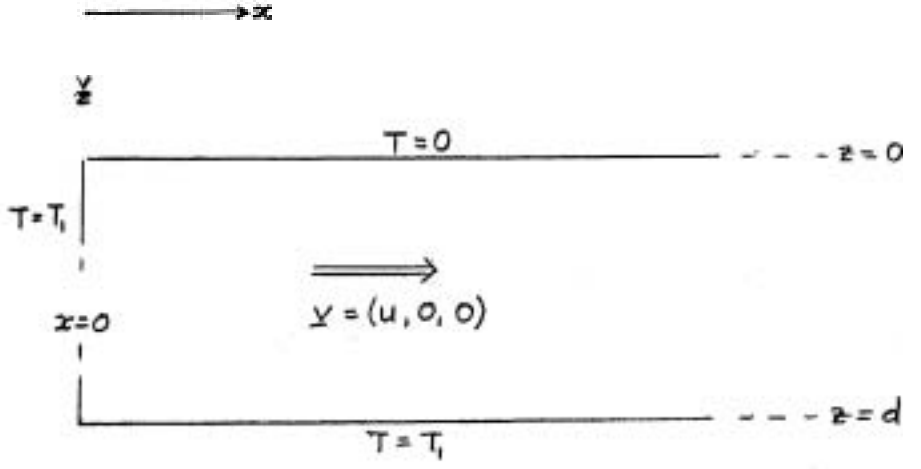

Fig.2 Geometry and boundary conditions of a thermal model (McKenzie, 1967) for the plates.

length scale than the plates themselves has been proposed to provide an efficient means of vertical heat transport in the upper mantle (Richter 1973, Richter and Parsons 1975). McKenzie and Weiss (1975) give other arguments for the existence of a small scale flow, in particular the overwhelming tendency of all flows studied numerically to be unstable to smaller scale disturbances.

The purpose of this study is to suggest a way in which the idea of the small-scale convective flow can be developed to provide a mechanism for maintaining a physical picture with the essential features of the plate model. In other words, two features must be explained. How are the isothermal boundary conditions on the

side and bottom boundary in Fig.2 maintained? Secondly, what determines the thickness of the plates and hence the age at which the linear relation between depth and $\sqrt{\epsilon}$ breaks down?

The scheme to be tested is illustrated in Fig.3. Material is assumed to ascend adiabatically at the ridge crest, and if we neglect the small adiabatic gradient this provides the isothermal side boundary condition. As the plate moves

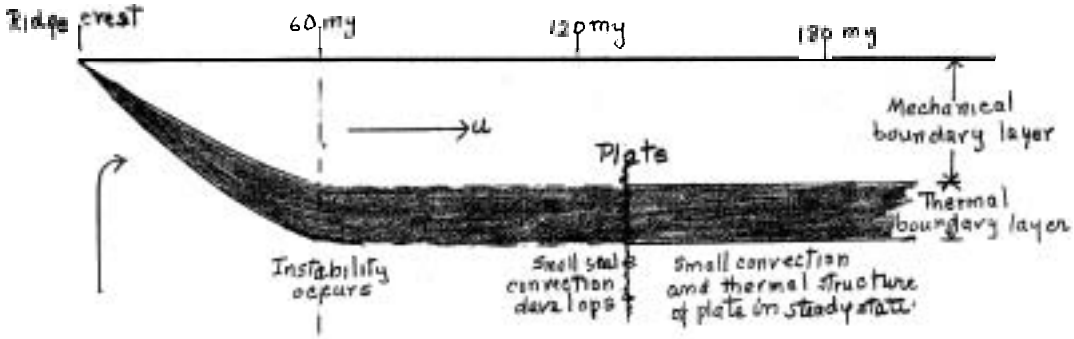

Fig.3 Sketch of the scheme to expalin the departure from the ϵ relationship at 60 m.y.

away from the ridge crest, the material cools conductively, the upper temperature being fixed at 0°C. Because of the very rapid variation of viscosity with temperature, it is assumed that the plate can be divided into two regions: an upper cold region which is essentially rigid, and a lower region which behaves approximately as a uniformly viscous fluid. It is proposed that at an age of 60 m.y. the cooling has proceeded sufficiently for the lower thermal boundary layer to become unstable. This is the point at which small-scale convection begins to develop. For ages larger than 60 m.y., material at the base of the plate is continuously being replaced in the thermal boundary layer. The bottom of the thermal boundary layer stays at the mean temperature produced when the small-scale convection reaches equilibrium with the heat sources within the mantle. The plate thickness is simply the sum of the mechanical and thermal boundary layers. Both are included as the definition of plate thickness based on the topographic observations must extend to a depth above which are included significant mean temperature, and hence density differences relative to the temperature profile under the ridge crest.

The difficulty with the proposal is to test whether the idea of an instability at this point is reasonable. In principle the stability of any two-dimensional flow could be examined exactly (e.g. Busse 1967). In practice, for this system, the calculation would be very difficult because of the variation of viscosity with temperature. In any case, we do not know what the large-scale flow, consisting of the plates and a return flow, really looks like. What I propose to do is to apply a local stability criterion to the thermal boundary layer in Fig.3, and show that it is not unreasonable to expect an instability to occur. Secondly, I shall show the results of some experiments, which again cannot directly prove the above assertion, but demonstrate enough similarities to provide confidence that the idea is a reasonable one.

2. Use of a boundary layer stability criterion.

a) Application to high Rayleigh number convection with internal heat sources.

The starting point is a scheme suggested by Howard (1966) as in some average sense equivalent to turbulent Rayleigh-Bénard convection. This is adapted to the

case of convection driven by internal heat sources, a mode of heating more appropriate in the earth, and comparisons will be made with numerical results for free-free boundary conditions. The steady state for such convection produces a mean temperature profile which is essentially isothermal from the bottom of the layer up to a thin boundary layer across which the temperature drops rapidly to match the zero temperature boundary condition on the upper surface. Following Howard (1966) we assume this situation can be modelled in a time-averaged sense by starting with a completely isothermal layer, temperature $T = T_1$, and at time $t = 0$ imposing an upper boundary condition $T = 0$, (Fig.4). An upper boundary layer develops by conductive cooling, the temperature being given by

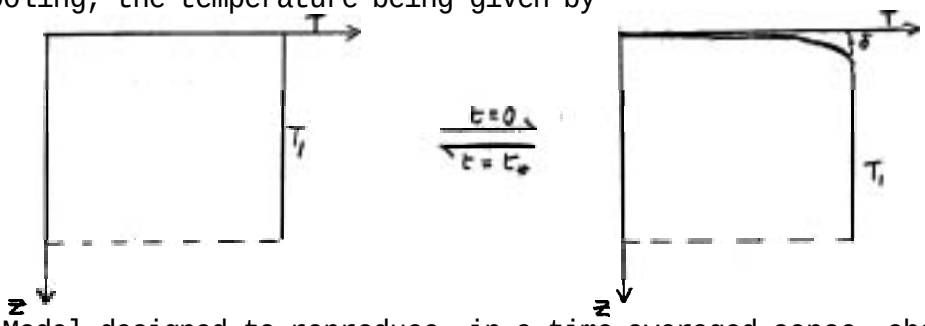

Fig.4 Model designed to reproduce, in a time-averaged sense, characteristics of convection driven by internal heat sources.

$$\frac{T}{T_1} = \operatorname{erf}\left\{\frac{z}{2\sqrt{\kappa t}}\right\} \tag{1}$$

This boundary layer becomes unstable at a time $t = t_*$ given by a local stability criterion

$$\frac{g\alpha T_1 \delta^3}{\kappa \nu} = R_c \tag{2}$$

where g is gravitational acceleration, α the thermal expansion coefficient, κ the thermal diffusivity, and ν the kinematic viscosity. The boundary layer thickness is taken to be

$$\delta = \sqrt{2\kappa t_*} \tag{3}$$

i.e., the thermal diffusion length scale at $t = t_*$. When the boundary layer becomes unstable, the fluid in the boundary layer is replaced in a time short compared to t_* (Howard 1966) so that the initial state is restored and the process repeats itself. The average heat flux over the period $(0, t_*)$ is

$$F = \frac{4kT_1}{\pi^{1/2}\delta} \tag{4}$$

where k is the thermal conductivity. In fact, in the internal heating problem, it is F that is specified and T_1 adjusts until a balance is attained with the internal heat sources. From (2) and (4) a relation between F and T_1 can be obtained

$$\log_{10} T_1 = 0.75 \log_{10} F - 0.25 \log_{10}\left\{\frac{64}{\pi^{3/2}}(\rho C_p)^3 \frac{\kappa^2 g\alpha}{\nu R_c}\right\} \tag{5}$$

with ρ the density and C_p the specific heat. McKenzie et al. (1974) obtained a similar relation based on their numerical calculations

$$\log_{10} T_1 = 0.76 \log_{10} F + 3.58 \tag{6}$$

Thus we see that the simple time-averaged model gives the correct form of the relation, and if we equate the constants in (5) and (6), using the values of the physical parameters given by McKenzie et al. (1974), a value of R_c is obtained that is to be applied to the stability of the boundary layer:

$$R_c = 473 \qquad (7)$$

Although the model is very crude, the value of R_c obtained provides some reassurance that reasoning based on the local stability of the boundary layer can give sensible results. The critical Rayleigh number for free-free boundaries is $R_c = 658$ with a constant temperature specified on the bottom boundary, and $R_c = 385$ with constant flux on the bottom boundary.

b) Application to the initiation of small-scale convection.

The scheme to be tested was illustrated in Fig.3. The decision to divide the developing lithosphere into two regions, one rigid, the other uniformly viscous, is based on the very rapid variation of viscosity with temperature. The Nabarro-Herring diffusion mechanism gives an expression for the viscosity

$$\eta = \frac{kTa^2}{10 m_0 D_0} \exp\left\{\frac{E+pV}{kT}\right\} \qquad (8)$$

where here k is Boltzmann's constant, a the mean grain radius, D_0 the reference constant in the diffusion coefficient, m_0 the mass of an oxygen ion, E an activation energy and V an activation volume, T the absolute temperature and p the pressure. In the upper 100 km the pressure effect is small; the temperature variation is shown in Fig.5, using the following values:

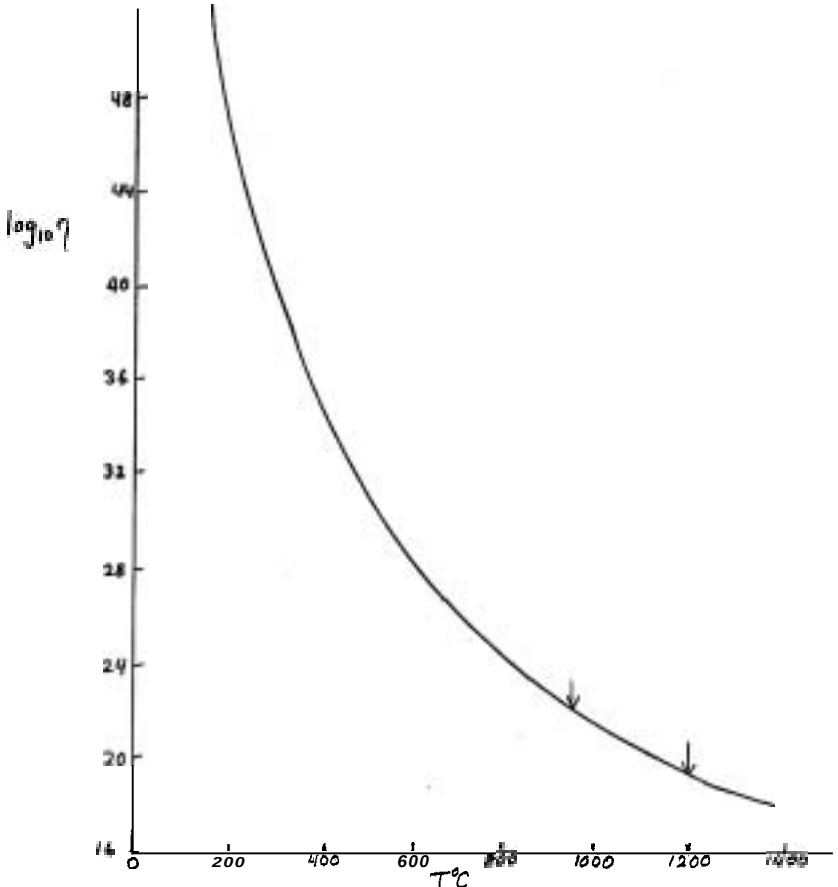

Fig.5 Plot of $\log_{10}\eta$, where η is the viscosity given by the Nabarro-Herring diffusion mechanism, for the temperature range expected in the plates.

$$a = 5.10^{-2}\,\text{cm}$$
$$D_0 = 5\,\text{cm}^2\text{s}^{-1} \qquad (9)$$

The value of the grain size to be used is subject to a great deal of uncertainty. The uniform temperature at the ridge crest is assumed to be

$$T_1 = 1200^{\circ}C \tag{10}$$

Decreasing the temperature by 300°C produces four orders of magnitude change in viscosity. To begin with, a temperature drop across the thermal boundary layer has to be guessed. I have picked 960°C as the temperature at which the behaviour goes from rigid to viscous, i.e.

$$\frac{T'}{T_1} = 0.8 \tag{11}$$

The initial temperature distribution is still given by (1) so that the thickness of the mechanical (rigid) boundary layer grows as

$$1.8\sqrt{\kappa t} \tag{12}$$

The temperature drop across the thermal boundary layer is obviously

$$\Delta T = 1200 - 960 = 240^{\circ}C \tag{13}$$

A thickness for the thermal boundary layer has to be defined somehow, and somewhat arbitrarily I have chosen

$$\frac{T''}{T_1} = 0.97 \tag{14}$$

to define the bottom of the thermal boundary layer. The thickness of the thermal boundary layer grows as

$$\delta = 1.2\sqrt{\kappa t} \tag{15}$$

Again a local stability criterion

$$\frac{g\alpha\Delta T\delta^3}{\kappa\nu} = R_c \approx 10^3 \tag{16}$$

can be applied to the thermal boundary layer. Rather than ask at what time t_* this occurs given ν, let us assert that the instability occurs at $t_* = 60$ m.y. as observed and ask what is the value of ν needed to satisfy (16). With the values

$$\begin{aligned} g &= 10^3 \text{ cm s}^{-2} \\ \alpha &= 3.10^{-5} {}^{\circ}C^{-1} \\ \kappa &= 8.10^{-3} \text{ cm}^2 \text{s}^{-1} \end{aligned} \tag{17}$$

this gives a value for the viscosity of

$$\nu = 11.10^{20} \text{ stokes} \tag{18}$$

This is reasonable judging by the values plotted in Fig.5. Using this value of ν, a check can be applied on the value 04 fixed as the temperature drop across the boundary layer. In the steady state ΔT and the heat flux are related as in (5) and (6). If we use the relation of McKenzie et *al.*, (1974), but include the fmplicit dependence on viscosity we have

$$\log_{10}\Delta T = 0.75\log_{10}F + 3.58 + 0.25\log_{10}\left(\frac{\nu}{\nu_0}\right) \tag{19}$$

where ΔT is in °C and F in W_m^{-2}. They used a reference viscosity

$$\nu_0 = 2.10^{21} \text{ stokes}$$

in which case for $\nu = \nu_0$ (19) reverts to (6). Substituting the value given in (18) with $F = 5.8 \cdot 10^{-2} W_m^{-2}$, we find that

$$\mathbf{\Delta T} = 220^{\circ}C \tag{20}$$

Hence the initial guess on the temperature drop across the thermal boundary layer turns out to have been quite close. From (12) and (15), when the instability occurs, the thickness of the mechanical boundary layer is 71 km, and that of the thermal boundary layer 49 km. The sum of these is 120 km which is the total plate thickness, consistent with the value of 115 km obtained by fits to the variation of depth with age. Thus the occurrence of such an instability explains the departure from the $\sqrt{t}$ behaviour at 60 m.y. and the observed thickness of the plate. For larger ages the amplitude of the small-scale flow increases to match the heat flow requirements of the cooling plate.

The last point we must demonstrate is that the temperature of the material intruded near the ridge crest is essentially that maintained in the main isothermal (adiabatic) part of the small-scale flow. In other words in moving from the region where the small-scale flow is established to the ridge crest the temperature change produced by the internal heat sources must be small. The observed heat flux is equivalent to uniform internal heating at a rate of 8.36×10^{-7} erg $s^{-1} cm^{-3}$ distributed in the upper mantle. The maximum temperature change these sources can produce in 120 m.y. in any given volume of material is less than 100° C even if no heat is lost from that volume. As the large-scale flow transports material from under the steady state portion of the plates to the ridge crest, there is little temperature change, and hence the temperatures on the side and bottom boundaries of the plate model can be considered identical.

3. Experiments

These were all performed in a convection tank based on the design of Chen and Whitehead (1968) and actually built to carry out the experiments described by Richter and Parsons (1975). The convection was observed by a shadowgraph technique, so that in the photographs shown below dark regions represent hot, upwelling fluid and, correspondingly, bright regions represent cold downwelling fluid. The layer of fluid is bounded above and below by horizontal glass surfaces which are maintained as isothermal boundaries to a good approximation. These are separated by machined spacers which control the depth of the fluid layer. The working fluid is in all cases a Dow Corning 200 silicone oil with a Prandtl number of 8,600, the large Prandtl number limit being appropriate for application to mantle convection. Values of the physical parameters of this oil are $\rho_0 = 0.971$ g cm^{-3}, $\nu = 10$ cm^2 s^{-1}, $\alpha = 9.6 \times 10^{-4}$ $^{\circ}C^{-1}$, and $\kappa = 1.16 \times 10^{-3} cm^2 s^{-1}$. The viscosity is to a good approximation independent of the temperature.

a) Transient experiment cooling from above.

This type of experiment has been explored previously, particularly in connection with the cooling of the surfaces of oceans and lakes. However, it seemed worthwhile to repeat it once or twice to check on the stability criterion used above, and also to obtain an idea of the form of the convection that occurs. Two runs were performed in which both boundaries were maintained at 400 C for a time greater than the thermal time constant, d^2/κ, of the tank, where d is the depth of the layer. This produces an initially isothermal layer of fluid. The heating of the bottom boundary was stopped at the same time as the temperature on the upper boundary was rapidly reduced. The bottom boundary temperature varies very slowly subsequently compared to that of the upper boundary, so that essentially the fluid was being cooled from above with zero heat flux at the bottom. The instability occurs in the cold upper boundary layer, cold (bright) fluid breaking away and forming concentrated downwellings. The boundary layer thickness at this point was estimated from the thermal diffusion length scale, $\delta = 2\sqrt{\kappa t_*}$, where t_* is the time from the initiation of cooling to the onset of the instability. This gave values

$$\delta \sim 1.8 \text{ cm} \qquad (21)$$

which were always smaller than the depth of the fluid layer (12 cm and 5 cm respectively). A rough value of the local Rayleigh number for the boundary layer at the onset of the instability was calculated using δ and the mean temperature difference over the interval $(0, t_c)$ between the initial temperature and that of the upper boundary. This gave

$$R_c \sim 2.10^3 \qquad (22)$$

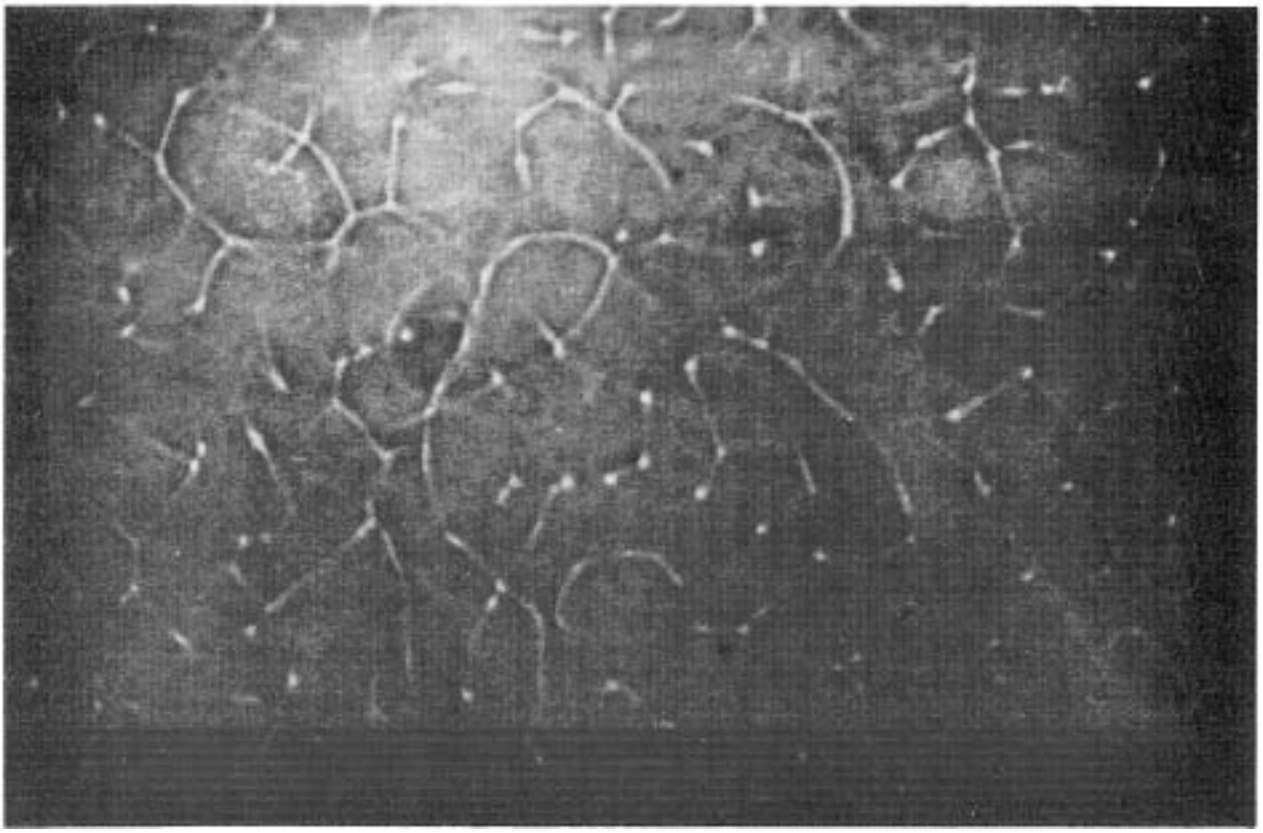

Fig.6 Example of the form of convection **produced** by **cooling** from above. Note the predominance of localized cold downwellings (bright regions).

again justifying considering only the stability of the boundary layer. The form of the convection that follows always consists of localised downwellings; no localised dark upwelling regions were observed so that the upwelling must occur over a diffuse area. A typical example of the developed form of the convection is shown in Fig.6, well before what is obviously a transient state begins to decay. This form of convection is observed in the numerical experiments for internal heating of McKenzie et *al.* (1974), and contrasts with Rayleigh-Bénard convection where upwelling and downwelling fluid occur symmetrically. Hence in the mantle we might expect the convection to occur in the form of localised downwellings falling from the base of the plate.

b) Interaction between Rayleigh-Benard convection and forced convection.

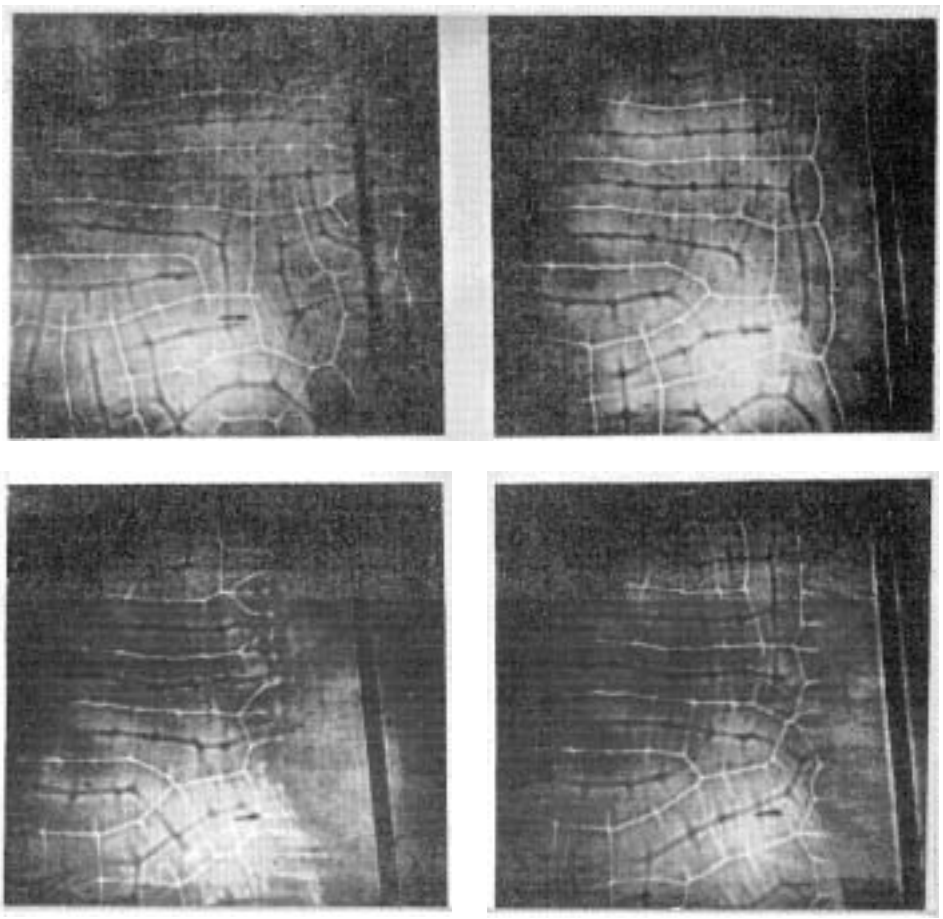

Fig,7 Steady state flows for a Rayleigh number of 5.10^4. Proceeding clockwise from the top left the forced flow has $\delta T = 0, 1, 2,$ and 3,4 respectively, Mote the region in which no Rayleigh-Bénard convection occurs near the pipe, which is the dark linear feature at the right of each photograph,

One would like to do an experiment exactly duplicating the situation being explored, i.e. forcing a flow by moving boundaries apart from each other at the same time as producing a small-scale convection with some appropriate mode of heating. This did not seem possible at the time, but it was possible to look at the interaction between another kind of forced flow and small-scale convection. The small-scale convection is represented by Rayleigh-Bénard convection driven by an adverse vertical temperature drop between the horizontal boundaries. The forced flow is produced by placing a copper pipe horizontally in the fluid. Hot water can be circulated through the pipe, and this heating forces a flow. The Rayleigh-Bénard convection is characterised by the Rayleigh number, R. To specify the forced flow, the temperature difference $\delta T'$ between the pipe and the mean temperature between the horizontal boundaries is nondimensionalised with respect to the vertical temperature drop $\Delta T'$ across the tank. Write this as

$$\delta T = \delta T'/\Delta T' \qquad (23)$$

The aspect ratio of the tank was 20, (the actual depth equalled 5 cm), and the pipe ran parallel to one side. It should be emphasised that the dynamics of this forced flow are different from the one we would really like to explore. However the feature in common can be seen in Fig.7. When there is a forced flow produced by heating from the pipe, there is a region near the pipe where no Rayleigh-Bènard small-scale convection occurs. The hot fluid produced in the forced convection must lose sufficient heat before it becomes unstable and cold fluid descends into the layer. On the other side of this boundary small-scale convection proceeds normally, with virtually no sign of any influence from the forced flow. Increasing the heating of the forced flow pushes the boundary between the two regions somewhat further from the pipe. Similar behaviour is observed at a higher Rayleigh number (Fig.8). The point at which the downwelling occurs is still a definite distance from the pipe and moves further away as the heating rate is increased. However, here we note that instabilities produced by heating on the bottom boundary are able to penetrate the forced flow. In the earth internal heating may be the more appropriate mode of heating for the small-scale flow so that these effects due to heating from below might not be so important. The common feature to be noted and compared to the scheme illustrated in Fig.3 is the finite region in which no downwellings occur until the fluid circulating in the forced flow has cooled sufficiently at the top boundary to become unstable, and then the small-scale flow starts to develop.

Acknowledgments

I would first of all like to thank the following individuals: Dan McKenzie, who suggested the starting point for the ideas developed here; Jack Whitehead, in whose laboratory the experiments were performed, and with whom one of the experiments in 3a was done; Robert Frazel, who helped modify the apparatus. Other fellows and staff members of the Geophysical Fluid Dynamics program contributed to an enjoyable stay in Woods Hole. I gratefully acknowledge the support of this program by the National Science Foundation.

References

Busse, F.H. 1967 On the stability of two-dimensional convection in a layer heated from below. J.Math.Phys. 46: 140.

Chen, M. and J.Whitehead 1968 Evolution of two-dimensional periodic Rayleigh convection cells of arbitrary wavenumbers. J.Fluid Mech. 31: 1.

Howard, L.N. 1966 Convection at high Rayleigh number, in Proc.11th Int.Congr. Appl.Mech., Munich, 1964, (ed.H.Gortler), p.1109.

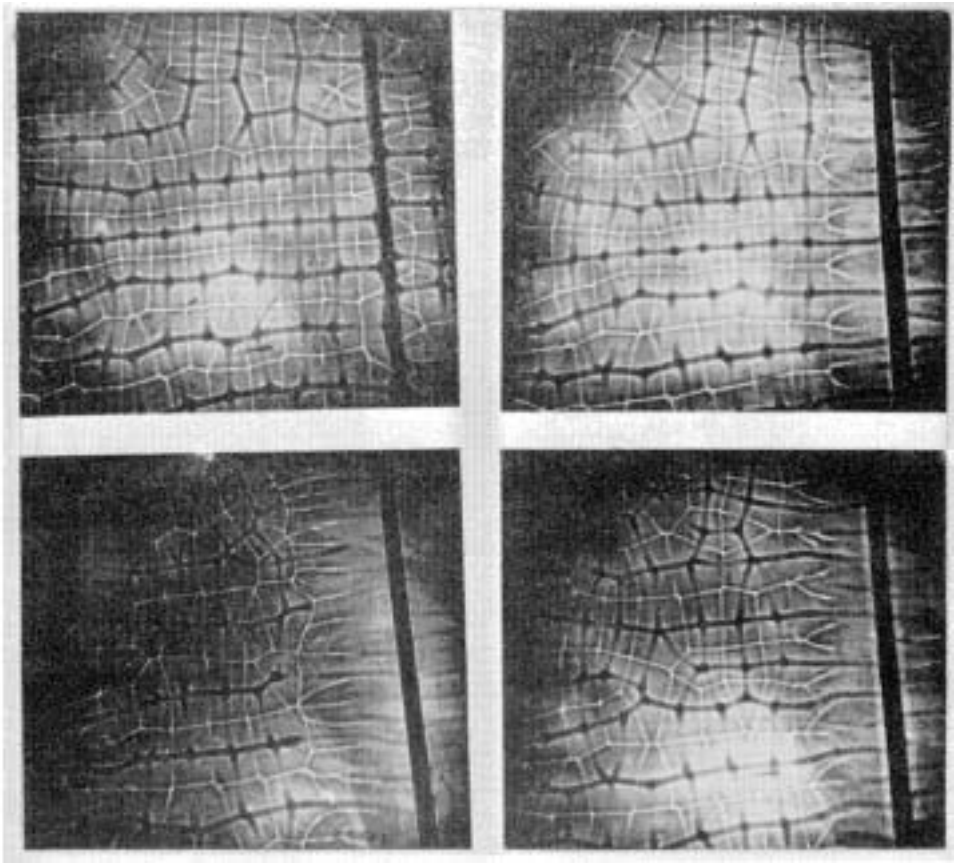

Fig.8 Steady state flows with R = 10^5. Clockwise from the top left the forced flow has ST = 0, 0.7, 1.2 and 2 respectively. In this case instabilities produced by heating at the bottom boundary can penetrate the forced flow.

McKenzie, D.P. 1967 Some remarks on heat flow and gravity anomalies. J.Geophys.Res. 72: 61.

McKenzie, D, and N. Weiss 1975 Speculations on the thermal and tectonic history of the earth. Geophys.J.R. Astr.Soc. (in press).

McKenzie, D.P., J.M.Roberts and N.O.Weiss 1974 Convection in the earth's mantle: towards a numerical simulation. J.Fluid Mech., 62: 465.

Parsons, B. and J.G.Sclater 1975 An analysis of the variation of ocean floor heat flow and bathymetry with age. Rev.Geophys.Space Phys. (submitted)

Richter, F.M. 1973 Convection and the large-scale circulation of the mantle. J.Geophys.Res., 78: 8735.

Richter, F.M. and B. Parsons 1975 On the interaction of two scales of convection in the mantle. J.Geophys.Res. 80: 2529.

INERTIAL CONVECTION AT LOW PRANDTL NUMBER

Michael Proctor

The properties of thermal convection at low Prandtl number (≪ kinematic viscosity/thermal conductivity) are of great interest in the study of the convectfve regions of the sun and stars, where the effective thermal conductivity of the stellar material is greatly enhanced by radiative processes. The Earth's liquid core is also largely metallic, and hence likely to be a good thermal conductor; Prandtl numbers there are thought to be rather less than unity. This type of convection is characterized by large Reynolds numbers (inertial forces become important) except at very low amplitudes, and appears easily to become turbulent owing to instabilities of the shear-flow type, Our understanding of turbulence is very limited, although Malkus, Busse and others have made progress towards a fuller understanding of thermal turbulence by considering its onset as a series of discrete transitions and instabilities, Other authors have chosen the opposite path - to ignore the instabilities (usually by suppressing three-dimensional motions) and to study the resulting laminar flow, both in order to elucidate the processes that drive to convection and limit its amplitude, and to obtain some rdea of the macroscopic order that exists even in a fully-developed turbulence, Prominent among these are the numerical studies of Moore and Weiss (1972) and Jones, Moore and Weiss (1975), who solve the full equations for the layer heated from below by finite difference methods. The first study is restricted to two-dimensional rolls, and the second to flows with symmetry about a vertical axis, Comparison of these papers shows a striking contrast between the Prandtl number dependence of the evolved steady flow in the two geometrfes, especially near to critical Rayleigh number for the onset of convection. In Fig.1 we show sketches of the dependence of Nusselt number against

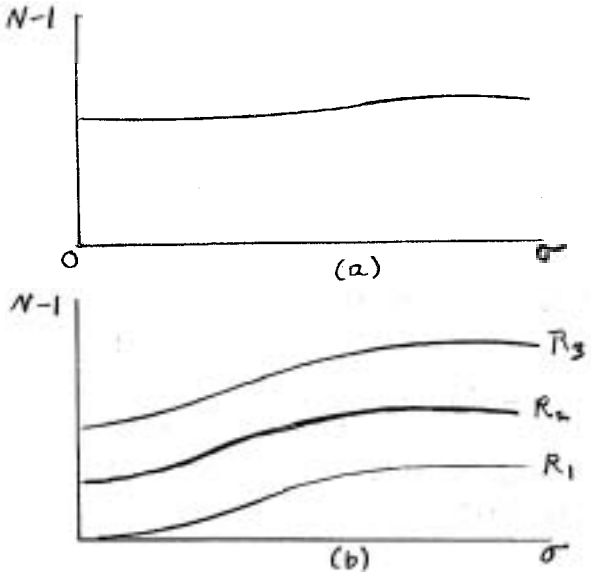

Fig.1

Fig.1 Sketches of Nusselt no. as a functnon of σ for (a) Rolls and (b) Cylinders: R_1 is below the 'second critical number' and R_1 and R_2 are above it,

the Prandtl number σ in the two cases. We notice that whale for rolls the σ-dependence is very weak, for cylinders the efficiency of convection is significantly inhibited for small σ. Further, below a certain Rayleigh number greater than the critical value to Nusselt number falls to 1 as $\sigma \to 0$, indicating that convection is suppressed in this limit. Another item of interest is that modified perturbation theory (e.g. Malkus and Veronis 1958), although satisfactory at all σ for the roll solutions, remains valid only for $(N - 1) = O(\sigma^2)$ for the cylinders at small σ

These results suggested the possibility that for $\sigma \to 0$ there was some sort of asymptotic limit in which inertial constraints played a dominant role. The discrepancy between rolls and cylinders could then be explained by noting that for rolls the inertial equation

$$\nabla_h (\underline{U} \cdot \nabla \underline{U}) \equiv 0 \tag{1.1}$$

is identically satisfied by the linear eigensolution, while for cylinders (1.1) is not satisfied, so that inertial adjustments become important at much lower amplitudes. Jones et *al.* demonstrated that a closed problem could be formulated in the limit $N \to 1; \sigma (N-1)^{-\frac{1}{2}} \to 1.$, in which (1.1) was satisfied to leading order. Their problem as posed was highly nonlinear, and they did not attempt to solve it directly. It is our purpose here to formulate two similar problems in which this nonlinear system is exactly soluble, so as to show how this problem differs from the conventional stability problem. In the next two sections we describe these problems and give some detail of their solution; in a conclusion we evaluate the results and assess their applicability to real turbulent convection and their relation to other types of problem.

2. The forced convection problem.

2.1 Formulation

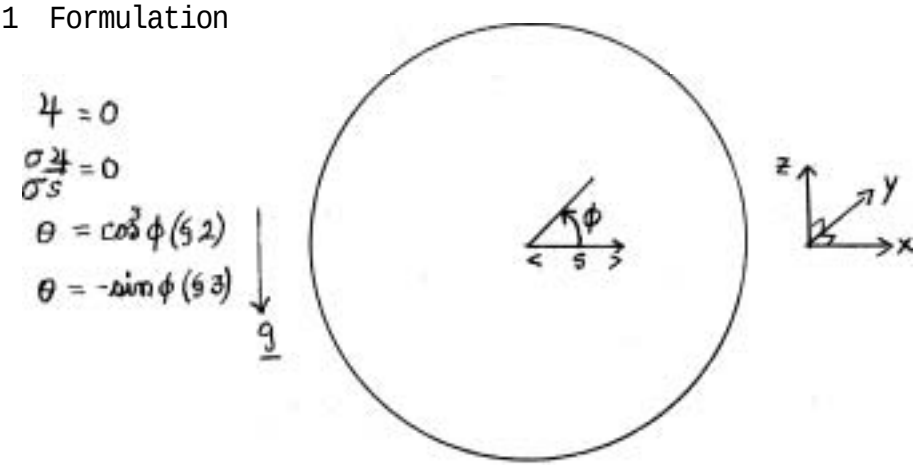

Fig.2. A sketch of the geometry and boundary conditions.

We consider two-dimensional motions of an incompressible fluid in a cylinder of nondimensional radius 1 with its axis along the y axis of a Cartesian coordinate system (Fig.2). s and ϕ are polar coordinates as shown, gravity is in the $-\hat{z}$ direction. The cylinder wall is supposed fixed, and the temperature of the wall is held fixed at the nondimensional temperature

$$\theta = \cos^3 \phi + T_0 \tag{2.1}$$

is that temperature increases to the right. The nondimensional equations of steady motions are, in the Boussinesq approximation

$$\begin{aligned} \sigma^{-1} \underline{U} \cdot \nabla \underline{U} + \nabla p &= R\theta \hat{\underline{z}} + \nabla^2 \underline{U} \\ \nabla^2 \theta &= \underline{U} \cdot \nabla \theta \\ \nabla \cdot \underline{U} &= 0 \end{aligned} \tag{2.2}$$

where

$$\underline{U} = \chi/a\,\underline{U}^*,\ \theta = \Delta T\theta^*,\ p = \frac{\chi\nu}{a^2}p^*,\ \underline{N} = a\underline{N}^*$$

$$\sigma = \nu/\chi,\ R = \frac{\alpha g \Delta T a^3}{\nu} \qquad (2.3)$$

and α is the coefficient of thermal expansion and χ is the thermal conductivity, ν the kinematic viscosity, and a typical length scale, (the radius of the cylinder), g the gravitational acceleration, and ΔT the maximum temperature contrast at the boundary. σ is the Prandtl number and R is the Rayleigh number. We also define a stream function $\psi(s,\phi)$ by

$$U_\phi = \frac{\partial\psi}{\partial s},\ U_s = -\frac{1}{s}\frac{\partial\psi}{\partial\phi} \qquad (2.4)$$

the boundary conditions are now

$$\psi = \frac{\partial\psi}{\partial s} = 0,\ \theta = \cos^3\phi \text{ on } s = 1 \qquad (2.5)$$

It is easily seen that (2.2) admits no solution unless motion occurs. In this respect it differs from the Rayleigh-Bénard problem discussed in § 3. As the temperature gradients drive the flow directly, this motion is known as fixed convection, and it has been studied by many authors in various limits. Here we give the standard perturbation treatment for the limit $R \to 0$, σ^{-1} finite, and contrast it with the solution in the (apparently new) limit of $R \to 0$, $\sigma R^{-1} \to 0$ which brings the inertial forces into predominance.

2.2 The Viscous Limit: $1 \gg \sigma \gg R$.

Since R is small, we expand all quantities in powers of R to give

$$\left.\begin{aligned}\theta &= \theta_0 + R\theta_1 + R^2\theta_2 + \cdots \\ \underline{U} &= R\underline{U}_1 + R^2\underline{U}_2 + \cdots\end{aligned}\right\} \text{etc.} \qquad (2.6)$$

where θ_1, $\underline{U}_2$, etc, may depend on σ. By substituting in (2.2) and equating powers of R we may solve a sequence of linear problems. The first equation is

$$\nabla^2\theta_0 = 0;\ \theta = \frac{1}{32}(3\cos\phi + \cos 3\phi) \text{ at } s = 1 \qquad (2.7)$$

and this has the solution

$$\theta_0 = \frac{1}{32}\left(3s\cos\phi + s^3\cos 3\phi\right) \qquad (2.8)$$

at O(R), we then have

$$\nabla p_1 = \theta_0\,\hat{\underline{e}} + \nabla^2\underline{U}_1 \qquad (2.9)$$

and this gives

$$\psi = \frac{1}{512}\left[6(2s^2 - s^4 - 1) - (s^6 - 2s^4 + s^2)\cos 2\phi\right] \qquad (2.10)$$

Note that the term $\sigma^{-1}R^2(\underline{U}_1\cdot\nabla\underline{U}_1)$ is small compared to the terms already considered in this limit. We may measure the vigour of the motion by the kinetic energy $E_2 \equiv -\frac{1}{2}\{\psi\nabla^2\psi_1\}$, where $\{\ \}$ denotes an integral over the cylinder and unit length in the y-direction. (2.10) gives

$$E_2 = \frac{3\pi}{2048} \times \frac{61}{60} \qquad (2.11)$$

independent of σ. We may continue the process by finding θ_1 from

$$\nabla^2\theta_1 = \underline{U}_1\cdot\nabla\theta_0 \qquad (2.12)$$

and then evaluating $\underline{U}_2$ from

$$\sigma^{-1}(\underline{U}_1\cdot\nabla\underline{U}_1)+\nabla p_2=\theta_1\hat{\underline{e}}+\nabla^2\underline{U}_2 \qquad (2.13)$$

Now, however, since $\nabla_h(\underline{U}_1\cdot\nabla\underline{U}_1)\not\equiv 0$ (as can be verified), $\underline{U}_2$ will be proportional to σ^{-1} to leading order (as $\sigma^{-1}>>1$). Our expansion for the energy E will therefore take the form

$$E=R^2E_2+\sigma^{-2}R^4E_4+\sim\sigma^{-3}R^6E_6+\cdots \qquad (2.14)$$

where E_4, E_6, etc. are independent of σ^{-1} to leading order. Although each term in the series is smaller than the last, it seems likely that the radius of convergence of the series tends to zero as $\sigma\to R$, and hence that (2.14) gives an extremely inaccurate estimate of E as this limit is approached. When $R^2>>\sigma$ (2.14) can give no information about E, even though $R<<1$, and we must seek an alternative formulation that enables us to escape from the constraints that are imposed by the perturbation approach, and to enter the regime in which inertial forces play a decisive role.

2.3 The Inertial Limit: $1>>R>>\sigma$

As noted in § 1, it is possible in some geometries to find steady flows for which the inertial forces are irrotational everywhere. Our geometry is one such, and this fact enables us to find a solution even though the kinetic energy and the Rayleigh number are small. The solution is not uniformly valid in the limit $R\to 0$ for fixed σ, but only in the (more restricted) limit

$$\left.\begin{aligned} R&\to 0\\ \sigma R^{-1}&\to 0\end{aligned}\right\} \qquad (2.15)$$

If we define $\eta=\sigma R^{-1}$, we can expand all quantities in powers of R as before, and obtain

$$\left.\begin{aligned} \underline{U}_1\cdot\nabla\underline{U}_1+\eta\nabla p_1&=\eta(\theta_0\hat{\underline{e}}+\nabla^2\underline{U}_1)\\ \nabla^2\theta_0&=0\end{aligned}\right\} \qquad (2.16)$$

to leading order; similar equations hold at higher orders in R. If we also expand in powers of η, so that

$$u_1=u_{10}+\eta u_{11}+\cdots \text{ etc.} \qquad (2.17)$$

then to leading order in η we must have

$$\nabla_h(\underline{U}_{10}\cdot\nabla\underline{U}_{10})\equiv 0 \qquad (2.18)$$

in terms of the streamfunction, this may be written

$$\nabla^2\psi_{10}=f(\psi_{10}) \qquad (2.19)$$

where f is arbitrary. Equation (2.19) states that streamlines and vorticity contours coincide to leading order. We determine f by noting that if we integrate (2.2) around <u>any</u> closed streamline $C(\psi)$ we obtain, (Batchelor 1956)

$$R\oint_C\theta\hat{\underline{e}}\cdot\underline{\sigma s}+\int_C\nabla^2\underline{U}\cdot\underline{\sigma s}\equiv 0 \qquad (2.20)$$

so that (2.20) does not contain the inertial terms - these only serve to redistribute energy around a streamline. (2.20) expresses the balance between thermal driving and viscous dissipation that must hold for each streamline. To leading order in R and η, (2.20) gives

$$\oint_{C_{11}}\theta_{10}\hat{\underline{e}}\cdot\underline{\sigma s}+\oint_{C_{11}}\nabla^2\underline{U}_{11}\cdot\underline{\sigma s}\equiv 0, \text{ where } C_{11} \text{ are the streamlines of } \underline{U}_{11}. \qquad (2.21)$$

and this can, in principle, be used to determine $f(\psi_{10})$ and hence the flow field. This problem is analogous to the one formulated but not solved analytically by Jones

et al. The difficulty is that the streamlines depend on the solution in general, so that the problem is highly nonlinear. However, in this geometry the solution is rendered extremely simple by the fact that the only solutions to (2.19) (which is second order) with the full viscous boundary conditions are of the form

$$\psi_{10} = \psi_{10}(s), \quad U_{10} = V_{10}(s)\hat{\phi} \tag{2.22}$$

so that all the streamlines are circles independently of the form of f. Since the equation for Θ_{00} is unaffected, giving the solution (2.8), (2.21) yields

$$\tfrac{1}{2}\left[\frac{35}{24}\right] + \alpha^2 V_{10} = 0 \tag{2.23}$$

where the $\frac{1}{2}$ comes from the streamline integration (reduced to a ϕ integration) and $\alpha^2 \equiv \frac{d^2}{ds^2} + \frac{1}{s}\frac{d}{ds} - 1/s^2$. Hence the part of Θ_0 proportional to $\cos\phi$ drives the flow, while that proportional to $\cos 3\phi$ has no effect, Hence ψ_{10} takes the form

$$\psi_{10} = \frac{1}{512}\left[6(2s^2 - s^4 - 1)\right] \tag{2.24}$$

and hence that the the kinetic energy to leading order will be

$$E_{20} = \frac{3\pi}{2048} \tag{2.25}$$

just under 2% less than in (2.11). This change may not be striking to the eye, but it is extremely important for a convergent representation of the solution. For it is now possible, as long as $\eta << R^{2n}$, to continue the expansion in powers of R, applying the analogues of (2.18) and (2.21) at each order, to produce a series for E that is independent of σ ;

$$E = R^2 E_{20} + R^4 E_{10} + \cdots \tag{2.26}$$

Hence we have isolated an asymptotic limit as $\sigma \to 0$, and all quantities are $O(1)$ except the inertial forces which are $O(\eta)$. This is clearly a much better representation of the solution as $\sigma \to 0$ than the previous one, since it is valid in a much larger region of parameter space. Figure 3 shows the dependence of E on R for any forced σ . For $R << O(\sigma)$ the curve lies near the viscous limit; for $R >> O(\sigma)$ it lies near the inertial limit. Between two limits is a transition zone in which $\eta = O(1)$ and the η expansion must be taken into account. It is hoped to treat the η expansion in the near future.

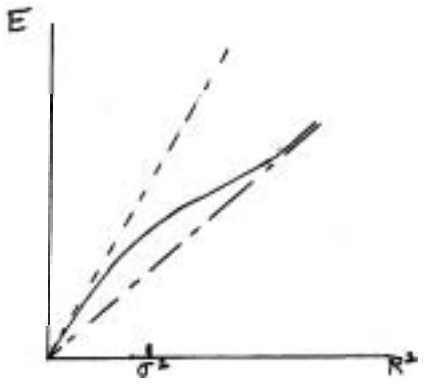

Fig.3 Graph of R^2 against E for the forced convection problem.
----- = viscous limit, — . — . — = inviscid limit.

3. The Rayleigh-Bénard problem.

3.1 Formulation.

For this problem, the geometry and scaling is exactly the same as in § 2, except that the temperature boundary condition is now given by

$$\theta = -\sin\phi \tag{3.1}$$

so that the fluid is heated from below and cooled from above. It is easily verified that (2.2) then has the static solution

$$\underline{U}_0 = 0, \quad \theta_0 = -z \tag{3.2}$$

and the problem then becomes one of the stability of the static state, Such a problem has been studied in many geometries by many authors, starting with Bénard (1900); Chandrasekhar (1968) gives a particularly full account. It was the recent study of Jones *et al.* (1975) that prompted the present work as in § 1. As in § 2, the equations may be attached in the two limits $1 \gg \sigma \gg \epsilon$ and $1 \gg \epsilon \gg \sigma$, where ϵ is a typical flow amplitude.

3.2 The viscous limit: $1 \gg \sigma \gg \epsilon$.

In this limit the problem may be attacked by the methods of modified perturbation theory, first applied to convection by Malkus and Veronis (1958). If we expand all quantities in powers of a small amplitude factor ϵ, so that

$$\left.\begin{aligned} \underline{U} &= \epsilon\,\underline{U}_1 + \epsilon^2\underline{U}_2 + \cdots \\ R &= R_0 + \epsilon R_1 + \cdots \\ \theta &= -z + \epsilon\theta_1 + \cdots \end{aligned}\right\} \tag{3.3}$$

and normalize ϵ by setting, $\{\theta_1\, \underline{U}_1 \cdot \hat{\underline{z}}\} = 1$, $\{\theta_1\, \underline{U}_n \cdot \hat{\underline{z}}\} = 0$, $n \neq 0$, then R can be determined as a function of ϵ. To leading order in ϵ, the equations are

$$\left.\begin{aligned} \nabla p_1 &= R_0\,\theta_1\,\hat{\underline{z}} + \nabla^2\underline{U}_1 \\ \nabla^2\theta_1 &= -\underline{U}_1 \cdot \hat{\underline{z}} \end{aligned}\right\} \tag{3.4}$$

since $\sigma^{-1}\epsilon\,(\underline{U}_1 \cdot \nabla\underline{U}_1)$ may be neglected to leading order in this limit. With the boundary conditions

$$\psi = \frac{\partial}{\partial s}\psi_1 = \theta_1 = 0 \quad \text{at } s = 1,$$

this is an eigenvalue problem for R_0. It appears that (3.4) possesses a variational principle (cf. Chandra, q.v.). R_0 can be found as the minimum of the functional

$$R[\underline{U}] \equiv \frac{\{|\nabla\underline{U}|^2\}}{\{|\nabla\theta|^2\}} \tag{3.5}$$

amang all $\underline{U}$ such that $\nabla\cdot\underline{U} = 0$ that satisfies the boundary conditions, θ being determined formally from (3.4b). Unfortunately it is not possible to solve (3.4) except as an infinite series, since the equations are not separable in s and ϕ. However, we may obtain an upper bound for the lowest eigenvalue by using a trial function $\underline{U}_T$ in (3.5); such an upper bound should be a good one since R_0 is an extremal. The lowest eigen mode is one that has circulation round the centre of the cylinder. The best estimate for the eigenvalue so far obtained is

$$R_0 \leq 380 \tag{3.6}$$

using a truncated ϕ expansion and Bessel function S-dependence. We do not give the details here, since (3.6) is probably fairly crude, and serves only to give an order of magnitude for R_c. The most accurate method of determining R_c is probably numerically using finite difference methods, In any case, our concern is not principally with this problem but with the inviscid one below, We note, though, that since Ψ_1 depends on ϕ, we have that

$$\nabla_h (\underline{U}_1 \cdot \nabla \underline{U}_1) \neq 0 \tag{3.7}$$

as in § 2. It follows that if we determine R_2, R_4, etc. by the standard methods we shall find that

$$R = R_0 + \epsilon^2 \sigma^{-2} R_2 + \cdots \tag{3.8}$$

to leading order in σ^{-1}, where R_2 is positive and independent of σ. Hence, as in § 2, (3.8) gives an accurate representation only for $\epsilon \ll \sigma$, and that for $\epsilon = O(\sigma)$ or larger the inertial terms must dominate the dynamics. Looked at another way, the nonlinear solution moves away from the eigen solution very rapidly in ϵ space due to the inertial terms. (3.8) clearly implies that ϵ^2 can rise only very slowly with increasing R; the inertial forces act to limit the amplitude of the system.

We treat the inertial limit below, The techniques used there are the same as in § 2, but the results are even more remarkable: for the inertial limit gives rise to an eigenvalue problem different from (3.4) and hence gives rise to a 'second critical eigenvalue' greater than R_c, as noted by Jones et al., and independent of σ.

3.3 The inertial limit: $\epsilon \gg \sigma$.

As in § 2, in this limit we can define a small parameter

$$\eta = \sigma \epsilon^{-1} \tag{3.9}$$

and consider $\epsilon \longrightarrow 0$, $\eta \longrightarrow 0$ together. If we expand all quantities in powers of ϵ and η:

$$\Psi = \sum_{i=1}^{\infty} \sum_{j=0}^{\infty} \epsilon^i \eta^j \Psi_{ij}, \text{ etc.} \tag{3.10}$$

Then to leading order in ϵ, (2.2) gives

$$\left.\begin{aligned} \underline{U}_{10} \cdot \nabla \underline{U}_{10} + \eta \nabla p_{10} &= \eta \left[R_{00} \theta_{10} \hat{\underline{z}} + \nabla^2 \underline{U}_{10} \right] \\ \nabla^2 \theta_{10} &= - \underline{U}_{10} \cdot \hat{\underline{z}} \end{aligned}\right\} \tag{3.11}$$

Then to leading order in η, we have

$$\nabla_h (\underline{U}_{10} \cdot \nabla \underline{U}_{10}) \equiv 0; \quad \Psi_{10} = \Psi_{10}(s), \underline{U}_{10} = V_{10}(s) \hat{\underline{\phi}} \tag{3.12}$$

as in (2.22). We determine Ψ_{10} by making use of (2.20); since the streamlines are circular in this case also, the integration is again trivial and we obtain

$$R_{00} \int^{2\pi} \theta_{10} \hat{\underline{z}} \cdot \hat{\underline{\phi}} \, d\phi + \int^{2\pi} (\nabla^2 \underline{U}_{10}) \cdot \hat{\underline{\phi}} \, d\phi \tag{3.13}$$

where

$$\nabla^2 \theta_{10} = - \underline{U}_{10} \cdot \hat{\underline{z}} \tag{3.14}$$

Now, $\underline{U}_{10}$ is given by (3.12) so that $\underline{U}_{10} \cdot \hat{\underline{z}} = V_{10}(s) \cos\phi$ Hence, if $\theta_{10} = \hat{\theta}_{10}(s) \cos\phi$, (3.14) becomes

$$\alpha^2 \hat{\theta}_{10} = - V_{10} \tag{3.15}$$

where α is defined as in (2.23). The integrals in (3.13) can now be evaluated to give

$$\hat{\theta}_{10} = V_{10} = 0 \quad \text{on} \quad s=1. \tag{3.16}$$

and (3.15), (3.16) are to be solved subject to the boundary conditions. It is easily verified that, up to arbitrary constants, the solution is given by

$$\left.\begin{aligned} \hat{\theta}_{10} &= J_1(\alpha s) \\ V_{10} &= \alpha^2 J_1(\alpha s) \\ J_1(\alpha) &= 0; \alpha = 3.82 \\ R_{00} &= 2\alpha^4 \simeq 432 \end{aligned}\right\} \tag{3.17}$$

This system, then, is much simpler in structure and in solution than the full eigenvalue problem. At leading order, the fluid is constrained to move in circles by the inertial forces. Since this is not the optimum mode for turning thermal into kinetic energy, the unstable temperature gradient needed will be greater than that given by R_0. R_{00} is independent of σ and thus represents an asymptotic limit of the equations. Although the system cannot attain this limit for forced σ, it can appear to have become unstable at $R = R_{00}$ if ϵ is not too small. It is possible to find $R = R(\epsilon, \eta)$ by standard methods in this limit. We give some details here of the ϵ expansion, but only touch on the η one, since it is not straightforward. As for $\S 2$, we hope to consider this more fully at a later date.

If we suppose $\eta \ll \epsilon^2$ and continue the ϵ expansion we find that, to leading order in η

$$\Psi_{20} = \Psi_{20}(s), \quad \Psi_{30} = \Psi_{30}(s) \tag{3.18}$$

The analogues of (3.13) give

$$R_{10}\int_0^{2\pi} \theta_{10}\, \underline{\hat{z}}\cdot\hat{\phi}+\, d\phi + R_{00}\int_0^{2\pi} \theta_{20}\, \underline{\hat{z}}\,\hat{\phi}\, d\phi + \int \nabla^2 \underline{U}_{20}\cdot \hat{\phi}\, d\phi = 0 \tag{3.19}$$

and

$$R_{20}\int_0^{2\pi} \theta_{10}\, \underline{\hat{z}}\cdot\hat{\phi}\, d\phi + R_{10}\int_0^{2\pi} \theta_{10}\cdot\underline{\hat{z}}\cdot\hat{\phi}\, d\phi + R_{00}\int_0^{2\pi} \theta_{30}\, \underline{\hat{z}}\cdot\hat{\phi}\, d\phi + \int \nabla^2 \underline{U}_{30}\cdot\hat{\phi}\, d\phi = 0$$

and we have the thermal equations

$$\left.\begin{aligned} \nabla^2\theta_{20} &= -\underline{U}_{20}\cdot\underline{\hat{z}} + \underline{U}_{10}\cdot\nabla\theta_{10} \\ \nabla^2\theta_{30} &= -\underline{U}_{30}\cdot\underline{\hat{z}} + \underline{U}_{20}\nabla\theta_{10} + \underline{U}_{10}\cdot\nabla\theta_{20} \end{aligned}\right\} \tag{3.20}$$

Taking (3.20a) first, we see that the inhomogeneous term can be written

$$-\frac{\alpha^2}{s} J_1^2(\alpha s)\sin\phi$$

so that, since $\underline{U}_{20}\cdot\underline{\hat{z}} = U_{20}\phi\cos\phi$, θ_{20} has two parts; the part proportional to $\cos\phi$ can be absorbed into θ_{10} without loss of generality, if we also absorb U_{20} into $\underline{U}_{10}$ and set $R_{10} = 0$. It can be checked easily that the part of θ_{20} proportional to $\&^+$ does not enter (3.19a), so that this procedure is self consistent.

If we now write

and

$$\left.\begin{aligned} \theta_{20} &= \hat{\theta}_{20}^{(\omega)} \sin\phi \\ \theta_{30} &= \hat{\theta}_{30}^{(\omega)} \cos\phi \\ \underline{U}_{30} &= V_{30}^{(\omega)}\, \hat{\underline{\phi}} \end{aligned}\right\}, \tag{3.21}$$

we obtain the following ordinary differential system

$$\left.\begin{aligned} \mathcal{L}^2 \hat{\theta}_{20} &= -\tfrac{\alpha^2}{5} J_1^2(\alpha s) \\ \mathcal{L}^2 \hat{\theta}_{30} &= -V_{30} + \tfrac{\alpha^2}{5} J_1(\alpha s)\, \hat{\theta}_{20} \\ \tfrac{R_{20}}{2}\hat{\theta}_{10} + \tfrac{R_{00}}{2}\hat{\theta}_{30} + \mathcal{L}^2 V_{30} &= 0 \end{aligned}\right\} \tag{3.22}$$

We now fix R_{20} by the requirement that (3.22) possess a solution. After some manipulation and use of the equations satisfied by V_{10}, $\hat{\theta}_{10}$ we find

$$\tfrac{R_{20}}{2}\int_0^1 \hat{\theta}_{10}^2\, s\, ds = -\int_0^1 \hat{\theta}_{10}\, \mathcal{L}^{-1}\left[\tfrac{\alpha^2}{5} J_1(\alpha s)\, \hat{\theta}_{20}\right] \tag{3.23}$$

and the integral on the right-hand side can be written

$$\alpha^2 \int_0^1 \left(\frac{\partial \hat{\theta}_{20}}{\partial s}\right)^2 s\, ds > 0 \tag{3.24}$$

so that R_{20} is positive and $O(1)$. We therefore conclude that there is no subcritical instabilfty in this limit. (It can be independently established that the principle of exchange of stabilities is valid for the eigenvalue problem (3.16); and R_{00} is the minimum of (3.5) among flows with circular streamlines, so this is to be expected.) Hence

$$R = R_{00} + \epsilon R_{20} + \cdots \tag{3.25}$$

We may now sketch the expansion in η. The equation for $\underline{U}_{11}$ is, from (3.11)

$$\underline{U}_{11}\cdot\nabla \underline{U}_{10} + \underline{U}_{10}\cdot\nabla \underline{U}_{11} + \nabla p_{10} = R_{00}\theta_{10}\hat{\underline{z}} + \nabla^2 \underline{U}_{10} \tag{3.26}$$

and $\underline{U}_{11}$ is given by

$$\nabla^2 \theta_{11} = -\underline{U}_{11}\cdot\hat{\underline{z}} \tag{3.27}$$

if we suppose that $\epsilon\eta$, etc. can be neglected. Once (3.26) has been solved for $\underline{U}_{11}$, the change in R may be calculated from the energy balance equation

$$R_{01}\left\{\theta_{10}\underline{U}_{10}\cdot\hat{\underline{z}}\right\} + R_{00}\left\{\theta_{11}\underline{U}_{10}\cdot\hat{\underline{z}}\right\} + \left\{\underline{U}_{11}\cdot\nabla'\underline{U}_{10} + \underline{U}_{10}\cdot\nabla^2\underline{U}_{11}\right\} = 0 \tag{3.28}$$

which is (2.20) integrated over all streamlines, We have not solved this as yet, but it seems plausible that $R_{01} < 0$. If this is the case, the expansion of R for small ϵ and η is given by

$$R - R_{00} = \epsilon^2 R_{20} + \sigma\epsilon^{-1} R_{01} \tag{3.29}$$

and this is sketched in Fig.4. The departure from the straight line $\epsilon = \frac{R-R_{00}}{R_{20}}$ occurs when $\sigma = O(\epsilon^3)$ so that as long as $\epsilon \ll 1$ it takes place well within the region of validity of the inertial limit, (3.29) with (3.8), then give a qualitative picture of $R = R(\epsilon)$ for small σ at all small ϵ. This picture is almost identical to the one found by Jones et *al.* in their cylindrical geometry (with a vertical cylinder), and it is clear that they were correct in supposing that their solutions reflected such a limit as the one here descrfbed.

4. Conclusion

In previous sections we have demonstrated vigorously the existence of an asymptotic solution to the problem of steady convection in the limit $\sigma \to 0$. This solution is formally nonlinear (although the equations in our particular geometry

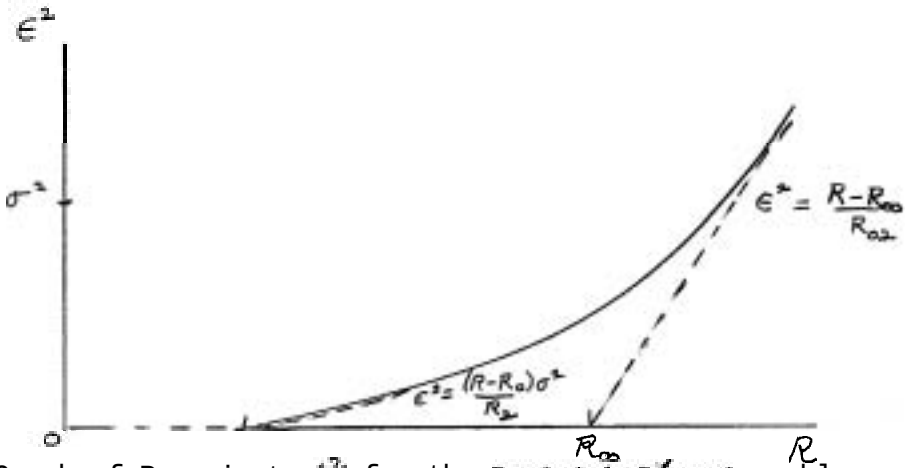

Fig.4 Graph of R against ϵ^2 for the Rayleigh-Bénard problem. (Note that $R_{oo} - R_o = O(1)$.

reduced to linear ones) and enables solutions to be obtained well outside the region of validity of normal perturbation theory. Physically, this limit is dominated by inertial constraints, so that the system acts as a 'flywheel'. The lower order viscous and diffusive terms serve to keep the flywheel in motion. In the Rayleigh-Bénard problem, this means that effective convection cannot occur until $R \geq R_{oo}$, yielding a criterion quite different from the normal marginal condition. The theory also explains why the very strong σ dependence shown at low amplitudes does not persist to higher ones. We believe that this limit may be relevant to any convective system where the flow pattern can be chosen so that inertial forces are irrotational everywhere. Certainly cellular convection between free boundaries seems to have the required freedom in general. If such a basic flow cannot occur, then the problem becomes more complicated, and it then seems likely that R_{oo} would go to infinity in the small σ limit. This work complements and justifies the work of Jones et *al.*, by basing their speculations on a sounder mathematical footing, and the results show a remarkable similarity with the nonlinear α-effect dynamo models of Malkus and Proctor (1975), for which a very similar dichotomy occurs in the basic eigenvalue problem depending on whether magnetic or viscous effects tend to zero most rapidly. Indeed, Fig.4 might have been taken directly from that paper. This suggests that the type of limit propounded here may occur in a variety of situations. The existence of such a limit in situations which exhibit subcritical instabilities would be particularly fascinating.

One last word should be said on the importance of this limit in the realistic situation where the flow is highly unstable. The experiments of Rossby (1969) show that, as in the laminar case, there is strong initial σ dependence of the Nusselt number at low amplitudes which becomes insignificant at higher amplitudes, suggesting that such a transition to almost inertial-dominated flow is occurring. There have been very few attempts to find such a transition by examining slightly supercritical flows, but Rossby (1962) in this summer program using mercury did find that the Nusselt number gradient went through a sharp transition at a Rayleigh number about 50% above critical. We reproduce his figure here as Fig.5. The band at the top of the diagram represents the scatter of his experiments; I have marked the 'second critical number' to aid understanding. This picture is so like Fig.4 that it would seem most desirable to attempt to repeat his experiments, since if they are not in error they would seem to go a long way to confirming the physicality of the work discussed here.

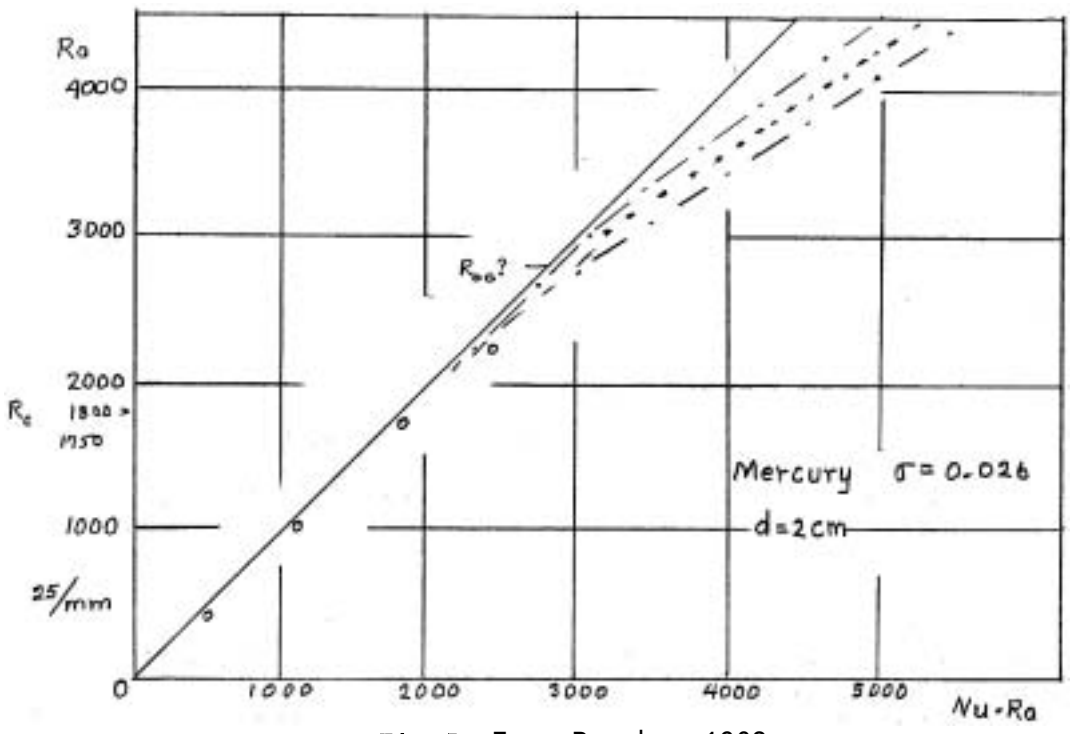

Fig.5 From Rossby, 1962.

Acknowledgement

The author wishes to thank the National Science Foundation and Massachusetts Institute of Technology for his support at the summer school, to Professor W. V.R. Malkus for arranging such support and for much help and construtive criticism throughout the summer, and to all the staff and fellows for much invaluable discussion.

References

Batchelor, G.K. 1956 J.Fluid Mech. 1: 177.

Bénard, H. 1900 Revue générale des Sciences Pures et Appliquées. 11: 1261.

Chandrasekhar, S. 1968 Hydrodynamic and Hydromagnetic Stability. O.U.P.

Jones, C.A., D.R.Moore, and N.O.Weiss. 1975 "Axisymmetric convection" (submitted to J.Fluid Mech.)

Malkus, W. V.R. and M.R.E.Proctor 1975 J.Fluid Mech. 67: 417.

Malkus, W. V.R. and G.Veronis 1958 J.Fluid Mech. 4: 225.

Moore, D.R. and N.O.Weiss 1972 J.Fluid Mech. 58: 289.

Rossby, H.T. 1962 G.F.D. Fellowship Lectures, Woods Hole, Massachusetts

Rossby, H.T. 1969 J.Fluid Mech. 36: 309.

PARTIAL DERIVATIVES OF LOVE NUMBERS AND RELAXATION SPECTRA OF THE EARTH

Masanori Saito

Introduction

Love numbers are a nondimensional triplet which describes elastic deformation of the earth subject to static external forces. Assuming the earth to be a non-rotating, self-gravitating, elastic sphere with spherical symmetry, we can calculate theoretical Love numbers for given earth models using the standard technique found in literatures (Longman, 1963; Farrell, 1972; Saito, 1974), which will be described briefly.

We seek the solution of the elastic-gravitational deformation of the earth in the following form:

$$u_r = y_1(r) Y_n(\theta,\varphi) \qquad u_\theta = y_3(r) \frac{\partial Y_n}{\partial \theta} \qquad u_\varphi = y_3(r) \frac{\partial Y_n}{\sin\theta \partial \varphi} \tag{1}$$

$$\psi = y_5(r) Y_n(\theta,\varphi)$$

where

r, θ, φ	: polar coordinates
$Y_n(\theta,\varphi)$	: spherical harmonic of degree n
$(u_r, u_\theta, u_\varphi)$	: displacement
ψ	: gravitational potential perturbation

ψ denotes the sum of the disturbing potential such as the tidal potential and the potential due to the deformation of the earth. In the following we normalize ψ in such a way that the disturbing potential has a unit amplitude on the surface, i.e., $\psi_{dist}(a,\theta,\varphi) = Y_n(\theta,\varphi)$. We further assume the following forms for stress, $\sigma_{r\theta}, \sigma_{\varphi r})$ and $\partial\psi/\partial r$:

$$\sigma_{rr} = y_2(r) Y_n(\theta,\varphi) \qquad \sigma_{r\theta} = y_4(r) \frac{\partial Y_n}{\partial \theta} \qquad \sigma_{\varphi r} = y_4(r) \frac{\partial Y_n}{\sin\theta \partial \varphi}$$

$$\frac{\partial \psi}{\partial r} - 4\pi G \rho u_r + \frac{n+1}{r}\psi = y_6(r) Y_n(\theta,\varphi) \tag{2}$$

where G is the gravitational constant and $\rho(r)$ the density. With these definitions the equations of equilibrium are written as

$$\dot{\underset{\sim}{y}} = \underset{\approx}{A}\, \underset{\sim}{y} \tag{3}$$

where $\underset{\sim}{y} = [y_1, \ldots, y_6]$, $\dot{\underset{\sim}{y}} = d\underset{\sim}{y}/dr$, and $\underset{\approx}{A}$ is a 6 x 6 matrix dependent on density and elasticity. The explicit dependence will be found in the references

The boundary conditions at the surface are given in terms of y_2, y_4 and y_6. We consider three independent cases.

(i) Tide: In this case the only external force is a tidal force. Thus the disturbing potential is $\psi_{dist} = (r/a)^n Y_n(\theta,\varphi)$ and the earth's surface is free $(\sigma_{rr} = \sigma_{r\theta} = \sigma_{\varphi r} = 0)$.

(ii) Load: A mass load on the surface exerts force in two ways: normal stress on the surface $(\sigma_{rr} \neq 0)$ and the gravitational body force. We normalize the surface mass load so that $\psi_{dist} = (r/a)^n Y_n(\theta,\varphi)$ inside the earth.

(iii) Shear: This type of external force has not been considered hitherto, but

I found it necessary to carry out the following analysis. We assume $\sigma_{rr} = 0$ but nonzero $\sigma_{r\theta}$ and $\sigma_{\varphi r}$. Note also $\psi_{dist} = 0$ is this case,

Boundary conditions in terms of y_2, y_4 and y_6 for the three cases are summarized in the following table,

Table 1. Boundary conditions for three cases.

	(i)	(ii)	(iii)
$y_2(a)$	0	0	0
$y_4(a)$	0	$-(2n+1)g(a)/4\pi Ga$	$(2n+1)g(a)/[4\pi Ga n(n+1)]$
$y_6(a)$	$(2n+1)/a$	$(2n+1)/a$	0

Here $g(r)$ denotes the gravity.

Given an earth model we can integrate Eq.(3) to get a solution $\underset{\sim}{y}_r$ that meets one of the three sets of boundary conditions. Once $\underset{\sim}{y}(r)$ has been obtained, Love numbers will be computed from $y_1(a)$, $y_3(a)$ and $y_5(a)$ for each case using the following table.

Table 2. Definitions of Love numbers.

	(i)	(ii)	(iii)
$g(a)y_1(a)$	h_n	h_n'	h_n''
$g(a)y_3(a)$	l_n	l_n'	l_n''
$y_5(a)$	$1+k_n$	$1+k_n$	k_n''

Nine Love numbers are defined in this table, but it will be shown below that only six of them are independent,

The Love numbers depend on density and elasticity structures in the earth. Although the dependence is completely described by Eq.(3), it is by no means clear. The problem we are concerned in this study is as follows: to what extent a particular Love number depends on one particular parameter, More, explicitly, we wish to establish quantitative relationships between variations of physical parameters and the corresponding variations in Love numbers.

Principle Equation (3) and the boundary conditions (Table 1) are equivalent to the following variational equation:

$$\delta\left\{\int_0^a F(\underset{\sim}{y}, \dot{\underset{\sim}{y}}, \underset{\sim}{p})\,dr - \underset{\sim}{f}\cdot\underset{\sim}{y}(a)\right\} = 0 \qquad (4)$$

where $\underset{\sim}{y} = [y_1, y_3, y_5]$, $\underset{\sim}{p}$ stands for a set of physical parameters, and $\underset{\sim}{f}$ the imposed boundary conditions. $F(\underset{\sim}{y}, \dot{\underset{\sim}{y}}, \underset{\sim}{p})$ is a quadratic homogeneous in $\underset{\sim}{y}$ and $\dot{\underset{\sim}{y}}$. The Euler equation to this variational equation is given by

$$\frac{d}{dr}\underset{\sim}{F}\dot{\underset{\sim}{y}} = \underset{\sim}{F}\underset{\sim}{y} \qquad (5)$$

and the boundary condition is

$$\underset{\sim}{F}\dot{\underset{\sim}{y}} = \underset{\sim}{f} \qquad (6)$$

In another word, Eqs.(5) and (6) are equivalent to Eq.(3) and Table 1 respectively,

Taking another set of solutions $\underset{\sim}{u} = [x_1, x_3, x_5]$ of Eq.(3), we find

$$\frac{d}{dr}(\underset{\sim}{u}\cdot\underset{\sim}{F}\dot{\underset{\sim}{v}}) = \dot{\underset{\sim}{u}}\cdot\underset{\sim}{F}\dot{\underset{\sim}{v}} + \underset{\sim}{u}\cdot\frac{d}{dr}\underset{\sim}{F}\dot{\underset{\sim}{v}} = \dot{\underset{\sim}{u}}\cdot\underset{\sim}{F}\dot{\underset{\sim}{v}} + \underset{\sim}{u}\cdot\underset{\sim}{F}\underset{\sim}{v}$$

and integrating from $r=0$ to a, we get

$$\underset{\sim}{u}\cdot\underset{\sim}{F}\dot{\underset{\sim}{v}}\Big|_0^a = \int_0^a G(\underset{\sim}{u},\underset{\sim}{v},\underset{\sim}{p})\,dr \tag{7}$$

where

$$G(\underset{\sim}{u},\underset{\sim}{v},\underset{\sim}{p}) = \dot{\underset{\sim}{u}}\cdot\underset{\sim}{F}\dot{\underset{\sim}{v}} + \underset{\sim}{u}\cdot\underset{\sim}{F}\underset{\sim}{v} \tag{8}$$

Because $F(\underset{\sim}{y},\dot{\underset{\sim}{y}},\underset{\sim}{p})$ is a homogeneous quadratic, it follows

$$G(\underset{\sim}{y},\underset{\sim}{y},\underset{\sim}{p}) = 2F(\underset{\sim}{y},\dot{\underset{\sim}{y}},\underset{\sim}{p})$$

$$G(\underset{\sim}{y},\underset{\sim}{u},\underline{p}) = G(\underset{\sim}{u},\underset{\sim}{v},\underline{p})$$

$$\underset{\sim}{G}_{u}(\underset{\sim}{u},\underset{\sim}{v},\underline{p}) = \underset{\sim}{F}\underset{\sim}{v}(\underset{\sim}{v},\dot{\underset{\sim}{v}},\underline{p})$$

$$\underset{\sim}{G}_{\dot{u}}(\underset{\sim}{u},\underset{\sim}{v},\underline{p}) = \underset{\sim}{F}_{\dot{v}}(\underset{\sim}{v},\dot{\underset{\sim}{v}},\underline{p})$$

and so on.

Now, suppose $\underset{\sim}{u}$ and $\underset{\sim}{v}$ are solutions to Eq.(5) for particular choice of $\underline{p}$. If we change $\underline{p}$ by $\delta\underline{p}$, then these solutions will also change, say, by $\delta\underset{\sim}{u}$ and $\delta\underset{\sim}{v}$. Hence from Eq.(7) we get, after some manipulation

$$(\underset{\sim}{u}\cdot\delta\underset{\sim}{F}\dot{\underset{\sim}{v}} - \underset{\sim}{F}\dot{\underset{\sim}{u}}\cdot\delta\underset{\sim}{v})\Big|_0^a = \int_0^a \underset{\sim}{G}_{\underline{p}}(\underset{\sim}{u},\underset{\sim}{v},\underline{p})\cdot\delta\underline{p}(r)\,dr \tag{9}$$

to the first order. Here $\underset{\sim}{F}\dot{\underset{\sim}{u}} = \underset{\sim}{F}\dot{\underset{\sim}{u}}(\underset{\sim}{u},\dot{\underset{\sim}{u}},\underline{p})$. The important point is that the variations in the solutions, $\delta\underset{\sim}{u}$ and $\delta\underset{\sim}{v}$, due to $\delta\underline{p}$ have disappeared except for the boundary values.

Variations in the elastic Love numbers.

The variational equation for the free oscillation of the earth has been given by Pekeris and Jarosch (1958). By setting frequency equal to zero, and using Eq.(8), we find

$$G(\underset{\sim}{u},\underset{\sim}{v},\underline{p}) = (\lambda+2\mu)r^2\dot{x}_1\dot{y}_1 + \lambda r\dot{x}_1 Y + \lambda r\dot{y}_1 X + (\lambda+\mu)XY +$$
$$+ n(n+1)\frac{r^2x_4y_4}{\mu^2} + n(n^2-1)(n+2)\mu x_3y_3 - \rho g r x_1 Y -$$
$$- \rho g r y_1 X + (n+1)\rho r(x_1y_5 + x_5y_1) - n(n+1)\rho r(x_3y_5 + x_5y_3) +$$
$$+ (4\pi G)^{-1}r^2x_6y_6 \tag{10}$$

$$X = 2x_1 - n(n+1)x_3 \qquad Y = 2y_1 - n(n+1)y_3$$

$$a^2\left[x_1y_2 + n(n+1)x_3y_4 + (4\pi G)^{-1}x_5y_6\right]_{r=a} = \int_0^a G(\underset{\sim}{u},\underset{\sim}{v},\underline{p})\,dr \tag{11}$$

$$a^2\left[(x_1\delta y_2 - x_2\delta y_1) + n(n+1)(x_3\delta y_4 - x_4\delta y_3) + (4\pi G)^{-1}(x_5\delta y_6 - x_6\delta y_5)\right]_{r=a} =$$
$$= \int_0^a \underset{\sim}{G}_{\underline{p}}(\underset{\sim}{u},\underset{\sim}{v},\underline{p})\cdot\delta\underline{p}\,dr \tag{12}$$

where x_i and y_i are two sets of solutions of Eq.(3), $\lambda(r)$ and $\mu(r)$ are Lame's elastic parameters, and $p=[\lambda,\mu,\rho]$. In taking variation of G, one should be careful about which x_i and y_i are to be taken to be independent. In the original variational equation (4), y_1, y_3 and y_5 are independent variables, and y_2, y_4, and y_6 are defined in terms of them. Therefore, in calculating derivatives of G, dependence of x_4 and y_4 on μ, for instance, should be taken into account, Also, dependence of g on ρ should be taken into account.

Interesting relations are derived from Eq.(11). Interchanging x_i and y_i and using the symmetry $G(\underset{\sim}{x},\underset{\sim}{y},p)=G(\underset{\sim}{y},\underset{\sim}{x},p)$, we find

$$a^2\left[(x_1y_2-x_2y_1)+n(n+1)(x_3y_4-x_4y_3)+(4\pi G)^{-1}(x_5y_6-x_6y_5)\right]_{r=a}=0 \qquad (13)$$

The left-hand side of this equation can be written in terms of imposed boundary conditions and Love numbers (Table 1 and 2). Let us write y_i^T, y_i^L and y_i^F for the solutions of case (i), (ii) and (iii) respectively. If we choose

$x_i = y_i^T$ and $y_i = y_i^L$ in Eq.(13) we find

$$1+k_n-h_n = 1+k'_n \qquad (14)$$

and another choice gives relations

$$k''_n = l_n = h''_n + l'_n \qquad (15)$$

Validity of Eq.(14) is demonstrated in the following table where Love numbers are taken from Farrell (1972) and Saito (1974). (Rather, consistency in their calculations is demonstrated by this table.)

Table 3. Comparison between h_n-k_n and $-k'_n$

n	h_n	k_n	$-k'_n$	h_n-k_n	
2	0.6114	0.3040	0.3075	0.3074	Farrell
3	0.2891	0.0942	0.1950	0.1949	
2	0.60847	0.30028	0.30819	0.30819	Saito
3	0.29145	0.09310	0.19835	0.19835	

It seems no one has ever noticed these relations. From Eqs.(14) and (15) it follows that only six of nine Love numbers are independent,

Similarly if we introduce any two of the three solutions into Eq.(12), we will have variations of Love numbers on the left-hand side and weighted integral of $\delta\underset{\sim}{p}$ on the right. Calculations are summarized in Table 4. In this table the first column indicates particular solutions used in the calculation; thus L, T imply $x_i=y_i^L$, $y_i=y_i^T$ in Eq.(12). $\delta g(a)$ is the variation in the surface gravity associated with the variation in density, Hence it is written as

$$\delta g(a) = \frac{4\pi G}{a^2}\int_0^a \delta\rho(r)\,r^2\,dr \qquad (16)$$

This term may be incorporated with the right-hand side integral.

Calculation of the right-hand side of Eq.(12) is also straightforward, even if cumbersome, The result is shown in Eq.(17).

Table 4. Left-hand side of Eq.(12).

x_i, y_i	left-hand side of (12) multiplied by $-4\pi G/(2n+1)a$
T, T	δk_n
T, L	$\delta(k_n - h_n) + h_n \frac{\delta g(a)}{g(a)}$
L, L	$\delta(k_n' - h_n') + 2h_n' \frac{\delta g(a)}{g(a)}$
S, T	$\delta l_n - l_n \frac{\delta g(a)}{g(a)}$
S, L	$\delta l_n' + (l_n - 2l_n') \frac{\delta g(a)}{g(a)}$
S, S	$\delta l_n'' - 2 l_n'' \frac{\delta g(a)}{g(a)}$

$$G_K = \frac{1}{(\lambda+2\mu)^2}(rx_2 + 2\mu X)(ry_2 + 2\mu Y)$$

$$G_\mu = \frac{4}{3(\lambda+2\mu)^2}(rx_2 - \tfrac{3}{2}KX)(ry_2 - \tfrac{3}{2}KY) + n(n+1)\frac{r^2 x_4 y_4}{\mu_2} + \\ + n(n^2-1)(n+2)x_3 y_3 \qquad (17)$$

$$G_\rho = (n+1)r(x_1 y_5 + x_5 y_1) - n(n+1)r(x_3 y_5 + x_5 y_3) - gr x_1 X - gr y_1 Y - \\ - r^2(x_1 y_6 + x_6 y_1) - 4\pi G r^2 \int_r^a \frac{\rho(r')}{r'}(x_1 Y + y_1 X)\,dr'$$

where K is the bulk modulus

$$K = \lambda + \tfrac{2}{3}\mu$$

Here we have chosen (K, μ, ρ) as an independent set of parameters. Equations (12) and (17), and Table 4 together with relations (14) and (15) completely determine variations of nine Love numbers in terms of δK, $\delta\mu$, $\delta\rho$ and y_i^T, y_i^L and y_i^S. The variations will be written, for example, as

$$\delta k_n = \int_0^a \left(\frac{\partial k_n}{\partial K}\delta K + \frac{\partial k_n}{\partial \mu}\delta\mu + \frac{\partial k_n}{\partial \rho}\delta\rho \right) dr \qquad (18)$$

"Partials" such as $\partial k_n / \partial K$, being functions of depth, are measures of dependence of Love numbers on each parameter at each depth.

To compute partial derivatives one must first solve Eq.(3) to get y_i's.

But as seen in Eq.(17), the partials at the surface $r = a$ can be obtained using available values of Love numbers. Since $(h''_n, l''_n, k''_n$ have not been computed, only partials of k_n, h_n, k'_n and h'_n are obtainable. The results follow.

$$\frac{aK}{k_2}\frac{\partial k_2}{\partial K} = -0.07 \qquad \frac{a\mu}{k_2}\frac{\partial k_2}{\partial \mu} = -0.10 \qquad \frac{a\rho}{k_2}\frac{\partial k_2}{\partial \rho} = 3.50$$

$$\frac{aK}{h_2}\frac{\partial h_2}{\partial K} = -0.57 \qquad \frac{a\mu}{h_2}\frac{\partial h_2}{\partial \mu} = -0.07 \qquad \frac{a\rho}{h_2}\frac{\partial h_2}{\partial \rho} = 3.62$$

$$\frac{aK}{k'_2}\frac{\partial k'_2}{\partial K} = -1.06 \qquad \frac{a\mu}{k'_2}\frac{\partial k'_2}{\partial \mu} = -0.03 \qquad \frac{a\rho}{k'_2}\frac{\partial k'_2}{\partial \rho} = 3.73$$

$$\frac{aK}{h'_2}\frac{\partial h'_2}{\partial K} = -5.16 \qquad \frac{a\mu}{h'_2}\frac{\partial h'_2}{\partial \mu} = -0.85 \qquad \frac{a\rho}{h'_2}\frac{\partial h'_2}{\partial \rho} = 3.71$$

It is interesting that the surface bulk modulus has the greatest effect on h'_2 while the effect of the rigidity is small. However it should be emphasized here that the partial derivatives given above are evaluated at the surface. Whether they increase with depth or not is left for future study.

Extension to non-elastic problems.

Peltier (1974) has shown that the visco-elastic response of the earth after the retreat of glacier could be solved using the corresponding principle (see also lecture note). The governing equation is identical to Eq.(3) except that λ and μ are to be replaced respectively by

$$\frac{\lambda s + K(\mu/\eta)}{+(\mu/\eta)} \quad \text{and} \quad \frac{\mu s}{s+(\mu/\eta)}$$

where η is the viscosity and s is the Laplace transform variable. In this problem h'_n is the most interesting quantity because it is related to post-glacial uplift of the earth's surface. Thus $\partial h'_n/\partial \eta$ together with observation of h'_n would give us some information on the viscosity distribution in the earth.

References

Farrell, W.E. 1972 Rev.Geophys.Space Phys., 10: 761-797.

Longman, I.M. 1963 J.Geophys.Res., 68: 485-496.

Peltier, W.R. 1974 Rev.Geophys.Space Phys., 12: 649-669.

Saito, M. 1974 J.Phys.Earth, 22: 123-140.

ON THE FLUID DYNAMICS OF RIDGE CRESTS

John N. Skilbeck

Introduction

Using a simple constant thickness plate model and imposing temperatures on its boundaries, McKenzie was able to calculate the mean uplift of the ocean floor due to thermal expansion of the lithosphere (Ref.1). This theoretical curve is a good fit to data from both fast- and slowly-spreading ridges except for a region about 10 km either side of the axis.

For ridges spreading at half-rates of 2.5 cm/yr or less (with the exception of the anomalous Reykjanes Ridge south of Iceland), one observes an axial depression in this region on the order of 1.5 km. For ridges spreading at 3 cm/yr or more, there is much smoother topography and possibly an axial horst in this region on the order of 200 m. In the latter case there is some dispute as to whether this horst is a distinct feature or whether McKenzie's thermal model adequately explains the topography all the way to the axis of faster-spreading ridges (Ref.2).

The problem to which this work is addressed is that of explaining how an axial valley can be formed and, if possible, why it is not there for faster-spreading systems. There have been several attempts already to explain this feature (Ref.3,4,5,6), although most of them involve rather complicated and sometimes unrealistic models from which it is difficult to extract the essential physics. The direction I have chosen to go in this problem, motivated by the nature of this summer school, is to look at the possibilities for a simple fluid dynamical explanation of these observations.

Although a major concern of plate tectonics for the moment is the season for a driving mechanism for plate motions, it is unlikely that this will be revealed until we understand clearly the things we observe at the surface. We know that plates are created at ridges and destroyed at trenches so that it would seem most important to try to understand features associated with these. It is to this end and with this philosophy that the work described here was undertaken.

1, Assumptions and Parameters

The physical parameters involved in this work are the mean mantle viscasity, μ, and the density contrast between mantle material and sea water, ρ. Taking mean values of 3.3 g/cc and 1.0 g/cc as the density of mantle and sea water respectively, we get

$$\rho \doteqdot 2.3\ g/cc$$

$$\frac{\mu}{\rho} \doteqdot 3 \times 10^{21}\ cm^2/sec.$$

Implicit in the above comments is the assumption that the upper mantle behaves as a Newtonian fluid (i.e. its properties can be described by a Newtonian viscosity). Although this may well be unreasonable, such behaviour ought to be understood before these effects are included.

A further assumption, based on the large value of μ/ρ, is that the flow is of low Reynolds number, i.e. viscosity terms in the Navier-Stokes equation are dominant over inertia terms. With the additional assumption of two-dimensionality (which is reasonable as ridges are quite linear features), this equation reduces to the biharmonic equation for the stream function ψ :

$$\nabla^4 \psi = 0$$

This can be solved for a variety of boundary conditions and the stresses induced by the flow can be derived. The topography is calculated on the following assumptions (see Appendix). These flow stresses act in particular on the whole length of the underneath part of the plate. Although, for forces spread over a distance small compared with its thickness, the plate may be regarded as rigid, for forces spread over much larger distances, the plate will simply bend to accommodate them (Ref.1). This calculation is only valid if the distortion of the surface is small enough not to affect the flow significantly.

2. Simplest Model of a Spreading Centre

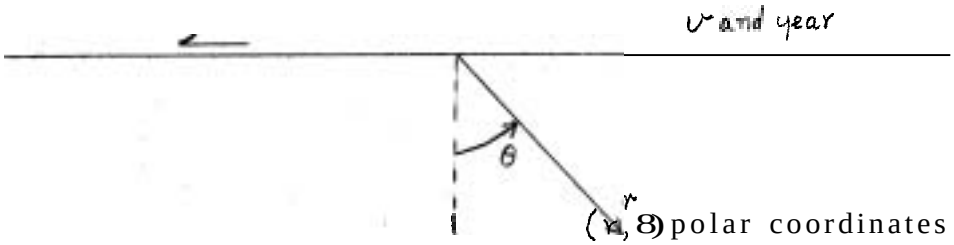

Fig.1 Simplest model of a spreading centre – V constant.

Figure 1 illustrates this idea. The fluid is semi-infinite in extent and symmetric about the line $\theta = 0$. This means that the stream function $\psi(r,\theta)$ must be antisymmetric in angle θ.

A simple similarity solution can be obtained if V is regarded as constant (see Appendix) and it is:

$$\psi(r,\theta) = -\frac{2V}{\pi} r\theta\cos\theta$$

The non-hydrostatic part of the normal stress (again see Appendix) is $-\frac{4\mu V}{\pi r}\cos\theta$ which vanishes on the upper surface $\theta = \pm \pi/2$ (except possibly at the origin). Consequently the upper surface does not deform.

This simple model clearly does not demonstrate the required features. A more general approach is now taken to look at the effect of a smooth transition in the horizontal velocity across the ridge axis and also the effect of considering a bottom boundary.

3. General Solution using Fourier Transforms

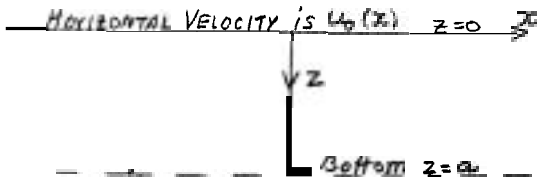

Fig.2 Diagram for solution using Fourier Transforms

Figure 2 shows the region considered. In the first place, d is taken to be infinite and finite d is accounted for later.

The biharmonic equation is solved by taking Fourier transforms in the x-directian, Such velocity boundary conditions as step-functions can be treated

using the theory of generalised functions (Ref.7). Using a sine transform (as ψ is antisymmetric), $\hat{\psi}(\kappa, z)$ the x-Fourier transform of $\psi(x,z)$ then satisfies:

$$\frac{d^4\hat{\psi}}{dz^4} - 2\kappa^2 \frac{d^2\hat{\psi}}{dz^2} + \kappa^4\hat{\psi} = 0$$

whose general solution is:

$$\hat{\psi}(\kappa,z) = Ae^{\kappa z} + Be^{-\kappa z} + Cze^{\kappa z} + Dze^{-\kappa z}$$

The boundary conditions are:

$$\hat{\psi}(\kappa,0) = 0, \quad \frac{d\hat{\psi}}{dz}(\kappa,0) = \hat{u}_0(\kappa) \qquad (\hat{u}_0(\kappa) \text{ is F.T of } u_0(x))$$

and that $\hat{\psi}$ is finite at $z = +\infty$.

The solution is then:

$$\hat{\psi}(\kappa,z) = \hat{u}_0 z e^{-\kappa z}$$

The pressure F.T. due to the shear stresses of the flow is given by:

$$\nabla\hat{p}_1 = \mu\nabla^2\hat{\underline{u}}$$

and yields: $\hat{p}_1 = -2\mu\kappa\hat{u}_0 e^{-\kappa z}$.

The non-hydrostatic part of the normal stress on a plane z = const. has a F.T. $\hat{\Delta}(\kappa,z)$, where

$$\hat{\Delta}(\kappa,z) = 2\mu\kappa^2\hat{u}_0 z e^{-\kappa z}$$

and this vanishes identically on the upper surface z = 0. There is consequently no topography.

Effect of Bottom Boundary

The same analysis can now be applied to include the effect of a bottom. If one is to model the plate as a constant thickness slab (equivalent to applying boundary conditions on a horizontal upper surface) the above indicates that such should be taken into account. The bottom boundary condition on the velocity is that both components vanish (no-slip).

The analysis is lengthy though not difficult and the result can be written:

$$\hat{\psi}(\kappa,z) = \hat{u}_0(A\sinh\kappa z + Cz\sinh\kappa z + Dz\cosh\kappa z)$$

The non-hydrostatic part of the normal stress on a plane z = constant has F.T.

$$\hat{\Delta}(\kappa,z) = -2\hat{u}_0\mu\kappa^2\left[(A + Cz)\cosh\kappa z + Dz\sinh\kappa z\right]$$

On the upper surface, z = 0, this has the form

$$\hat{\Delta}(\kappa,0) = -2\mu\kappa^2 A\hat{u}_0$$

where the constant $A = \dfrac{-d^2\kappa}{(\sinh^2 d\kappa - d^2\kappa^2)}$

The kernal of the expression for $\hat{\Delta}(\kappa,0)$ is:

$$\mathbb{K}(\kappa d) = \frac{2\mu d^2\kappa^3}{(\sinh^2 d\kappa - d^2\kappa^2)}$$

$$= \frac{2\mu\kappa}{\left\{\left(\frac{\sinh d\kappa}{d\kappa}\right)^2 - 1\right\}}$$

For infinite d, $K(\kappa,d) \equiv 0$ and the result reduces to the previous one.

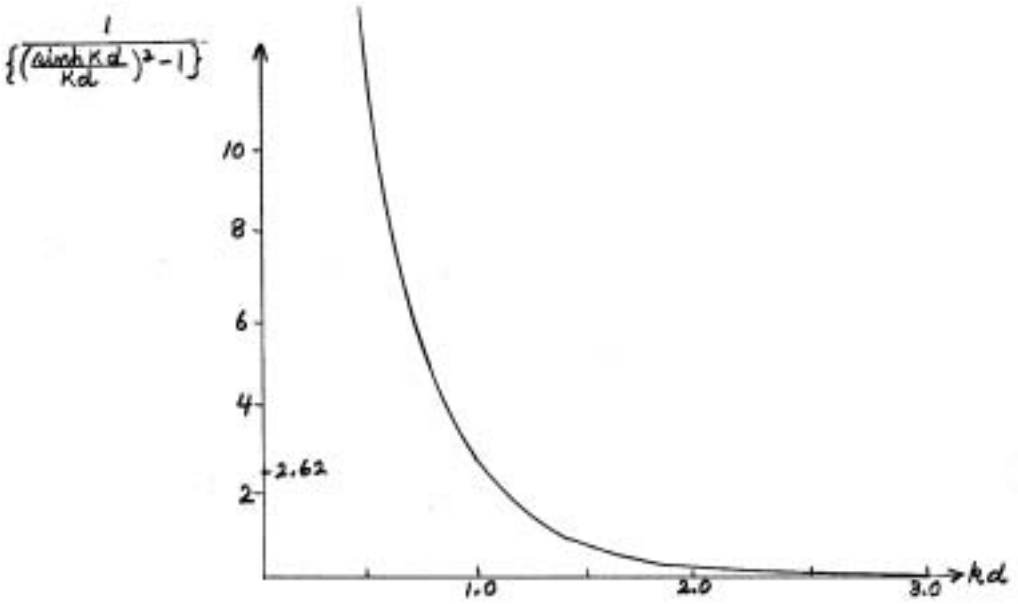

Fig. 3 Take d to be 10^3 km

L (km)	$\frac{1}{2\mu} K(d/L)$
1000	2.62×10^{-3}
10,000	3×10^{-2}
10	7×10^{-43}

This function goes very rapidly to zero (as $e^{-2\kappa d}$) as κd increases above 1 and so we would only expect the bottom to have an effect on features whose linear scale is of order d. If we consider a depth d to be that of the upper mantle (d=700 km), we would expect to see no effect on topography of dimensions 30 km. There is no evidence for putting the effective boundary at 30 km depth as it would require the viscosity to change by several orders of magnitude there.

In conclusion, one feels justified in neglecting the bottom in further analysis though this means that we must model the plate by other than a horizontal boundary. The following model is an attempt to do this.

4. Wedge Model of Plates near a Spreading Centre

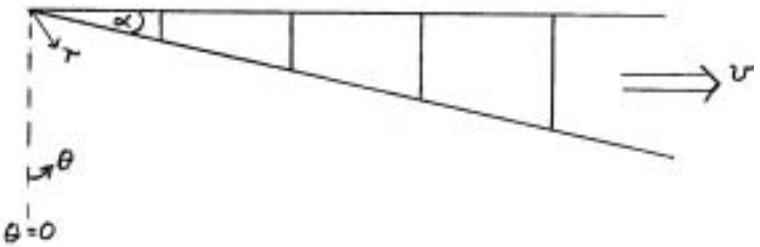

Fig.4 Diagram of Wedge Model for plate near spreading centres.

This idea is illustrated in Fig.4 A solution to the biharmonic equation for these boundary conditions can be obtained using Moffatt's similarity solution (see Appendix) with $\Psi(r-\theta) = -\Psi(r,\theta)$ and the plate velocity, v, constant. This solution is:

$$\Psi(r,\theta) = rv(A_1 \sin\theta - D\theta\cos\theta)$$

where $A = \frac{2\sin^2\alpha}{(\pi - 2\alpha - \sin 2\alpha)}$ and $D = \frac{2}{(\pi - 2\alpha - \sin 2\alpha)}$

Streamlines for wedge angles of 5^o, 15^o and 40^o are shown in Figs.S, 6 and 7.

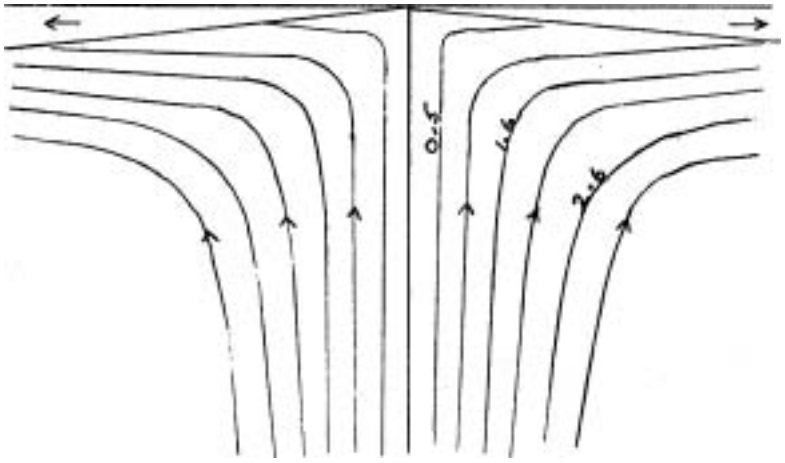

Fig.5 Streamlines for wedge angle $\alpha = 5^o$. Contours are of non-dimension stream functions.

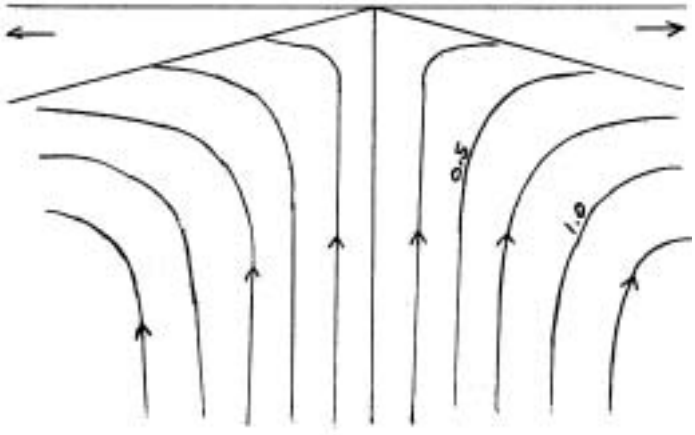

Fig.6 Streamlines for wedge angle $\alpha = 15^o$. Contours at each interval of non-dimensional stream function.

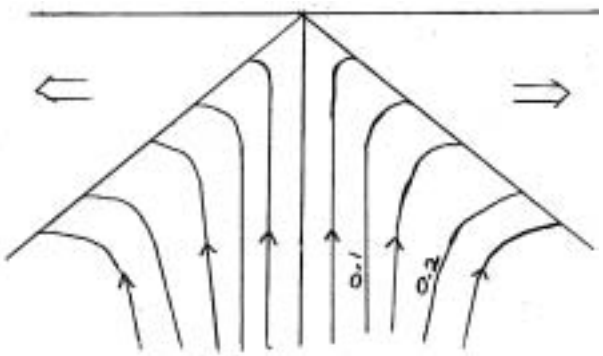

Fig.7 Streamlines for wedge angle $\alpha = 40^{\circ}$. Contours are of the non-dimensional stream function.

Again from the Appendix, the perturbation to the pressure due to the shear stresses of the flow is:

$$P_1 = \frac{-2\mu v D \cos\theta}{r}$$

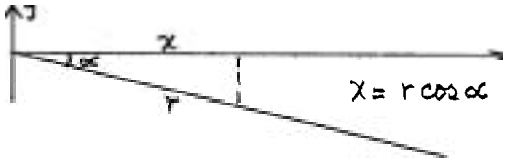

and on the surface $\theta = \frac{\pi}{2} - \alpha$ (bottom of the wedge) this is

$$P_1 = -\frac{2\mu v D \sin\alpha}{r} = -\frac{\mu v D \sin 2\alpha}{x} \qquad (1)$$

If we assume that the plate is rigid and transmits this force to the upper surface, (Ref.1), it will deform the upper surface until this force is balanced by the hydrostatic pressure. We can now calculate this deformation. From the Appendix it is given by:

$$-P_0 - P_1 = 0$$

With y measured vertically upwards

$$P_0 = -\rho g y$$

so

$$\rho g y + \frac{\mu v D \sin 2\alpha}{x} = 0$$

and hence

$$xy = -\frac{2\mu v \sin 2\alpha}{\rho g (\pi - 2\alpha - \sin 2\alpha)} \qquad (2)$$

These surfaces are hyperbolae.

For very small x, the pressure P, and hence the deformation y become large. Since the plate has only finite strength it will break when the force on it exceeds some critical value and the solution is not valid thereafter.

Definition of α

Figure 8 illustrates a possible definition of the wedge angle α. As the plate spreads from the axis it cools and thickens - it's thickness being proportional to the square root of it's age, provided this is $\lesssim$ 60 my. After 60 my the plate thickness becomes roughly constant. It is unlikely that an α based on this thickness at 60 my will be a good representation, as the observations considered here are highly local to the ridge axis (60 my is equivalent to 1200 km for a 2 cm/yr spread-

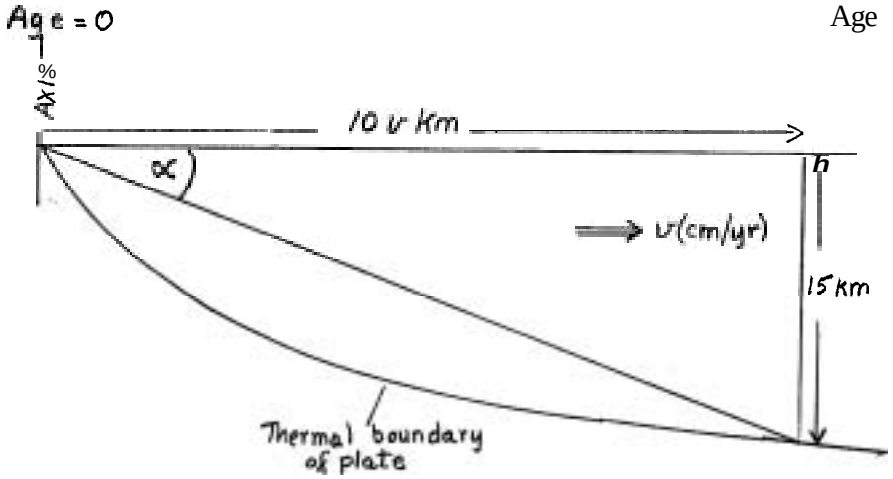

Age = 1 my = time for plate to become a thickness of order the scale of the feature considered. (15 km)

Fig.8 Suggested Definition of Wedge Angle α

ing rate). A more sensible definition of α is that it is the angle from the ridge crest to the point where the plate is 15-20 km thick - the scale of our axial valleys. Either the thermal thickness (defined by the coding curve proportional to age) or the mechanical thickness (somewhat less than this) would be a reasonable choice. Since we have calculated the topography on the assumption of plate rigidity (up to a given breaking stress), the mechanical thickness is probably the more appropriate.

Figure 8 shows that the thermal thickness $\sim$ 15 km at 1 my. As an estimate, let us assume that the mechanical thickness at a given age is half the thermal thickness, so that we have:

$$\tan\alpha = 3/4v \quad (v \text{ in cm/yr})$$

We use this expression in the following estimation. Note that in the limit as $\alpha \to 0$, Eq. (2) becomes $xy = 0$ which implies $y = 0$ except at $x = 0$. This is the result of the spreading centre model of Section 2.

Estimation of Topography

Equation (2) gives the shape of the deformed upper surface as a hyperbola. The infinity at the origin is not realistic as the plate has finite strength and one can calculate the depth, y_c, at which $|p_1|$ exceeds some critical value, p_1^{crit}. I take p_1^{crit} = 100 bars (Ref. 8)

$$-p_0 - p_1 = 0 \quad \text{(from Appendix)}$$

and hence $\rho g y_c = -p_1^{crit}$

and using values from Section 1, this gives:

$$y_c \doteq -420\,m$$

I take this point to define the edge of the axial valley.

Equation 1 then tells us the half-width, x_c, of the axial valley

$$x = -\frac{\mu v D \sin 2\alpha}{p_1}$$

and with μ and p_1 in cgs units and v in cm/yr and $\tan\alpha = \frac{3}{4}v$ this becomes:

$$x_c = \frac{\mu \cos^2\alpha}{(\pi - 2\alpha - \sin 2\alpha)} \times 10^{-20} \text{ km}$$

v(cm/yr)	α (nearest degree)	x_c (km)
1	37	49.6
1.5	26	39.1
2	20	34.0
4	10	28.3
8.5	5	24.6

This model predicts an axial depression at all spreading rates with widths, x_c, shown in the previous table. As can be seen, for $v \lesssim 2.5$ cm/yr, these values are too big by a factor of about 2, although this is readily accounted for by the uncertainty in the viscosity μ. If we take a viscosity one-half of that suggested in Section 1, then x_c agrees well with observations. The associated gravity anomaly can then be calculated up to the edge of the valley and is negative and of the same order of magnitude as Lambeck's positive anomaly (Ref.9) (see Fig,9 and Appendix).

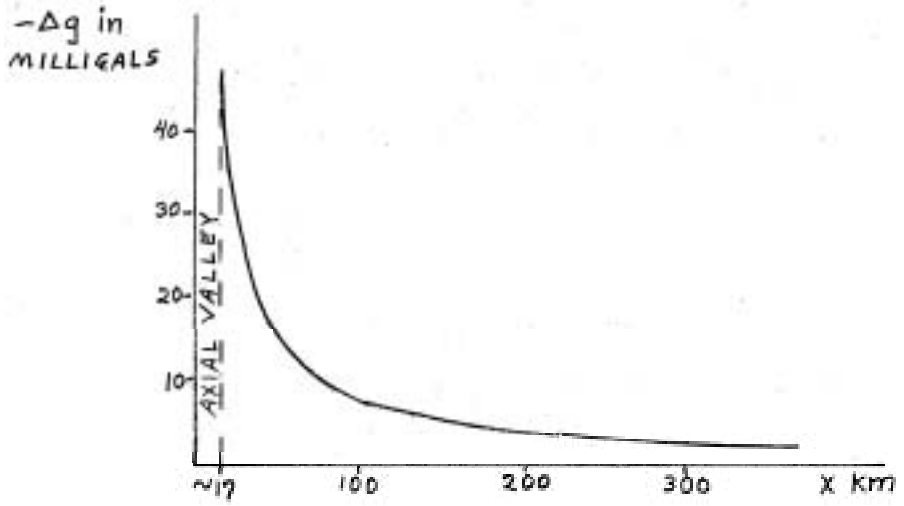

Fig.9 Gravity Anomaly for spreading rate 2cm/yr with $\frac{4\mu}{\rho} = 1.5 \times 10^{21} \text{cm}^2/\text{sec}$. Compare Fig.7 (Ref.9). See Appendix.

This is encouraging as there is no observed gravity anomaly associated with ridges.

For the faster spreading rates, the topography is one or two orders of magnitude too big. If such a dip does exist in this case then to show no gravity anomaly it must be of linear dimension much less than the sea depth. (Under such conditions the sea attenuates the effect strongly and no anomaly will be observed.) This requires a valley width of only a few hundred meters. If this were so nothing would be observed topographically as such a small depression would be quickly filled with sediment. To get such small topography from this model, a much reduced (by 1 or 2 orders of magnitude) viscosity would be needed for faster spreading ridges.

Such an assertion is not altogether unreasonable. Faster spreading ridges are more likely to be able to support magma chambers as material upwells and moves out before it has a chance to cool and solidify. The viscosity in this case would easily satisfy this avove requirement. There is evidence for and against this idea. Against it there is geochemical work. If there are magma chambers under faster

spreading systems and not under slower ones, one would expect to see a difference in the constitution of the rocks which reach the surface in the two places. So far no difference has been detected. However, there is recent seismic evidence of a low velocity zone under the fast spreading ridge of Baha, California (Ref.10) while such a structure has not been found by workers on the slowly spreading mid-Atlantic Ridge, it is by no means an automatic conclusion that this structure is a magma chamber though it could perhaps be so. In addition to this, the anomalous Reykjanes Ridge south of Iceland hints at the possible connection between such structures and the topography. This ridge is slowly spreading and yet has no axial valley which might lead one to suggest (in the light of this model) that, because of the frequent magnetic eruptions around Iceland, magma chambers lower the effective viscosity there.

Conclusions

The effects of modelling the plate as having a constant thickness with a horizontal lower boundary have been shown to produce insignificant topography of the scale being considered (— 30 km) unless the lower boundary is at a depth of order 30 km also. There is' no evidence for this as it would require a large change in viscosity there. To get out of this difficulty account was taken of the fact that the plate thickens with distance from the ridge axis (as it cools) and the wedge model proposed.

This model predicts an axial depression at all values of the spreading rate. For reasonable values of the viscosity the width of this depression is in the range 15-25 km (for $v \lesssim 2.5$ cm/yr) which is in good agreement with observations. There is an associated negative gravity anomaly of roughly the same size as Lambeck's positive one. This is encouraging as no anomaly is observed in these regions.

At higher velocities, the topography is 1-2 orders of magnitude too big. An explanation for this difference is suggested with reference to recent work though it is mentioned that there is evidence against it.

This model is very simple yet gives the desired result and as such is possibly a better starting point for further work than some of the more complicated earlier models.

Appendix

A solution to

$$\nabla^4 \psi = 0$$

can easily be obtained in polar coordinates if the velocity on boundaries $\theta = \theta_1$ and $\theta = \theta_2$ is given and constant. It is due to Moffatt (Ref.11) and is:

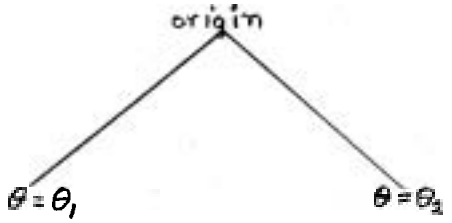

$$\psi = r\Theta(\theta)$$

Substitution shows Θ satisfies

$$\frac{d^4\Theta}{d\theta^4} + 2\frac{d^2\Theta}{d\theta^2} + \Theta = 0$$

the general solution to which is:

$$\Theta(\theta) = A\sin\theta + B\cos\theta + C\theta\sin\theta + D\theta\cos\theta$$

McKenzie (Ref.12) shows that for this form of stream function the deviatoric stress tensor is:

where $\sigma'_{r\theta} = \frac{\mu}{r}\left(\frac{d^2\Theta}{d\theta^2} + \Theta\right)$

and the perturbation to the pressure from this shear stress is;

$$p_1 = -\frac{\mu}{r}\left(\frac{d^2\Theta}{d\theta^2} + \frac{d\Theta}{d\theta}\right)$$

In particular, the equation determining the surface deformation (provided it is small enough not to distort the original from significantly) is:

$$-p_0 - p_1 = 0$$

where p_0 is the hydrostatic pressure.

With reference to the gravity anomaly shown in Fig.9, a viscosity one-half that suggested in Section 1 is used. For a spreading rate of 2 cm/yr the elevation, y, at distance, x, from the axis is given by:

$$y = -\frac{7.5}{x}\ \text{km} \qquad \text{(where } x \text{ is in km)}$$

The gravity anomaly Δg is approximately equal to $42\rho y$ mgals. as an infinite slab 1 km thick of density 1 gm/cc gives an anomaly of 42 mgals. With ρ as suggested in Section 1,

$$\Delta g \doteq -\frac{750}{x}\ \text{mgals.} \qquad (x \text{ in km})$$

which is plotted in Fig.9.

References

McKenzie, D.P. 1967 J.Geophys.Res. 72: 6261.

2. Parsons, B.E. and J.G.Sclater (in press)

3. Sleep, N.H. and S. Biehler 1970 J.Geophys.Res. 75: 2478.

Sleep, N.H. 1975 J.Geophys.Res. (in press)

Anderson, R.N. and H.C.Noltimier 1973 Geophys.J.R.astr.Soc. 34: 137.

6. Lachenbruch, A.H. 1973 J.Geophys.Res. 78: 3395.

Lighthill, M.J. "Introduction to Fourier Analysis and Generalised Functions", Cambridge University Press.

8. Rayleigh, C.B. and S.H.Kirby 1970 Am.Mineral.,Spec.Pap.3: 113.

9. Lambeck, K. 1972 Geophys.J.R.astr.Soc. 30: 37.

10. Orcutt, J. *et al.* 1975 Nature, 256: 475.

11. Batchelor, G.K. "Fluid Dynamics", Cambridge University Press.

12. McKenzie, D.P. 1969 Geophys.J.R.astr.Soc. 18: 1.

Acknowledgements

I would like to thank Drs. Peter Molnar and Tanya Atwater for bringing this problem to my attention, and to Dr. Dan McKenzie whose help and guidance was always an inspiration. Thanks are due to the staff of the GFD school, and also to Drs. Barry Parsons, Mike Proctor and Jay Melosh and fellow student Allen Waxman for many profitable conversations.

SUBCRITICAL INSTABILITY IN STELLAR SEMICONVECTION ZONES

Allen M. Waxman

1. Introduction

A star of initially uniform chemical composition evolves to a state in which composition gradients do exist and it may do so in a variety of ways. In the core of a star nuclear reactions occur which fuse lighter nuclei into heavier ones and therefore the possibility of composition gradients can be realized. The cores of stars more massive than a few solar masses, tend to be convectively unstable and so one may expect the core itself to be homogeneous. However, this poses the question of the stability of the region immediately outside the convective core where a discontinuity in composition may then exist. This problem was considered by Ledoux (1947) who showed that a discontinuity in composition was not possible and instead the star would set up a narrow zone of continuously varying composition. By considering an adiabatic displacement of a parcel of gas through a zone of varying temperature composition and the resulting buoyancy of the fluid, Ledoux took into account the stabilizing effect of the composition gradient.

Schwarzschild and Härm (1958) discuss the formation of a zone of varying composition and draw the distinction between the processes responsible in low and high mass stars; (the division between low and high mass being at about 10 solar masses). For stars of low mass the boundary of the convective core shrinks (in mass fraction enclosed) as hydrogen is depleted at the center leaving behind a 'frozen in' composition gradient. The composition at a given point would correspond to the homogeneous core composition at the time the boundary passed that point. In massive stars the radiation pressure lowers the effective gravity in the region outside the core hence lowering the local adiabatic temperature gradient. Thus this region tends to be more unstable and one finds that the convective core grows (in mass fraction) with time. Schwarzschild and Härm argue that one cannot have a discontinuity in composition at the boundary of this outward-moving core if electron scattering is the dominant form of opacity, (as is the case for massive stars). As a gram of hydrogen outside this boundary has more electrons than a gram of helium on the inside of this boundary, a discontinuity in composition would be accompanied by a jump in the opacity. The larger opacity outside the core would raise the temperature gradient there and convection would set in joining this region to the convective core. The convection would mix in enough helium to lower the opacity (and therefore the temperature gradient) just enough to maintain a marginally stable state; hence, they coined the phrase 'semiconvection zone'. Unlike Ledoux, however, they do not account for the added stability of composition gradients.

The question still remains as to what is the correct criterion for stability in the presence of composition gradients. The various methods for handling convection in regions of varying composition in evolution calculations are summarized by Stothers (1970). He states that a semiconvection zone which joins the convective core to the radiative envelope must exist though he is undecided about the stabilizing effects of a composition gradient.

The problem of convection in the presence of composition gradients is a familiar one in the thermohaline problem of the oceans (Veronis, 1964, 1968). We will use this work as a guide to our investigation of the stability of these zones of varying composition. We will restrict the analysis to a special case which admits some simplifications in the governing equations and so makes the problem more tractable. Though we will consider the problem in the context of the Boussinesq approximation we will explore the effects of a temperature and composition-dependent conductivity as is relevant to the stellar case. We will also carry the analysis into the non-

linear regime via the techniques of modified perturbation theory and explore the possibility of subcritical instability. The results obtained add some insight to the stabilizing effects of composition gradients in semiconvection zones though the question of 'the correct stability criterion' still remains open.

II. The Governing Equations

The configuration to be studied is shown in Fig.1. Here we have a fluid layer heated from below. The lower bounding plate is maintained at temperature and composition μ_L while the top plate is maintained at $T_U < T_L$ and $\mu_U < \mu_L$. We will consider the bounding surfaces as perfect conductors of heat and μ. μ is the mean molecular weight of the fluid and represents the number of atomic mass units per particle of fluid and hence reflects the composition. We will restrict ourselves to studying the stability of two-dimensional disturbances, i.e. rolls. Gravity is downwards as shown. We will also exclude the possibility of heat sources within the fluid as energy generation is essentially negligible in semiconvection zones. The fluid between the plates is primarily a hydrogen plasma with a gradient of ionized helium, If the fluid between the plates were to represent the entire semiconvection zone, the composition could vary from pure helium at the lower boundary ($\mu = 4/3$) to almost pure hydrogen at the top ($\mu = 1/2$). However, if we restrict ourselves to a smaller region of the zone we can take advantage of some simplifications that will become apparent. One major assumption is that of the Boussinesq approximation. As the fluid is compressible we must take into account the density stratification of the fluid in its hydrostatic state. The Boussinesq equations are discussed by Malkus (1964) and by Spiegel and Veronis (1960) for a compressible fluid with a homogeneous composition. The resulting equations of motion and continuity are

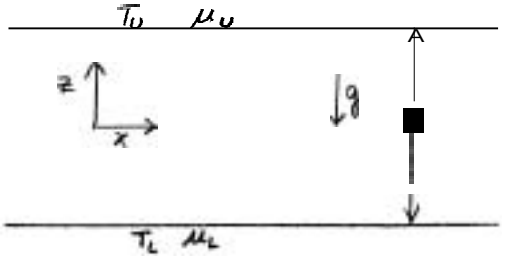

Fig.1

$$\frac{\partial \underset{\sim}{v}}{\partial t} + \underset{\sim}{v}\cdot\nabla\underset{\sim}{v} = -\frac{1}{\rho_m}\nabla P' - g\frac{\rho'}{\rho_m}\hat{k} + \nu\nabla^2\underset{\sim}{v} \qquad (1)$$

$$\nabla\cdot\underset{\sim}{v} = 0. \qquad (2)$$

In Eqs.(1) and (2) $\underset{\sim}{v}$ is a perturbation velocity on the basic hydrostatic state. ρ_m is the mean density of the fluid layer and P' and ρ' are perturbations in the pressure and density respectively. The basic hydrostatic state has been subtracted from (1). The kinematic viscosity ν has been taken as constant here and we feel this justified because the diffusion of momentum is so small compared to the diffusion of heat. That is to say we are dealing with a very low Prandtl number fluid. We will now derive the heat equation for an ideal gas with gradients in the chemical composition.

Consider a mixture of two gases. We can write the first law of thermodynamics for this mixture as

$$dq = C_v dT - P/\rho^2\, d\rho - \mu_1 dn_1 - \mu_2 dn_2 \qquad (3)$$

where μ_1 and μ_2 are the chemical potentials of components 1 and 2 in one gram of the mixture. n_1 is the number of particles of type 1 per gram of mixture and if m_1 is the mass of a particle of type 1 then $n_1 m_1$ is the mass fraction of type 1 per gram. In (3), $C_v dT$ is the differential change in internal energy per gram of mixture and dq is a differential of heat added to a gram of mixture. As there are no sources or sinks of fluid we must have

$$n_1 m_1 + n_2 m_2 = 1. \tag{4}$$

Defining the concentration of type 1 as $C = n_1 m_1$ and utilizing (4) we may rewrite (3) as

$$dq = C_V dT - P/\rho^2 d\rho - \mu_{chem} dC \tag{5}$$

where the relative chemical potential is

$$\mu_{chem} = \frac{\mu_1}{m_1} - \frac{\mu_2}{m_2}.$$

If we multiply (5) by ρ and note that the energy added per unit time per unit volume is due to viscous dissipation Φ_{vis} in the fluid and the divergence of the heat flux vector $\underset{\sim}{f}$ we may write (5) as

$$\Phi_{vis} - \nabla \cdot \underset{\sim}{f} = \rho C_V \frac{DT}{Dt} - \frac{P}{\rho} \frac{D\rho}{Dt} - \rho \mu_{chem} \frac{DC}{Dt} \tag{6}$$

(where we have made use of the substantial derivative $\frac{D}{Dt} = \frac{\partial}{\partial t} + \underset{\sim}{v} \cdot \nabla$ as we are following a particular element of fluid). We will now define the mean molecular weight via the equation of state for an ideal gas (which is applicable to semiconvection zones).

$$P = \frac{\rho k T}{\mu m_p} \tag{7}$$

In (7) k is Boltzman's constant and m_p is a proton mass. We may associate the pressure P in (7) with that in (6) if we assume that radiation pressure is negligible in the region of interest. This is a fair approximation for stars less than about 10 solar masses. We will adopt this assumption for the analysis. If X is the mass fraction of hydrogen, Y the fraction of helium, and $Z_1 = 1 - X - Y$ is the fraction of the remaining 'heavy elements' we may express μ as (Chandrasekhar, 1939)

$$\mu = \frac{2}{1 + 3X + \frac{1}{2}Y}. \tag{8}$$

We will assume that Z_1 is constant throughout the fluid layer as Z_1 is only a few percent in the regions surrounding helium cores. Solving (8) for Y in terms of μ gives

$$\frac{1}{\mu} = \text{constant} - \frac{5}{4} Y$$

which can be inserted into (7). Taking the logarithmic derivative of (7) and substituting this expression for $\frac{1}{\mu}$ in (6) gives

$$\Phi_{vis} - \nabla \cdot \underset{\sim}{f} = \rho C_V \frac{DT}{Dt} + \frac{P}{T} \frac{DT}{Dt} - \frac{DP}{Dt} - \frac{5}{4} \frac{\rho k T}{m_p} \frac{DY}{Dt} - \rho \mu_{chem} \frac{DY}{Dt}. \tag{9}$$

In (9) we have associated helium with the type 1 particle, i.e., $C = Y$. We may simplify (9) by noting that $\frac{P}{T} = \rho (C_p - C_v)$ where C_p and C_v are the specific heats at constant pressure and volume respectively and both are at constant composition. The Bussinesq approximation allows for further simplification in that we may replace the $\frac{DP}{Dt}$ term by $w \frac{dP_b}{dz} = -w \rho g$ where w is the z-component of velocity and P_b is the basic hydrostatic pressure field. We may also replace the heat flux vector by $K_{rad} \nabla T$ where K_{rad} is the radiative conductivity which dominates any molecular heat transport processes due to temperature or concentration gradients (Landau and Lifshity, 1959; §58). We may also neglect the viscous dissipation term as compared to the heat conduction term in the context of the Boussinesq approximation (their ratio is

$$\text{D/scale height} \times \text{Prandtl number} << 1)$$

and in addition we evaluate the density and heat capacities at some mean reference point in the fluid. We will, however, take the conductivity as variable. Incorporating these simplifications in (9) we obtain the following heat equation:

$$\frac{DT}{Dt} + \frac{g}{C_p} w - \frac{1}{\rho_m C_p}\left(1 + \frac{4}{5}\frac{m_p \mu_{chem}}{\kappa T}\right)_m \frac{P}{\mu}\frac{D\mu}{Dt} - \nabla\cdot(\chi \nabla T) = 0 \qquad (10)$$

In (10) we have replaced Y by its expression in terms of μ and have redefined the conductivity as $\chi = \frac{K_{rad}}{\rho_m C_p}$. We have also allowed ourselves to evaluate the coefficient of $\frac{P}{\mu}\frac{D\mu}{Dt}$ at the reference point. This is because we expect the ratio of the relative chemical potential to the thermal energy per proton to be small. This is reasonable as the relative potential represents the change in electrostatic energy of a gram of fluid when a proton (and its electron) is removed and a helium nucleus (and its two electrons) are added. This energy is small because at stellar densities' ions are surrounded by Debye spheres and hence, their charges are shielded from other ions (Landau and Lifshitz, 1958; §§ 24 and 74). An important assumption in the justification of the Boussinesq approximation is that the depth of the fluid layer be much less than an adiabatic scale height. This scale height for uniform composition is given by $H_s = \frac{C_s T_m}{g}$ and may be obtained from

$$\frac{ds}{dz} = \frac{\partial s}{\partial T}\Big)_p \frac{dT}{dz}\Big|_{ad} + \frac{\partial s}{\partial P}\Big)_T \frac{dP}{dz} = 0$$

and from the hydrostatic pressure balance. This yields $\frac{dT}{dz}\Big|_{ad} = -g/C_p$ and thus the scale height H_s. In zones of varying composition we often have the depth D of order 1/2 H_s and a fairly constant gravity as well. Hence we will take g as constant and proceed with confidence that $D/H_s << 1$ is satisfied.

We also need an equation which describes the diffusion of helium through the fluid. We will assume that the diffusion of helium is driven only by concentration gradients and take the diffusion coefficient as constant. This is a good assumption as diffusion in stars is essentially negligible compared to any convective mixing. Even the original gradient outside the core is dominated by evolutionary effects and not diffusion. However we are limiting our discussion to a very narrow region at the onset of convection and so will make use of the following diffusive equation.

$$\frac{DY}{Dt} = k_Y \nabla^2 Y \qquad (11)$$

As we are more interested in the mean molecular weight we may replace Y by its expression in terms of μ and obtain

$$\frac{D\mu}{Dt} = k_Y \nabla^2 \mu - 2 k_Y \frac{1}{\mu} \nabla\mu \cdot \nabla\mu. \qquad (12)$$

Let us divide (12) by μ_m (the reference μ) and expand $\frac{1}{\mu}$ in a Taylor series about μ_m. If we scale variations in μ by $\Delta\mu \equiv \mu_L - \mu_U$ and define the small quantity $\eta = \frac{\Delta\mu}{\mu_m}$, equation (12) becomes

$$\eta \frac{D\hat{\mu}}{Dt} = \eta k_Y \nabla^2 \hat{\mu} - 2\eta^2 k_Y \nabla\hat{\mu}\cdot\nabla\hat{\mu} + O(\eta^3) \qquad (13)$$

where $(\Delta\mu)\hat{\mu} = \mu$. If we divide through (13) by η and consider the limit of $\eta \longrightarrow 0$ we obtain

$$\frac{D\mu}{Dt} = k_Y \nabla^2 \mu, \qquad (14)$$

having multiplied by $\Delta\mu$. All we have done is linearized the right-hand side of the diffusion equation for μ (the nonlinear advective term is still contained in $\frac{D}{Dt}$) however, this is not unlike the small parameter expansion procedure used by Malkus (1964) to justify the use of the Boussinesq approximation for homogeneous fluids. We will make use of (14) in our study.

Equation (1) still contains the density perturbation and so we must provide an equation of state which governs these density fluctuations. The equation of state governing these fluctuations may be obtained by expanding the ideal gas law(7)

around a reference density and keeping only first order terms. The influence of pressure perturbations on the density is of less importance than temperature perturbations if $D/H_s \ll 1$, (see Spiegel and Veronis, 1960). Keeping within the Boussinesq limitations we must have the variations of density, temperature, and concentration between the plates small compared to their mean values. Therefore we may write the equation of state as

$$\rho \cong \rho_m \left(1 - \frac{T'}{T_m} + \frac{\mu'}{\mu_m}\right). \tag{15}$$

Equations (1), (2), (10), (14), and (15) complete our set of governing equations, however, we must still specify the forms of the transport coefficients. The kinematic viscosity in (1) may be expressed in terms of the dynamical viscosity, $\nu = \eta/\rho_m$ where η has a contribution from both the gas and the radiation field. We may approximate the gas's viscosity by that of a pure hydrogen plasma whose momentum transport is dominated by the Coulomb interaction. The form as given by Spitzer is

$$\eta_{gas} = \frac{0.4\sqrt{m_p}(kT)^{5/2}}{e^4 \ln \Lambda_D} \tag{16}$$

where the Debye length is given by

$$\Lambda_D = \frac{3}{2e^3}\sqrt{\frac{m_p k^3 T^3}{\pi \rho}}$$

and 'e' is the magnitude of the charge on the electron. The momentum transfer by radiative stresses in a moving fluid may be expressed in terms of a radiative viscosity given by (Thomas, 1930)

$$\eta_{rad} = \frac{4}{15}\frac{aT^4}{cK\rho}. \tag{17}$$

(For a more transparent discussion see Ledoux and Walraven, 1958, § 49 β.) In (17) K is the opacity and for our discussion we will use the electron scattering opacity. For pure scattering the coefficient in (17) should be 8/27 (Masaki, 1971). In terms of the mass fraction of hydrogen

$$K \cong 0.19(1+X)$$

or using the relationship between X, Y and Z, and Eq. (8) we may write

$$K = 0.19\left[\frac{2+Z}{5} + 4/5\mu^{-1}\right]. \tag{18}$$

Diffusion in stars is discussed by Aller and Chapman (1960) and a form for the diffusion coefficient relevant to stellar interiors is given there. Though the coefficient can be modified if a substantial part of the pressure is due to radiation it is still many orders of magnitude smaller than the conductivity. Typically it is about 1/100 of the gaseous kinematic viscosity which is itself ~ 1/10 the radiative kinematic viscosity.

To obtain a radiative conductivity we refer to the relationship between the radiative flux (integrated over all frequencies) and the corresponding radiative stresses (Chandrasekhar, 1939, V and VI). We may write

$$\nabla\left(\tfrac{1}{3}aT^4\right) = -\frac{K\rho}{c}\mathcal{F}$$

where $\frac{ac}{4}$ = Stefar-Boltzman radiation constant and 'c' is the speed of light. If we express the flux in terms of a temperature gradient and a conductivity from the above relation we obtain

$$K_{rad} = \frac{4}{3}\frac{acT^3}{K\rho} \tag{19}$$

The dependence of $\chi = \frac{K_{rad}}{\rho_m c_p}$ on the composition is evident from (18) and (19). To investigate the effects of a conductivity given by (19) we proceed as follows: We expand χ in a Taylor series around a reference point and truncate the expansion after the second derivatives in ρ, T, μ and their cross derivatives. We obtain the derivatives from (19) and use (15) to eliminate ρ. As the range of μ is between 4/3 and 1/2 we will take ξ 1. Furthermore, we separate the T and μ fields into their unperturbed and perturbed parts, e.g. $T = T_b + T'$ and write $T_b = T_m + T_0$ where T_0 now represents the variation of T_b around its mean value. We then scale T_0, T' and μ_0, μ' by $\Delta T = T_L - T_U$ and $\Delta\mu = \mu_L - \mu_U$ respectively. If we define the two small parameters

$$\delta = \frac{\Delta T}{T_m} \quad , \quad \xi = \frac{\Delta\mu}{\mu} \tag{20}$$

we may write the conductivity as

$$\frac{\chi}{\chi_m} \tilde{=} 1 + 3\delta T_0 + \tfrac{2}{3}\xi\mu_0 + 3\delta^2 T_0^2 - \tfrac{2}{9}\xi^2\mu_0^2 + \delta\xi T_0\mu_0 + T'\left[4\delta + \tfrac{15}{2}\delta^2 T_0 + \tfrac{4}{3}\delta\xi\mu_0\right] -$$
$$-\mu'\left[\tfrac{1}{3}\xi + \tfrac{1}{2}\delta\xi T_0 + \tfrac{7}{9}\xi^2\mu_0\right] + \tfrac{11}{2}\delta^2(T')^2 + \tfrac{4}{9}\xi^2(\mu')^2 - \tfrac{13}{6}\delta\xi T'\mu'. \tag{21}$$

We can make use of the equation of motion in its more convenient form by eliminating the x and y components of (1) as well as P'. By taking $\partial/\partial z$ of the divergence of (1), utilizing (2), and subtracting from that the Laplacian of the z-component of (1) we obtain

$$\left(\frac{\partial}{\partial t} - \nu\nabla^2\right)\nabla^2 w = g\left(\frac{\Delta_2 T'}{T_m} - \frac{\Delta_2\mu'}{\mu_m}\right) + L_{(v)} \tag{22}$$

where

$$L_{(v)} = \frac{\partial^2}{\partial z \partial x}(v\cdot\nabla u) + \frac{\partial^2}{\partial z \partial y}(v\cdot\nabla v) - \Delta_2(v\cdot\nabla w).$$

In (22) we have replaced ρ' with Eq. (15), written the velocity components as $v = (u, v, w)$ and defined $\Delta_2 = \frac{\partial^2}{\partial x^2} + \frac{\partial^2}{\partial y^2}$. For two-dimensional rolls $v = 0$ and $= 0$. (Equation (22) has the unscaled quantities T' and μ' which are scaled in (21).) Before going on to scale the governing equations and discuss their solution we will obtain from them the stability criteria of Ledoux and Schwarzschild.

III. The Ledoux and Schwarzschild Limits

The stability criteria used by Schwarzschild and Ledoux were obtained from simple buoyancy arguments concerning the adiabatic displacement of a blob of fluid. For adiabatic motion we replace all the transport coefficients by zero. Equations (10), (14), and (22) become

$$\left(\frac{\partial}{\partial t} + v\cdot\nabla\right)T + \frac{g}{c_p}w - \frac{1}{\rho_m c_p}\left(1 + \frac{4}{5}\frac{m_p\mu_{chem}}{kT}\right)_m \frac{P}{\mu}\frac{D\mu}{Dt} = 0 \tag{23}$$

$$\frac{D\mu}{Dt} = 0 \tag{24}$$

$$\frac{\partial}{\partial t}\nabla^2 w = g\left(\frac{\Delta_2 T'}{T_m} - \frac{\Delta_2\mu'}{\mu_m}\right) + L_{(v)}. \tag{25}$$

Equation (24) eliminates the $\frac{D\mu}{Dt}$ term from (23). We replace the variables T and μ by the sum of their unperturbed plus perturbed parts, e.g. $T = \bar{T}_{(z)} + T'$. We then linearize (23) - (25) and remembering that

$$\left.\frac{dT}{dz}\right|_{ad} = -g/c_p$$

we obtain

$$\frac{\partial T'}{\partial t} + w\left(\frac{d\bar{T}}{dz} - \left.\frac{d\bar{T}}{dz}\right|_{ad}\right) = 0 , \qquad \frac{\partial \mu'}{\partial t} + w\frac{d\bar{\mu}}{dz} = 0 \qquad (26)\,(27)$$

and

$$\frac{\partial}{\partial t}\nabla^2 w = g\left(\frac{\Delta_2 T'}{T_m} - \frac{\Delta_2 \mu'}{\mu_m}\right) \qquad (28)$$

We assume that w, T', and μ' can be written in the form

$$T' = \hat{T}_{(z)} e^{\sigma t} f_{(x,y)}, \quad \mu' = \hat{\mu}_{(z)} e^{\sigma t} f_{(x,y)}, \quad w = \hat{w}_{(z)} e^{\sigma t} f_{(x,y)}$$

where the plan form $f_{(x,y)}$ satisfies $\frac{\partial^2 f}{\partial x^2} + \frac{\partial^2 f}{\partial y^2} + a^2 f = 0$, (i .e. closely packed cells of horizontal wave number 'a'). Substitution into (26) through (28) yields

$$\sigma\hat{\mu} + \hat{w}\frac{d\bar{\mu}}{dz} = 0$$

$$\sigma\hat{T} + \hat{w}\left(\frac{d\bar{T}}{dz} - \left.\frac{dT}{dz}\right|_{ad}\right) = 0$$

$$\sigma\left(\frac{\partial^2}{\partial z^2} - a^2\right)\hat{w} = -ga^2\frac{\hat{T}}{T_m} + ga^2\frac{\hat{\mu}}{\mu_m}$$

which can be combined into the one equation

$$\frac{\sigma^2}{ga^2}\left(\frac{\partial^2}{\partial z^2} - a^2\right)\hat{w} = \hat{w}\left[\frac{1}{T_m}\frac{d\bar{T}}{dz} - \frac{1}{T_m}\left.\frac{dT}{dz}\right|_{ad} - \frac{1}{\mu_m}\frac{d\bar{\mu}}{dz}\right]. \qquad (29)$$

At marginal stability the growth rate $\sigma = 0$ (disregarding any overstability). In general $\hat{w} \neq 0$ and therefore the square bracket in (29) must vanish at $\sigma = 0$. If we choose the reference point at the position of the displaced blob we obtain the Ledoux criterion for marginal convective instability,

$$\frac{d\ln\bar{T}}{dz} = \left.\frac{d\ln T}{dz}\right|_{ad} + \frac{d\ln\bar{\mu}}{dz}. \qquad (30)$$

For a homogeneous fluid $\frac{d\ln\bar{\mu}}{dz} = 0$ and we obtain from (30) the Schwarzschild criterion.

IV. Scaling the Equations and the Basic State

The governing equations in dimensional form are (2), (10), (14), and (22) with the conductivity χ scaled by χ_m in (21). At this point it is convenient to scale the equations by taking (dimensionless quantities are capped)

$$(X, Y, Z) = D(\hat{X}, \hat{Y}, \hat{Z}), \quad t = \frac{D^2}{\chi_m}\hat{t}, \quad \underset{\sim}{v} = \frac{\chi_m}{D}\underset{\sim}{\hat{v}}, \quad \chi = \chi_m\hat{\chi},$$

$$T = (\Delta T)\hat{T}, \quad \mu = (\Delta\mu)\hat{\mu}, \quad P = \rho_m g D\hat{P}, \quad \gamma = \left.\frac{dT}{dz}\right|_{ad} = -g/c_p = \frac{\Delta T}{D}\hat{\gamma}.$$

The dimensionless numbers which are relevant to the problem are then the thermal Rayleigh number $R_T = \frac{g\frac{\Delta T}{T_m}D^3}{\chi_m\nu}$, the concentration Rayleigh number $R_\mu = \frac{g\frac{\Delta\mu}{\mu_m}D^3}{\chi_m\nu}$, the Prandtl number $\sigma = \nu/\chi_m$ and the ratio of concentration to heat diffusivities $\tau = \kappa_T/\chi_m$. In terms of these scaled quantities the equations become (dropping the caps)

$$\left(\frac{1}{\sigma}\frac{\partial}{\partial t} - \nabla^2\right)\nabla^2 w = \frac{1}{\sigma}L_{(v)} + R_T\Delta_2 T - R_\mu\Delta_2\mu \qquad (31)$$

$$\nabla \cdot \underset{\sim}{v} = 0 \tag{32}$$

$$\left(\frac{\partial}{\partial t} - \tau \nabla^2\right)\mu = -\underset{\sim}{v} \cdot \nabla \mu \tag{33}$$

$$\frac{\partial T}{\partial t} + \underset{\sim}{v} \cdot \nabla T - \gamma w + \left(1 + \frac{4}{3}\frac{m_p \mu_{chem}}{kT}\right)\gamma \frac{P}{\mu}\frac{D\mu}{Dt} - \nabla \cdot (\chi \nabla T) = 0. \tag{34}$$

In Eq. (31) we have replaced the scaled perturbations T' and μ' by $T = T_b + T^I$ and $\mu = \mu_b + \mu'$ as T_b and μ_b are only functions of z while Δ_1 is an (x,y) differential operator. As it stands now there is not much that can be done with Eq. (34), however we can simplify it even more if we assume that

$$\zeta/\delta \ll 1.$$

Let us consider the dimensionless product $\hat{\gamma}\frac{\hat{P}}{\hat{\mu}}$ which appears in (34). If we write its equivalent in unscaled variables and make use of the ideal gas law we find

$$\left|\hat{\gamma}\frac{\hat{P}}{\hat{\mu}}\right| = \frac{g}{c_p}\Big/\frac{\Delta T}{D}\,\frac{P}{\rho_m g D}\,\frac{\Delta\mu}{\mu} = \frac{\Delta\mu}{\mu}\,\frac{P}{\rho_m c_p \Delta T} = \frac{\Delta\mu}{\mu}\,\frac{T}{\Delta T}\,\frac{\rho}{\rho_m}\,\frac{k/\mu m_p}{c_p}.$$

As variations of ρ, μ, and T must be small compared to their mean values we may approximate them by ρ_m, μ_m, and T_m. As $k/\mu_m m_p \approx c_p$ (within a factor of 2) we use (20) to find

$$\left|\hat{\gamma}\frac{\hat{P}}{\hat{\mu}}\right| \approx \zeta/\delta \ll 1$$

by assumption. As this expression is so small while the coefficient γ of the γw term in (34) is of order unity for a system in laminar convection, we feel that it is justified to evaluate the entire coefficient of $\frac{D\mu}{Dt}$ at the reference point. We define

$$K_\mu = \gamma \frac{P_m}{\mu_m}\left(1 + \frac{4}{3}\frac{m_p \mu_{chem}}{kT}\right) \ll 1 \tag{35}$$

and rewrite (34) as

$$\frac{\partial T}{\partial t} - \gamma w + K_\mu \frac{\partial \mu}{\partial t} - \nabla \cdot (\chi \nabla T) + \underset{\sim}{v} \cdot (\nabla T + K_\mu \nabla \mu) = 0 \tag{36}$$

As mentioned above we will consider roll solutions to the equations, therefore $\Delta_2 = \frac{\partial^2}{\partial x^2}$. In addition we will restrict our attention to steady convection only and therefore $\frac{\partial}{\partial t} = 0$. Though it is known from the thermohaline problem that the fluid is unstable to oscillatory modes at a lower R_T than for non-oscillatory modes we will restrict the analysis to steady modes only. Kato (1966) has shown that mixing can occur by overstability when dealing with an isolated fluid region, however Auré (1969) has shown that overstable convective modes are damped by the radiative envelope in B stars departing from the main sequence. We feel that this justifies the study of steady modes only. Moreover we will be looking for the possibility of a subcritical steady mode which the star might lock into before any oscillatory modes may develop. However we can not rule out the possibility of overstable modes in the limit of vanishing frequency as these set in at Rayleigh numbers lower than critical. In the limit of this study the governing system of equations becomes

$$\nabla^4 W + R_T \frac{\partial^2}{\partial x^2} T - R_\mu \frac{\partial^2}{\partial x^2}\mu = -\frac{1}{\sigma} L(\underset{\sim}{v}) \tag{37}$$

$$\frac{\partial u}{\partial x} = -\frac{\partial w}{\partial z} \tag{38}$$

$$\tau \nabla^2 \mu - \underset{\sim}{v} \cdot \nabla \mu = 0 \tag{39}$$

$$\nabla^2 T + \gamma W - \underline{\nu}\cdot(\nabla T + K_\mu \nabla \mu) + \nabla\cdot\left[(\chi - 1)\nabla T\right] = 0 \tag{40}$$

together with (21). We might mention that typical values for σ and τ in semiconvective zones are $\sigma \sim 10^{-4}$, $\tau \sim 10^{-9}$.

Equations (37) - (40) and (21) still contain the basic state temperature and composition profiles which we may solve for now before going on to the perturbation problem. If we take the mean quantities T_m and μ_m to be the average of those values on the plates, we have the following scaled boundary conditions on the basic state $T_b = T_m + T_0$ and $\mu_b = \mu_m + \mu_0$;

$$T_0 = (\pm)\tfrac{1}{2} \quad \text{and} \quad \mu_0 = (\pm)\tfrac{1}{2} \text{ at } z = \begin{pmatrix} 0 \\ 1 \end{pmatrix}. \tag{41}$$

As the basic state is hydrostatic and z-dependent, only the governing equations reduce to

$$\frac{d^2 \mu_0}{dz^2} = 0 \tag{42}$$

$$\frac{d}{dz}\left(\chi_0 \frac{dT_0}{dz}\right) = 0 \tag{43}$$

with χ_0 given by the first six terms in (21). Eqs. (42) and (43) may be integrated directly with (41) to give

$$\mu_0 = \tfrac{1}{2}(1 - 2z) \tag{44}$$

and

$$\chi_0 \frac{dT_0}{dz} = \text{constant}. \tag{45}$$

As χ_0 makes (45) nonlinear, it is to our advantage to make use of the smallness of δ and η. We can obtain an approximate solution by expanding T_0 in a series of powers of δ and η and require each order in δ and η to satisfy (45) separately. We must also adjust our boundary conditions. We may write

$$T_0 = \sum_{\substack{m=0 \\ n=0}}^{\infty} T_0^{(m,n)} \delta^m \eta^n \tag{46}$$

and

$$T_0^{(0,0)} = (\pm)\tfrac{1}{2} \text{ at } z = \begin{pmatrix} 0 \\ 1 \end{pmatrix}$$
$$T_0^{(m,n)} = 0 \text{ for } (m,n) \neq (0,0) \text{ at } z \begin{pmatrix} 0 \\ 1 \end{pmatrix}. \tag{47}$$

Substituting (21) and (46) into (45) and considering the expansion through second order in small quantities, we obtain the following set of equations for T_0 :

$$\frac{dT_0^{(0,0)}}{dz} = \text{constant}$$

$$\frac{dT_0^{(1,0)}}{dz} + 3T_0^{(0,0)}\frac{dT_0^{(0,0)}}{dz} = \text{constant}$$

$$\frac{dT_0^{(0,1)}}{dz} + \frac{2}{3}\mu_0 \frac{dT_0^{(0,0)}}{dz} = \text{constant}$$

$$\frac{dT_0^{(2,0)}}{dz} + 3T_0^{(0,0)}\frac{dT_0^{(1,0)}}{dz} + 3T_0^{(1,0)}\frac{dT_0^{(0,0)}}{dz} + 3T_0^{(0,0)^2}\frac{dT_0^{(0,0)}}{dz} = \text{constant}$$

$$\frac{dT_0^{(0,2)}}{dz} + \frac{2}{3}\mu_0 \frac{dT_0^{(0,1)}}{dz} - \frac{2}{9}\mu_0^2 \frac{dT_0^{(0,0)}}{dz} = \text{constant}$$

$$\frac{dT_0^{(1,1)}}{dz} + 3T_0^{(0,1)}\frac{dT_0^{(0,0)}}{dz} + 3T_0^{(0,0)}\frac{dT_0^{(0,1)}}{dz} + \frac{2}{3}\mu_0 \frac{dT^{(1,0)}}{dz} + \mu_0 T_0^{(0,0)} = \text{constant}$$

The solution subject to (47) is

$$T_0 \cong \tfrac{1}{2}(1-2z) + \tfrac{3}{2}z(1-z)\delta + \tfrac{1}{3}z(1-z)\eta - \tfrac{11}{4}z(1-z)(1-2z)\delta^2 - \tfrac{1}{9}z(1-z)(1-2z)\eta^2 -$$

$$- z(1-z)(1-2z)\delta\eta + \cdots \tag{48}$$

We may now substitute (48) into (21) to obtain the final form of χ which we will use in the perturbation problem. Letting T and μ in (37)-(40) be written as $T = T_m + T_0 + T'$ and $\mu = \mu_m + \mu_0 + \mu'$ subtracting the basic state from (37)-(40), and dropping the primes on perturbation quantities we obtain the set of equations governing the perturbations.

$$\nabla^4 w + R_T \frac{\partial^2}{\partial x^2} T - R_\mu \frac{\partial^2}{\partial x^2}\mu = -\frac{1}{\sigma} L_{(\underset{\sim}{v})} \tag{49}$$

$$L_{(\underset{\sim}{v})} = \frac{\partial}{\partial x}\left[w\left(\frac{\partial^2}{\partial x^2}, \frac{\partial^2}{\partial z^2}\right)u - u\left(\frac{\partial^2}{\partial x^2} + \frac{\partial^2}{\partial z^2}\right)w\right]$$

$$\frac{\partial u}{\partial x} = -\frac{\partial w}{\partial z} \tag{50}$$

$$\nabla^2\mu + \frac{w}{\tau} = \frac{1}{\tau}\underset{\sim}{v}\cdot\nabla\mu \tag{51}$$

$$\nabla^2 T + (\gamma + K\mu)w - w\frac{dT_0}{dz} + \nabla_0\left[(\chi-1)\nabla T + (\chi-\chi_0)\frac{dT_0}{dz}\hat{k}\right] = \underset{\sim}{v}\cdot\left[\nabla T + K\mu\nabla\mu\right] \tag{52}$$

$$(\chi-1) \cong \tfrac{3}{2}(1-2z)\delta + \tfrac{1}{3}(1-2z)\eta + \tfrac{3}{2}\left(\tfrac{1}{2} + z - z^2\right)\delta^2 - \tfrac{1}{18}(1-2z)^2\eta + \tfrac{1}{4}\delta\eta +$$

$$+ T^{(0,2)}\left[4\delta + \tfrac{15}{4}(1-2z)\delta^2 + \tfrac{3}{2}(1-2z)\delta\eta\right] + 4T^{(1,2)}\delta^2 + 4T^{(0,1)}\delta\eta -$$

$$- \mu^{(0,2)}\left[\tfrac{1}{2}\eta + \tfrac{7}{18}(1-2z)\eta^2 + \tfrac{1}{4}(1-2z)\delta\eta\right] - \tfrac{1}{3}\mu^{(0,1)}\eta^2 - \tfrac{1}{3}\mu^{(1,0)}\delta\eta +$$

$$+ \tfrac{11}{2}T^{(0,2)0}\delta^2 + \tfrac{4}{9}\mu^{(0,0)^2}\eta^2 - \tfrac{13}{6}T^{(0,2)}\mu^{(0,0)}\delta\eta + \cdots \tag{53}$$

In (53) we have already expanded the perturbation quantities in powers of δ and η. This will be part of the general expansion procedure we will use to study the nonlinear system (49)-(53). We may mention that in the derivation of the μ-diffusion equation we made a similar expansion and threw out higher order terms while we have retained them here. We have done this because of the dependence of K_{rad} on T and μ as implied by (19). The dependence on these variables is rather strong and we can imagine ourselves creating new small parameters which reflect this strong dependence. For example if $K_{rad} \sim T^n$ then we can expand T about T_m and create the small parameter $n\frac{\Delta T}{T_m}$ which emphasizes the dependence through n. In our case $n = 3$ so we have absorbed n into the coefficients of $(\chi - 1)$. We will use equations (49)-(53) as a model for our system and we will study this model within its limitations.

V. The Perturbation Problem

We will study the perturbation equations (49)-(53) for both perturbations of infinitesimal amplitude and for small but finite amplitude. To do so we will make use of the modified perturbation techniques used by Malkus and Veronis (1958) to study Rayleigh-Bénard convection at finite amplitude. The justification of the approach is elaborated on in terms of Taylor expansions in a parameter space by

Millman and Keller (1969).

In addition to the two expansion parameters δ and η which we have been using we will also make use of the perturbation amplitude ϵ. We will expand the perturbations T, μ, w, and u as $T = \sum_{\ell=1}^{\infty} \sum_{m=0}^{\infty} \sum_{n=0}^{\infty} T_\ell^{(m,n)} \epsilon^\ell \delta^m \eta^n$ and similarly for μ, w, and u. We then substitute these expansions into Eqs.(49)-(53) and solve them at each order of ϵ, δ, and η separately. Thus $(\ell,m,n) = (1,0,0)$ will yield the linearized homogeneous problem and for other values of (ℓ,m,n) we will obtain additional inhomogeneous terms. For a solution to exist the equation must satisfy certain solubility conditions. That is the inhomogeneous terms must be orthogonal to the adjoint solution to the homogeneous problem. In general this will not be the case and so we will expand the eigenvalue as well and choose it so that this condition is met. For the stellar case we may consider the composition as given and so keep the concentration Rayleigh number R_μ fixed. We will expand the thermal Rayleigh number as

$$R_T = \sum_{\substack{\ell=0 \\ m=0 \\ n=0}}^{\infty} R_\ell^{(m,n)} \epsilon^\ell \delta^m \eta^n .$$

To eliminate the arbitrary addition of the homogeneous solution to the solution of higher order $(\ell,m,n) \neq (1,0,0)$ we will define ϵ by an orthogonality relation to be given below. We will also refer to $(x-l)_\ell^{(m,n)}$ which will depend on the index ℓ of the perturbations which appear in (53).

We will require the perturbations in T and μ to vanish at the boundaries $z = (0,1)$ as we have assumed the plates to be perfect conductors of heat and helium. As fixing any sort of boundary conditions on the gas motions in a star is somewhat artificial we feel that stress-free boundaries are more realistic than rigid boundaries. The vanishing of the shear stress $\frac{\partial u}{\partial z}$ at $z = (0,1)$ (for all x) combined with (50) yields $\frac{\partial^2 w}{\partial z^2} = 0$ at $z = (0,1)$ and with the requirement that there be no net mass flux through the plates implies $w = 0$ at $z = (0,1)$. As a convenience from now on we will let $D = \frac{d}{dz}$.

$(\ell,m,n) = (1,0,0)$

Upon substituting the expansions given above into Eqs.(49)-(53) the equations we obtain may be written as

$$(D^2 - a^2)^2 w_1^{(0,0)} - a^2 R_0^{(0,0)} T_1^{(0,0)} + a^2 R_\mu \mu_1^{(0,0)} = 0 \qquad (54)$$

$$(D^2 - a^2) \mu_1^{(0,0)} + \frac{w_1^{(0,0)}}{\tau} = 0 \qquad (55)$$

$$(D^2 - a^2) T_1^{(0,0)} + (\gamma + 1 + K\mu) w_1^{(0,0)} = 0 \qquad (56)$$

We have chosen a periodic x-dependence of wavenumber 'a' to achieve a separation of variables. We will restrict our attention to solutions at all orders of ϵ, δ, η which have a periodicity of $\frac{2\pi}{a}$ in the x-direction. This implies that the x-dependence at each individual order will be a harmonic of the fundamental wavenumber 'a'. Taking $(D^2 - a^2)$ of (54) we may combine (54)- (56) into one equation.

$$(D^2 - a^2)^3 w_1^{(0,0)} + \left[(\gamma + 1 + K\mu) R_0^{(0,0)} - R_\mu / \tau \right] a^2 w_1^{(0,0)} = 0 \qquad (57)$$

As $T_1^{(0,0)} = \mu_1^{(0,0)} = 0$ at $z = (0,1)$ Eq.(54) implies $(D^2 - a^2)^2 w_1^{(0,0)}$ vanishes as well at $z = (0,1)$. This is the well-known Rayleigh equation with the expression in square brackets being the eigenvalue. The z-dependence of the solution must be $\sin n\pi z$ as seen from taking D^2 of (57) and using the boundary conditions over and over again. The eigenvalue will then be $\frac{(n^2\pi^2 + a^2)^3}{a^2}$ and will take on its minimum value of $\frac{27\pi^4}{4}$ at $a^2 = \pi^2/2$. We may use the solution for $w_1^{(0,0)}$ in (55), (56), and (50) to obtain expressions

for $\mu_1^{(0,0)}$, $T_1^{(0,0)}$ and $u_1^{(0,0)}$. The solution to this linearized problem at the eigenvalue minimum is

$$W_1^{(0,0)} = 2 \sin \pi z \cos ax$$

$$\mu_1^{(0,0)} = \frac{2}{\tau(\pi^2+a^2)} \sin \pi z \cos ax$$

$$T_1^{(0,0)} = 2\frac{(\gamma+1+K\mu)}{(\pi^2+a^2)} \sin \pi z \cos ax \qquad (58)$$

$$u_1^{(0,0)} = -\frac{2\pi}{a} \cos \pi z \sin ax$$

and

$$R_0^{(0,0)} = \left(\frac{27\pi^4}{4} + \frac{R\mu}{\tau}\right) \Big/ (\gamma+1+K\mu).$$

We note that the ϵ-expansion is valid only within some radius of convergence. For $\ell = 1$ we have ignored the nonlinear terms in the equations. As can be seen from (49) and (51) this is only valid for $\epsilon \ll \sigma$ and $\epsilon \ll \tau$. This is a severe restriction as σ and τ are very small for stars. $R_0^{(0,0)}$ is the critical Rayleigh number for the problem. According to the solution of the linearized problem the system becomes unstable to infinitesimal disturbances for $R_T > R_0^{(0,0)}$. For Rayleigh numbers lower than $R_0^{(0,0)}$ the disturbances decay while for Rayleigh numbers greater than $R_0^{(0,0)}$ they grow exponentially. We will see from the finite amplitude corrections that this is not the case. Before going on to those corrections let us see what effect the temperature - composition dependent conductivity has on the eigenvalue.

At this point let us define ϵ by the following relation,

$$\epsilon = \frac{a}{2\pi} \int_{-\pi/a}^{\pi/a} dx \int_0^1 dz \, (W_1^{(0,0)} W). \qquad (59)$$

We also note that the general Rayleigh operator $\left[\nabla^6 - C_0^{(0,0)} \frac{\partial^2}{\partial z^2}\right]$ (where $C_0^{(0,0)}$ is the expression in the square brackets of (57)), together with the homogeneous boundary conditions at z (9) and the $\frac{2\pi}{a}$ periodicity in x constitutes a self-adjoint operator.

$(\ell, m, n) = (1, 1, 0)$

At this order of ϵ, δ, γ we are still concerned with the linearized form of Eqs. (49)-(52), however the first order effects of the temperature dependence of χ will come in. Again we may choose the planform of the variables to be $\sim \cos ax$ as this now appears in the inhomogeneous terms. The equations become

$$(D^2-a^2)^2 W_1^{(1,0)} - a^2 R_0^{(1,0)} T_1^{(0,0)} - a^2 R_0^{(0,0)} T_1^{(1,0)} + a^2 R_\mu \mu_1^{(1,0)} = 0 \qquad (60)$$

$$(D^2-a^2)\mu_1^{(1,0)} + \frac{W_1^{(1,0)}}{\tau} = 0 \qquad (61)$$

$$(D^2-a^2)^3 T_1^{(1,0)} + (\gamma+1+K\mu) W_1^{(1,0)} = 3(\gamma+2+K\mu)(1-2z) \sin \pi z \cos ax +$$
$$+ \frac{14\pi}{\pi^2+a^2} (\gamma+1+K\mu) \cos \pi z \cos ax \qquad (62)$$

Taking (D^2-a^2) of (60), we may combine (60) - (62) and using (58) obtain

$$(D^2-a^2)^3 W_1^{(1,0)} + a^2 C_0^{(0,0)} W_1^{(1,0)} + R_0^{(1,0)} 2a^2(\gamma+1+\kappa\mu)\sin\pi z\cos ax =$$

$$= R_0^{(0,0)} a^2 \cos ax \left[3(\gamma+2+\kappa\mu)(1-2z)\sin\pi z + \frac{14\pi}{\pi^2+a^2}(\gamma+1+\kappa\mu)\cos\pi z\right]. \qquad (63)$$

As $T_1^{(1,0)} = \mu_1^{(1,0)} = T_1^{(0,0)} = 0$ at $z = \begin{pmatrix} 0 \\ 1 \end{pmatrix}$ we find from (60) that $D^4 W_1^{(1,0)} = 0$ as $W_1^{(1,0)} = D^2 W_1^{(1,0)} = 0$ at $z = \begin{pmatrix} 0 \\ 1 \end{pmatrix}$. From (63) we see that $W_1^{(1,0)} \sim \cos ax$. Multiplying (63) by the adjoint of $W_0^{(0,0)}$ and integrating by parts we obtain as the solubility condition of (63) that $R_0^{(1,0)} = 0$. To satisfy the boundary conditions on $W_1^{(1,0)}$ we will need to make use of the complimentary solutions of the homogeneous equation (57). If we let the solutions of (57) have the dependence $e^{\lambda z}$ we obtain the algebraic equation

$$(\lambda^2-a^2)^3 + a^2 C_0^{(0,0)} = 0, \qquad C_0^{(0,0)} = \frac{(\pi^2+a^2)^3}{a^2}.$$

The six roots are $\lambda_{1,2} = \pm i\pi$; $\lambda_{3,4} = \pm a\left[1+\tfrac{1}{2}(1+\pi^2/a^2)(1+i\sqrt{3})\right]^{1/2}$, and $\lambda_{5,6} = \pm\sqrt{\lambda_3^{2*}}$ where (*) means complex conjugate. If we define

$$\lambda = a\left[1+\tfrac{1}{2}(1+\pi^2/a^2)(1+i\sqrt{3})\right]^{1/2} \qquad (64)$$

we may write the complete solution of (63) as

$$W_1^{(1,0)} = W_1^{(1,0)}(z)\cos ax$$

where $W_1^{(1,0)}(z) = A_1 z\sin\pi z + A_2 z\cos\pi z + A_3 z^2\cos\pi z + A_4\cos\pi z + A_5 e^{\lambda z} +$

$$+ A_6 e^{-\lambda z} + A_7 e^{\lambda^* z} + A_8 e^{-\lambda^* z} - A_{11}\sin\pi z. \qquad (65)$$

The first three coefficients in (65) come from the particular solution and are given by

$$A_1 = \frac{a^2 R_0^{(0,0)}}{2(\pi^2+a^2)^3}\left[\frac{14}{3}(\gamma+1+\kappa\mu) - \frac{(5\pi^2+a^2)}{\pi^2}(\gamma+2+\kappa\mu)\right],$$

$$A_2 = \frac{-a R_0^{(0,0)}}{2(\pi^2+a^2)^2}(\gamma+2+\kappa\mu), \quad A_3 = -A_2.$$

To satisfy the six boundary conditions on $W_1^{(1,0)}(z)$ we may adjust the six free constants. However the $a\sin\pi z$ term cannot affect the boundaries implying that at most only fire of the boundary conditions are linearly independent. By setting up the 6x6 matrix equation for the coefficients and performing the usual row operations we find that the matrix has a rank of five and at the same time obtain the solution for the coefficients. The matrix equation, off of which the solutions may be read is

$$\begin{pmatrix} (\pi^2+\lambda^2)(\pi^2+\lambda^{*2}) & 0 & 0 & 0 & 0 \\ (\pi^2+\lambda^{*2})(e^{-\lambda}+1) & (\lambda^{*2}-\lambda^2)(e^{-\lambda}-e^{\lambda}) & 0 & 0 & 0 \\ (\pi^2+\lambda^{*2}) & (\lambda^{*2}-\lambda^2) & (\lambda^{*2}-\lambda^2) & 0 & 0 \\ (e^{-\lambda^*}+1) & (e^{-\lambda^*}+1) & (e^{-\lambda^*}+1) & (e^{-\lambda^*}-e^{\lambda^*}) & 0 \\ 1 & 1 & 1 & 1 & 1 \end{pmatrix} \begin{pmatrix} A_4 \\ A_5 \\ A_6 \\ A_7 \\ A_8 \end{pmatrix} =$$

$$= \begin{pmatrix} 2(2\pi^2+\lambda^2+\lambda^{*2})(\pi A_1+A_3)+8\pi^2 A_3 \\ 2(e^{-\lambda}+1)(\pi A_1+A_3) \\ 2(\pi A_1+A_3) \\ 0 \\ 0 \end{pmatrix}. \tag{66}$$

The coefficient A_{11} in (65) is determined by the orthogonality condition (59). The solutions to (61) and (62) may be written as $\mu_1^{(1,0)} = \mu_1^{(1,0)}(z)\cos ax$ and $T_1^{(1,0)} = T_1^{(1,0)}(z)\cos ax$

where $\mu_1^{(1,0)}(z) = \frac{1}{\tau(\lambda^2+a^2)}\left[(A_1+\frac{4\pi}{\pi^2+a^2}A_2)z\sin\pi z + A_2 z\cos\pi z - A_3 z^2\cos\pi z - \right.$

$$\left. -\left(\frac{2\pi}{\pi^2+a^2}A_2+A_{11}\right)\sin\pi z+\left(\frac{2\pi}{\pi^2+a^2}A_1-\frac{2(a^2-3\pi^2)}{(\pi^2+a^2)^2}A_2+A_4\right)\cos\pi z\right] -$$

$$-\frac{1}{\tau(\lambda^2-a^2)}\left(A_5 e^{\lambda z}+A_6 e^{-\lambda z}\right)-\frac{1}{\tau(\lambda^{*2}-a^2)}\left(A_7 e^{\lambda^* z}+A_8 e^{-\lambda^* z}\right)+$$

$$+A_9\cosh az + A_{10}\sinh az \tag{67}$$

and $T_1^{(1,0)}(z) = \tau(\gamma+1+K\mu)\mu_1^{(1,0)}(z) - \frac{3(\gamma+2+K\mu)}{(\pi^2+a^2)}(1-2z)\sin\pi z + \frac{2\pi}{(\pi^2+a^2)^2}(\gamma-5+K\mu)\left[\cos\pi z - \right.$

$$\left. -\cosh az + (\operatorname{csch} a + \coth a)\sinh az\right]. \tag{68}$$

The coefficients A_9 and A_{10} are chosen to make $\mu_1^{(1,0)}$ satisfy its boundary conditions. We see that to first order in δ though the structure of the eigenfunctions is certainly modified, the critical eigenvalue is not. Also, as the (1,1,0) solutions are all proportional to $\cos ax$ they do not affect the mean fields (the horizontally averaged μ and T fields). We need not write down the form of $w_1^{(1,0)}$ but only say that it is obtained from $w_1^{(1,0)} = -\frac{1}{a^2}D w_1^{(1,0)}(z)\sin ax$ Physically, the fields themselves are given by the real parts of (65), (67), and (68). As we are considering solutions near the critical eigenvalue we would expect the horizontal wavenumber to remain very close to $a = \pi/\sqrt{2}$. This was shown to be true for the Rayleigh-Bénard problem at finite amplitude by Malkus and Veronis (1958).

$(\ell, m, n) = (1, 0, 1)$

The results of the (1,0,1) problem are very similar to the (1,1,0) results. We find $R_0^{(0,1)} = 0$ and eigenfunctions of the same form as those of the (1,1,0) case, Hence to first order in both δ and η the critical Rayleigh number is unaffected.

$(\ell, m, n) = (1, 2, 0)$

By the time we get to second order in δ the equations become very unmanagable, however it is at this order that we first encounter corrections to the critical eigenvalue. Let us consider one particular term to demonstrate the point, To eliminate $T_1^{(2,0)}$ from Eq. (49) for $w_1^{(2,0)}$ we will have to take ∇^2 of (49) and introduce (52) for $T_1^{(2,0)}$ into that equation. Thus the equation will contain the following terms due to the $w\frac{dT_2}{dz}$ term in (52):

$$a^2 R_0^{(0,0)}\left(w_1^{(1,0)} D T_0^{(1,0)} + w_1^{(0,0)} D T^{(2,0)}\right).$$

These terms will be multiplied by $\sin\pi z$ and integrated over z to determine $R_0^{(2,0)}$. Upon doing so we find that the $W_1^{(0,0)} D T_0^{(2,0)}$ term does not contribute, however the $W_1^{(1,0)} D T_0^{(1,0)}$ term does. This can be seen by considering only the first term in (65). The integration over x does not vanish as both $w_0^{(0,0)}$ and $W_1^{(1,0)} \sim \cos ax$. The z integration will be $-\int_0^1 (\sin\pi z)(z\sin\pi z)(1-2z) \neq 0$.

We would also expect nonvanishing $R_0^{(0,2)}$ and $R_0^{(1,1)}$ as $R_0^{(2,0)} \neq 0$. Thus the critical Rayleigh number is modified at second order in the small quantities δ, η.

$(\ell, m, n) = (2,0,0)$

For $\ell \geq 2$ the governing equations will contain additional inhomogeneous terms reflecting the nonlinear terms on the right-hand sides of (49)-(52). As $L(x)$ in (49) will always contain the factor W or D^2W of an order of W already known (which satisfied certain boundary conditions) it will not affect the boundary conditions of a higher order W. As can be seen for $\ell = 2$, $L(x)$ contains W_1 and D^2W_1, both of which vanish at $z = \binom{0}{1}$. As T_2 and μ_2 must vanish on the boundaries as well as W_2 and D^2W_2 we must have D^4W_2 vanish there also. This same argument applies for all higher orders of W and so from now on we can take as our boundary conditions at

$$z = \binom{0}{1} \qquad \mu = T = W = D^2W = D^4W = 0.$$

At $(\ell, m, n) = (2, 0, 0)$ the equations become

$$\nabla^4 W_2^{(0,0)} + R_0^{(0,0)} \frac{\partial^2}{\partial x^2} T_2^{(0,0)} + R_1^{(0,0)} \frac{\partial^2}{\partial x^2} T_1^{(0,0)} - R\mu \frac{\partial^2}{\partial x^2} \mu_2^{(0,0)} = 0$$

$$\nabla^2 \mu_2^{(0,0)} + \frac{W_2^{(0,0)}}{\tau} = \frac{2\pi}{\tau^2(\pi^2+a^2)} \sin 2\pi z$$

$$\nabla^2 T_2^{(0,0)} + (\gamma + 1 + K\mu) W_2^{(0,0)} = \frac{2\pi}{\pi^2+a^2}\left[\gamma + 1 + K\mu(1+\tau^{-1})\right] \sin 2\pi z.$$

We note that the inhomogeneous terms are independent of x and so will not enter into the $\nabla^6 W_2^{(0,0)}$ equation. Taking ∇^2 of the $W_2^{(0,0)}$ equation, eliminating $T_2^{(0,0)}$ and $\mu_2^{(0,0)}$ and using the expression for $T_1^{(0,0)}$ we find that choosing a $\cos ax$ dependence for $W_2^{(0,0)}$ yields

$$(D^2 - a^2)^3 W_2^{(0,0)}(z) + \left[(\gamma + 1 + K\mu) R_0^{(0,0)} - \frac{R\mu}{\tau}\right] a^2 W_2^{(0,0)} + 2(\gamma + 1 + K\mu) a^2 R_1^{(0,0)} \sin\pi z = 0.$$

Multiplying by $W_1^{(0,0)}(z)$ and integrating by parts we find that we must choose $R_1^{(0,0)} = 0$. If we do so we see that the equation and boundary conditions that $W_2^{(0,0)}$ must satisfy and they are the same as those for $W_1^{(0,0)}$ (see (57)) and so by the orthogonality condition (59) we must choose $W_2^{(0,0)} = 0$. The equations for $\mu_2^{(0,0)}$ and $T_2^{(0,0)}$ may then be solved giving

$$\mu_2^{(0,0)} = \frac{-1}{2\pi\tau^2(\pi^2+a^2)} \sin 2\pi z \tag{69}$$

and

$$T_2^{(0,0)} = \frac{-1}{2\pi(\pi^2+a^2)} \left[\gamma + 1 + K\mu(1+\tau^{-1})\right] \sin 2\pi z. \tag{70}$$

As $\mu_2^{(0,0)}$ and $T_2^{(0,0)}$ are independent of x we see that the first effect of the nonlinear terms is to modify the horizontally averaged fields. Eqs. (69) and (70) show that the convection mixes the fluid into a more uniform state. As $W_2^{(0,0)} = 0$, Eq. (50) implies that $u_2^{(0,0)}$ is independent of x. If we go back to Eq. (1) and consider the x-component for the steady state we find that

$$D^2 u_2^{(0,0)} \sim \frac{\partial P_2^{(0,0)}}{\partial x}.$$

If $D^2 u_2^{(0,0)}$ were nonzero we would have a horizontal pressure gradient which was linear with x and hence would diverge as $x \to \infty$. This is clearly unphysical and so we must have $D^2 u_2^{(0,0)} = 0$, or $u_0^{(0,0)} = az + b$ with 'a' and 'b' constants. The vanishing of the shear stress at the boundaries implies $a = 0$ leaving a constant horizontal velocity of the system. As this may be transformed away by a constant translation of the origin we may set $u_2^{(0,0)} = 0$ without any loss of generality.

$(\ell, m, n) = (2, 1, 0)$

At this order we find that all the inhomogeneous terms in (49)-(52), except for the $R_1^{(1,0)}$ term, are proportional to $\cos 2ax$ or, as in (51) and (52), are independent of x. The equation we obtain for $w_2^{(1,0)}$ is of the form

$$(\nabla^6 - C_0^{(0,0)} \frac{\partial^2}{\partial x^2}) w_2^{(1,0)} + R_0^{(0,0)} f(z) \cos 2ax + R_1^{(1,0)} g(z) \cos ax = h(z) \cos 2ax .$$

Multiplying by $w_1^{(0,0)}$, requiring $w_2^{(1,0)}$ to have an harmonic period of $\frac{2\pi}{a}$ in the x-direction, and integrating over a period of $\frac{2\pi}{a}$ in x and from $z = 0 \to 1$ we find $R_1^{(1,0)} = 0$. This is then also true for $R_1^{(0,1)}$ as the equations at $(\ell, m, n) = (2, 0, 1)$ have the same form as here. As the equations for $u_2^{(1,0)}$ and $T_2^{(1,0)}$ have inhomogeneous terms which are functions of z only, we find that the horizontally-averaged fields are now modified by the δ and η terms in the expansion, The fields will also have components proportional to $\cos 2ax$. This applies to $u_2^{(0,1)}$ and $T_2^{(0,1)}$ also. If we go on to higher orders of δ and η we will find that

$$R_1^{(2,0)} = R_1^{(0,2)} = R_1^{(1,1)} = 0 \quad \text{as well.}$$

All inhomogeneous terms, at any order of δ and η for $\ell = 2$, will be formed either by products of $\ell = 1$ terms or by products of an $\ell = 2$ term with a term from the basic state. This will always yield inhomogeneous terms in the sixth order equation for $w_2^{(m,n)}$ which are proportional to $\cos 2ax$ and so will not modify the Rayleigh number. We may conclude that $R_1^{(m,n)} = 0$ for all (m, n).

$(\ell, m, n) = (3, 0, 0)$

At this order Eqs. (49)-(53) yield the following sixth order equation,

$$(\nabla^6 - C_0^{(0,0)} \frac{\partial^2}{\partial x^2}) w_3^{(0,0)} + R_2^{(0,0)} 2a^2 (\gamma + 1 + K\mu) \sin \pi z \cos ax =$$
$$= R\mu \frac{2a^2}{\tau^2 (\pi^2 + a^2)} \sin \pi z \cos 2\pi z \cos ax - R_0^{(0,0)} \frac{2a^2}{(\pi^2 + a^2)} \left[\gamma + 1 + K\mu (1 + \tau^{-1} + \tau^{-2})\right] \sin \pi z \cos 2\pi z \cos ax . \tag{71}$$

As above, we multiply (71) by $w_1^{(0,0)}$ and integrate choosing $R_2^{(0,0)}$ so as to remove any secular terms. We find

$$R_2^{(0,0)} = \frac{1}{2(\gamma + 1 + K\mu)} \left\{ \frac{R_0^{(0,0)}}{(\pi^2 + a^2)} \left[\gamma + 1 + K\mu (1 + \tau^{-1} + \tau^{-2})\right] - \frac{R\mu / \tau^3}{(\pi^2 + a^2)} \right\} . \tag{72}$$

The dependence of $R_2^{(0,0)}$ on $R\mu$ is given in (58). We also note that for a stabilizing composition gradient ($R\mu > 0$) the form of $R_2^{(0,0)}$ implies that $(\gamma + 1 + K\mu) > 0$ for ΔT near or larger than the negative of the adiabatic gradient. Though the signs are consistent for $\Delta T < -g/c_p$ it is not possible to convect as there is no potential energy available to drive any motion. Therefore for $(\gamma + 1 + K\mu) > 0$ (72) and (58) give us a condition for $R_2^{(0,0)} < 0$. It may be written as

$$R\mu \left[1 - \tau^3 (1 + F)\right] > \frac{27\pi^4}{4} \tau^3 (1 + F) \tag{73}$$

where $F = \frac{K\mu (1 + \tau)}{\tau^3 (\gamma + 1 + K\mu)}$.

As $K\mu \sim \gamma < 0$ for $\Delta T > 0$ and $(\gamma + 1 + K\mu) > 0$ we have $F < 0$. As $\tau < 1$ we have

$[1-\tau^2(1+F)]>0$ and therefore we obtain $R_2^{(0,0)} < 0$ for

$$R_\mu > \frac{27\pi^4}{4}\tau\left[\frac{K_\mu(1+\tau)+(\gamma+1+K_\mu)\tau^2}{-(\gamma+1+K_\mu)\tau^2+(\gamma+1-\tau K_\mu)}\right]. \qquad (74)$$

As K_μ and τ are both very small numbers we conclude that instability to finite amplitude perturbations sets in below critical for almost any $R_\mu > 0$.

It can be shown that as $\tau < 1$ the right-hand side of (74) becomes negative for

$$\frac{|K_\mu|}{(\gamma+1)} > \frac{\tau^2}{1+\tau+\tau^2} \approx \tau^2.$$

This would imply the possibility of a subcritical instability even for $R_\mu < 0$. But for $R_\mu < 0$ and $R_T > 0$ both the temperature and concentration fields are destabilizing A small but finite kick will homogenize the system and as $\tau < 1$ the thermal field will be reestablished first. This would leave the system less unstable than before because we would have destroyed the destabilizing concentration field. Hence a subcritical instability for $R_\mu < 0$ is unphysical and the analysis is applicable only for $\frac{|K_\mu|}{(\gamma+1)} < \tau^2$.

With $R_2^{(0,0)}$ determined we can solve (71) for $W_3^{(0,0)}$ to find

$$W_3^{(0,0)} = \frac{R_2^{(0,0)} 2a^2(\gamma+1+K_\mu)}{(9\pi^2+a^2)^3-(\pi^2+a^2)^3}\sin 3\pi z \cos ax \qquad (75)$$

and $u_3^{(0,0)} = -\frac{1}{a} D W_3^{(0,0)}(z) \sin ax.$

$\mu_3^{(0,0)}$ and $T_3^{(0,0)}$ will have terms $\sim \sin 3\pi z \cos ax$ and $\sim \sin \pi z \cos ax$. Their coefficients are unimportant for now.

As the first finite amplitude results were obtained at $(\ell, m, n) = (3,0,0)$ the dependence of χ on T and μ can change things only slightly but as $\delta \ll 1$ and $\eta \ll 1$ they cannot remove the subcriticality. Therefore, as in the thermohaline case we conclude that stellar semiconvection zones are subcritically unstable as well.

It is of some interest to consider even higher order terms in the expansion. If we go on to $(\ell, m, n) = (4,0,0)$ we find that $R_3^{(0,0)} = 0$ and that $W_4^{(0,0)} \sim \sin 2\pi z \cos 2ax$ and $\sim \sin 4\pi z \cos 2ax$. In addition the mean fields of μ and T are modified by terms $\sim \sin 2\pi z$ and $\sim \sin 4\pi z$. We see that these higher order terms bring out more structure of the effects of convection on the horizontally averaged fields. The results of the previous orders may then be applied at $(\ell, m, n) = (2,0,0)$ to obtain $??^{+(0,0)}$. In deriving $R_4^{(0,0)}$ we drop some terms that are clearly smaller than others by several orders of τ. The expression we obtain is

$$R_4^{(0,0)} = \frac{1}{2(\gamma+1+K_\mu)}\left\{\frac{R_2^{(0,0)}}{\pi^2+a^2}\left[\gamma+1+K_\mu(1+\tau^{-1}+\tau^{-2}+\tau^{-3})\right] - \frac{R_0^{(0,0)}}{\pi^2+a^2}\left(\frac{5\pi^2+a^2}{9\pi^2+a^2}\right)\left(\left[\gamma+1+K_\mu(1+\tau^{-1}+\tau^{-2}+\tau^{-3}+\tau^{-4})\right]+\right.\right.$$

$$\left.\left.+\left[\gamma+1+K_\mu(1+\tau^{-1}+\tau^{-2})\right]E_1\right) + \frac{R_\mu}{\pi^2+a^2}\left(\frac{5\pi^2+a^2}{9\pi^2+a^2}\right)(\tau^{-5}+E_1\tau^{-3})\right\}. \qquad (76)$$

Here

$$E_1 = \frac{R_2^{(0,0)} 2a^2(\gamma+1+K_\mu)}{(9\pi^2+a^2)^3-(\pi^2+a^2)^3}.$$

Remembering that the results were valid only for $\frac{|K_\mu|}{\gamma+1} < \tau^2$ and that $|K_\mu| \approx |\gamma|\,\eta/\delta$ we see for $|\gamma|$ of order unity $\eta/\delta \sim \tau^2$ or $R_\mu \sim \tau^2 R_T$ and that as we are in the neighborhood of critical $R_T \sim \left(\frac{27\pi^4}{4} + R_\mu/\tau\right)/(\gamma+1+K_\mu)$. With this ordering in

mind we may write approximate relations for $R_0^{(a,\omega)}$, $R_2^{(a,\omega)}$, and $R_4^{(a,\omega)}$. We obtain

$$(\gamma+1+K\mu)R_0^{(a,\omega)} = \frac{27\pi^4}{4} + \frac{R\mu}{\tau} > 0$$

$$(\gamma+1+K\mu)R_2^{(a,\omega)} \approx \frac{-R\mu}{2\tau^3(\pi^2+a^2)} \sim \frac{-1}{\tau} < 0 \tag{77}$$

$$(\gamma+1+K\mu)R_4^{(a,\omega)} \approx \left(\frac{5\pi^2+a^2}{9\pi^2+a^2}\right)\frac{-R\mu}{2\tau^5(\pi^2+a^2)} \sim \frac{-1}{\tau^3} < 0$$

As $a^2 = \pi^2/2$ and $R_T^{(a,\omega)} \cong R_{(0)}^{(a,\omega)} + \epsilon^2 R_2^{(a,\omega)}$ we find

$$(\gamma+1+K\mu)R_T^{(a,\omega)} \approx 657 + \frac{R\mu}{\tau} - \epsilon^2\frac{R\mu/\tau^3}{30} + \epsilon^4\frac{11}{19}\frac{R\mu/\tau^5}{30}. \tag{78}$$

Since $R\mu \sim \tau^2$ we see that (78) is convergent for $\epsilon \ll \tau$ which was a restriction on the expansion procedure, If we minimize $R_T^{(a,\omega)}$ with respect to ϵ^2 we find that $R_T^{(a,\omega)}$ takes on a minimum at

$$\epsilon^2_{min} = \frac{-R_2^{(a,\omega)}}{2R_4^{(a,\omega)}} \approx \tau^2.$$

outside the limit of our radius of convergence. If applicable, this implies

$$(\gamma+1+K\mu)R_{T\,min}^{(a,\omega)} \approx 657 + R\mu/\tau \tag{79}$$

Let us go back and consider Eqs. (50) and (52). Let us also add the basic state temperature to the perturbation temperature and the basic state μ to the perturbation μ, Taking note of (43) we obtain

$$\frac{\partial u}{\partial x} = -\frac{\partial w}{\partial z} \tag{80}$$

and

$$\nabla\cdot(\chi\nabla T) + \gamma w - \underset{\sim}{\chi}\cdot[\nabla T + K\mu\nabla\mu] = 0. \tag{81}$$

Averaging (80) over the x-direction (either one period of $\frac{2\pi}{a}$ or the infinite domain) yields $\frac{d\overline{w}}{dz} = 0$ or $\overline{w}$ = constant. (An overbar means horizontal average.) As W must vanish at $z = (0)$ we have $\overline{w} = 0$. As (80) states that $\nabla\cdot\underset{\sim}{\chi} = 0$ we can replace $\underset{\sim}{\chi}\cdot\nabla$ in (81) by $\nabla\cdot(\underset{\sim}{\chi}T)$ and similarly for [illegible]. Then averaging (81) over x gives

$$\frac{d}{dz}\left\{\chi\frac{d\overline{T}}{dz} - \overline{wT} - K\mu\,\overline{w\mu}\right\} = 0 \tag{82}$$

Separating T and μ into its horizontally averaged components (which includes distortions due to the convection) and its fluctuating components by $T = \overline{T} + \tilde{T}$ and $\mu = \overline{\mu} + \tilde{\mu}$ and noting that $\overline{w} = 0$ we can rewrite (82) as

$$\frac{d}{dz}\left\{-\chi\frac{d\overline{T}}{dz} + \overline{w\tilde{T}} + K\mu\,\overline{w\tilde{\mu}}\right\} = 0 \tag{83}$$

Integrating (83) over z we find

$$Nu = -\chi\frac{d\overline{T}}{dz} + \overline{w\tilde{T}} + K\mu\,\overline{w\tilde{\mu}} \tag{84}$$

where Nu is a constant of integration and therefore is independent of z. If we integrate (84) over z again (denoting the z integration by brackets) we obtain

$$Nu = \left\langle -\chi \frac{d\bar{T}}{dz} \right\rangle + \left\langle \overline{w\tilde{T}} \right\rangle + \left\langle K_\mu \overline{w\tilde{\mu}} \right\rangle . \qquad (85)$$

To order $(m,n) = (0,0)$ we have $\chi = 1$ and we see that (85) is the heat flux nondimensionalized by a linear temperature gradient $(\Delta T/D)$, that is (85) is the Nusselt number. Substituting in the ϵ-expansions for the variables of order $(m,n) = (0,0)$, noting that $w_2^{(0,0)} = 0$ and that $w_3^{(0,0)}$ is orthogonal to $\bar{T}_1^{(0,0)}$ and $\tilde{\mu}_1^{(0,0)}$ we find to order ϵ^4 that

$$Nu = 1 + \epsilon^2 \left[\left\langle \overline{w_1^{(0,0)} \tilde{T}_1^{(0,0)}} \right\rangle + K_\mu \left\langle \overline{w_1^{(0,0)} \tilde{\mu}_1^{(0,0)}} \right\rangle \right] + \epsilon^4 \left[\left\langle \overline{w_1^{(0,0)} \tilde{T}_3^{(0,0)}} \right\rangle + K_\mu \left\langle \overline{w_1^{(0,0)} \tilde{\mu}_3^{(0,0)}} \right\rangle \right]. \qquad (86)$$

$\tilde{\mu}\tilde{\mu}$ contributes to the heat flux because the exchange of an H nucleus with a He nucleus via diffusion implies the removal of two particles $(H^+ + e^-)$ with the addition of three particles $(He^{+2} + 2e^-)$, i.e., the ions drag their free electrons along.

Substituting in the eigenfunctions and performing the integrations we find

$$Nu = 1 + \epsilon^2 \sqrt{\frac{32}{9\pi^4}} (\gamma+1) \left[1 + \frac{K_\mu}{(\gamma+1)} (1+\tau^{-1}) \right] - \epsilon^4 \sqrt{\frac{32}{81\pi^8}} (\gamma+1) \left[1 + \frac{K_\mu}{(\gamma+1)} (1+\tau^{-1}+\tau^{-2}+\tau^{-3}) \right]. \qquad (87)$$

From (87) we see that the restriction that $\frac{|K_\mu|}{(\gamma+1)} < \tau$ is consistent with a Nusselt number always ≥ 1, (remember that $K_\mu < 0$ as $K_\mu \sim \gamma$). We can solve for ϵ^2 in terms of the known quantities $R_0^{(0,0)}$, $R_2^{(0,0)}$, $R_4^{(0,0)}$ and the specified $R_T^{(0,0)}$. The solution of the quadratic equation is

$$\epsilon^2_{(R_T)} \cong \frac{-R_2^{(0,0)}}{2R_4^{(0,0)}} \pm \frac{1}{2R_4^{(0,0)}} \left[R_2^{(0,0)2} + 4R_4^{(0,0)} \left(R_T - R_0^{(0,0)} \right) \right]^{1/2}.$$

For $R_T > R_0^{(0,0)}$ we must choose the (+) sign while for $R_T < R_0^{(0,0)}$ we have two values for ϵ^2. The heat flux is proportional to $Nu\, R_T$ and we find that the slope of the heat flux vs. $R_T^{(0,0)}$ curve at $R_0^{(0,0)}$ is

$$\left. \frac{d(Nu R_T^{(0,0)})}{dR_T} \right|_{R_T = R_0^{(0,0)}} = Nu + R_T \frac{dNu}{d\epsilon^2} \frac{d\epsilon^2}{dR_T} \approx 1 \pm \frac{R_T(\gamma+1)}{|R_2^{(0,0)}|} \sqrt{\frac{32}{9\pi^4}}$$

at $R_T^{(0,0)} = R_0^{(0,0)}$. As $|R_T^{(0,0)}| \sim$ [illegible] we have slopes of $1 \pm O[(\gamma+1)^2\tau]$. The general shape of the curve is given in Fig.2.

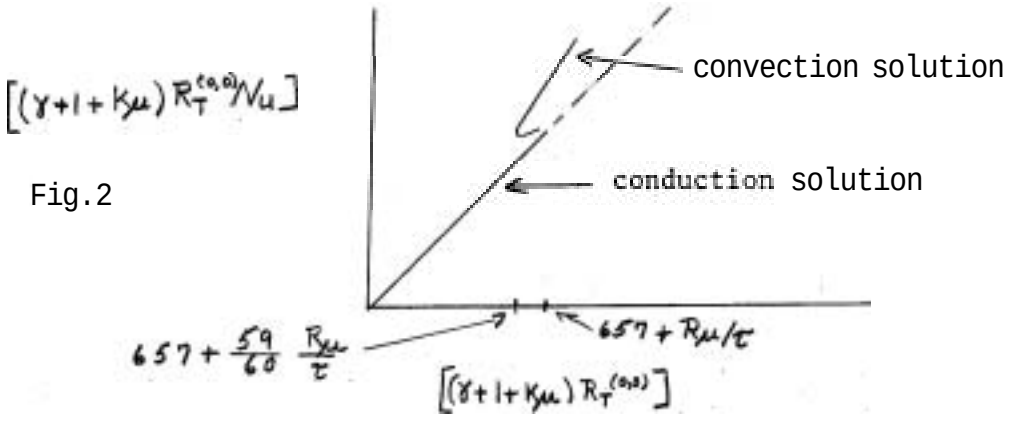

Fig.2

Though we have considered only steady solutions to the equations we would expect the lower branch of the convective solutions to represent steady finite amplitude convection which itself is unstable to infinitesimal perturbations. This is because for a prescribed Rayleigh number the lower branch solutions convect less heat than those on the upper branch. As we would expect the fluid to convect in the mode which releases the most potential energy the fastest (Malkus and Veronis,

1958) we suspect that the upper branch is the physically realized solution.

VI Conclusion

We have investigated the stability of finite amplitude two-dimensional disturbance in a compressible fluid layer with a stabilizing gradient of solute and a destabilizing temperature gradient. We have considered only steady convective solutions and have made an attempt to take into account the temperature and composition dependence of the conductivity. We have found that the steady convective solutions bifurcate from the conductive solution in a subcritical manner and that the variable conductivity does not remove this subcritically. Though we have restricted our investigation to a very special ordering of the relevant parameters we feel that the qualitative nature of the instability is demonstrated even though the minimum in the heat flux vs. R_T curve was outside the radius of convergence of the ϵ -expansion.

With reference to stellar semiconvection zones we would like to determine with somewhat more confidence the minimum R_T for which there exists a convective solution. Because of the parameter range we were working in, we found that the subcriticality did not change things very much, however we feel that this would not be the case in stars. It is still unclear whether the Ledoux or the Schwarzschild stability criterion is the more realistic in the stars. In some sense our results indicate that the Ledoux criterion is too restrictive while Schwarzschild's is not restrictive enough.

Acknowledgments

I would like to thank Dr, Edward Spiegel very much for suggesting this problem to me and for his guidance throughout this work. I would also like to thank the other members of the staff for helpful discussions.

References

Aller, L. and S.Chapman 1960 Ap.J. 132: 461. Diffusion in the Sun.

Auré, J.-L. 1969 GFD Woods Hole Notes II: 1. Overstable Damping in a Stellar S Semiconvective Zone.

Chandrasekhar, S. 1939 Univ.Chicago Press; Dover 1958. An Introduction to the Study of Stellar Structure.

Kato, S. 1966 Pub.Ast.Soc.Japan, 18: 374.

Landau, L. and E.Lifshity 1958 Pergamon Press. Statistical Physics.

Landau, L. and E.Lifshity 1959 Pergamon Press. Fluid Mechanics.

Ledoux,P. 1947 Ap.J. 105: 305. Stellar Models with Convection and with Discontinuity of the Mean Molecular Weight.

Ledoux,P. and T.Walraven 1958 Springer-Verlag. Handbuch der Physik LI.

Malkus, W.V.R. 1964 Woods Hole G.F.D.Notes I: 1-12. Boussinesq Equations.

Malkus, W.V.R. and G.Veronis 1958 J.Fluid Mech. 4: 225. Finite Amplitude Cellular Convection.

Masaki 1971 Pub.Ast.Soc.Japan, 23: 425.

Millman, M. and J.Keller 1969 J.Math.Phys. 10: 342. Perturbation Theory of Nonlinear Boundary-Value Problems.

Schwarzschild, M. and R.Harm 1958 Ap.J., 128: 348. Evolution of Very Massive Stars,

Spiegel, E. and G. Veronis 1960 Ap.J., 131: 442. On the Boussinesq Approximation for a Compressible Fluid (see correction by Veronis, 1962 Ap.J.135: 655).

Spitzer, L. Physics of Fully Ionized Gases,

Stothers,R. 1970 M.N.R.A.S., 151: 65. Internal Structure of Upper Main-Sequence Stars.

Thomas,L. 1930 Quart.J.Math., 1: 239. The Radiation Field in a Fluid in Motion.

Veronis,G. 1964 J.Marine Research, 23: 1. On Finite Amplitude Instability in Thermohaline Convection.

Veronis,G. 1968 J.F.M. 34: 315. Effect of a Stabilizing Gradient of Solute on Thermal Convection.